HERARCHICALLY SLAVED MULTI-PULSING MODE-LOCK DYNAMICS

A THESIS SUBMITTED TO
THE GRADUATE SCHOOL OF ENGINEERING AND SCIENCE
OF BILKENT UNIVERSITY
IN PARTIAL FULFILLMENT OF THE REQUIREMENTS FOR
THE DEGREE OF
MASTER OF SCIENCE
IN
MATERIALS SCIENCE AND NANOTECHNOLOGY

By
Aladin Choura
September 2021

HIERARCHICALLY SLAVED MULTI-PULSING MODE-LOCK DYNAMICS

By Aladin Choura

September 2021

We certify that we have read this thesis and that in our opinion it is fully adequate, in scope and in quality, as a thesis for the degree of Master of Science.

Fatih Ömer İlday (Advisor)

Mehmet Burçin ünlü

Serim İlday

Approved for the Graduate School of Engineering and Science:

Ezhan Karaşan
Director of the Graduate School

ABSTRACT

HERARCHICALLY SLAVED MULTI-PULSING MODE-LOCK DYNAMICS

Aladin Choura
M.S. in Materials Science and Nanotechnology
Advisor: Fatih Ömer İlday
September 2021

Passive mode-locking is the self-assembly of optical energy in a laser cavity towards narrow pulses. Often, the energy available in the cavity goes into multiple coexisting pulses with little control on their number, their energies, or their temporal positions. This phenomenon is vaguely known as pulse energy quantization and has been anecdotally linked to pulse splitting induced by optical nonlinearity. Research has focussed mainly on avoiding pulse energy quantization and any complex behavior associated with it while driving the pulses to higher and higher energies. The complex multi-pulsing behavior is often regarded as an output of a black box filled with complex nonlinear dynamics with little hope to control it. There's a want for a clear and workable understanding of these dynamics.

The central point of this thesis is that standard, few-dimensional, nearly deterministic nonlinear dynamics offers this understanding; while mode-locking is indeed the result of noisy interactions of thousands of optical modes shaping the optical pulses, due to fast pulse-shaping processes involved in mode-locking, the pulse shapes tend to be slaved to one or few order parameters, mainly the pulse energy. Then, the complex behavior is understood as the result of a much simpler nonlinear dynamical system. This understanding is supported by our experiments on a multi-pulsing Mamyshev oscillator, and in return, it guides us towards reliably controlling it. With this control, multiple pulsation, which has been little more than a scientific curiosity, becomes technologically valuable for applications such as ablation-cooled material removal and frequency metrology.

First, we address the issue of multiple pulsation. We define an energy map which describes the evolution of each pulse. Using the energy map, we show that stable coexistence of multiple pulses is permitted despite their competition on the gain if the growth of a pulse is self-limiting, i.e., if the energy map features

a stable fixed point even at a constant gain. The energy map similarly explains the intimately related phenomena of period-doubling, non-identical pulses, and response to perturbations. The physical processes leading to these phenomena in our laser and others are discussed in parallel, and analogies to other systems are drawn. Many attractors are permitted by the energy map, highlighting the effect of bifurcations, hysteresis, and kinetics of pulse formation. Accordingly, we present guidelines for the control of multi-pulsing lasers and a procedure to control the number of pulses in a Mamyshev oscillator.

Having controlled the number of pulses, we turn our attention to the temporal organization they take. Pulses coexisting in a laser cavity tend to evolve towards stable patterns due to long-range interactions between them. Several interaction mechanisms have been proposed in the literature, but the pulse interactions are still poorly understood. This is due partially to the multitude of possible interaction mechanisms and partially to the focus of their discussion on the physical processes that allow the pulses to interact without analyzing the dynamics that result from these interactions. We argue that the temporal organization dynamics is slaved and present the form of the dynamical system for all long-ranged interaction mechanisms and use it to derive for the first time the stability criterion for harmonic mode-locking. A comparison between the interaction mechanisms suggests the dominance of acoustically mediated interactions in our oscillator. We show theoretically that the acoustic effect is coupled to the single-pulse evolution dynamics and influences the individual pulse energies, which in turn, slave their speeds. This is a distinguishing feature of pulse interactions in our oscillator. We show experimentally that these interactions permit multiple stable fixed points for a given number of pulses and demonstrate noise-induced transitions as well as bifurcation based on parameters of single-pulse mode-lock dynamics, confirming our interaction theory. Lastly, we demonstrate drastic manipulation of the acoustic interactions using a novel secondary loop, allowing richer pulse patterns, and further supporting our interactions theory.

Keywords: nonlinear dynamics, complex behavior, self-organization, slaving principle, bifurcation, noise-induced transitions, mode-lock, multiple pulsation, pulse energy quantization, pulse interactions, harmonic mode-locking, high repetition rate .

ÖZET

HİYERARŞİK OLARAK BAĞIMLI ÇOKLU DARBE MOD-KİLİT DİNAMİĞİ

Aladin Choura
Malzeme Bilimi ve Nanotechnology, Yüksek Lisans
Tez Danışmanı: Fatih Ömer İlday
Eylü 2021

Pasif mod kilitleme, optik enerjinin bir lazer boşluğunda dar darbelere doğru kendiliğinden toplanmasıdır. Çoğu zaman, boşlukta mevcut olan enerji, sayıları, enerjileri veya zamansal konumları üzerinde çok az kontrol ile birden fazla birlikte var olan darbelere gider. Bu fenomen, belirsiz bir şekilde darbe enerjisi kuantizasyonu olarak bilinir ve optik doğrusal olmayanlığın neden olduğu darbe bölme ile anekdot olarak bağlantılıdır. Araştırma, esas olarak, darbeleri daha yüksek enerjilere yönlendirirken darbe enerjisi kuantizasyonundan ve bununla ilişkili herhangi bir karmaşık davranıştan kaçınmaya odaklanmıştır. Karmaşık çoklu darbe davranışı, genellikle, onu kontrol etmek için çok az umutla karmaşık doğrusal olmayan dinamiklerle dolu bir kara kutunun çıktısı olarak kabul edilir. Bu dinamiklerin açık ve uygulanabilir bir şekilde anlaşılmasına yönelik bir ihtiyaç var.

Bu tezin merkezi noktası, standart, birkaç boyutlu, neredeyse deterministik doğrusal olmayan dinamiklerin bu anlayışı sunduğudur; Mod kilitleme, mod kilitlemede yer alan hızlı darbe şekillendirme mekanizmaları nedeniyle, optik darbeleri şekillendiren binlerce optik modun gürültülü etkileşimlerinin gerçekten bir sonucu olsa da, darbe şekilleri bir veya birkaç düzen parametresine (order parameter), darbe enerjisi gibi, bağımlı (slaved) olma eğilimindedir. Dolaysıyla, karmaşık davranış, çok daha basit, doğrusal olmayan dinamik bir sistemin sonucu olarak anlaşılır. Bu anlayış, çoklu darbe bir Mamyshev osilatörü üzerindeki deneylerimizle desteklenir ve karşılığında, onu güvenilir bir şekilde kontrol etmeye yönlendirir. Bu kontrol ile, bilimsel bir meraktan fazla olamayan çoklu darbe lazerleri, ablasyon soğutmalı malzeme kaldırma ve frekans metrolojisi gibi uygulamalar için teknolojik olarak değerli hale gelir.

İlk olarak, çoklu darbe sorununu ele alıyoruz. Her darbenin evrimini

tanımlayan bir enerji haritası tanımlarız. Enerji haritasını kullanarak, bir darbenin büyümesi kendi kendini sınırlandırıyorsa, yani enerji haritası sabit bir kazançta bile stabil bir sabit noktaya sahipse, kazanç üzerindeki yarışmaya rağmen birden fazla darbenin aynı zamanda bulunmasına izin verildiğini gösteriyoruz. Enerji haritası benzer şekilde, pertürbasyonlara tepki, özdeş olmayan atımlar ve periyot ikiye katlanması gibi yakından ilişkili fenomenleri açıklar. Lazerimizde ve diğerlerinde bu fenomenlere yol açan fiziksel süreçler paralel olarak tartışılır ve farklı bilimsel sistemlerle analojiler çizilir. Enerji haritası tarafından birçok çekiciye izin verilir, bu da çatallanmaların, histerezisin ve darbe doğumun kinetiğinin etkisini vurgular. Buna göre, çok darbeli lazerlerin kontrolü için yönergeler ve Mamyshev osilatöründeki darbelerin sayısını kontrol etmek için bir prosedür sunuyoruz.

Darbe sayısını kontrol ettikten sonra, dikkatimizi aldıkları zamansal organizasyona çeviriyoruz. Bir lazer boşluğunda bir arada bulunan darbeler, aralarındaki uzun menzilli etkileşimler nedeniyle kararlı modellere doğru gelişme eğilimindedir. Literatürde birkaç etkileşim mekanizması önerilmiştir, ancak darbe etkileşimleri hala tam olarak anlaşılamamış durumdadır. Bunun nedeni kısmen olası etkileşim mekanizmalarının çokluğu ve kısmen de bu etkileşimlerden kaynaklanan dinamikleri analiz etmeden darbelerin etkileşime girmesine izin veren fiziksel süreçler üzerindeki tartışmalarının odak noktasıdır. Zamansal organizasyon dinamiklerinin bağımlı olduğunu savunarak, tüm uzun menzilli etkileşim mekanizmaları için dinamik sistem formunu sunuyoruz ve bu dinamik sistemi kullanarak, ilk kez harmonik mod kilitlemeye izin veren kriterini türetiyoruz. Literatürdeki etkileşim mekanizmaları arasındaki karşılaştırmak, osilatörümüzde akustik olarak aracılık edilen etkileşimlerin baskınlığını gösterir. Teorik olarak, bu darbe etkileşimlerde, akustik etkin ile birlikte, tek darbeli evrim dinamiklerinin yer bulduğunu, bireysel darbe enerjilerini etkilediğini, ve darbe hızları, darbe enrjilerine bağımlı olduğunu gösteriyoruz. Bu, osilatörümüzdeki darbe etkileşimlerinin ayırt edici bir özelliğidir. Deneysel olarak, bu etkileşimlerin belirli sayıda darbe için birden fazla stabil sabit noktaya izin verdiğini ve gürültü kaynaklı geçişlerin yanı sıra tek darbeli mod-kilit dinamiği parametrelerine dayalı çatallanma gösterdiğini ve etkileşim teorimizi doğruladığını gösteriyoruz. Son olarak, daha zengin darbe organizasyona izin veren ve etkileşim teorimizi daha da destekleyen yeni bir ikincil döngü kullanarak akustik etkileşimlerin dramatik manipülasyonunu gösteriyoruz.

Anahtar sözcükler: doğrusal olmayan dinamik, karmaşık davranış, kendi kendine organizasyon, bağımlılık ilkesi, gürültü kaynaklı geçiş, mod kilitleme, çoklu darbe mod kilitleme, darbe energjisi kuantizasyonu, darbe etkileşimleri, harmonik mod kilitleme, yüksek darbe oranı.

Acknowledgement

This thesis would not come to exist without my advisor Ömer İlday. I thank him for his accommodating and insightful supervision and for enduring my mentally taxing arguments. His struggle to understand my thoughts was crucial for me to put this thesis in a human-readable language.

I thank my committee members, Serim Ílday and Burçin ünlü for serving on my committee and evaluating my dense thesis.

I am indebted to all past and present members of UFOLAB for creating the scientific and technical infrastructure that made this work possible. I especially thank Hamit Kalayicioğlu and Parviz Ilahi for their very generous technical, scientific, and personal support. I owe them hundreds of hours of diverse discussions, often late at night.

I also would like to thank Bülend Ortaç, who gave me a far head start by teaching me the fundamentals of lasers, and Seymur Jahangirov and Serim Ílday for seeding my interest in complex systems. I'm also indebted to my many professors and teachers without whom I wouldn't have had the scientific foundation to pursue this research.

Above all, I thank my family, who take the credit for inclining me to education and science since my childhood and who never stopped giving me their support throughout my education abroad.

This work was supported by Türkiye Bilimsel ve Teknik Araştırma Kurumu. I'm grateful to the taxpayers for funding my research and I hope it will serve their interests well in return.

Contents

List of Figures

Chapter 1

Introduction

The earliest interest in mode-locking may be attributed to its clear display of self-organization [1, 2, 3], a complex dynamical system of tens or hundreds of thousands of optical modes organize in phase and amplitude to form a wave packet with the same shape and spectrum every roundtrip through the laser cavity. With this fundamental interest, experimental and theoretical research approached both single-pulsing and multi-pulsing mode-lock dynamics, and so, multiple pulsation received significant experimental and theoretical research [4, 5, 6]. However, the focus was on the only regime of mode-lock available at the time, the so-called soliton regime [7].

As mode-locking received more and more technological interest, research drifted towards avoiding pulse quantization rather than controlling and exploiting it. This drift was motivated by the demand for single-pulsing lasers with high pulse energies for applications such as ultrafast ablation [8] and multi-photon spectroscopy [9]. To this end, new mode-lock regimes [10, 11, 12, 13, 14] have found great success in raising the pulse energy before the onset of multiple pulsation, with some regimes providing higher pulse energies than others. This dependence on the mode-lock regime gives the impression that multiple pulsation is inseparably connected to the full complexity of mode-lock dynamics.

However, multiple pulsation is not limited to any particular mode-lock regime, and it is more strongly influenced by the particular laser cavity design and parameters. For example, the so-called Mamyshev oscillator [15, 16] has been reported to produce single pulses with record-high energy [17] as well as much more complex [18, 19, 15] multiple pulsation and related behaviors, including period-doubling and non-identical pulses. This prevalence of complex multi-pulsing behaviors promises and motivates a simple and general dynamical description of these phenomena valid for a large family of mode-lock regimes and cavity designs.

In this thesis, we present such a simple and general description in parallel to an experimental account of a homemade Mamyshev oscillator, where we demonstrate a high level of control. In doing so, we approach two higher aims from mode-lock studies:

1. To solidify concepts from mode-lock dynamics with instructive analogies reaching far beyond mode-locking and laser systems in general.

2. To develop general principles and specific recipes for robust and reliable control of complex mode-lock behavior for technological applications.

In chapter 2, we discuss basic concepts of nonlinear dynamics, highlighting dynamical phenomena that will appear throughout this text. We then discuss nonlinear pulse evolution processes and put them in the context of mode-locking and its known regimes. These processes and regimes will be referenced when explaining multi-pulsing trends in later chapters. Lastly, we define multiple pulsation and related phenomena, highlighting questions to be answered in later chapters.

In chapter 3, we discuss the Mamyshev oscillator. We explain its working principle and general characteristics and present an overview of its reported behaviors in the literature. We then present our experimental setting.

In Chapter 4, we discuss the dynamics governing the number of pulses. We

present a procedure to control the number of pulses in our laser, in addition to period-doubling and different-energy pulses. We introduce the concept of an energy map and use it to demonstrate our quantization mechanism and explain the experimental phenomena reported in this chapter.

In chapter 5, we focus on the pulse interactions. We present a control procedure to achieve harmonic mode-locking (equidistant pulse pattern) in our laser. Then we analyze the pulse interactions theoretically by formalizing the dynamical system of interacting pulses. We then present an overview of interaction mechanisms in the literature and argue for the dominance of acoustically mediated interactions in our oscillator. We review the theory of acoustic interactions and adapt it to our oscillator. This discussion leads to the stability criterion of harmonic mode-locking, which we derive for the first time. Lastly, we introduce a technique to drastically manipulate the acoustic interactions using a secondary loop.

In chapter 6, we summarize and conclude by assessing the extent to which the two higher aims above are achieved.

Chapter 2

Basic Concepts

In section 1 of this chapter, we introduce concepts of nonlinear dynamics which will be demonstrated by experimental phenomena throughout this thesis. As the terminology is non-standard in this field, we fix it for the rest of this thesis, adopting it mostly from [20]. In section 2, we discuss some relevant pulse evolution processes in light of the dynamical concepts thus introduced. These processes are concatenated to form the mode-lock regimes, as discussed in section 3. Lastly, we outline the multi-pulsing phenomena of interest in section 4.

2.1 Concepts in Nonlinear Dynamics

A dynamical system is a system whose components evolve in time and can be described as:

$$\dot{\mathbf{x}} = \mathbf{f}(\mathbf{x}) \tag{2.1}$$

or

$$\mathbf{x}_{n+1} = \mathbf{f}(\mathbf{x}_n), \tag{2.2}$$

where $\mathbf{x}$ and $\mathbf{f}$ are vectors whose number of dimensions equals that of the number of degrees of freedom, and the system may be described as *complex* if the number of its parts, its degrees of freedom, is large. Equation. 2.1 describes a system

that continuously evolves in time and maybe termed *differential dynamical system* whereas equation. 2.2 describes a *map*, where the evolution occurs in discrete steps. The space spanned by all possible $\mathbf{x}$ values is called the *phase space*, and the state of a system occupies a point in the phase space. Pulse propagation through a medium is best described by a differential dynamical system whereas pulse evolution in a laser one roundtrip after another is a map (see section 3); the dynamical variables in each are the values of the electric field envelope at each point, which can be approximated by a finite number of points in the time-domain or Fourier domain.

Dynamical systems may be classified as *dissipative* or *conservative*. In dissipative systems, an ensemble of systems with nearby initial states changes its density in the phase space along with their evolution. It can be shown [20, 21] that systems with non-trivially conserved quantities cannot be dissipative. This is why non-dissipative systems are called conservative. Dissipative systems accommodate *attractors*, which are points, asymptotic trajectories, or other topological entities in the phase space to which all nearby states are attracted. The region in the phase space from which systems evolve towards an attractor is that attractor's *basin of attraction*. The boundaries between different basins of attraction are called *basin boundaries*. Dynamical systems may feature *invariant* sets in the phase space, sets from which states never leave without any external perturbation. These include *fixed points*, closed trajectories, and possibly others. If states go back to an invariant set after any sufficiently small perturbation from it, the invariant set is *stable*, and it is an attractor. Conservative systems allow invariant sets but not attractors. Examples of these invariants and attractors are presented in section 2.

In a complex system, the majority of its degrees of freedom may relax towards a state that is determined by few much slower degrees of freedom. The fast degrees of freedom are said to be *slaved* to the slower ones, which are called *order parameters*. With this assumption, the complex system may be approximated by a simpler one described in terms of the order parameters only. This so-called *slaving principle* [22] is central for this thesis; it is the essence of the energy map (chapter 4) as well as our pulse interactions model (chapter 5).

Dynamical systems may be further classified as *linear* or *nonlinear* depending on whether or not $\mathbf{f}$ accepts linear superposition. Linear systems feature a limited number of known behaviors. Most notably, a linear system features a single fixed point which may or may not be stable. Nonlinear systems, on the other hand, accommodate a large variety of behaviors such as multiple attractors. For example, nonlinearity allows our laser to accommodate different numbers of identical pulses, non-identical pulses and *period-doubled* states (chapter 4). It also allows multiple pulse patterns (chapter 5).

Figure 2.1 shows an example of a 2-dimensional nonlinear dissipative dynamical system featuring three stable fixed points and demonstrating the slaving principle.

Any quantities involved in $\mathbf{f}$ other than the dynamical variables, $\mathbf{x}$, are *parameters* (pump power for example) and their possible values span the *parameter space*. The behavior of a dynamical system is often qualitatively dependent on its parameters; a change in the parameters may, for example, create or destroy a fixed point (chapter 5: the destruction of a fixed delay in a double-pulsing state) or change its stability (chapter 4: destabilization of pulse energy) when a boundary in the parameter space is crossed. Such critical qualitative response to a change of parameters is called *bifurcation*. *Multistability* is the case where multiple attractors coexist in a shared region in the parameter space so that the choice of the attractor actually occupied by the system depends on the history of the motion in the parameter space. This results in bifurcations that are not reversible, also known as *hysteresis*. In chapter 4, we show hysteresis in the number of pulses, and in chapter 5, we show hysteresis in their temporal organization.

The appearance of multiple attractors and/or a large number of bifurcations is often described as *complex behavior*. Complex behavior correlates with nonlinearity rather than the complexity of the system itself. A simple, few dimensional dynamical system may give rise to the same complex behavior as a system with complicated interactions between many degrees of freedom. Indeed, collapsing a complex system to a few order parameters by the slaving principle does not miss the complexity in its behavior.

So far we have considered *deterministic* systems, where *additive noise* is negligible; in actual systems, a noise term should be added to equations 2.1 and 2.2. Weak noise may lead the system to an attractor if one exists, even if the system starts outside its basin of attraction. Once the system comes near an attractor, weak noise is attenuated. On the other hand, sufficiently strong noise may carry the state from one attractor to another across basin boundaries. Accordingly, we may compare the stability of attractors against *noise-induced transitions* [23], with attractors enjoying stronger noise attenuation and larger basins of attraction being more stable. The system prefers attractors with higher stability. If the state of the system remains at a non-preferred attractor due to weakness of the noise, we describe this state as *kinetically stable*. Typical Mamyshev oscillators allow many kinetically stable states due to their strong suppression of noise (chapter 3). In particular, we induce transitions in the pulse patterns using injected noise, occasionally leading to rarely attained but kinetically stable patterns (chapter 5). Moreover, mode-lock pulses are commonly born out of noise but not in Mamyshev oscillators.

Lastly, we note that the parameters may be susceptible to *parameter noise* as well, which includes, for example, fluctuations in the pump power. The system may be considered *robust* if the additive noise can not cause unintended noise-induced transitions and the parameter noise can not cause unintended bifurcations.

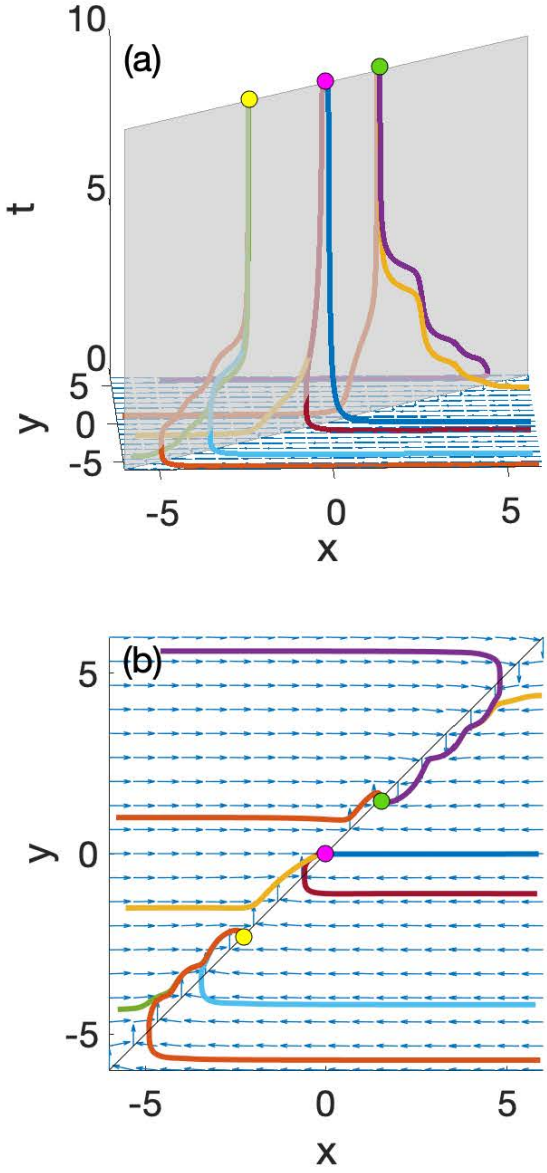

Figure 2.1: Behavior of a nonlinear dissipative dynamical system, $\dot{x} = 20(y - x), \dot{y} = sin(xy) - 0.4y$. (a) shows the evolution in time from multiple initial conditions. (b) shows the same trajectories projected onto the 2-dimensional phase space. This system is dissipative, which allows it to have attractors. The attractors shown are three stable fixed points, marked by yellow, pink, and green dots; these points attract all trajectories in their respective basins of attraction. Note also that x approaches the $x = y$ line much faster than y approache the fixed points; x is slaved to the order parameter y so that the dynamics is effectively one-dimensional.

2.2 Pulse evolution processes

As a pulse travels through a laser cavity, it undergoes multiple processes. The most important processes in the context of mode-lock lasers are listed below:

Dispersion [24]: A pulse is a localized electromagnetic wave packet that results from the superposition of multiple frequency components and moves with the group velocity of its central frequency. However, the group velocity varies along the frequency spectrum of the pulse so that different parts of the pulse move faster than others, broadening the pulse and dispersing its frequency components over its temporal profile. As a result, the pulse acquires a frequency chirp, where the instantaneous frequency varies along the pulse. Positive or normal chirp is conventionally the case where high-frequency components are delayed so that the lagging edge of the pulse is blue-shifted. Naturally, the effect of dispersion on the pulse shape increases with its spectral width. The pulse propagation under the sole effect of dispersion is mathematically expressed as:

$$\frac{\partial A}{\partial z} = -i\frac{\beta_2}{2}\frac{\partial^2 A}{\partial \tau^2}, \tag{2.3}$$

where A is the complex amplitude, z is the propagation distance, β_2 is the group velocity dispersion, also known as second order dispersion and τ is the time delay variable. Figure 2.2 shows the evolution of a Gaussian pulse under positive dispersion

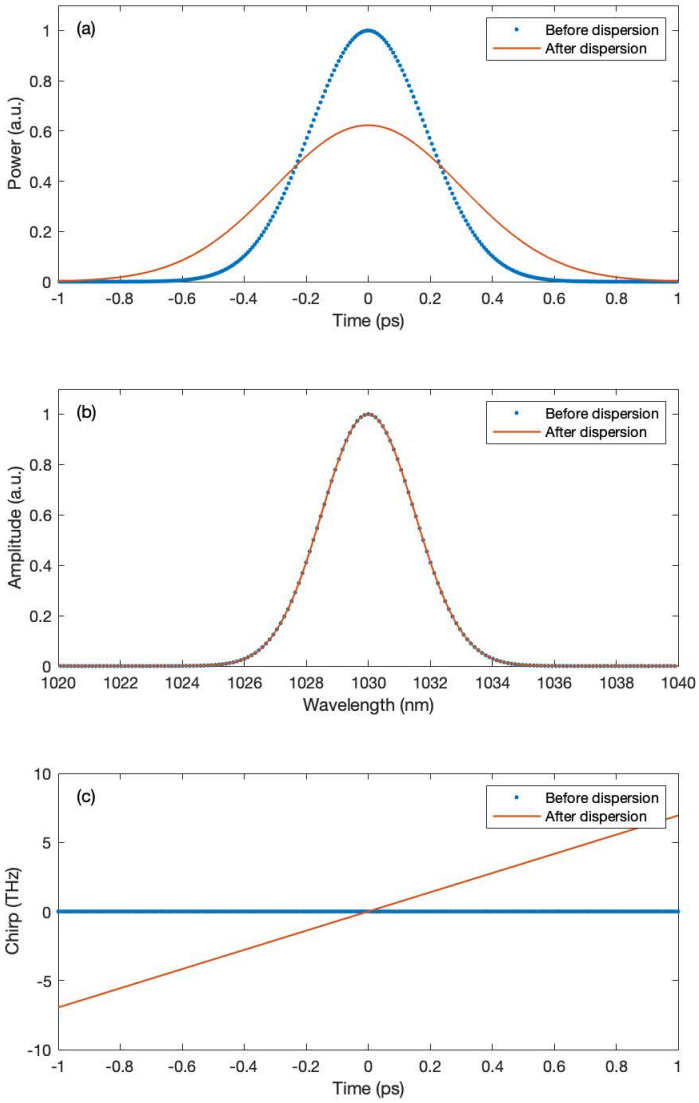

Figure 2.2: Gaussian pulse evolution under positive dispersion. Dotted blue lines represent the initial pulse, and solid orange lines represent the pulse after dispersive propagation. (a): pulse shape in time (amplitude squared). The pulse broadens due to dispersion. (b): pulse spectrum. Dispersion doesn't change the spectrum. (c): frequency chirp. The pulse broadens in time despite keeping the same spectrum because dispersion delays its frequency components with respect to each other, resulting in this chirp

Kerr nonlinearity[25]: The commonly known linear electromagnetic wave equation assumes the induced polarization of the material to be linear in the electric field so that the refractive index is independent of the optical power. Due to this linearization, the spectrum of a pulse never changes along its propagation. With sufficiently intense pulses, however, the refractive index does depend on the optical power, changing the spectrum and contributing to the chirp. Mathematically the pulse propagation solely under the effect of Kerr nonlinearity is modeled by:

$$\frac{\partial A}{\partial z} = i\gamma \left|A\right|^2 A, \tag{2.4}$$

where γ is the coefficient of Kerr nonlinearity. It is inversely proportional to the area of the optical beam.

Kerr nonlinearity alone does not change the pulse shape; starting with negligible chirp, Kerr nonlinearity broadens the spectrum while also adding chirp so that, despite the decrease in the transform-limited pulse duration due to spectral broadening, the actual pulse duration and shape remain the same; Kerr nonlinearity blue-shifts frequency components towards the lagging edge and red-shifts frequency components towards the leading edge of the pulse. With more and more Kerr nonlinearity, the spectrum broadens and acquires modulations while compressing within the same initial pulse envelope. Figure 2.3 shows the evolution of a transform-limited Gaussian pulse under pure Kerr nonlinearity.

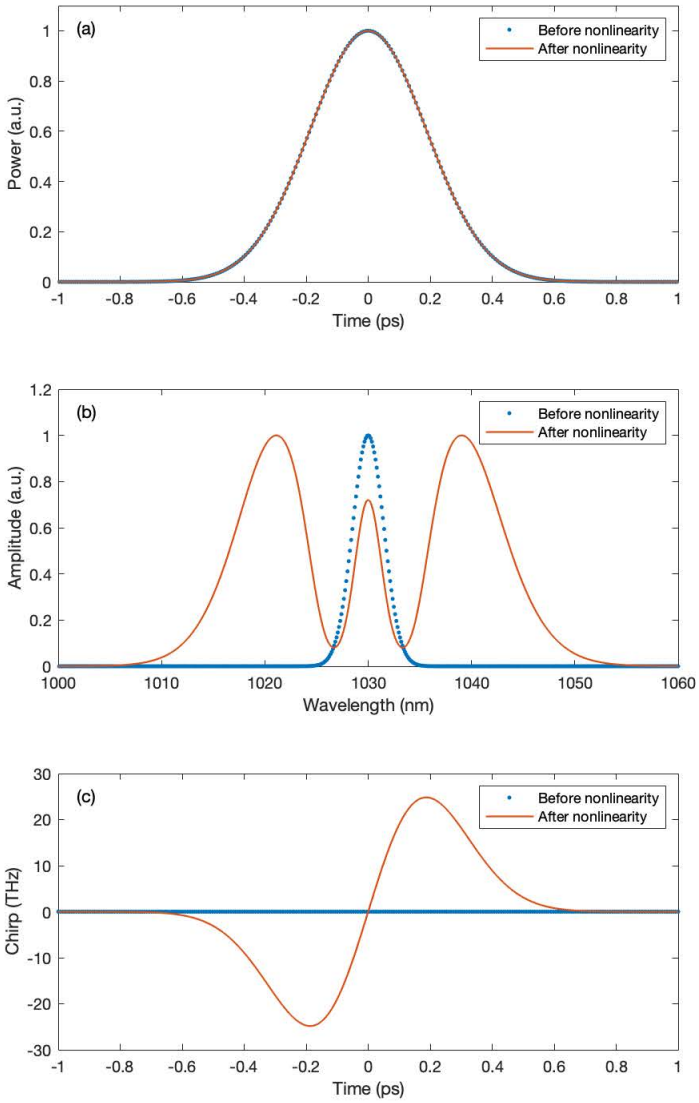

Figure 2.3: Gaussian pulse evolution under pure Kerr nonlinearity. Dotted blue lines represent the initial pulse, and solid orange lines represent the pulse after evolution. As shown in (a), the initial and final pulse shapes coincide. (b) shows broadening and modulation of the spectrum. (c) shows the chirp the pulse acquires during this evolution. The chirp maintains the pulse shape despite the broadening and modulation of the spectrum

With the addition of dispersion, we distinguish the following three cases:

1. Conservative solitons[7]: if dispersion is negative, its combined effect together with Kerr nonlinearity allows an infinite set of oscillatory invariants called solitons. Although dispersion and Kerr nonlinearity are conservative processes, solitons behave almost like attractors; an initial pulse sufficiently close to a soliton becomes closer to that soliton with a smaller amount of energy. This comes at the cost of a long and shallow pedestal dispersing away from the soliton as it forms. The simplest and most common type of solitons is the so-called fundamental Soliton which is a fixed point in the phase space; the effects of negative dispersion and Kerr nonlinearity exactly negate each other at a transform-limited $sech^2$ pulse shape (amplitude squared) with its energy and width related by:

$$E\tau_0 = \frac{2\,|\beta_2|}{|\gamma|}, \tag{2.5}$$

where E is the energy and τ_0 is the width. Interestingly, there are materials that enjoy negative Kerr nonlinearity together with positive dispersion. The same $sech^2$ solution is valid for those materials as well.

Figure 2.4 shows the evolution of a transform-limited Gaussian pulse to a fundamental soliton with a dispersive waves pedestal.

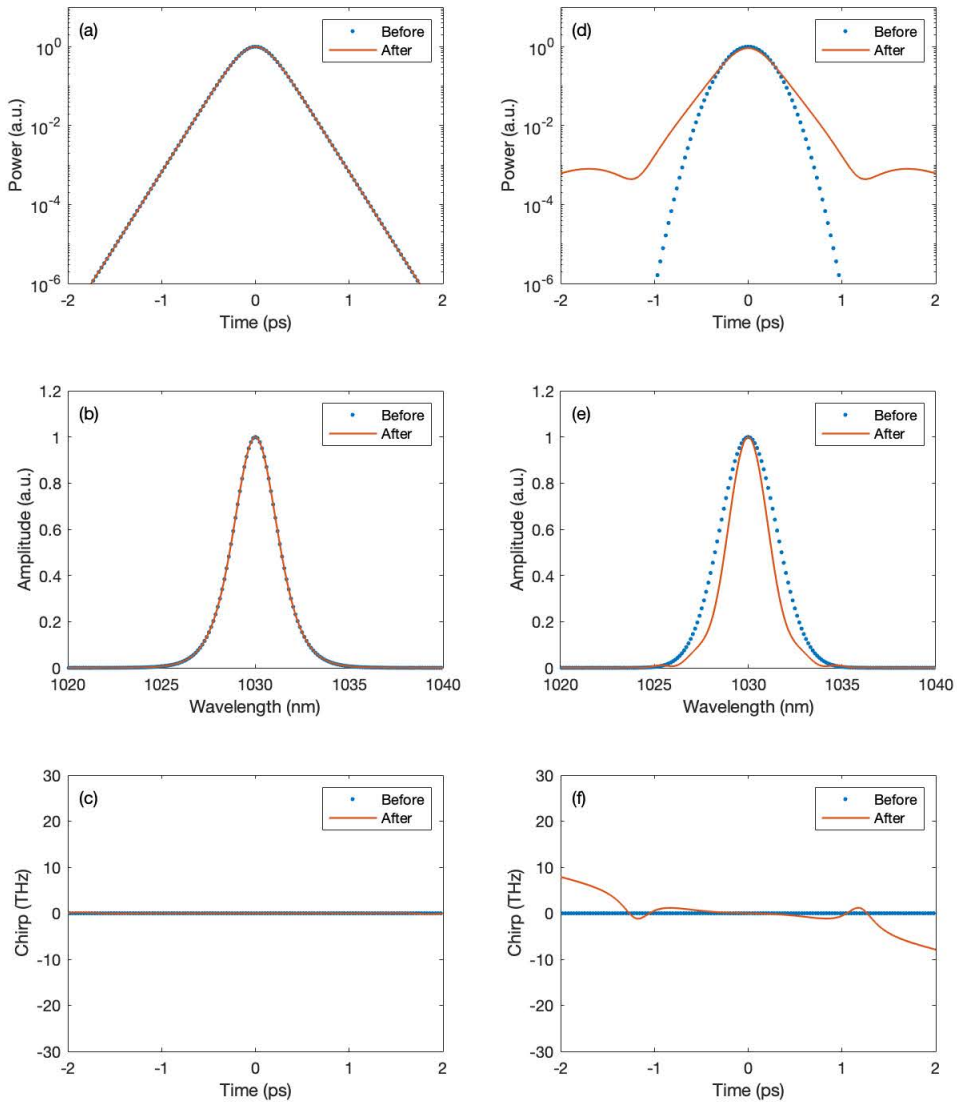

Figure 2.4: Soliton evolution. Dotted blue lines represent the initial pulse, and solid orange lines represent the pulse after propagation. (a, b, c) evolution of an initial fundamental soliton. The pulse does not change at all because the initial soliton width and energy are precisely set according to equation 2.5; (d, e, f) evolution of a Gaussian pulse with the same energy and a similar width. As can be seen from the semi-log plot of the temporal shape, the pulse evolves to a $Sech^2$ shape at the expense of energy lost to dispersive waves. This decrease in the energy causes spectral narrowing and temporal broadening

2. Passive similariton[26]: under Kerr nonlinearity together with comparably strong positive dispersion, the temporal and spectral shapes of a pulse broaden while remaining generally smooth. A near-parabolic pulse broadens and flattens while preserving its shape; its shape evolves self-similarly. This self-similar solution behaves almost like an attractor: initial short pulses experience higher nonlinearity and spectral broadening so that, due to dispersion, their width broadens faster than initially wider pulses, and after a sufficient propagation length, different pulses with the same energy and initial bandwidth get roughly the same peak power. However, since this process is conservative, the details of the initial pulse shape and chirp are not dissipated, and the shape of the pulse after propagation is determined by its initial state.

3. Active similariton[27]: Passive similaritons can not be attractors because they evolve under strictly conservative processes. If a pulse experiences amplification, the evolution becomes dissipative since the pulse energy is not conserved. Indeed, amplification results in the similariton attractor, where the pulse shape is parabolic and grows self-similarly. Any initial input pulse will evolve asymptotically towards an exact similariton. The only initial pulse parameter that influences the asymptotic behavior is the initial pulse energy.

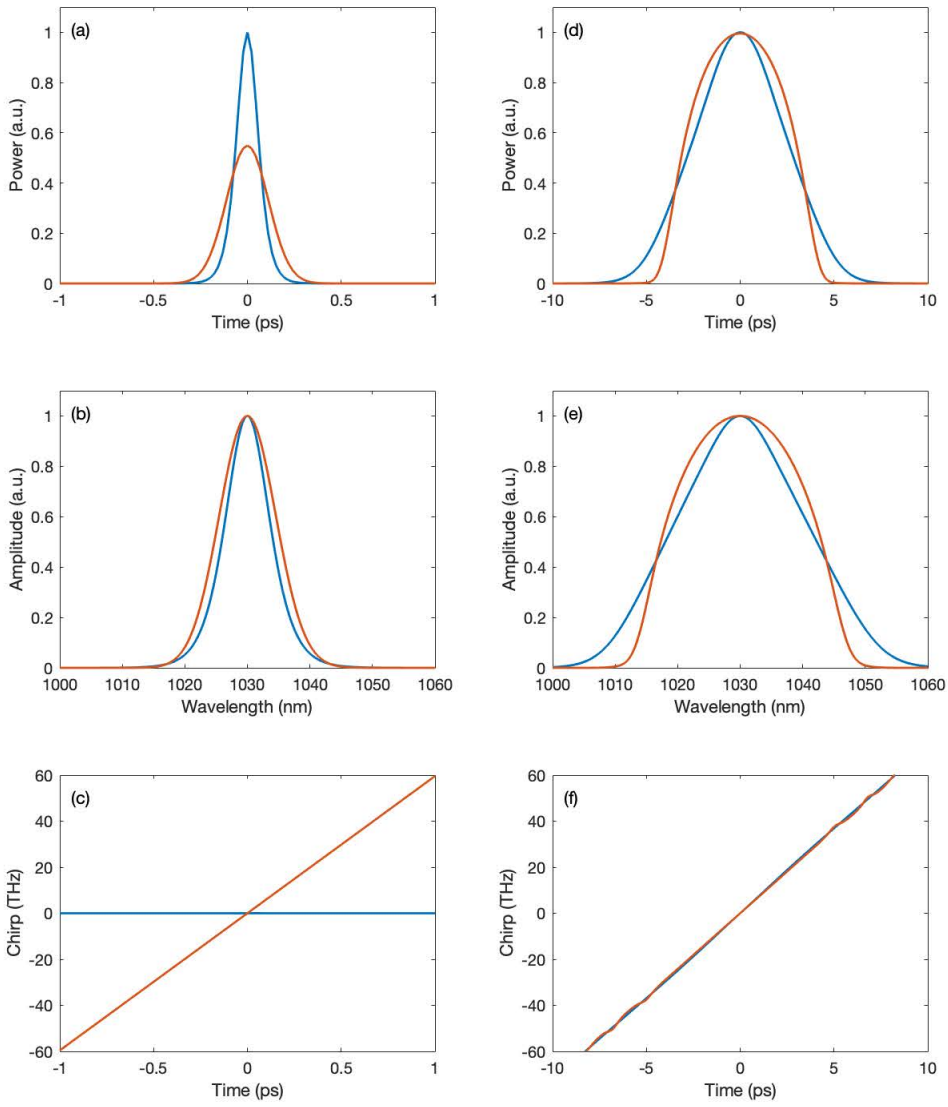

Figure 2.5: The evolution of two different pulses under Kerr nonlinearity and positive dispersion. Blue lines represent an initial transform-limited $sech^2$ pulse, and orange lines represent a Gaussian pulse with the same energy, and roughly the same spectral width chirped to twice the pulse duration. (a, b, c) the state of the two pulses before the evolution; (d, e, f) the state of the two pulses after the evolution. After this evolution, the pulse durations, peak powers, and chirps become similar. Also, the initial chirped Gaussian becomes closer to a parabola, and both pulse shapes become very similar to their respective spectra

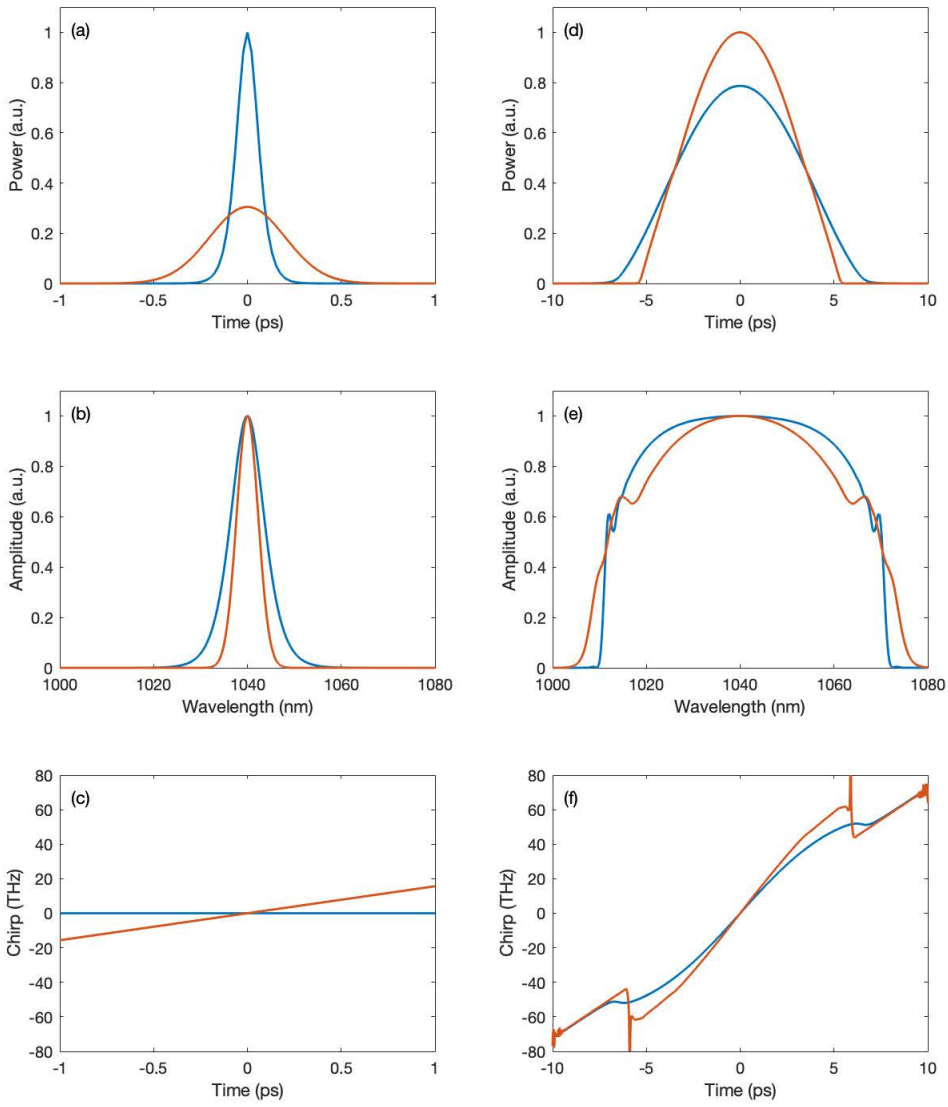

Figure 2.6: Pulse evolution towards the active similariton attractor. Blue lines represent an initial transform-limited initial $sech^2$ pulse, while the orange lines represent a Gaussian pulse with the same energy and half the spectral width chirped to four times the temporal width. (a, b, c) the states of the pulses before active similariton evolution; (d, e, f) the states after active similariton evolution. The very different pulses evolve towards the similariton attractor, acquiring a parabolic temporal shape with similar temporal and spectral widths and similar chirps.

Spectral filtering: The effect of spectral filtering depends on the input pulse and filter width; cutting a highly chirped pulse in the spectral domain cuts it in the time domain as well. A transform-limited pulse, on the other hand, broadens due to spectral filtering. Spectral filtering is a highly dissipative process; a sufficiently narrow filter determines the output pulse shape as the Fourier transform of the filter shape, almost regardless of the input pulse shape and spectrum. In this extreme case, the only information preserved by the filter is the filtered pulse energy and temporal position. Note that gain media typically effect wide spectral filtering due to their limited gain bandwidth. Figure 2.7 demonstrates the effect of narrow spectral filtering.

Saturable absorption: Historically, saturable absorbers were materials whose absorptivity decreases with intensity. This process transmits the peak of a pulse and attenuates wings, pedestals, noise and continuous wave. With high gain, this allows mode-lock pulses to grow from noise ripples by imposing lower loss on them compared to the lower-intensity background. Then after the pulse grows, it saturates the gain such that noise ripples feel a net loss and decay. Different combinations of optical elements can act as saturable absorbers. The most common of these are interferometric saturable absorbers, where Kerr nonlinearity imparts a phase shift that determines the loss at a subsequent interferometric element. In this case, the transmission depends sinusoidally on the power [28, 29].

Other pulse propagation processes become significant with very short pulses. These include self-steepening (dependence of group velocity on optical intensity), Raman scattering (frequency shift due to interactions with optical phonons), and higher-order dispersion (nonlinear dependence of group velocity on frequency). We will encounter these processes only briefly and rarely.

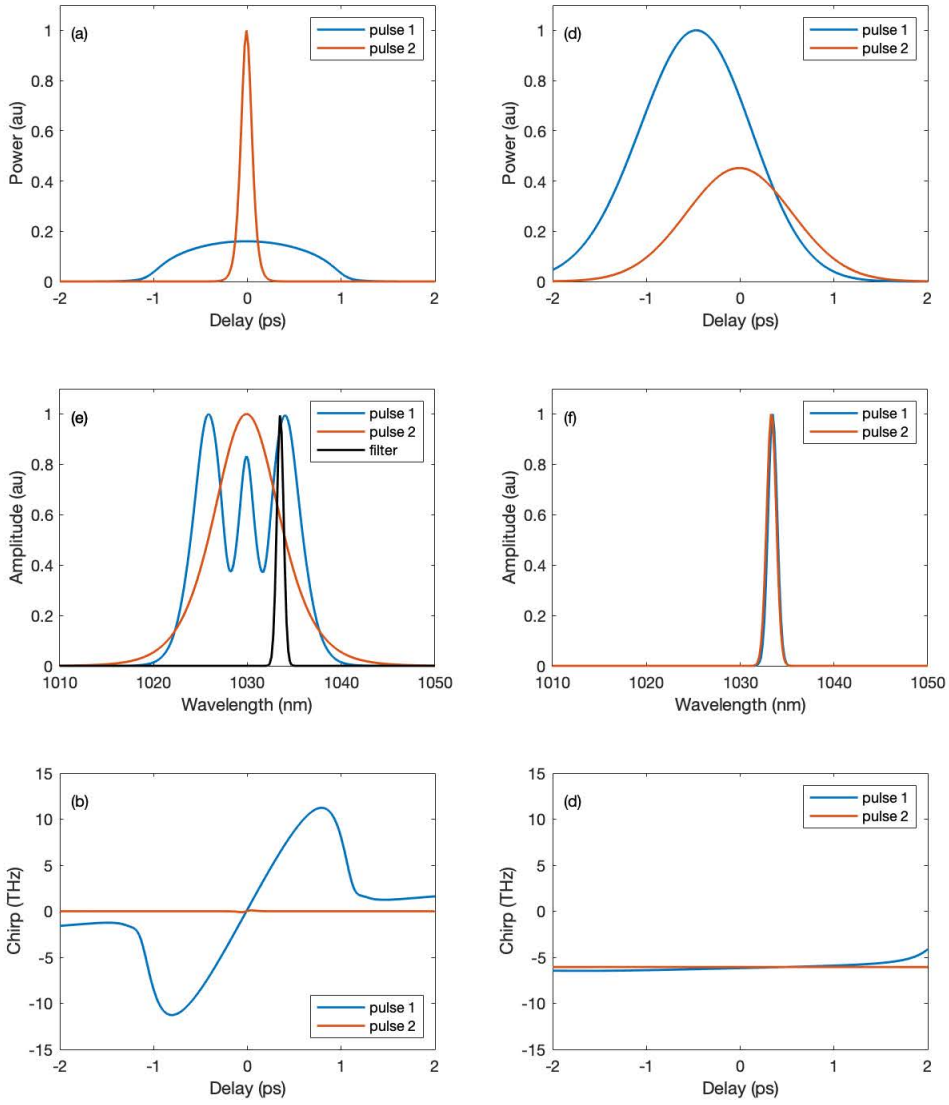

Figure 2.7: The effect of narrow filtering. The orange and blue lines represent two very different pulses. (a, b, c) the states of the pulses before filtering. The narrow black Gaussian at ∼1035 nm is the spectral filter; (d, e, f) the state of the pulses after filtering. Due to the small width of the filter, both pulses are nearly identical to a transform-limited Gaussian, and they differ only in energy, according to the spectral power at the filter wavelength. Note also the temporal shift experienced by the blue pulse after filtering. This is caused by the initial chirp.

2.3 Regimes of Mode-lock

A mode-locked cavity involves some of the processes discussed above together with linear amplification and losses. It is commonly modeled by a variant of the so-called Ginzberg-Landau equation [30] which takes all the processes above into account:

$$\frac{1}{T_R}\frac{\partial A}{\partial t} = gA + (\frac{1}{\Omega} - i\frac{\beta_2}{2})\frac{\partial^2 A}{\partial \tau^2} + (\alpha + i\gamma)\left|A\right|^2 A + \delta\left|A\right|^4 A, \tag{2.6}$$

where the α and δ terms are the first and second Taylor expansion terms of the transmission of the saturable absorber, the $\frac{1}{\Omega}$ term represents the spectral filtering, g is the net gain and T_R is the cavity roundtrip time. All of the parameters in this equation are averaged over the different elements in the cavity. Therefore, with this model, the pulse is taken to experience all the processes at all parts of the cavity at the same time. With this model, a pulse is considered mode-locked if the complex amplitude, $A(\tau, t)$ is a stable solution to this equation.

In actual lasers, these processes are concentrated at different elements in the cavity. In modern fiber lasers, the change experienced by a pulse in a single pass through each element in the cavity is typically so large that mixing and averaging these processes does not accurately model the laser dynamics. Instead, we should think of a roundtrip through the laser cavity as a periodic concatenation of these processes. A roundtrip through the cavity acts as a complex nonlinear map that evolves the pulse in discrete roundtrips. Then, a pulse is considered mode-locked if its energy and temporal and spectral shapes are at a stable fixed point of this map.

Mode-locked lasers with different combinations of the pulse evolution processes above are considered to be different regimes of mode-locking as they involve qualitatively different pulse-shaping dynamics. The following are the known mode-lock regimes so far:

Soliton: Soliton shaping radiates dispersive waves, which are attenuated by a saturable absorber, turning the soliton into a true attractor. However, the periodic changes in the pulse energy or optical properties experienced by the

pulse as it travels around the cavity displace the pulse from the fixed point of the fundamental soliton so that the soliton radiates dispersive waves every roundtrip.

Dispersion-managed soliton[10]: In this regime, a positive dispersion section is introduced to the soliton laser so that the pulse stretches and compresses significantly every roundtrip. Due to the stretched pulse duration, the peak power decreases, modifying the interaction with the saturable absorber. For this reason, dispersion managed solitons tend to have higher energy than fixed solitons.

Similariton[11]: In this regime, the pulse propagates as a passive similariton through most of the cavity, then experiences amplification and mild filtering (due to gain bandwidth), linear loss, saturable absorption, and partial dispersion compensation. These processes return the pulse back to the beginning of passive self-similar propagation. Disturbances in the initial state of passive similariton propagation translate to the wings of the pulse rather than the peak power. The wings are attenuated by spectral filtering and saturable absorption, making the passive similariton a true attractor.

Dissipative soliton[12]: This regime involves large positive dispersion with no significant dispersion compensation. The pulse grows in duration and spectrum due to dispersion and Kerr nonlinearity. Then, a bandpass filter, commonly with sharp edges, cuts the pulse in time and spectrum every roundtrip. The delay between the spectral components within the filter band is stabilized against dispersion by Kerr nonlinearity, which compresses newly generated frequencies within the same pulse envelope. Saturable absorption starts mode-locking from noise then attenuates background noise.

Amplifier similariton[14]: Here the pulse evolves towards a similariton within a long gain fiber every roundtrip. A narrow filter is placed after the gain in order to reset the bandwidth of the pulse and to pre-shape the pulse close to the similariton attractor even before entering the gain fiber. Saturable absorption starts mode-locking from noise and attenuates background noise.

Soliton-similariton[13]: As in the amplifier similariton regime, the pulse evolves

to the similariton attractor within the gain fiber. After the similariton evolution, the pulse passes through a spectral filter followed by negative-dispersion fiber, where the pulse compresses and evolves into a soliton. The compressed soliton then reseeds the active similariton evolution similarly to the effect of the narrow Gaussian filter in the amplifier similariton regime.

2.4 Multiple pulsation

A single pulsing laser hosts one pulse in its cavity and outputs one pulse per cavity period, where a cavity period is the time of flight of a pulse round the cavity; the output is a regular pulse train at a repetition rate of inverse the cavity period.

Multiple pulsation is the situation where the optical energy is divided among multiple, usually identical, pulses hosted simultaneously in the cavity, and the output still retains the periodicity with the cavity period but with multiple pulses in it.

What is the general dynamics governing the number of pulses and their energies, and how can we control it?

At the opposite extreme, we see period-doubling, where the pulse energy changes periodically (figure 2.8) or even chaotically [31] from one roundtrip to another; the output does not follow the period of the cavity itself. Moreover, this behavior can occur together with multiple pulses in the cavity [32]!

What are the dynamics governing period-doubling, and what relation does it have with multiple pulsation?

One usually finds multiple coexisting pulses adopting stable patterns, where their temporal spacings are fixed. They may be as close as overlapping or up to orders of magnitude further apart. This is evidence of long-distance pulse interactions. What mediates these interactions, and how do they result to the experimentally observed patterns? Do these interactions involve the pulse shaping

processes we discussed above?

In particular, the long-range interactions allow the pulses to adopt equidistant temporal spacings so that the output shows a regular pulse train with a repetition of a harmonic of the fundamental repetition rate of the cavity. The laser is said to be n^{th}-order harmonically mode-locked (HML) if it outputs n equidistant pulses per cavity period. We can judge the regularity of the pulse train by plotting the Fourier spectrum of the output power (at radio frequencies, RF); an imperfect HML involves radio frequency components other than the n^{th}-order harmonics. The so-called supermode suppression ratio (SSR), which is illustrated in figure 2.9, quantifies this imperfection.

What determines the possibility of an HML state and fixes its SSR? Is it possible to manipulate these long-range interactions for other (non-equidistant) patterns?

The following chapters address these questions.

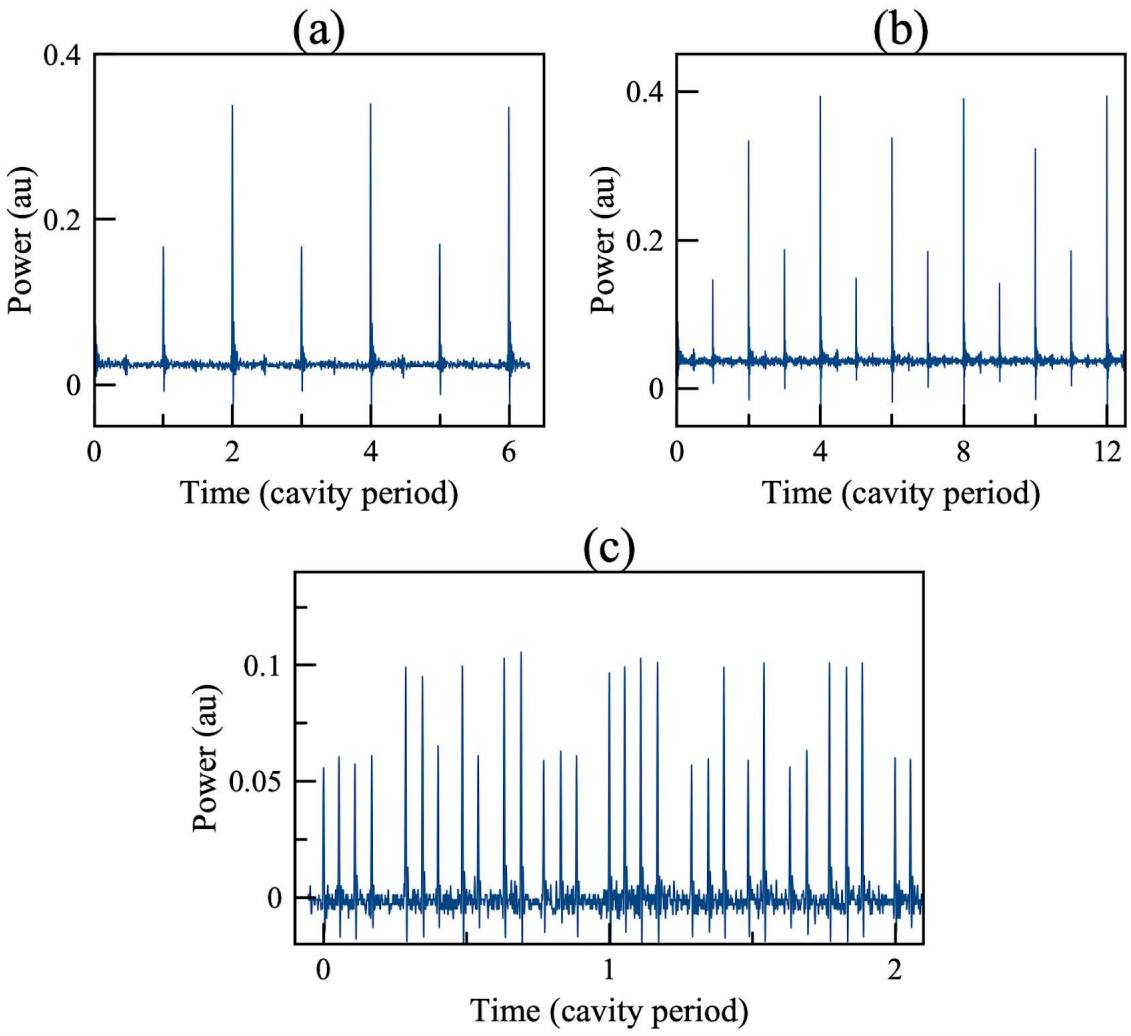

Figure 2.8: Period-doubling mode-locked states. (a): period-doubled single-pulsing output. (b): period-quadrupled single-pulsing output. (c): period-doubled multipulsing output

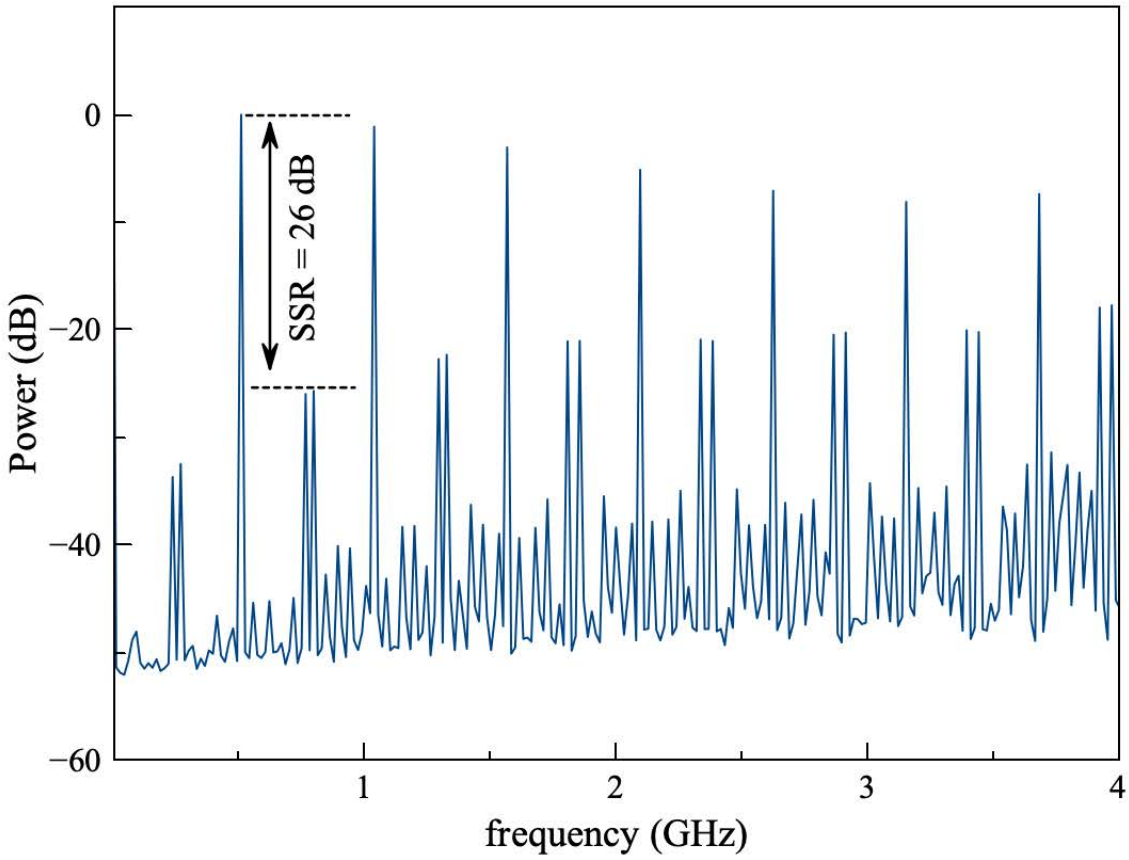

Figure 2.9: SSR shown on the RF spectrum of a 35^{th}order HML state of our oscillator. SSR is conventionally measured between the strongest RF line, corresponding to the repetition rate of the HML state, and the second-strongest between zero and twice the repetition rate.

Chapter 3

The Mamyshev Oscillator

This chapter discusses the Mamyshev oscillator, which can be considered a variant of the amplifier similariton or dissipative soliton regimes with the so-called Mamyshev regenerator as an alternative to the saturable absorber. First, we introduce the working principle of the Mamyshev regenerator and compare it to saturable absorbers. In section 2, we discuss and connect the ideas of pulse birth, noise attenuation, and kinetic stability with the Mamyshev oscillator as an extreme example. This discussion predicts a large variety of Mamyshev oscillator behaviors, for which we review the literature in section 3. In section 4, we present experimental details of our Mamyshev oscillator setup.

3.1 Mamyshev regeneration as a saturable absorber

The Mamyshev regenerator was first developed as a tool for optical data regeneration [33]; it restores attenuated pulses and strongly attenuates background noise picked by the optical signal in its transmission. By discriminating against continuous wave and background noise, Mamyshev regenerators achieve the essential purpose of saturable absorbers.

The working principle of the Mamyshev regenerator is illustrated in figure 3.1. Propagation through a nonlinear medium is sandwiched between two spectral filters with negligible spectral overlap; a sufficiently high-energy pulse passing through the first filter will experience high enough Kerr nonlinearity for its spectrum to broaden and reach the wavelength of the second filter. Then, part of the pulse energy passes through the regenerator and, with amplification, the pulse can be restored. Conversely, continuous wave and noise ripples passing through the first filter do not experience sufficient spectral broadening to reach the subsequent filter, and their transmission through the regenerator is, consequently, orders of magnitude lower than that of pulses. The regenerator is turned to an oscillator by propagating the output of the second filter through another nonlinear amplifier leading the pulses back to the first filter, as shown in figure 3.1.

As discussed in chapter 2, it is not enough for a regenerator or a saturable absorber to favor pulsation over continuous wave for stable mode-locking; a roundtrip propagation through the oscillator must also map all pulse parameters back to themselves. This condition is easily met in a Mamyshev oscillator because, as discussed in chapter 2 (see figure 2.7), the filters tend to enforce their own shape on the pulse, almost regardless of the processes occurring in the amplification arms as long as those processes result in an appropriate amount of spectral energy at the wavelength of the filters.

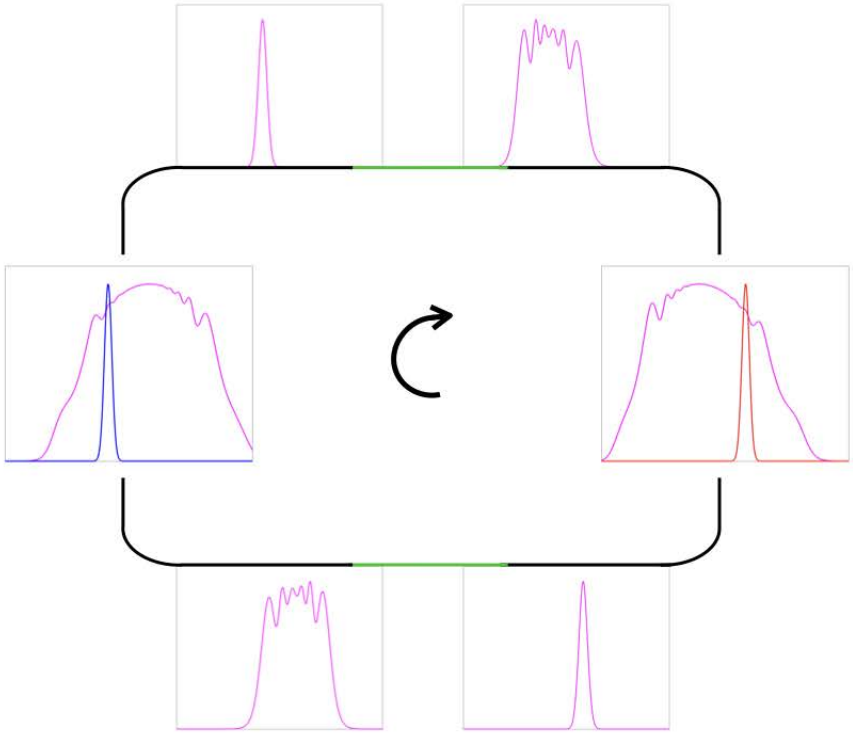

Figure 3.1: illustration of the working principle of a Mamyshev oscillator. There are two non-overlapping spectral filters. After each filter, the pulse experiences gain to compensate the filtering and other losses, and nonlinearity, for its spectrum to broaden and reach the next filter. With insufficient nonlinearity, the light can not survive both filters.

3.2 Seeding, Noise and Kinetic Stability

Commonly, mode-locked pulses grow out of noise ripples on continuous wave background. This growth occurs because saturable absorbers apply less loss on the noise ripples compared to the background. Then, as these noise ripples grow to pulses, they lower the gain by consuming more power. This way, a continuous wave background will experience less gain than loss and decay.

This process is not possible in most Mamyshev oscillators due to their prohibition of noise and continuous wave background. A noise ripple does feel slightly less loss than a uniform background, but, commonly, neither the continuous wave nor the noise ripples on it are allowed. Even if the filters are brought to a distance that allows continuous wave *and* imposes less loss on noise ripples, the net gain felt by these noise ripples will be so low that they disperse before growing into pulses. This is common in oscillators with whose saturable absorbers are weak at low powers [34], especially with positive dispersion [35]. For this reason, pulses in a Mamyshev oscillator are commonly started by external seeding, whereby pulses are injected from an external source. Once the seeding is done, the pulses stabilize inside the Mamyshev oscillator, and the seed source is no longer required.

The requirement of external seeding implies kinetic stability of most attractors; for example, a noise ripple cannot grow to a pulse and change the number of pulses or survive for long enough to collide with a pulse and change the temporal organization of the pulses. Noise-induced transitions are highly unlikely. To induce such transitions experimentally, we either bring the filters close to each other to allow background noise or inject low-energy seed pulses. In practice, kinetic stability allows a plethora of indefinitely stable states that exist at the same cavity parameters. Without kinetic stability, some attractors may not be occupied for long enough to be even observed. This is in perfect analogy with metastable states in thermodynamics, where the lifetime of the metastable state decreases dramatically with temperature. A mode-locked Mamyshev oscillator is a near-zero temperature system.

3.3 Mamyshev in the literature

The preceding discussion suggests that every attractor in a typical Mamyshev oscillator should enjoy long-term stability. Indeed, a large number of such states are observed and reported in the literature. For example, in [15], simulations revealed stable pulses with different energies at the same cavity parameters, in addition to identical pulses coexisting simultaneously in the cavity and period-doubled states. Some of these phenomena were reported in the experimental study of [19], where the transition between different states does not occur without external seeding; the number of pulses didn't change upon increasing the pump power. In [36], long-term stable harmonic mode-locking with 48 dB of supermode suppression ratio was reported. These reports support the kinetic stability of Mamyshev oscillators.

At the opposite extreme, [37] demonstrated a km-long Mamyshev oscillator that spontaneously harmonically mode-locks from noise. In this case, the nonlinear propagation arms are so long that even noise ripples can experience sufficient spectral broadening to evolve to pulses. The output of such a laser is highly noisy, and kinetically stable states are unlikely.

Mild pulse starting procedures have also been reported. These include pump modulation [38], slowly increasing the filter offset [16], injecting high intensity noise [39] or a combination of these techniques [40].

It is worth noting that Mamyshev oscillators are also considered ideal for single-pulsing operation. This is due partly to their stability and partly to their ability to generate short pulses with high energies. For this goal, the spectral filtering and amplification arms are designed to support amplifier similariton propagation as much as possible [39, 17].

3.4 Our Mamyshev Oscillator

A detailed schematic presentation of our system is presented in figure 3.2a: two all-polarization maintaining amplification arms with normal dispersion, separated by two Gaussian spectral filters with adjustable central wavelengths. The defining feature in our laser is that one of the two amplification arms is designed to support Kerr nonlinearity-dominant pulse propagation. We, therefore, name it the "Kerr arm". The other amplification arm supports amplifier similariton propagation to achieve short pulse durations. We, therefore, name it the "similariton arm".

Kerr-dominant pulse propagation is achieved by starting from a narrow filter so as to suppress the effect of dispersion. The pulses pass through a short, large-core (10 µm) fiber to decrease spectral and temporal broadening before amplification. Then, amplification is delivered as abruptly as possible, and the pulses pass to a small-core (6 µm) fiber to promote Kerr nonlinearity. The dominance of Kerr nonlinearity in this arm is ultimately limited by the pulse energy and the resulting spectral width, which strengthens dispersion towards the end of the arm.

Pulses are seeded externally. In our setup, the seed comes from an all-normal dispersion oscillator [14, 12] mode-locked by nonlinear polarization evolution [28] with a repetition rate of 40 MHz. The seed pulses see the same filter as the cavity pulses even at their entrance, making our results rather insensitive to the choice of the seed source. It's possible to start our Mamyshev oscillator without an external seed by modulating the pump of one of the amplification arms or modulating the signal at the repetition rate of the cavity with an acousto-optic modulator (AOM) while increasing the filter offset. However, these techniques allowed only poor control over the resulting state.

In our experiments on pulse interactions, we implemented a secondary loop that takes the laser's output from a polarization beam splitter (PBS) after the HP arm. It then passes the output pulses through a polarization-maintaining fiber and re-injects them back to the cavity by reflection off the same PBS with

an orthogonal polarization, so they join the cavity signal. Because these delayed-reinjected pulses have orthogonal polarization, they do not survive the polarizing isolator after the Kerr arm. Hence, they only drive pulse interactions within the Kerr arm. The secondary loop is shown in figure 3.2b.

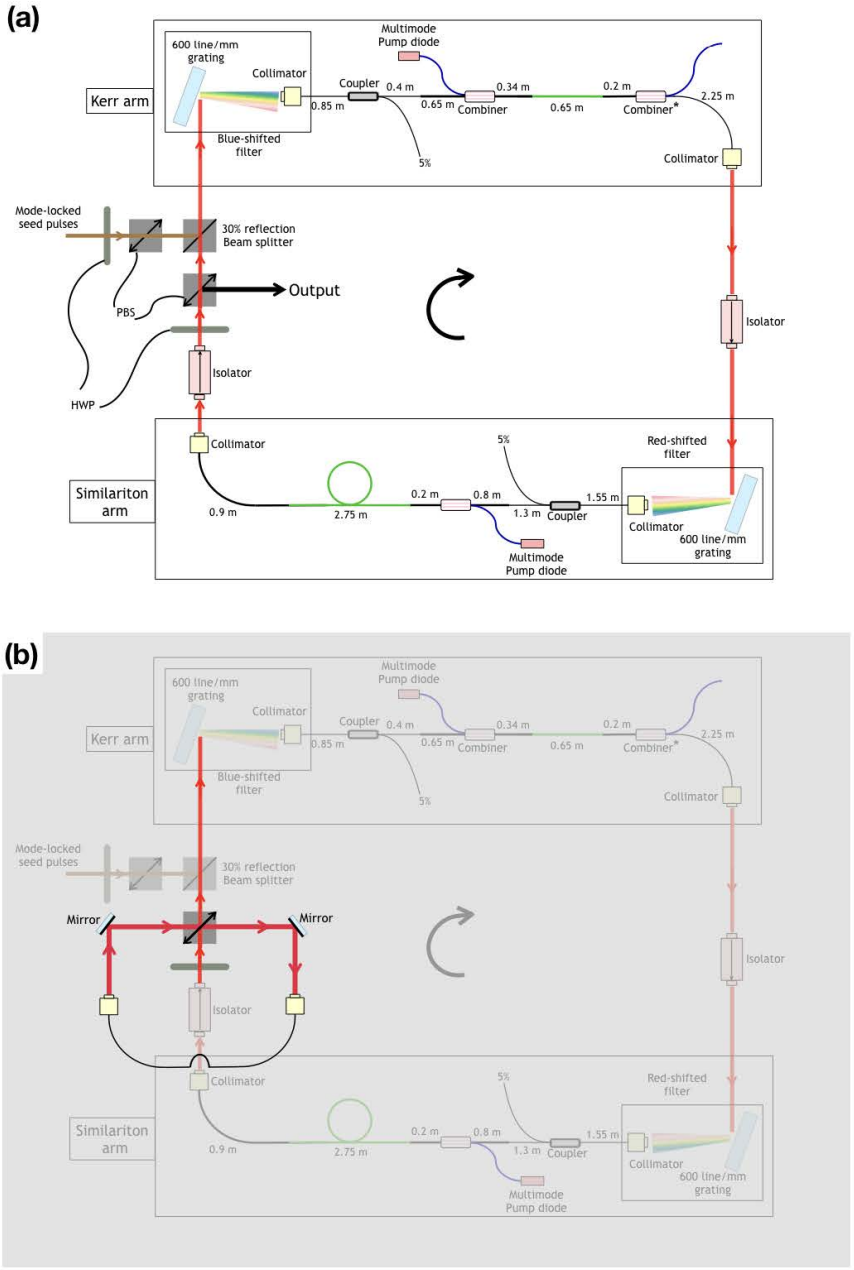

Figure 3.2: (a) detailed schematic representation of our Mamyshev oscillator. The green lines represent Yb-doped gain fibers with a $10\mu m$ core diameter; the thick (thin) black lines represent passive fibers with $10\mu m$ ($6\mu m$) core diameter; the thick blue lines represent multimode fibers carrying the pump. The combiner with an asterisk is used as a pump stripper and a mode-field adaptor. PBS: polarizing beam splitter; HWP: half waveplate; (b) detailed schematic representation of the orthogonally polarized secondary loop. The cavity is shaded to highlight the elements of the secondary loop. The secondary loop is used for pulse interaction experiments only

Chapter 4

Pulse Energy Quantization and the Energy Map

In this chapter, we focus on the dynamics governing the number of pulses. Section 1 presents the control procedure to achieve any desired number of pulses and related experimental observations. In section 2, we review the literature for experiments and theories concerning multiple pulsation. Multiple "quantization mechanisms" and dynamical models are discussed. Section 3 presents our quantization mechanism and models its dynamics using a simple equation we term "the energy map." This model explains the control procedure and the experimental observations outlined in section 1.

4.1 Control procedure and experimental observations

Achieving a particular desired number of pulses is done by following two steps:

1. We set the filter offset to 3-5 nm and increase the pump powers well beyond the powers necessary to support the desired number of pulses. At these

settings, we temporarily block the cavity, preventing lasing while the seed is allowed into it. If the seed pulse energy is appropriate, after unblocking the cavity, a large number of pulses is seeded, and the seed is unlikely to change the number of pulses afterward.

2. We decrease the number of pulses one-by-one by slowly increasing the filter offset and/or decreasing the pump powers until we reach the desired number of pulses.

The result of the first step alone is not well-controlled; even at the same settings, the laser admits multiple numbers of pulses. Seeding with a high repetition rate (40 MHz) of seed pulses does not lead to a precise number of pulses. However, the number of pulses seeded generally increases with the pump powers.

Pulse death is then employed to reach the desired number of pulses after seeding. Figure 4.1 demonstrates the process of pulse death by increasing the filter offset. Increasing the filter offset demands broader spectra, which increases the minimum required pulse energy and decreases the maximum allowed number of pulses at the same pump powers; if we move the filters outside their respective spectra, one or more pulses die. The death of some pulses increases the gain felt by the remaining pulses, increasing their energies and broadening their spectra to reach the distant filters. Similarly, decreasing the pump powers kills pulses by decreasing their spectral width, with pulse death leaving more energy to the remaining pulses and broadening their spectra.

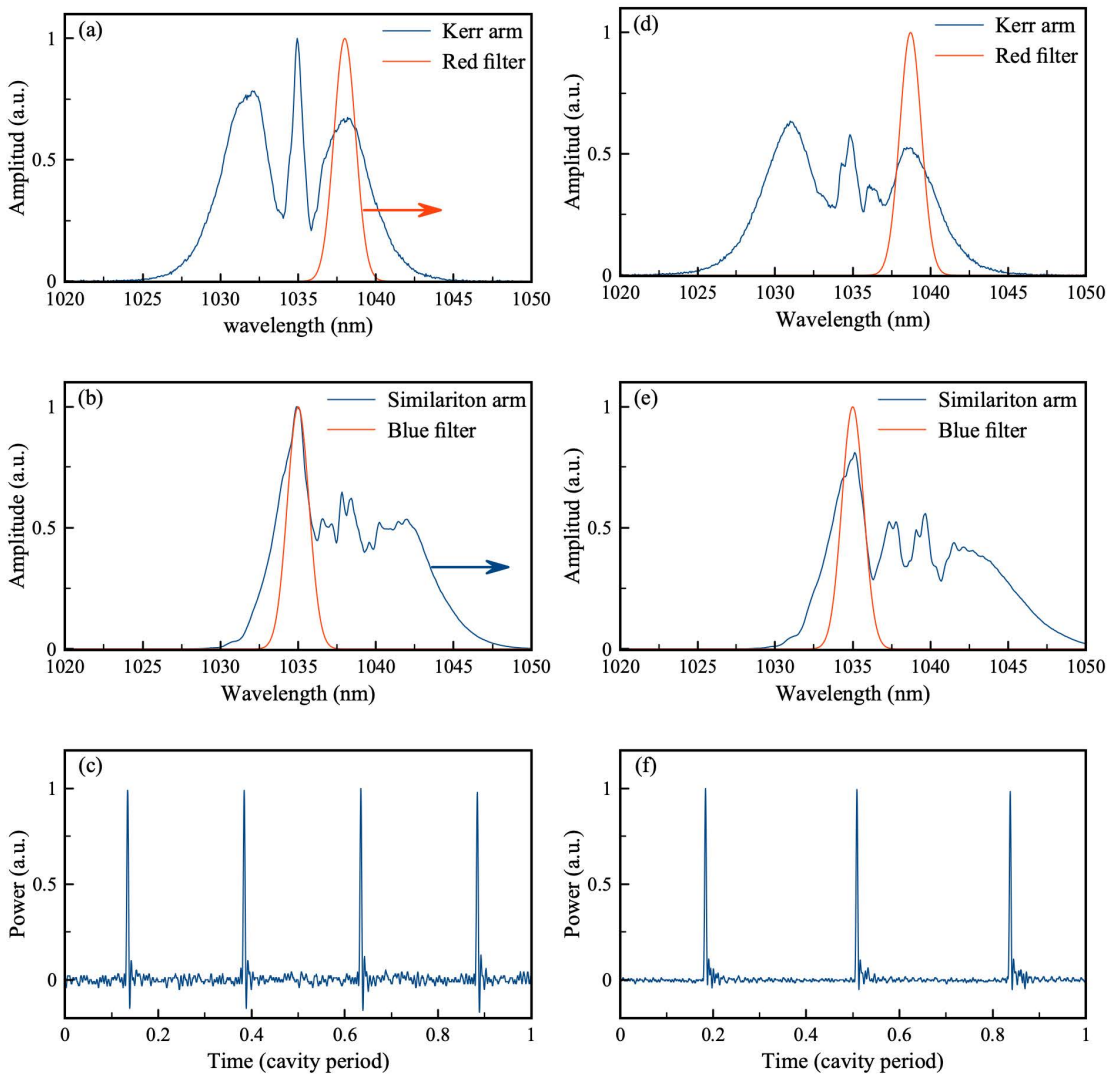

Figure 4.1: Pulse death by increasing the filter offset: (a, b) the spectra and the following filters before increasing the filter offset; the arrows show where the filter after the Kerr arm and the spectrum of the similariton arm are moved when the filter offset is increased, (c) oscilloscope trace showing four pulses in a cavity roundtrip time, (d, e) the spectra and the following filters after increasing the filter offset, (f) oscilloscope trace showing three pulses in a roundtrip time. Increasing the filter offset decreased the number of pulses and increased their spectral widths.

This procedure for pulse death suggests that a multi-pulsing state is stable as long as the filters are within the spectra and the loss due to filtering is low. Figure 4.2 shows a counter-example where the state is stable while the red filter is at the wing of the Kerr arm spectrum. *Decreasing* the filter offset destabilizes this multi-pulsing state, resulting in period-doubling, which is a state where the pulses take two different pulse energies that alternate every roundtrip. To get this result, we specifically adjusted the pump powers so that after decreasing the filter offset, one filter met a steep "outer" slope (a slope that falls away from the central wavelength) and the other filter met a steep inner slope. By repeating this process, we see that the pattern of high and low energies within a roundtrip is random. In other words, the "phases" of these oscillations for different pulses are uncorrelated. We also observed periodic states with longer periods and, possibly, chaotic states, depending on the precise filter offset and pump powers. However, distinguishing between these higher-period and chaotic states is difficult because they live in very small ranges of pump powers, so the laser jumps between these states very frequently with pump fluctuations. For this reason, we focused only on the period-2 state.

Additionally, by carefully adjusting the filter positions relative to the spectra, we get coexisting pulses with different but constant energies. Figure 4.3 shows the onset of different pulses with filter adjustment. In order to produce such different-energy pulses, both filters are positioned at steep outer slopes in the spectra. In this example, too, we destabilized the multi-pulsing state by decreasing the filter offset. The resulting different-energy pulses have quite different speeds so that they collide in a fraction of a second. Then they either appear to pass through each other or become closely bound, or merge, resulting in one high-energy pulse. Pulse merging is the only process we observed to change the number of pulses while the filter offset and pump powers are sufficient, and the seed is blocked. Otherwise, the number of pulses remains stable indefinitely.

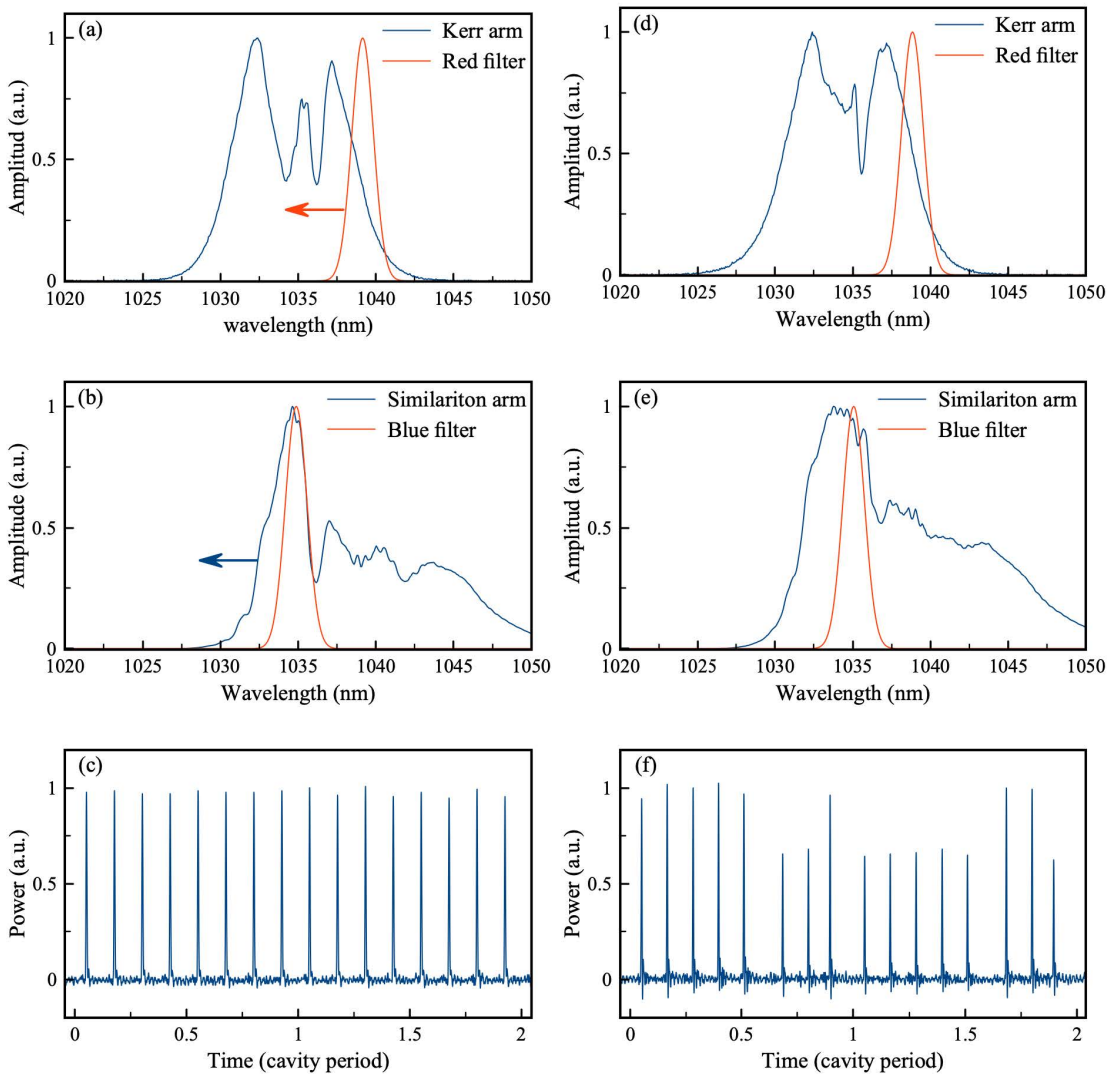

Figure 4.2: Period-doubling upon decreasing the filter offset. (a, b) the spectra and filters before decreasing the filter offset. The arrows show the direction where the red filter and the spectrum of the similariton arm are moved when decreasing the filter offset, (c) oscilloscope trace showing eight pulses per cavity roundtrip with constant pulse energies. (d, e) the spectra and filters after decreasing the filter offset. The spectra appear to be smeared as they are superpositions of different spectra from pulses with different energies, (d) oscilloscope trace showing eight pulses that are period-doubled. Pulses with high energies in the first cavity period have lower energies in the second cavity period and vice versa.

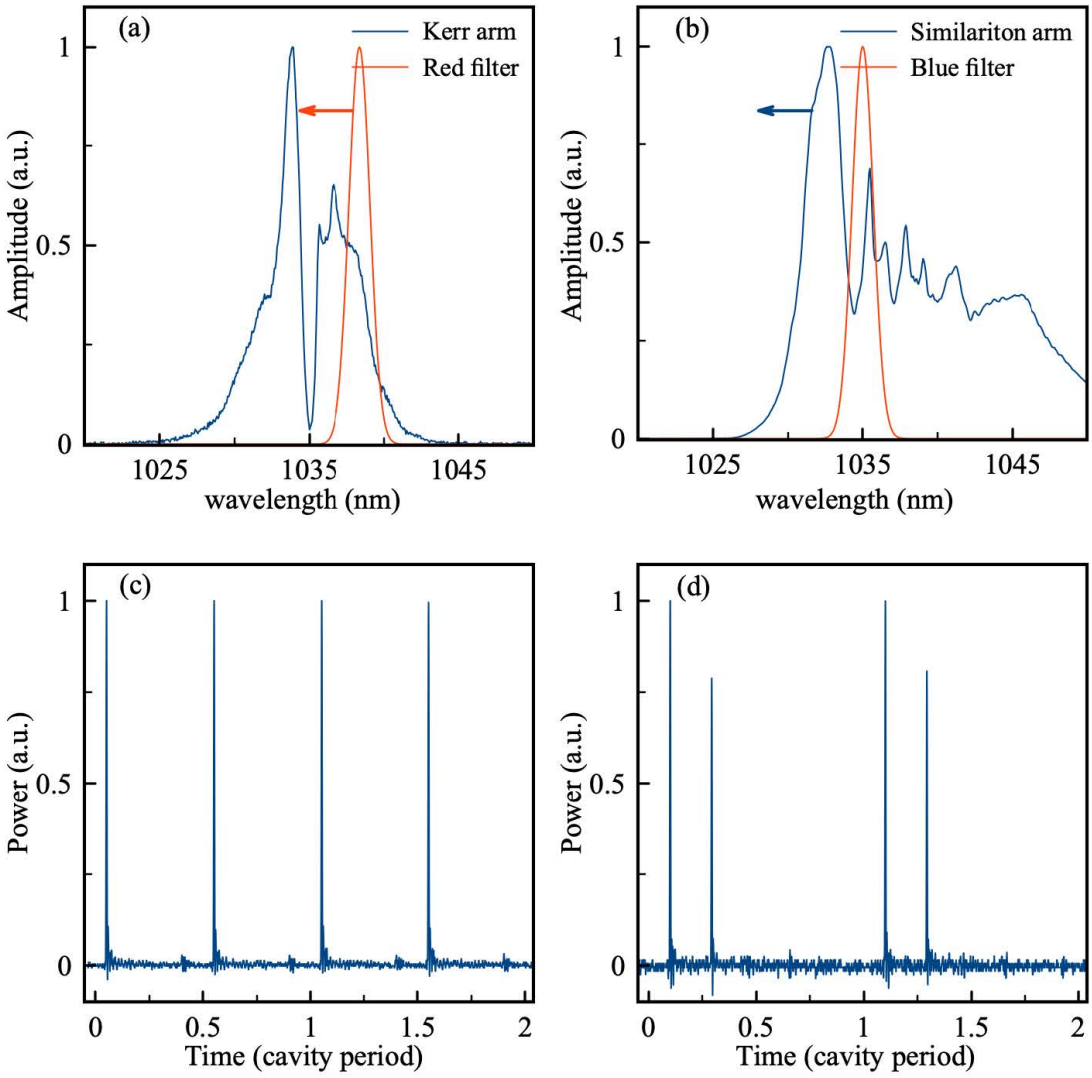

Figure 4.3: Different energy pulses produced by filter adjustment. (a, b) The spectra and filter positions just before reaching the state of different energy pulses. The arrows show the directions where the red filter is moved, (c) the pulse train before reaching the two-energies state showing two identical pulses per roundtrip. (d) a snapshot of the pulse train after reaching the state of different energy pulses. The two pulses are moving relative to each other.

4.2 Multiple pulsation in the literature

Multiple pulsation has been reported in soliton lasers [6, 5, 41], Dispersion-managed soliton lasers [42, 43, 44], similariton lasers [45], amplifier similariton lasers [46] and dissipative soliton lasers [47, 48]. Moreover, multiple pulsation is seen with all types of saturable absorbers, such as real saturable absorbers [49, 6], interferometric saturable absorbers [5, 41] and in Mamyshev oscillators [36, 19]. These references also cover different gain materials, waveguides, and cavity shapes. To our knowledge, no mode-locked laser is immune to multiple pulsation when pumped sufficiently. In all of these experimental reports, the pulses appear identical. To our knowledge, our laser is the second to produce coexisting non-identical pulses after [19].

Most of the research regarding multiple pulsation merely aims to raise the pulse energy after which multiple pulsation starts, rather than controlling its dynamics. In this regard, lasers with large waveguides such as solid-state lasers and photonic crystal fiber lasers [50] tend to support higher pulse energies. Similarly, lasers with long pulse durations such as similariton and dissipative soliton lasers tend to support higher pulse energies compared to soliton lasers, where the pulse has a transform-limited duration. Moreover, most modes of nonlinear pulse propagation, especially the soliton, feature some sort of pulse splitting when subjected to excessive nonlinearity. From these tendencies, one might infer that multiple pulsation is caused by pulse splitting when the pulse suffers excessive nonlinearity in its propagation through the waveguide.

While this picture provides a possible mechanism for the *birth* of new pulses, it does not address the stability of the resulting multi-pulsing state. Before addressing the stability of the multi-pulsing state, It is useful to take a step back and consider analogical systems to identify the fundamental aspects of this problem. Essentially, a multi-pulsing mode-locked state is a coexistence between multiple entities that compete over the same resource. We find similar systems in Ecology and Economy. In Ecology, it has been shown through the Lotka-Volterra model [51] that competing species can coexist if the competition within a species

is stronger than the competition between different species. In other words, the growth of a species must inhibit its own further growth through a mechanism other than the depletion of the common resources. In political economy, it has been shown [52] that nonlinear taxation promotes competitive balance as opposed to monopolies. In this example, we regard the market demand as the common resource that feeds the competing businesses and the nonlinear taxation as the mechanism that inhibits further growth independently from resource depletion.

These analogical systems instruct us to look for mechanisms that apply a higher loss to pulses with higher energy. Such mechanisms may be collectively described as "pulse quantization mechanisms," a term that's vaguely associated with multiple pulsation in the literature. From [6] and [5], three families of quantization mechanisms can be inferred:

1. Emission of dispersive waves: In a real soliton laser, the gain, loss, dispersion, Kerr nonlinearity, and saturable absorption do not all act simultaneously but are generally concentrated at different elements in the cavity. This means that a soliton is perturbed periodically from its fundamental soliton shape. The recovery after each perturbation produces low-intensity dispersive waves, which are attenuated by the saturable absorber. The higher the pulse energy, the higher loss that the pulse suffers due to dispersive wave emission.

2. Over-driving the saturable absorber: The purpose of a saturable absorber is to apply a lower loss to high-energy pulses, as compared to continuous wave and noise ripples. This means that the saturable absorber is expected to resist the quantization mechanisms. However, this behavior does not persist for indefinitely high energies. For example, the loss through a real saturable absorber ideally approaches a constant at high powers. This allows other quantization mechanisms to result in multiple pulsation without resistance from the saturable absorber. Moreover, the loss through interferometric saturable absorbers depends sinusoidally on the power, which means that the pulses start feeling higher and higher loss beyond an optimum pulse energy.

3. Spectral filtering: The higher the pulse energy, the stronger the Kerr nonlinearity and, consequently, the wider the spectrum becomes. In the presence of a spectral filter, the wider the spectrum, the higher the loss. Moreover, even without placing a filter in the cavity, the gain itself acts as a spectral filter by amplifying the nonlinearly generated spectral components less than the spectral components at the central wavelength. As a result, increasing the pulse energy increases the loss.

To the best of our knowledge, there are no experimental reports of multiple pulsation where neither of these three mechanisms applies except for [37], where the gain is provided by the Raman process, which is nearly instantaneous so that the pulses don't compete over a common gain.

Period-doubling is not exclusive to our laser or separate from multiple pulsation; it is commonly observed in lasers with interferometric saturable absorbers with excessive pump powers just before the birth of a new pulse. In [32] for example, increasing the pump power leads to period-doubling, followed by the birth of a new pulse, followed by period-doubling (for all of the existing pulses), and so on... In [53], the birth of a new pulse is difficult and, so, increasing the pump power does not immediately result in multiple pulses. In this case, it is reported that, with increasing pump power, the pulse energy follows the so-called "period-doubling route to chaos" [20], a universal phenomenon. These reports indicate that period-doubling is related to the strength of the quantization mechanism and not particularly related to the mode-lock regime or any technical details in the cavity.

It is not readily clear how the quantization mechanisms result in this behavior because their action is often perceived in the context of continuous pulse evolution [54], in which the very existence of cavity periods is denied. In [47, 55, 53, 56], the evolution of the pulses is modeled by a map instead of a differential system. The dynamical variables are the pulse energies. Each step of the map represents the evolution of the pulse energies after one roundtrip through the cavity. In every roundtrip, the pulses are assumed to pass through a fast saturable gain and an interferometric saturable absorber, where they're assumed to have a fixed shape.

Despite its simplicity, this model produces multiple pulsation, period-doubling, and non-identical pulses. In the next section, we will improve, justify and adapt this model to our laser and use it to explain the phenomena in the previous section and their control procedures.

4.3 Our synthetic quantization mechanism

Let us consider the process of narrow filtering in our laser, illustrated in figure 4.4 (figure 2.7, repeated here for the reader's convenience). Two very different pulses are incident on the filter, yet the filtered pulses have nearly identical spectral and temporal shapes. The only major difference is in their energy. Therefore, given the pulse energy at the input of an amplification arm in our laser, the whole state of the pulse at the input is approximately determined. This, in turn, determines the spectral shape at the output of the arm, which determines the pulse energy transmitted through the subsequent filter, and so on.

Let us follow the evolution of the pulse energy along a roundtrip. Given the energy of the pulse at the output of the Kerr arm, which we name E_k, its spectrum is approximately determined so that the pulse energy after the subsequent filter can be approximated by a function, $\tilde{f}_{s,k}(E_k)$, that maps the energy at the output of the Kerr arm to that at the input of the similariton arm. Figure 4.5f shows our experimental measurement of this function. Following the filter, the pulse energy changes due to the gain provided in the gain fiber as well as the losses, such as output coupling. Then, we may write the pulse energy at the output of the similariton arm, E_s, as:

$$E_s = g_s \tilde{f}_{s,k}(E_k) \equiv f_{s,k}(E_k, g_s), \tag{4.1}$$

where g_s is the net gain in the similariton arm and $f_{s,k}(E_k, g_s)$ is a function that maps the pulse energy at the output of the Kerr arm to that at the output of the similariton arm, taking into account the effects of the filter and the net gain in the similariton arm. Similarly, the pulse energy at the output of the similariton arm determines the energy of the pulse when it arrives again to the output of the

Kerr arm:

$$E_k = g_k \tilde{f}_{k,s}(E_s) \equiv f_{k,s}(E_s, g_k), \tag{4.2}$$

where g_k is the net gain in the Kerr arm and the functions $\tilde{f}_{k,s}$ and $f_{k,s}$ map the pulse energy from the similariton arm to the Kerr arm.

Using equations 4.1 and 4.2, we can express the pulse energy as a function of itself in the previous roundtrip. Denoting the roundtrip number by n, the evolution of the pulse energy at the output of the Kerr arm can be expressed as:

$$E_{k,n} = f_{k,s}(f_{s,k}(E_{k,n-1}, O, g_s), O, g_k) \equiv f_k(E_{k,n-1}, O, g_s, g_k), \tag{4.3}$$

where f_k is the energy map when observing the pulse at the output of the Kerr arm and O is the filter offset, which we made explicit here to emphasize the dependence of the energy map on it.

In a typical gain material, the gain decreases with the total energy from all the pulses in the cavity. In the references we cited above, the gain is assumed to adapt instantly to any changes in the total energy, which is not physical. Unlike these references, we have taken the gain in the two arms as *parameters* despite the fact that they evolve according to the total energy in the cavity. This is because the gain evolves in a much longer time scale than the pulses. By taking the gain as a parameter, the energies of different pulses are decoupled from each other, resulting in this single-dimensional energy map.

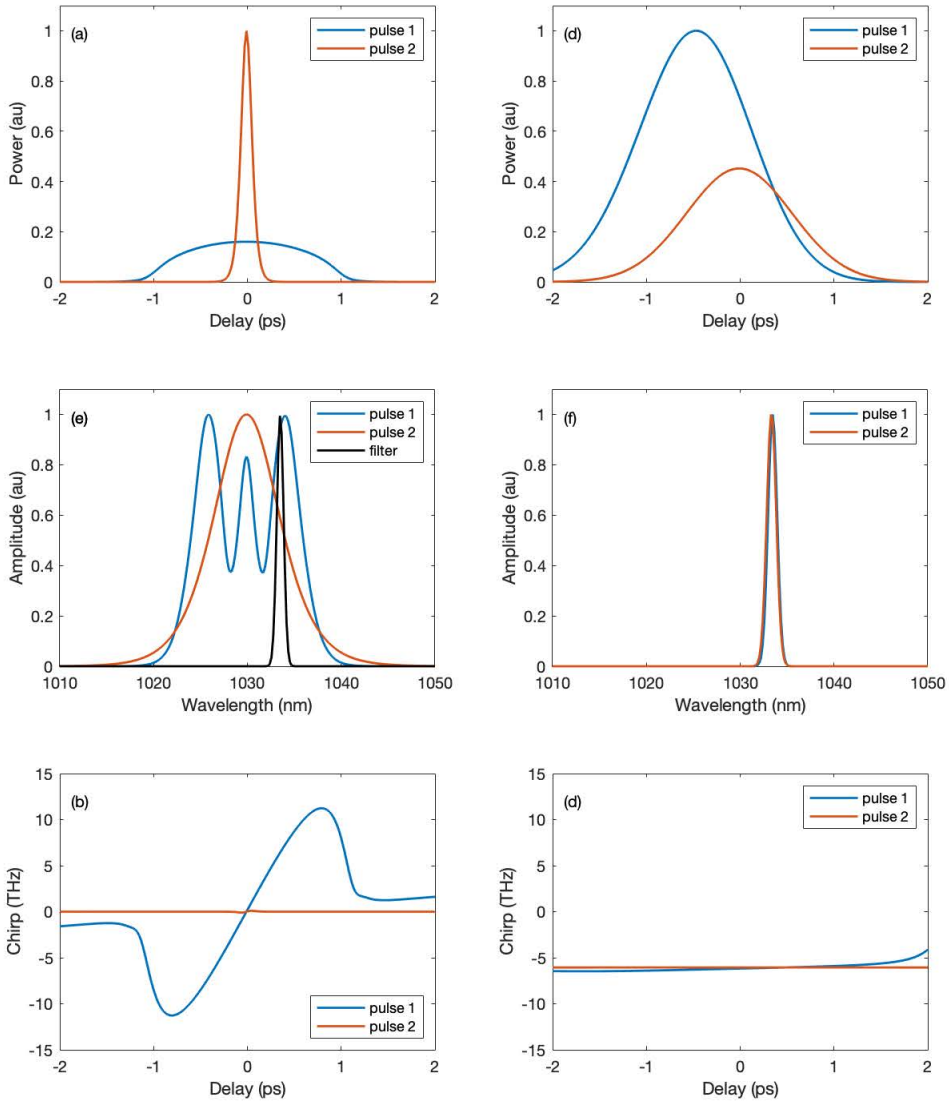

Figure 4.4: The effect of narrow filtering. The orange and blue lines represent two very different pulses. (a, b, c) the states of the pulses before filtering. The narrow black Gaussian at ∼1035 nm is the spectral filter; (d, e, f) the state of the pulses after filtering. Due to the small width of the filter, both pulses are nearly identical to a transform-limited Gaussian, and they differ only in energy, according to the spectral power at the filter wavelength.

The assumption of a constant pulse shape is not necessary to reach the energy map. All that is required is for some process in the cavity to bring any input pulse shape close to a function of the pulse energy within one pass. We say that the pulse shape is *slaved* to the pulse energy. In chapter 2, we discussed the soliton and similariton evolutions and highlighted that they, too, bring the pulse shape close to a function of the energy. Therefore, we expect the energy map model to reliably describe the behavior of fiber lasers with sufficiently long similariton or soliton evolution sections.

In our laser, the energy map can be qualitatively inferred just by looking at the spectra, and our quantization mechanism arises from the response of the spectra to increasing the pulse energy. To illustrate this fact, we passed seed pulses through the blue filter, the Kerr arm, then the red filter with an offset of $\sim$3 nm. We varied the pump power while measuring the spectrum and pulse energy at the output of the Kerr arm and the pulse energy transmitted through the red filter. The result is shown in figure 4.5. As we increase the pulse energy, the spectrum broadens, and its red-most spectral lobe moves with respect to the filter. Around the pulse energy E_1, increasing the pulse energy brings the spectral lobe closer to the filter. The behavior of the filter in this range resembles that of a regular monotonic but strong saturable absorber and is the main characteristic of a Mamyshev regenerator. As we increase the pulse energy further, the red-most lobe starts to surpass the filter, and soon after the peaks of the spectral lobe and the filter match, the transmitted pulse energy peaks at E_2. Further increasing the pulse energy pushes the spectral lobe further away from the filter and decreases the transmitted pulse energy. This corresponds to the region around E_3. Soon before the local minimum in the spectrum reaches the filter, the transmitted pulse energy reaches a local minimum at E_4 then starts to increase again. As shown in figure 4.5f, the curve of the transmitted pulse energy through the red filter (which corresponds to the function $\tilde{f}_{s,k}$ in equation 4.1) closely follows the shape of the spectrum. Our quantization mechanism arises from the motion of the spectral lobe relative to the filter, and it starts taking effect when the spectral lobe reaches the filter.

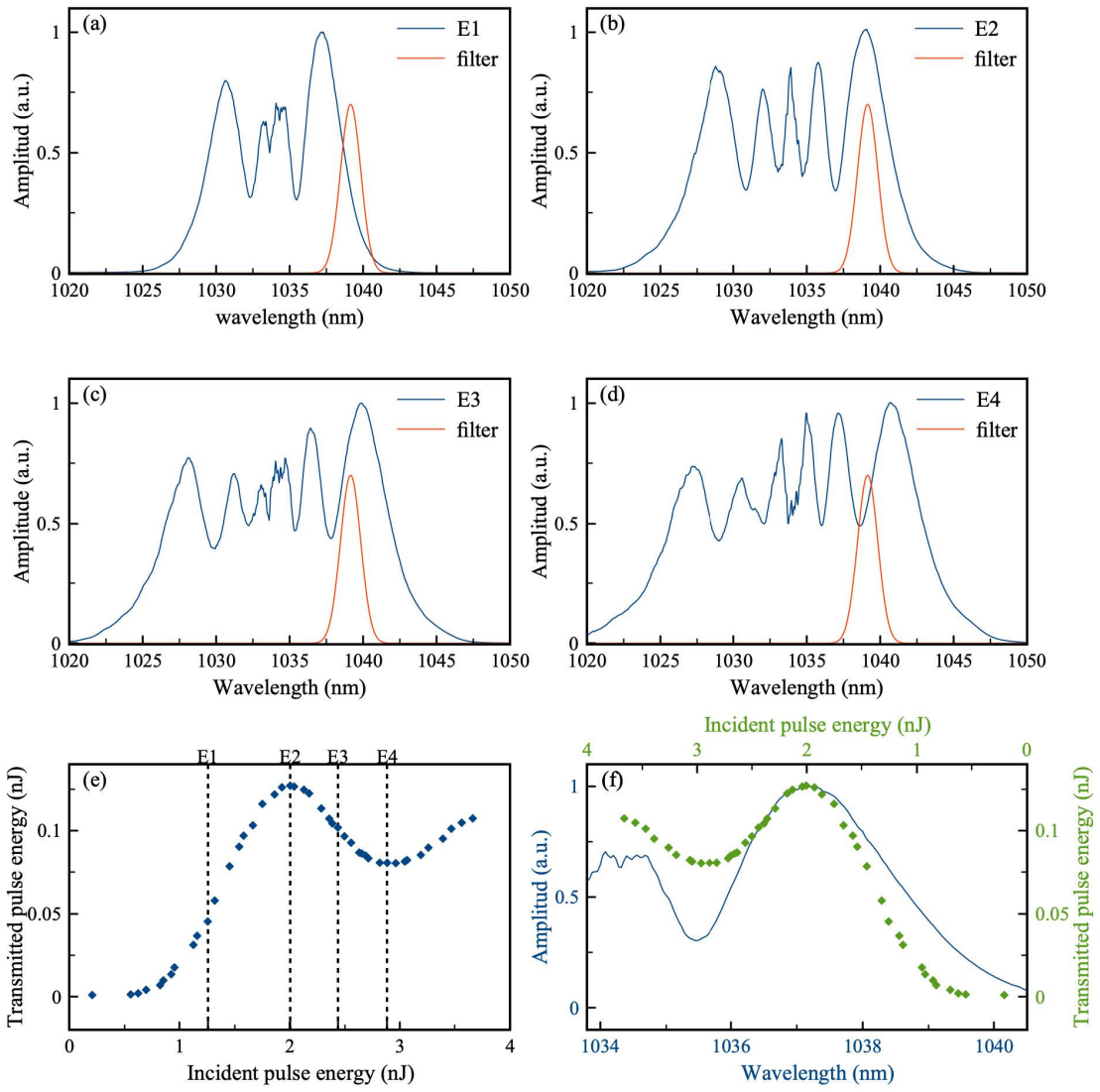

Figure 4.5: Our synthetic quantization mechanism. (a, b, c, d) amplified seed spectra at the pulse energies E_1, E_2, E_3, and E_4, respectively, (in ascending order); (e) the transmitted energy versus the incident energy at the filter. The pulse energies $E_1 - E_4$ are marked on this plot to illustrate the correspondence between the spectral shape and the transmission through the filter; (e) the spectrum (taken at E_1) plotted together with the filter transmission (plotted in reverse) to illustrate the similarity between the spectrum and the filter transmission. This similarity allows us to infer the shape of the energy map qualitatively based on the spectra.

Mathematically, for a pulse to be at a fixed point, the energy map must map its energy back to itself:

$$E_k^* = f_k(E_k^*, O, g_s, g_k). \tag{4.4}$$

For this state to be stable, any small perturbations to the pulse energy must decay. For sufficiently small perturbations,

$$\begin{aligned} E_k^* + \Delta E_n =& f_k(E_k^* + \Delta E_{n-1}, O, g_s, g_k) \\ \approx& f_k(E_k^*, O, g_s, g_k) + \frac{\partial f_k}{\partial E_k}\Delta E_{n-1} \\ \implies \Delta E_n \approx& \frac{\partial f_k}{\partial E_k}\Delta E_{n-1} \\ =& \frac{\partial f_{k,s}}{\partial E_s}\frac{\partial f_{s,k}}{\partial E_k}\Delta E_{n-1}. \end{aligned} \tag{4.5}$$

The evolution of the perturbation depends on the slope of the energy map, which, in turn, follows the slopes of the spectra at the positions of the filters. To illustrate this point, we, again, passed seed pulses through the Kerr arm and the two filters, but this time we applied small sinusoidal modulation to the pump power. Such modulations appear on the radio frequency spectrum as sidebands. We measured and compared the intensity of these sidebands relative to the main peak before and after the filter. This is shown in figure 4.6. When the filter sees a steep slope in the spectrum, the perturbations (sidebands) are amplified by the filter; when the filter sees a near-zero slope, the perturbations are attenuated nearly completely. Similar behavior is seen even in a mode-locked state of our laser (figure 4.7); modulating the Kerr arm while the oscillator is mode-locked produces sidebands in the radio frequency spectrum that get attenuated at the filter. In this case, by carefully adjusting the filter position, we attenuated the modulations by a factor of 22 dB. This is, to our knowledge, the first report of a mode-locked oscillator with a position-dependent RF spectrum.

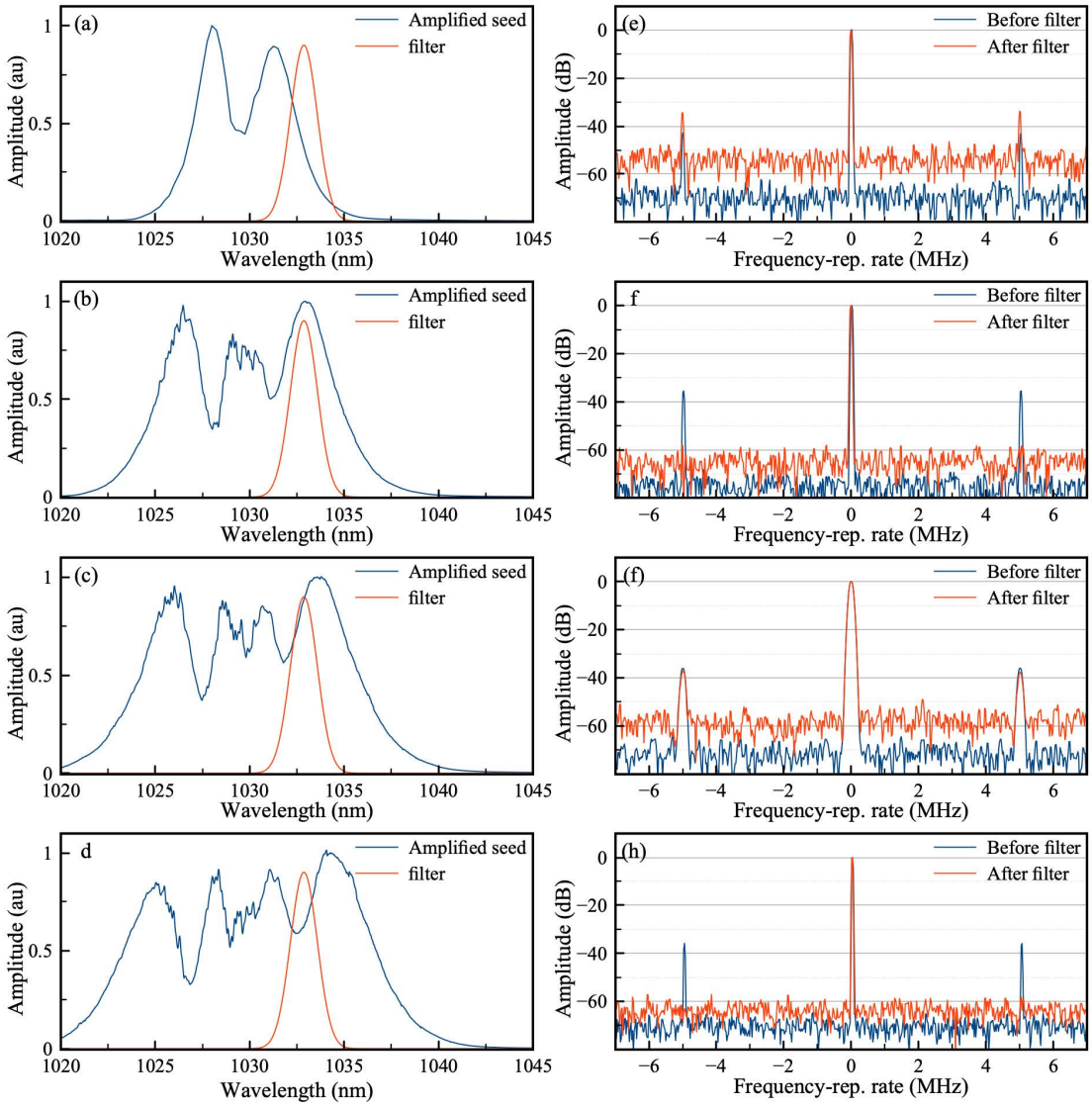

Figure 4.6: Pump modulation experiment with seed pulses at different pulse energies. (a, b, c, d) the optical spectra at increasing pulse energies; (e, f, g, h) the corresponding radio frequency spectra showing the modulation sidebands relative to the main peak before and after the filter. The filter amplifies the perturbations when it meets a steep slope in the spectrum and attenuates them in the vicinity of a maximum or minimum in the spectrum.

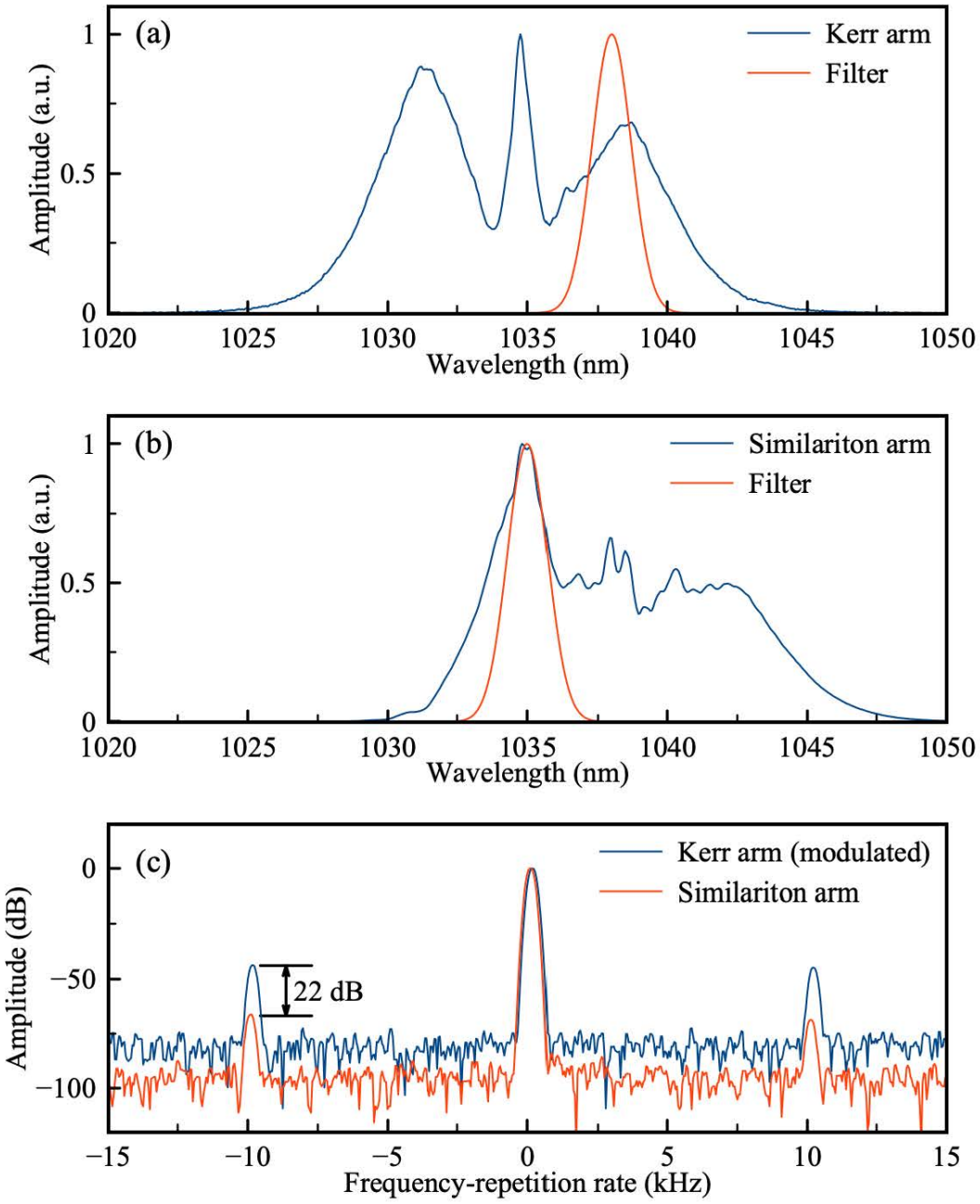

Figure 4.7: Pump modulation experiment during mode-locked oscillator operation. (a, b) the spectra at the output of the Kerr and similariton arms, respectively. The filters are positioned to optimize the filtered pulse energy; (c) the radio frequency spectra before and after the red filter, showing an abrupt 22 dB attenuation of the sidebands by the filter.

We now explain the dynamics behind the behavior we reported in section 1 by plotting the trajectories of the pulse energy on the energy map. Consider the energy maps plotted in figure 4.8. The shape of these maps is typical of our laser: E_{n+1} starts near zero at small E_n as the spectral lobes are far from the filters. Then E_{n+1} increases as increasing E_n brings the spectral lobes closer to the filters then E_{n+1} peaks and starts decreasing after the spectral lobe at one of the arms surpasses its subsequent filter. The difference between the two energy maps in figure 4.8 is in the gain, specifically the gain in the Kerr arm, which merely scales up the pulse energy before it reaches the exit of the Kerr arm, where it is measured. As one would expect, all trajectories on the low-gain map go to the stable fixed point at zero pulse energy. This is because the low-gain map is below the $E_{n+1} = E_n$ line. By contrast, the high-gain map intersects the $E_{n+1} = E_n$ line at two additional pulse energies. At the lower one (marked by a cross), the slope is larger than one and, so, the trajectories diverge away from it. It is an unstable fixed point. At the higher point (marked by a dot), the slope is smaller than one, and so, the trajectories converge towards it. It is a stable fixed point. The pulses are stable at this pulse energy regardless of their number as long as the pump power is consistent with it so as to keep the gain at the value that supports this energy map.

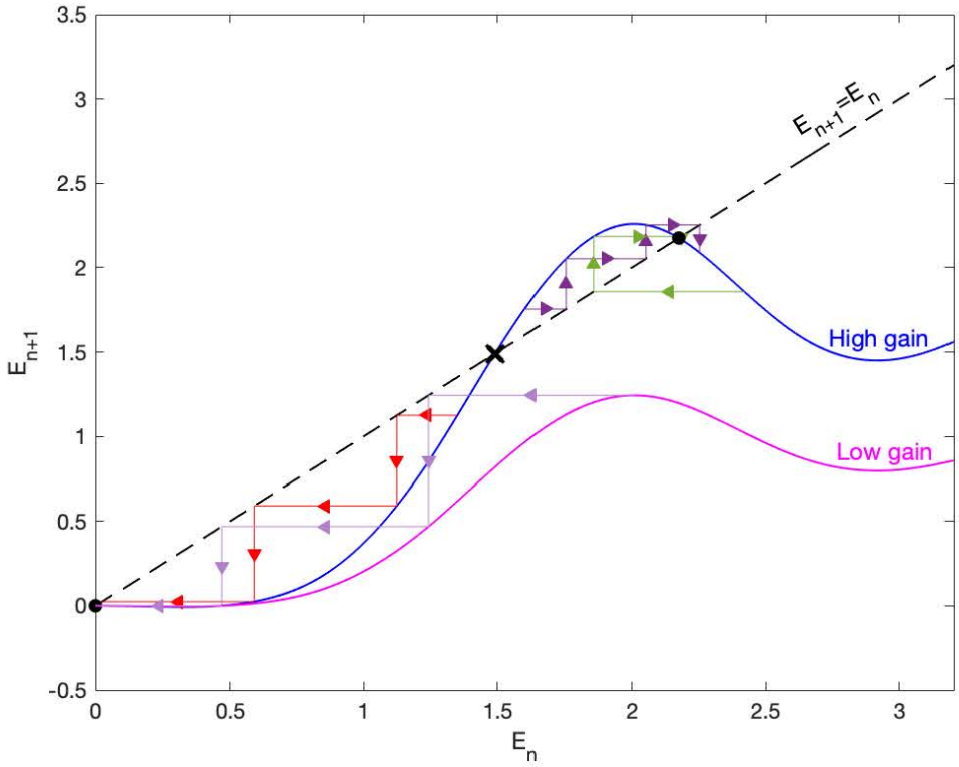

Figure 4.8: Dynamic trajectories on the energy maps. The high gain curve represents a typical energy map in our oscillator with sufficient gain to support one or more pulses, and the low gain curve represents what the energy map would look like if we could abruptly decrease the gain. The arrows show the trajectories followed by the pulse energies. The intersection points between the energy maps and the $E_{n+1} = E_n$ line are the fixed points. The pulses evolving on the high-gain map diverge away from the unstable fixed point, marked by a cross, and converge towards one of the two stable fixed points, marked by dots. A stable mode-lock state has all of its pulses at a dot other than the zero-energy one. The only stable fixed point on the low-gain map is the zero-energy point, and all the pulses evolving on this map from all initial energies go to this point within a few roundtrips.

When reading these maps, one must keep in mind that this behavior applies to all the pulses in the cavity, each according to its initial condition. This means that if we could abruptly lower the gain or, equivalently, increase the filter offset so as to bring the energy map below the $E_{n+1} = E_n$ line, *all* of the pulses in the cavity would die. Of course, this would cause the gain to increase, raising the peak of the energy map above the $E_{n+1} = E_n$ line, but this takes tens or hundreds of roundtrips, by which time, all of the pulses would have been long dead.

This may seem to contradict the control procedure we outlined in section 1, where we claimed that we could reliably deliver the state to a precise number of pulses by decreasing the pump powers and/or increasing the filter offset so as to kill pulses one-by-one. Figure 4.9 illustrates the behavior when this control procedure is followed. The key is to move the parameters so as to lower the energy map only slowly. As we approach the point of saddle-node bifurcation, where the stable and unstable fixed points meet, it becomes likely for the energy of a pulse to fluctuate below the unstable fixed point, leading it to the zero-energy point. This is similar to quantum tunneling. The death of one pulse decreases the total energy in the cavity and the rate of stimulated emission from the gain fiber, which slowly increases the energy accumulated in it and the gain it provides. As the gain increases, the energy map moves away from the bifurcation point, making the death of more pulses nearly impossible. The bifurcation point itself is never crossed because merely approaching it is enough to result in pulse death and, subsequently, gain increase. This is similar to the regulatory effect of the Zener tunneling diode.

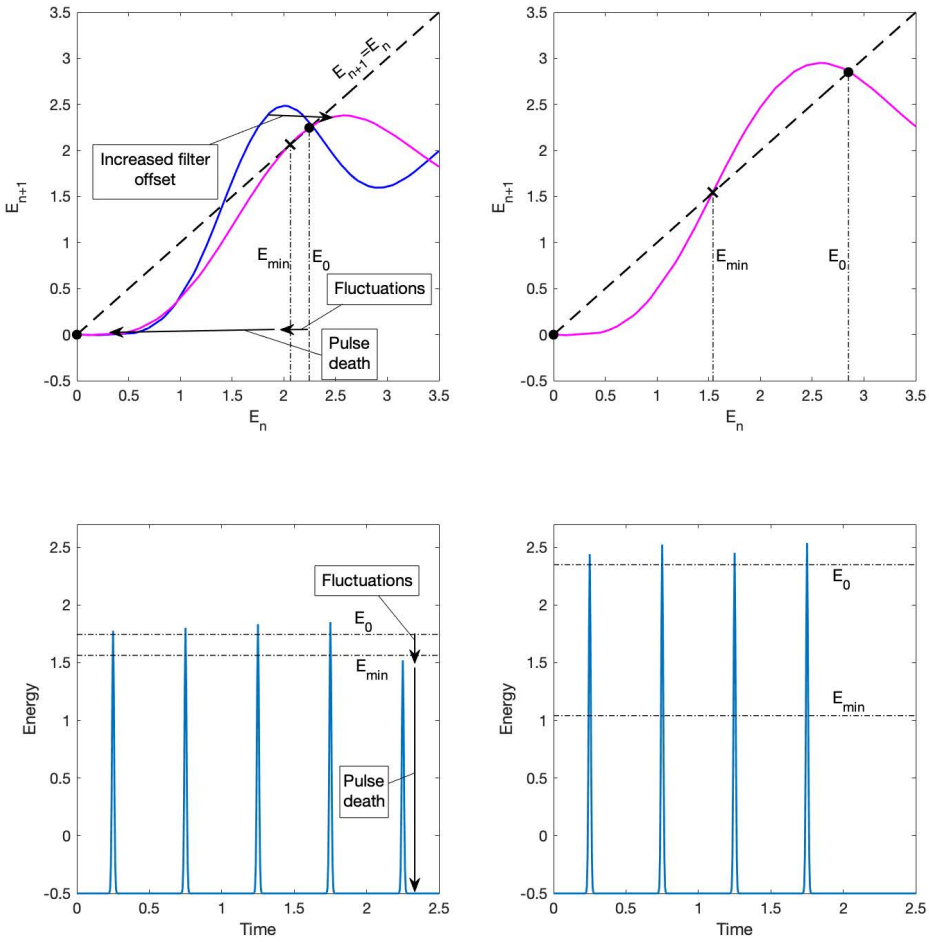

Figure 4.9: Dynamics of pulse death. (a) the change in the energy map while increasing the filter offset. This change brings the stable and unstable fixed points E_0 and E_{min} close to each other, making fluctuations from E_0 to below E_{min} likely; (b) visualization of pulse death through fluctuations upon bringing E_0 and E_{min} close to each other. (c) the energy map after the gain adapts to the lower number of pulses. This pushes E_0 and E_{min} away from each other, making more pulse-killing fluctuations highly unlikely; (d) visualization of the increased pulse energy, E_0, and the lowered threshold, E_{min}, after the gain adapts.

On the other hand, consider the case where the gain is initially high due to the absence of pulses but is then suddenly lowered upon seeding an excessively large number of pulses. These pulses will circulate at the stable fixed point E_0 for a short period of time during which they will consume the energy stored in the gain fiber, which lowers the gain it provides and leads towards the saddle-node bifurcation. If this decrease in the gain took place at a time scale of seconds, like when we manually decrease the pump power, we would expect as many pulses to remain as can be supported by the pump power. However, as the bifurcation point is approached quickly, at the time scale of the gain itself, the pulse-killing fluctuations can not find the time to occur until the gain comes so close to the bifurcation point that they become likely enough to be experienced nearly simultaneously by multiple numbers of pulses with comparable probabilities. This explains why the seeding step we mentioned in section 1 produces a large but random number of pulses.

This is, to our knowledge, the second type of bifurcation where "branch selection" is controlled by slowing down the bifurcation parameter [57].

The combined system of pulse energies together with the adaptive gain permits multi-pulsing states with different numbers of pulses even at the same external parameters (pump powers and filter offset). This is an example of multistability. Most of these states are long-term stable. This can be attributed to the fact that pulses can not be born or killed by any reasonably probable fluctuations. In other words, noise-induced transitions are highly unlikely, and all of these multi-pulsing states are kinetically stable. The only noise-induced transition is the one that occurs near a bifurcation point. If the laser was self-starting and if it follows the so-called minimum loss dictum [58], then the number of pulses would keep increasing and saturating the gain until their energy is such that they experience the lowest possible loss. But the minimum loss state corresponds to the tangential point between the energy map and the $E_{n+1} = E_n$ line, where pulse death is highly likely. The fact that our laser is not self-starting is a valuable advantage.

Additionally, the stability of the multi-pulsing states relies on the stability

of the external parameters. If, for example, the filter positions were sensitive to temperature fluctuations or small mechanical vibrations, the energy map itself would fluctuate in time, resulting in pulse death. In reality, Mamyshev oscillators are stable against disturbances from their environment so that the only significant parameter noise is seen in the pump powers, which fluctuate on the order of $0.1 - 1\%$ in our system, which is small compared to the large ranges of pump powers where most of these multi-pulsing states live. The combination of kinetic stability and environmental stability is what makes the multi-pulsing operation of our laser robust.

The energy map also explains the period-doubling shown in figure 4.2. when the filter offset is decreased, the two filters match steep slopes: one outer slope and one inner slope. This makes the slope of the energy map less than -1. One may say that the quantization mechanism here is too strong; if we were to model the evolution of the pulse energy continuously (by a differential equation), we would falsely conclude that this state is exceptionally stable. This is not the case with the discrete roundtrip-to-roundtrip evolution we have in real oscillators. According to the linearization in equation 4.5, this leads to oscillatory divergence away from the fixed point. Then, the state converges to the period-doubled state when the trajectory approaches the nearby local minimum or maximum in the energy map. Such a trajectory is drawn in figure 4.10. Physically, when the pulse energy is low, the similariton spectrum is narrow so that the filter picks the intense, blue-most peak in it. This makes the pulse energy in the following roundtrip high so that the similariton spectrum becomes broad and the filter misses the intense lobe, making the pulse energy in the following roundtrip low again, completing a double period.

Lastly, we explain the coexistence of different-energy pulses of figure 4.3. The red filter is at the outer slope of the Kerr arm. This means that the pulse energy is well within the monotonic range of the red filter transmission (the region between 0 and E_2 in figure 4.5e). This implies that the energy map takes the qualitative shape of the spectrum of the similariton arm with some deformation; It is expected to feature two local maxima, corresponding to the first and second spectral lobes, with a local minimum in between as we have drawn in figure 4.11.

If the $E_{n+1} = E_n$ line passes near both the local minimum and the second local maximum, we get two stable fixed points besides the zero-energy point. These two stable fixed points correspond to two different energies of pulses that can coexist at the same gain in the cavity.

We would like to emphasize the synthetic nature of our quantization mechanism. It arises from the nonlinearly shaped spectra, which can be engineered to produce interesting dynamics, as we have shown with period-doubling and different-energy pulses. Of particular interest is our ability to tune the minimum required pulse energy in real-time by changing the filter offset. This would not be possible if the quantization effect was inherent in the pulse propagation dynamics as with solitons.

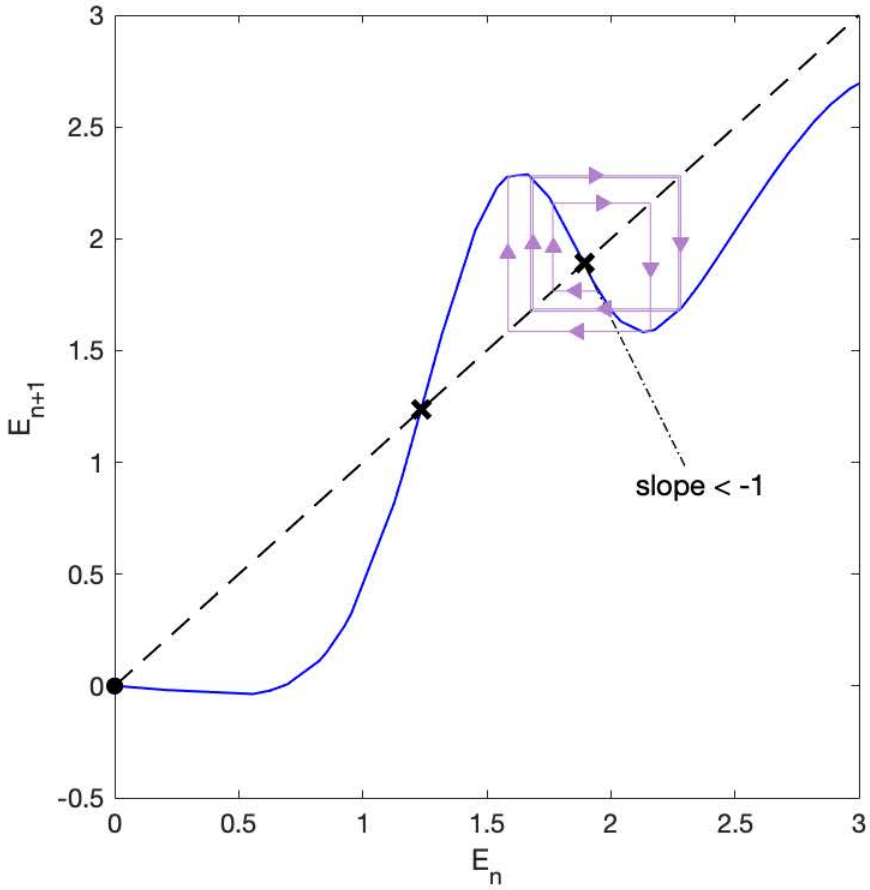

Figure 4.10: The evolution towards a period-doubled state. The pulse energy is unstable here because the slope is less than -1. The arrows show a trajectory starting from a perturbation from this unstable fixed point, which diverges away from it and converges to a period-doubled state.

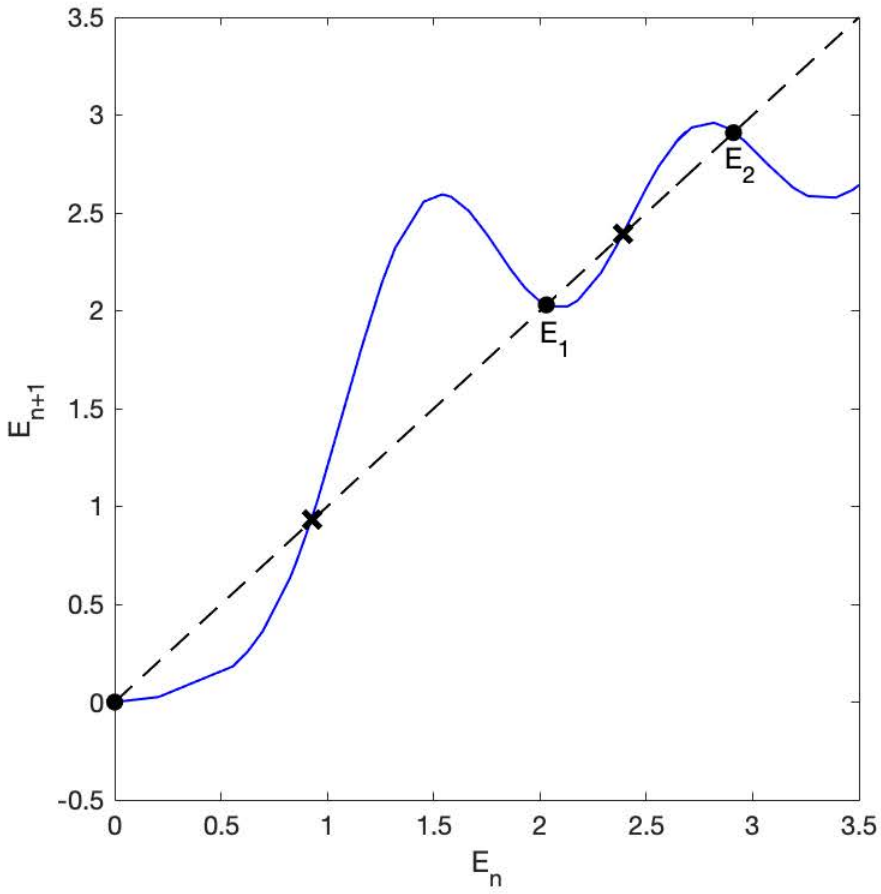

Figure 4.11: The energy map that supports coexisting but different pulses. The energy map is qualitatively similar to the spectrum of the similariton arm (figure 4.3b). E_1 and E_2 represent the two coexisting pulse energies. They are stable fixed points because they intersect the $E_{n+1} = E_n$ line with small slopes.

Chapter 5

Pulse Interactions

In the previous chapter, we discussed the dynamics governing the number of pulses and the procedure to control it without discussing the temporal organization they take. In this chapter, we outline our experimental observations regarding the temporal organization of the pulses and present the procedure to achieve harmonic mode-locking. The rest of the chapter addresses the question: what governs the temporal organization of the pulses in the nanosecond scale and how to control it? We start in section 2 by formulating the dynamical system using what little is readily known about the pulse interactions. In section 3, we summarize and compare the physical processes proposed in the literature to explain the pulse interactions. The acoustically mediated interaction theory stands out in this comparison and, so, we review it in detail in section 4, filling some of the gaps left in the literature. In section 5, we adapt the acoustic theory to our Mamyshev oscillator and show that it involves pulse-shaping processes like Kerr nonlinearity and spectral filtering. With that, we explain the control procedure that achieves harmonic mode-locking in our laser. The acoustic interaction theory suggests a way to manipulate the pulse interactions via a secondary loop. Section 6 presents this technique and its experimental results, which show unprecedented manipulation of pulse patterns, verifying our interaction theory and pointing at promising technological applications.

5.1 Experiments with harmonic mode-locking

Following the control procedure mentioned below, we achieved harmonic mode-locking beyond 1.2 GHz (83^{rd} harmonic) in our laser while keeping short pulse durations and strong supermode suppression. For example, we obtained harmonic mode-locking at 1 GHz with pulses compressible down to ∼117 fs and with a supermode suppression ratio of ∼50 dB. The repetition rate and pulse energy are limited by the pump power; at high repetition rates, the power limitation forces us to lower the pulse energy, which decreases the nonlinearity and spectral width, leading to longer de-chirped pulse durations. At 1.2 GHz (figure 5.1), the pulse energy at the output of the similariton arm is ∼2 nJ and the de-chirped pulse duration is 150 fs. Decreasing the repetition rate down to 261 MHz (figure 5.2), for example, allows us to increase the pulse energy at the output of the similariton arm to ∼11 nJ, which decreased the de-chirped pulse duration below 100 fs, albeit with a pedestal forming around the pulse. The 1 GHz state (figure 5.3) is a good compromise between the pulse duration and the repetition rate, where the pulse energy at the output of the similariton arm is ∼3 nJ. If we can increase the average power, higher repetition rates are expected with ∼100 fs pulse durations.

Achieving harmonic mode-locking in our laser is done by the combination of two things:

1. We adjust the filter positions with respect to the spectra at the Kerr and similariton arm outputs; for all harmonic orders, there is a range of filter positions that allows harmonic mode-locking.

2. We perturb the state of the laser by sending a stream of low-energy seed pulses into the cavity. These pulses are too weak to seed new pulses in the cavity, but they do change the temporal organization. For example, they can break apart bound pulses or prevent them from forming.

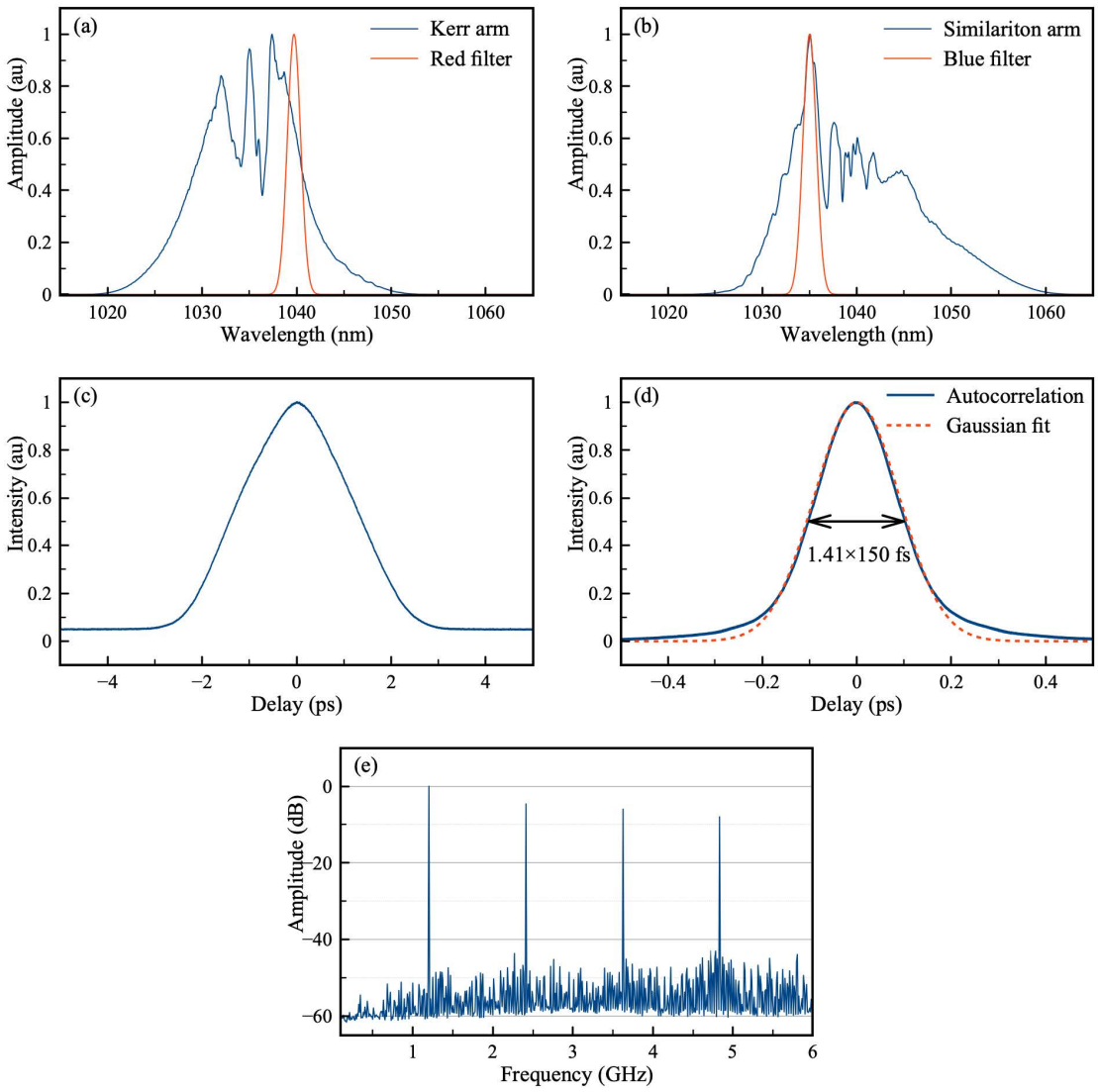

Figure 5.1: Harmonically mode-locked state at 1.208 GHz ((83rd harmonic): (a) spectrum at the output of the Kerr arm and the subsequent filter, (b) spectrum at the output of the similariton arm and the subsequent filter, (c) intensity autocorrelation trace of the laser output (from the similariton arm), (d) intensity autocorrelation trace of de-chirped laser output showing a pulse duration of 150 fs, (e) radio frequency spectrum showing a supermode suppression ratio of ∼45 dB

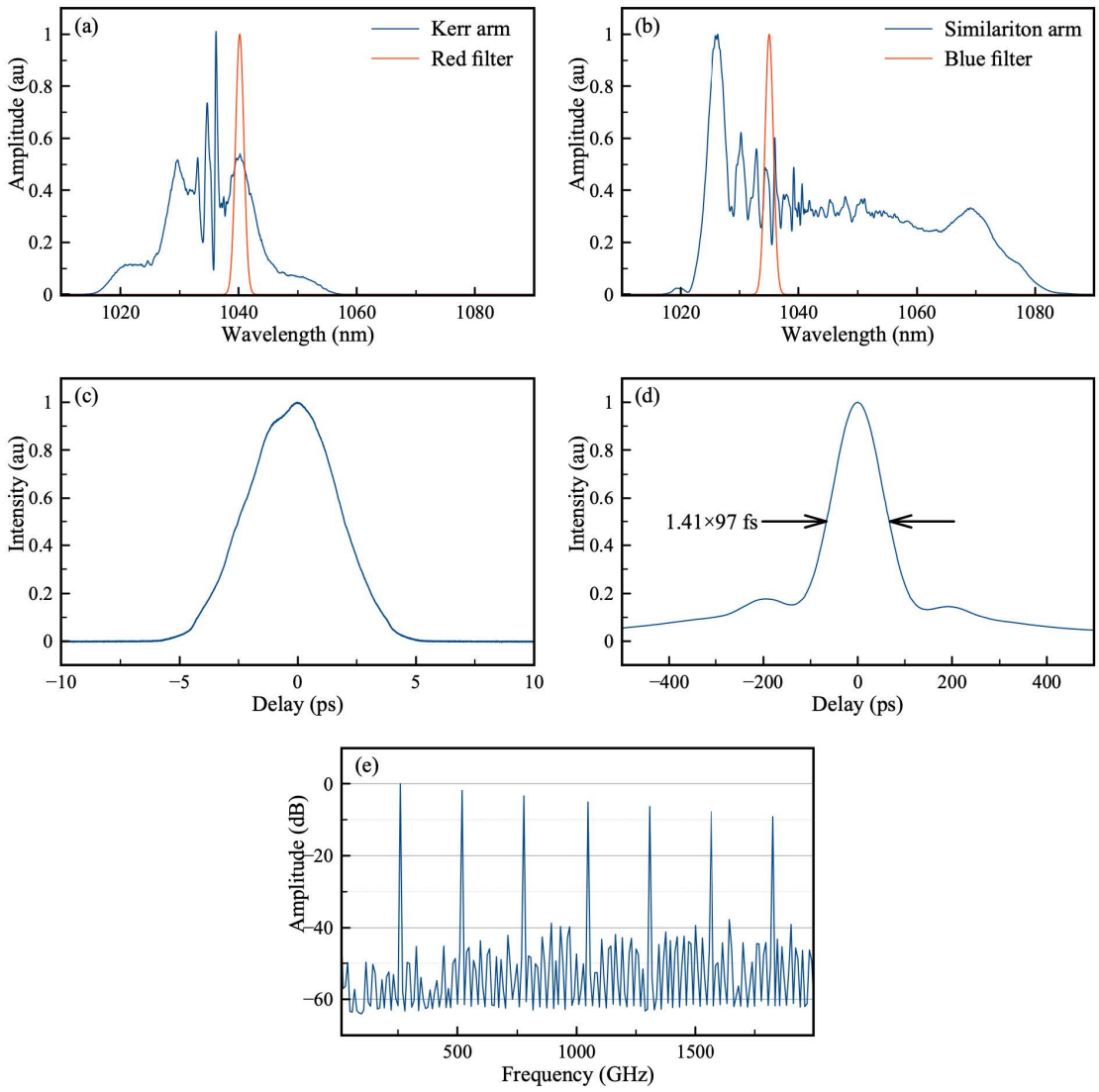

Figure 5.2: Harmonically mode-locked state at 261 MHz (18^{th} harmonic): (a) spectrum at the output of the Kerr arm and the subsequent filter, (b) spectrum at output of the similariton arm and the subsequent filter, (c) intensity autocorrelation trace of the laser output (from the similariton arm), (d) intensity autocorrelation trace of de-chirped laser output showing a pulse duration of ∼97 fs, (e) radio frequency spectrum showing a supermode suppression ratio of ∼45 dB

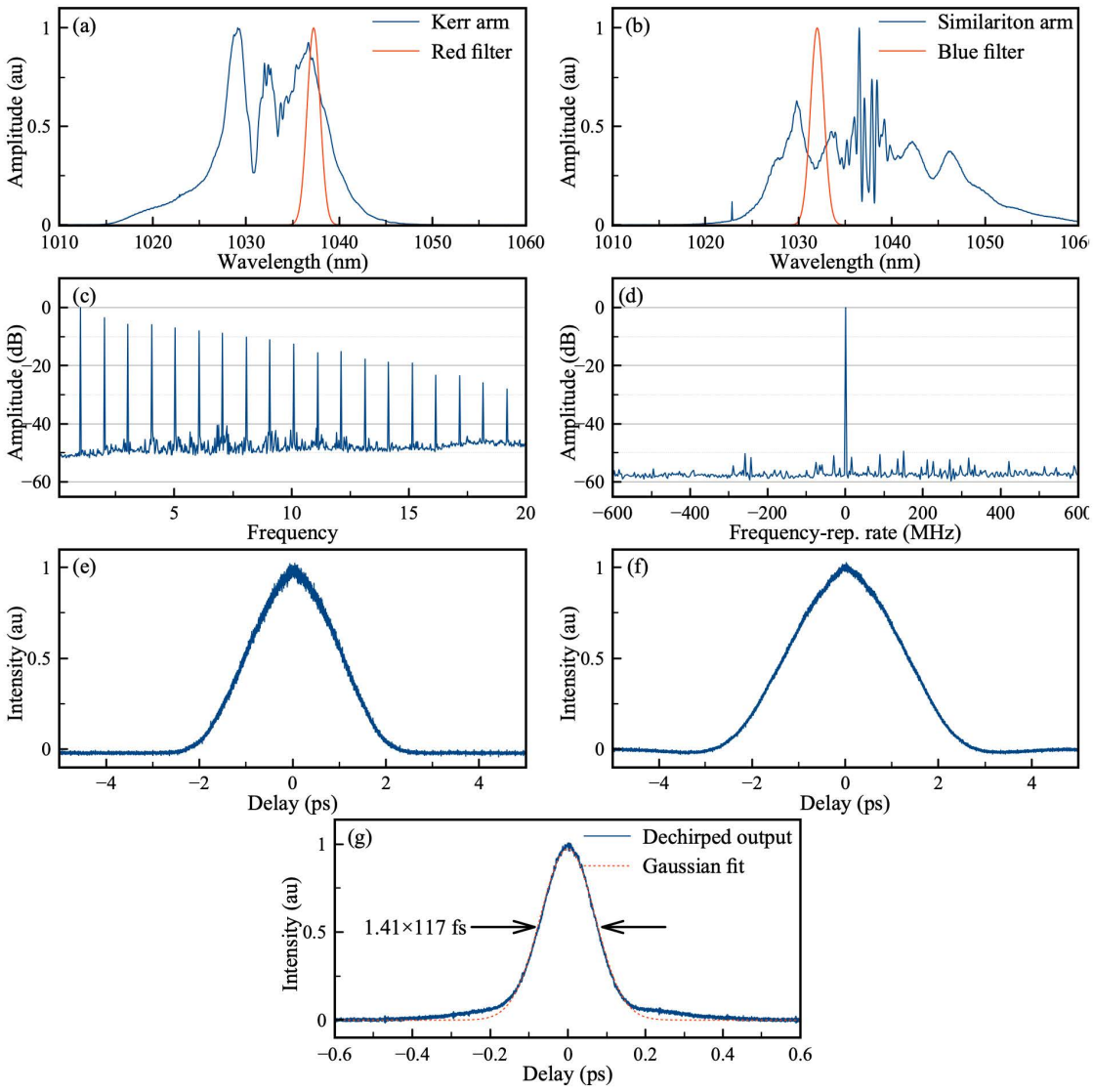

Figure 5.3: Harmonically mode-locked state at 1.007 GHz ((67th harmonic): (a) spectrum at the output of the Kerr arm and the subsequent filter, (b) spectrum at output of the similariton arm and the subsequent filter, (c) radio frequency spectrum spanning 20 GHz, (d) radio frequency spectrum centered around the first line showing a supermode suppression of 50 dB, (e) intensity autocorrelation trace at the output of the Kerr arm, (f) Intensity autocorrelation trace at the output of the similariton arm (laser output), (g) Intensity autocorrelation trace of de-chirped laser output (similariton arm)

The first measure is a necessary condition for harmonic mode-locking. Once a harmonically mode-locked state is reached, it remains stable for as long as the filter positions are appropriate. We have verified that our laser supports harmonic mode-locking at every harmonic order at least up to 1.2 GHz with only one exception, the 72^{nd} harmonic (1.048 GHz), where the supermode suppression ratio was suspiciously low ($\sim$30 dB).

Reaching a harmonically mode-locked state may or may not require perturbation, depending on the initial pulse pattern right after the most recent change in the number of pulses. Usually, killing a pulse by increasing the filter offset leads the state to harmonic mode-locking without perturbation. Essentially, the perturbation step is an intentional noise-induced transition from a kinetically trapped state to harmonic mode-locking and, therefore, it is unnecessary if the system happens to start in the basin of attraction of harmonic mode-locking.

The relative speeds of the pulses are on the order of nanoseconds per second. It takes on the order of seconds for the temporal organizations of the pulses to stabilize. For example, it's possible to bring the filter positions close to each other to allow a noisy continuous wave-like signal to perturb the pulse pattern then go back to an appropriate filter position before the state settles, hoping that when it does, it settles at harmonic mode-locking.

Quite often, the laser goes to states that are best described as "nearly harmonically mode-locked." They are stable states whose pulses appear almost equidistant, but their radio frequency spectra exhibit intense and stable supermodes. Transitions from those states to harmonic mode-locking are achieved by following the procedure above. Two examples of this phenomenon are presented in figure 5.4 for transition via filter adjustment and figure 5.5 for transition via perturbation. Furthermore, we have found few states where harmonic mode-locking is less favorable compared to their nearly harmonically mode-locked neighbors. For these states, a perturbation is more likely to lead the pulses to a nearly harmonically mode-locked state, and several trials are needed before harmonic mode-locking is randomly reached. After that, the state is indefinitely stable. For these states, harmonic mode-locking may be regarded as kinetically stable.

Finally, given a harmonically mode-locked state, it is possible to optimize the supermode suppression by fine-tuning the filter offset. In most cases, this involves increasing the filter offset and pushing the pulse energy quantization to its limits. The highest supermode suppression ratio achieved involved a filter offset almost large enough to cause pulse death (figure 5.4). This ratio is $\sim$60 dB, and it is to our knowledge the highest supermode suppression ratio of any passively harmonically mode-locked laser [45, 46].

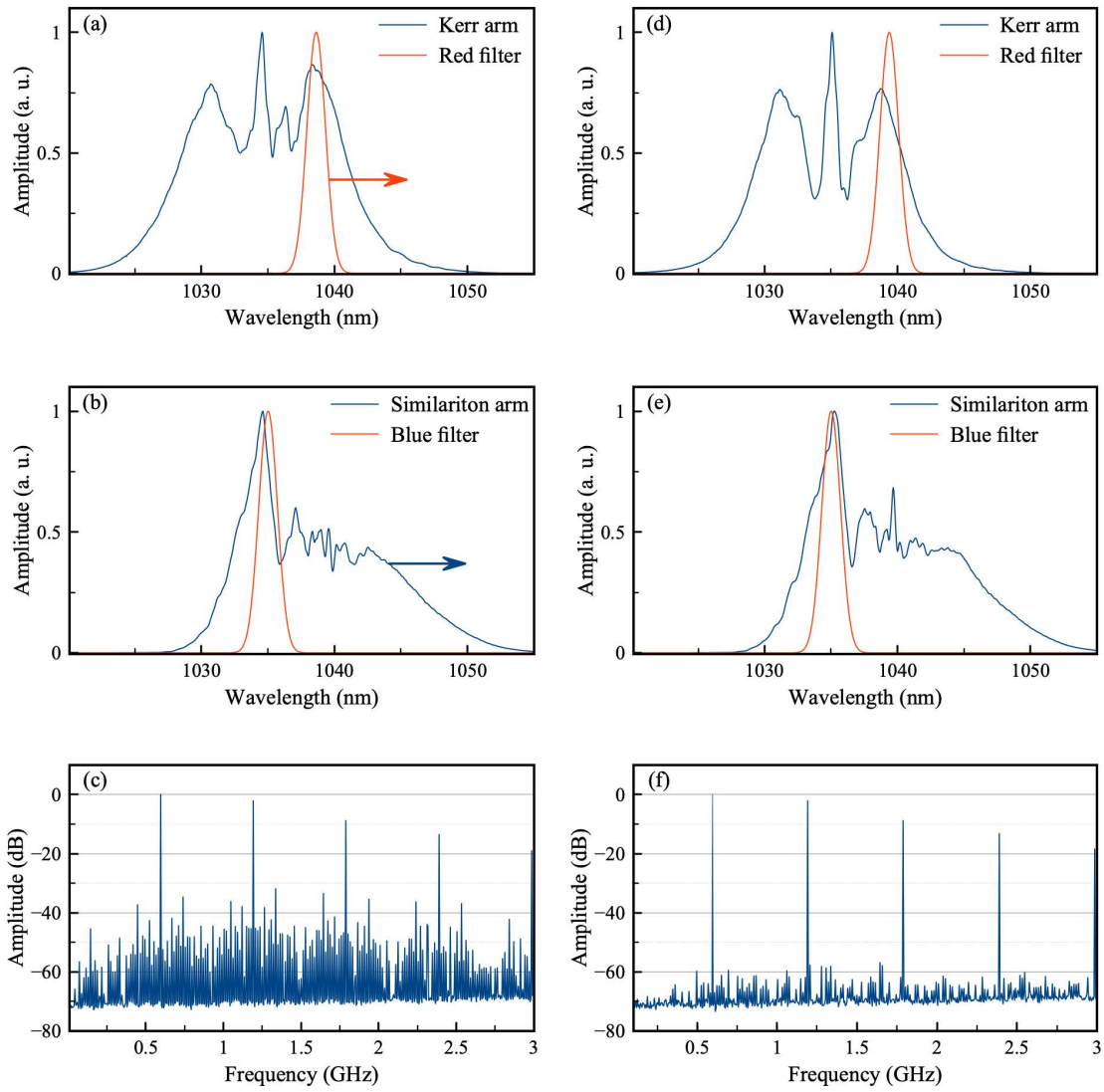

Figure 5.4: harmonic mode-locking and supermode suppression optimization by filter adjustment: (a, b, c) spectra and radio frequency trace of a nearly harmonically mode-locked state (597 MHz, 41^{st} harmonic); the filter offset is small and the arrows show where the red filter and the similariton arm spectrum will be moved to optimize the supermode suppression ratio, (d, e, f) spectra and radio frequency trace after increasing the filter offset. The suppression of supermodes is optimized by adjusting the filter positions relative to the spectra such that they lie on steep slopes. Pulse energy fluctuations are only weakly attenuated, and the state is at risk of pulse death (see chapter 4).

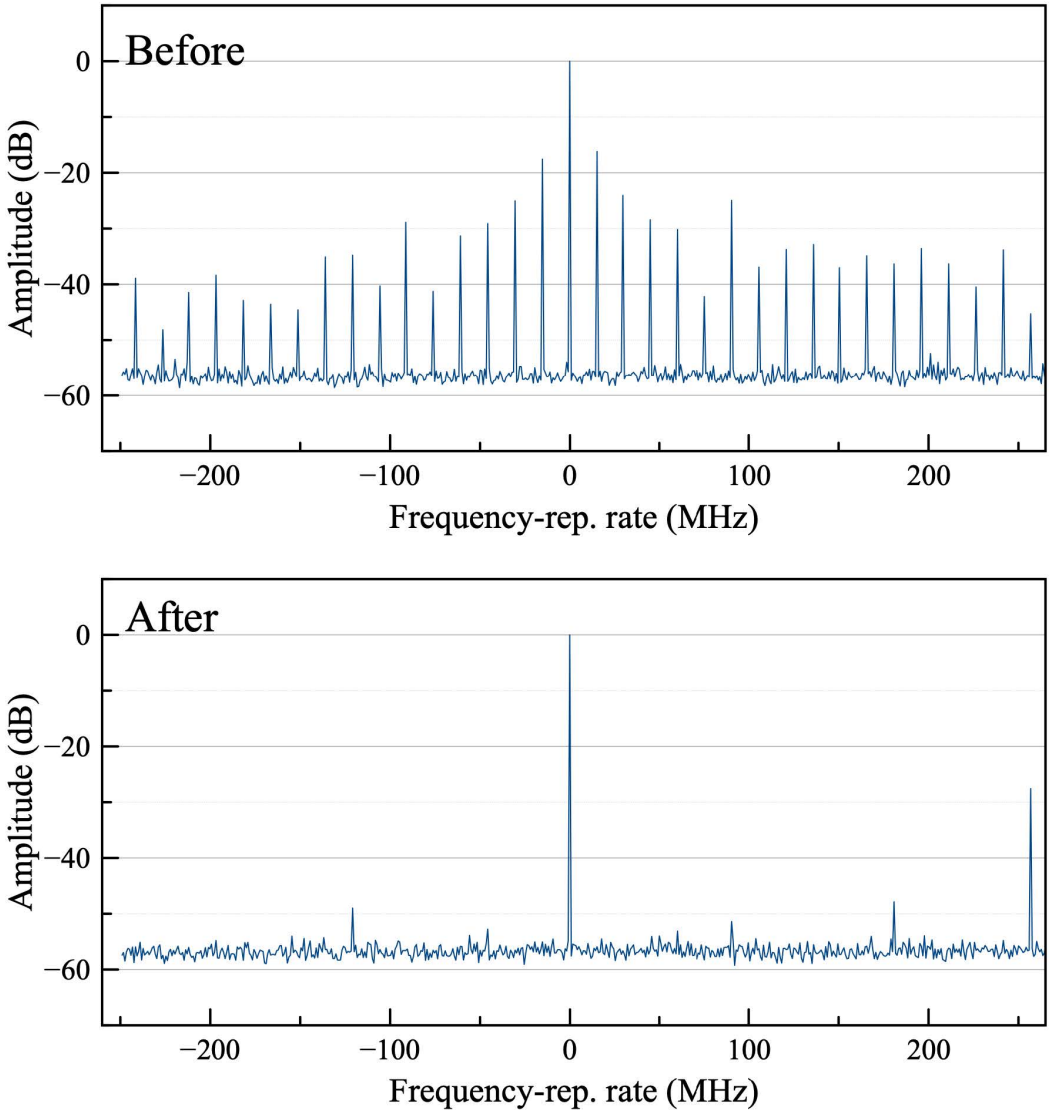

Figure 5.5: Perturbation-induced transition from a nearly harmonically mode-locked state to a harmonically mode-locked state (512MHz): RF spectra before and after perturbation by a stream of low-energy seed pulses

5.2 The dynamical system of interacting pulses

For a multi-pulsing state with N pulses, there are $N-1$ degrees of freedom describing the temporal positions of the pulses within the cavity period. We denote the temporal position of the i^{th} pulse by τ_i, which may be measured with respect to the $i-1^{st}$ pulse or a reference pulse within a period or the center of mass of the pulses in a period. The temporal positions of the pulses evolve according to their speeds:

$$\dot{\tau_i} = V_i(\tau_1, \tau_2, ..., \tau_N, \Gamma_1, \Gamma_2, ...), \tag{5.1}$$

where V_i corresponds to the speed of the i^{th} pulse (in nanosecond/second), and the Γ's represent all external parameters such as the pump powers and the filter positions. Equation 5.1 may seem like a tautology, but it's actually an extreme simplification. To see this, consider two states, A and B, with the same number of pulses and the same temporal positions, except that in B, one of the pulses happens to take a shifted wavelength at some point in its evolution. Clearly, the speeds of the pulses in A and B cannot both be described by equation 5.1 even though they have the same pulse pattern; the wavelength shift in B introduces an error to equation 5.1 that lasts until the wavelength shift is corrected by the spectral filtering in the cavity. Therefore, describing the evolution of the temporal positions of the pulses by equation 5.1 assumes that the evolution of the pulse properties such as the central wavelength and, consequently, the pulse speeds happens at a time scale that is negligibly small compared to that of the evolution of the pulse positions. This is an application of the slaving principle, and in this example, it is very similar to the Born-Oppenheimer approximation in quantum mechanics. It is valid for the weak pulse interactions over nanosecond-long delays, where the pulse pattern evolves on the time scale of seconds. It does not apply to, for example, overlapping pulses, whose temporal positions evolve at the same time scale as their energies, phases, central wavelengths, etc.

We restrict our discussion to the pulse interactions over nanosecond-long delays, where equation 5.1 applies, and focus our analysis on harmonic mode-locking. A harmonically mode-locked pulse pattern enjoys translational symmetry. This means that the pulse speeds are identical and, consequently, harmonic mode-locking is necessarily a fixed point. This is true regardless of the pulse interaction mechanism. To determine whether harmonic mode-locking is a stable or unstable fixed point, we analyze the response of the system to small perturbations, $\delta\tau_j$ and linearize:

$$\begin{aligned}\dot{\tau}_i = \delta\dot{\tau}_i &= V_i(\tau_{h,1} + \delta\tau_1, \tau_{h,2} + \delta\tau_2, ..., \tau_{h,N} + \delta\tau_N, \Gamma_1, \Gamma_2, ...) \\ &\approx \sum_{j=1}^{N} \frac{\partial V_i}{\partial \tau_j}\delta\tau_j,\end{aligned} \tag{5.2}$$

where $\tau_{h,i}$ is the temporal position of the i^{th} pulse in the state of harmonic mode-locking and we have taken the temporal positions with respect to a point that moves with the pulse pattern so that $V_i(\tau_{h,1}, \tau_{h,2}, ..., \tau_{h,N}, \Gamma_1, \Gamma_2, ...)$ is zero.

If we include the temporal positions of all N pulses (which adds one redundant variable), then we can simplify equation 5.2 further by noting the translational symmetry:

$$\frac{\partial V_i}{\partial \tau_j} = \frac{\partial V_{i+1}}{\partial \tau_{j+1}};\ \tau_{N+1} = \tau_1. \tag{5.3}$$

This condition defines a circulant matrix, whose eigenvalues are:

$$\gamma_k = \sum_{j=1}^{N} \frac{\partial V_1}{\partial \tau_j} e^{i\frac{2\pi}{N}(j-1)k};\ k = 0, 1, ...N-1. \tag{5.4}$$

Here, γ_0 corresponds to translating the whole pulse pattern and is zero if the pulse positions are measured with respect to a point that moves with the pulse pattern. In order to guarantee that harmonic mode-locking is a stable fixed point, all the remaining $N-1$ eigenvalues have to be negative.

It should be noted that the mere fact that harmonic mode-locking is a stable fixed point does not guarantee that the state of the laser will be harmonically mode-locked; if V_i is nonlinear in the pulse positions τ_j's, then it can have multiple attractors, such as the near harmonic mode-locked states we reported.

5.3 Pulse interaction mechanisms in the literature

To our knowledge, there are six families of pulse interaction mechanisms presented in the literature: the coherent overlap theory [44, 6, 59] treats the interactions between pulses with significant overlap, making it irrelevant in the nanosecond range. Interactions mediated by dispersive waves [5, 60] suggest that pulses interact via light that breaks off of the pulse, commonly due to soliton formation. The effective range, however, depends on how far this light disperses before it's attenuated by the saturable absorber and is typically tens to hundreds of picoseconds. In oscillators with saturable absorbers as strong as the Mamyshev regenerator, the attenuation is nearly instantaneous, and the range of effect of such mechanism depends on the total group velocity dispersion delay in a single roundtrip, which is in the order of picoseconds. Noise [61], gain depletion [62] and electronic excitation-mediated interaction mechanisms [5, 63] allow truly long-range interactions as they involve the gain, which is typically slow. However, these interactions are monotonic; they are either repulsive, pushing towards Harmonic mode-locking, or attractive, pulling towards a single bunch of bound pulses, but not oscillatory. If they were dominant, they would not allow the nearly harmonically mode-locked states. Moreover, in fiber lasers, the gain typically stores an amount of energy that is much larger than the pulse energy, and so, the oscillation in the population inversion, which is essential for these mechanisms, is extremely small. For example, following [63], we estimate the electronic de-excitation upon the amplification of one pulse in a gain fiber in our laser to cause oscillation in the refractive index on the order of 10^{-12}, which causes a wavelength shift on the order of 10^{-8} nm. By contrast, the refractive index modulation due to absorption and electronic excitation in a semiconductor material in [5] is on the order of 10^{-2} and the associated wavelength shift is on the order of 10^{-5} nm. Nevertheless, it is straight-forward to extend our analysis of the interactions below to include the interactions mediated by the gain.

The only remaining interaction mechanism from the literature is the acoustic

interaction mechanism, which is both long-ranged and non-monotonic and, as we show in the following sections, is on an order of magnitude that is consistent with experiments.

A large body of literature exists on the acoustic interactions in fiber lasers, starting from the first long-range interaction observed outside an oscillator [64], followed by the formulation and numerical evaluation of acoustic interactions in a single pair of pulses outside an oscillator [65] and a train of pulses in oscillators with mild spectral filtering [66], to the recent Raman-like gain [67] and ∼2 GHz harmonic mode-locking [68] with tight confinement of acoustic and optical modes in photonic crystal fibers, to the utilization of torsional acoustic vibrations to rotate the polarization of continuous wave background in an all-non-polarization-maintaining laser mode-locked by nonlinear polarization evolution [69]. These works grant importance and confidence to the acoustic interaction theory.

5.4 The acoustic interaction mechanism

Here, we present a pedagogical review of the acoustic interaction mechanism starting from first principles. This review is adopted partially from [70, 65, 66, 5].

As an optical pulse passes through a point along a fiber, Its electric field induces polarization in the glass material. The interaction between this induced polarization and the electric field lowers the electric potential energy (per unit volume) associated with the field by the amount:

$$u = -\frac{1}{2}\epsilon\epsilon_0 < E^2 > . \tag{5.5}$$

This amount increases if the glass material is pulled towards the fiber axis because then the induced polarization becomes stronger. This change in the potential energy equals:

$$\Delta u = -\frac{1}{2}\epsilon_0 < E^2 > \frac{\partial\epsilon}{\partial\rho}\Delta\rho, \tag{5.6}$$

where ρ is the density. Therefore, there must exist a negative pressure around the fiber core pulling the glass material inwards and doing the following work per

unit volume:

$$\begin{aligned} w = p_e \frac{\Delta V}{V} = -p_e \frac{\Delta \rho}{\rho_0} = -\Delta u \\ \Longrightarrow p_e = \frac{1}{2}\epsilon_0 < E^2 > \gamma_e. \end{aligned} \tag{5.7}$$

This phenomenon is called electrostriction and the constant $\gamma_e = \rho_0 \frac{\partial \epsilon}{\partial \rho}$ is the electrostriction constant. It can be estimated by the Lorentz-Lorenz law as:

$$\gamma_e = \frac{(n^2-1)(n^2+2)}{3}, \tag{5.8}$$

where n is the refractive index. As this negative pressure pulls the fiber material towards the core, the density changes according to the continuity equation:

$$\frac{\partial^2 \rho}{\partial t^2} = -\nabla^2 p_e = -\frac{1}{2}\epsilon_0 \gamma_e \nabla^2 < E^2 > . \tag{5.9}$$

On the other hand, the resulting change in the density induces an elastic force according to Hook's law:

$$\frac{\partial^2 \rho}{\partial t^2} = v^2 \nabla^2 \rho, \tag{5.10}$$

which is a linear wave equation and can be solved by the separation of variables. If we approximate the fiber as cylindrically symmetric, the separation of variable reads:

$$\begin{aligned} \rho(r,t) = R(r)T(t) \\ \frac{\frac{d^2T}{dt^2}}{T(t)} = \frac{v^2 \nabla^2 R(r)}{R(r)} = -v^2 K^2, \end{aligned} \tag{5.11}$$

where we have chosen the separation constant as $-v^2K^2$. First we treat the radial part. Multiplying by $\frac{2\pi r R}{v^2 K^2}$, we get:

$$\frac{2\pi r}{K^2}\frac{d^2R}{dr^2} + \frac{2\pi}{K^2}\frac{dR}{dr} + 2\pi r R = 0. \tag{5.12}$$

We also take the following boundary condition:

$$\begin{aligned} \frac{dR}{dr}|_{r=0} = 0 \\ R(r_{clad}) = 0 \end{aligned} \tag{5.13}$$

where r_{clad} is the radius of the glass fiber. The condition at $r = 0$ merely assumes that the density varies smoothly. The condition at $r = r_{clad}$, however, is artificially imposed for convenience. The combination of equation 5.12 and the boundary condition implies that the solutions of the radial part form a complete basis that is orthogonal with respect to the inner product:

$$\int_0^{r_{clad}} R_1(r)R_2(r)2\pi r dr = 0. \tag{5.14}$$

Now, we multiply equation 5.12 with $rK^2/2\pi$ and look for solutions of the form:

$$\begin{gathered} R(r) = J(kr) \\ r^2\frac{d^2J(Kr)}{dr^2} + r\frac{dJ(Kr)}{dr} + K^2r^2J(kr) = 0 \\ x^2\frac{d^2J(x)}{dx} + r\frac{dJ(x)}{dx} + x^2J(x) = 0, \end{gathered} \tag{5.15}$$

where we have defined $x \equiv Kr$. This is a Bessel equation of order zero. The boundary condition necessitates that the solution is the Bessel function of the first kind and that K is such that:

$$\begin{gathered} J(K_m r_{clad}) = 0 \\ \Longrightarrow K_m \approx \frac{(m - 1/4)\pi}{r_{clad}}. \end{gathered} \tag{5.16}$$

where m denotes the acustic mode.

The temporal part has a purely sinusoidal behavior. However, this results from the frictionless model of equation 5.10. Experiments show [71, 72] that such oscillations in fused silica glass decay exponentially with an exponent that's parabolic in the oscillation frequency. For example, an acoustic plane wave behaves like:

$$\rho = e^{i(Kx - wt)}e^{-\alpha w^2 t}; \alpha \approx 4.1 \times 10^{-5} ns. \tag{5.17}$$

This behavior can be captured if we add viscous friction to equation 5.10:

$$\begin{gathered} \frac{\partial^2\rho}{\partial t^2} - v^2\nabla^2\rho - 2A\frac{\partial}{\partial t}\nabla^2\rho = 0 \\ (iw + \alpha w^2)^2 + v^2K^2 - 2AK^2(iw + \alpha w^2) = 0 \\ \Longrightarrow A \approx \alpha v^2. \end{gathered} \tag{5.18}$$

Now, adding the elastic, the viscous friction, and the electrostrictive forces together, we get:

$$\frac{\partial^2\rho}{\partial t^2} - v^2\nabla^2\rho - 2A\frac{\partial}{\partial t}\nabla^2\rho = -\frac{1}{2}\epsilon_0\gamma_e\nabla^2 < E^2 > . \tag{5.19}$$

The electric field can be written in terms of the optical power passing through the fiber and its spatial distribution, which is approximated as a Gaussian:

$$< E^2 >= \frac{n}{c\epsilon\epsilon_0}\frac{1}{\pi a^2}e^{-(\frac{r}{a})^2}P(t), \tag{5.20}$$

where c is the speed of light and we have approximated the group velocity by $\frac{c}{n}$. The spatial distribution of the optical mode practically satisfies the boundary condition 5.13. This means that we can exploit the completeness and orthogonality of the radial solutions above to express the spatial distribution of the electric field as:

$$\begin{aligned} \frac{1}{\pi a^2}e^{-(\frac{r}{a})^2} &= \sum_{m=1}^{\infty} S_m J(K_m r); \\ S_m &= \int_0^{r_{clad}} J(K_m r)\frac{1}{\pi a^2}e^{-(\frac{r}{a})^2}2\pi r dr. \end{aligned} \tag{5.21}$$

The spatial overlap factor, S_m, determines how strongly the optical mode excites the m^{th} acoustic mode. It depends on the core diameter of the fiber (through the parameter a) and the natural frequency of the acoustic mode, as illustrated in figure 5.6.

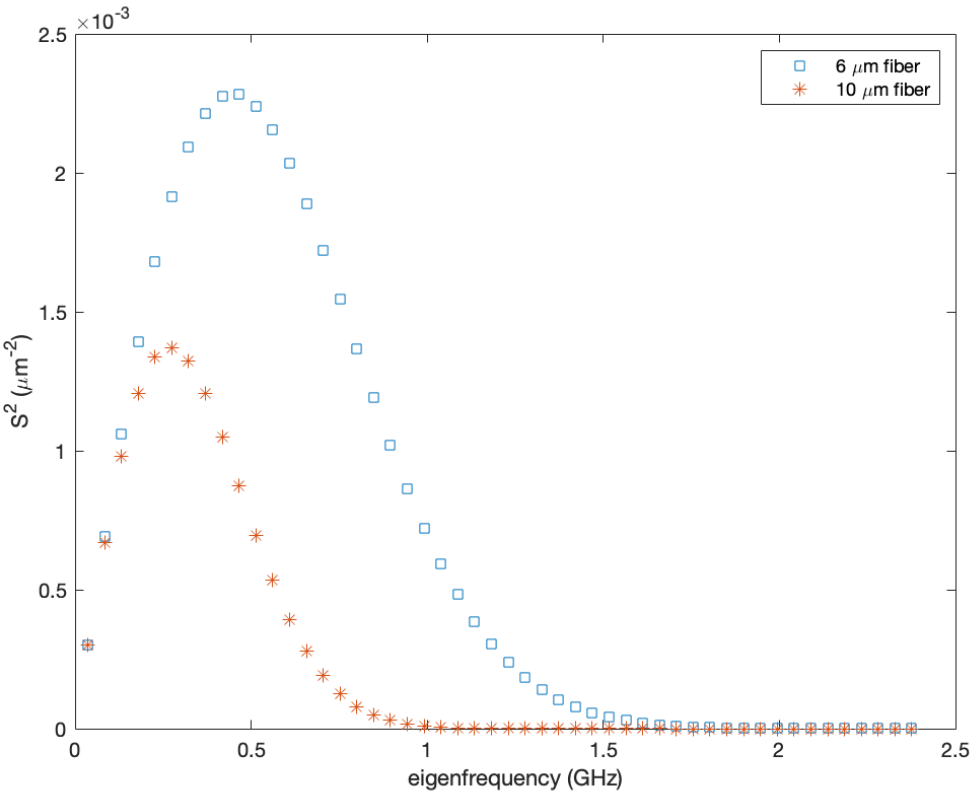

Figure 5.6: The spatial overlap factor for each acoustic mode versus the natural frequencies (eigenfrequencies) of the modes $\frac{v^2 K_m^2}{2\pi}$ for two different fiber core diameters, $6\mu m$ ($a = 3/\sqrt{2}$) and $10\mu m$ ($a = 5/\sqrt{2}$). Fibers with narrower core diameters excite acoustic modes with higher frequencies

In time, the optical signal can have any pattern and is not limited to the natural frequencies of the acoustic modes. Therefore, we look for a solution of the form:

$$\rho(r,t) = \sum_{m=1}^{\infty} J(K_m r) \int_{-\infty}^{+\infty} \widetilde{\rho}_m(w) e^{iwt} dw. \tag{5.22}$$

Substituting this ansatz into equation 5.19, we solve for the density perturbation:

$$\rho(r,t) = \frac{n\gamma_e}{2c\epsilon} \sum_{m=1}^{\infty} J(K_m r) \int_{-\infty}^{+\infty} \frac{S_m K_m^2 \widetilde{P}(w)}{v^2 K_m^2 - w^2 + 2iAwK_m^2} e^{iwt} dw. \tag{5.23}$$

The density perturbation influences the pulses by modifying the refractive index of the fiber. Taking $\epsilon = n^2$, we find

$$\begin{aligned} \delta n(r,t) &= \frac{1}{2n} \frac{\partial \epsilon}{\partial \rho} \rho(r,t) \\ &= \frac{{\gamma_e}^2}{4cn^2\rho_0} \sum_{m=1}^{\infty} J(K_m r) \int_{-\infty}^{+\infty} \frac{S_m K_m^2 \widetilde{P}(w)}{v^2 K_m^2 - w^2 + 2iAwK_m^2} e^{iwt} dw \\ \delta n_{\text{effective}}(t) &= \frac{{\gamma_e}^2}{4cn^2\rho_0} \sum_{m=1}^{\infty} \int_{-\infty}^{+\infty} \frac{S_m^2 K_m^2 \widetilde{P}(w)}{v^2 K_m^2 - w^2 + 2iAwK_m^2} e^{iwt} dw, \end{aligned} \tag{5.24}$$

where we have averaged the refractive index perturbation over the optical mode, bringing another factor of S_m. As we're only interested in this effective index modulation, we will drop its subscript.

The refractive index modulation affects the speeds of the pulses in two ways: it directly modulates the speeds:

$$\dot{\tau}_i = \frac{L_{\delta n} \delta n(\tau_i)}{cT_R}, \tag{5.25}$$

where, $L_{\delta n}$ is the length of the fiber where δn is in effect, and T_R is the cavity roundtrip time. Note the dependence of the index modulation on the temporal position of the pulse, τ_i; different pulses at different temporal positions experience different index modulations and speeds.

Additionally, the refractive index modulation affects the pulses in another way, by causing the following wavelength shift:

$$\delta\lambda(\tau_i) = \frac{cL_{\delta n}}{\lambda} \frac{d(\delta n)}{dt} \Big|_{\tau_i}. \tag{5.26}$$

The effect of the wavelength shift depends on the rest of the laser dynamics. For the soliton and dispersion-managed soliton regimes, the only regimes known at the time when this theory was developed, the pulses experience only weak filtering every roundtrip, and the small frequency shift accumulates one roundtrip after another. Then, with dispersion (see chapter 2), the speeds of the pulses are modulated. For soliton lasers, this effect is much stronger than the direct effect of the refractive index modulation [5]. We show this with the order of magnitude analysis below.

Figure 5.7 shows the refractive index modulation and the corresponding wavelength shift for regular pulse trains at two different frequencies. They are calculated for the post-amplification section of the Kerr arm in our Mamyshev oscillator (pulse energy=$2nJ$ and $L_{\delta n} = 2.5m$). As can be inferred from this figure, the order of magnitude of the refractive index modulation and the wavelength shift in our laser are 10^{-9} and $10^{-4}nm$, respectively. These values would be one order of magnitude lower in a soliton laser due to its lower pulse energy. The index modulation corresponds to relative pulse speeds on the order of 0.1 nanosecond per second, which is one or two orders of magnitude slower than what we observe on the oscilloscope. We want to estimate the order of magnitude of the effect of the wavelength shift (for a soliton laser), and for that, we must model the filtering process first. We use a Gaussian spectral shape for both the pulse and the filter:

$$\text{pulse spectrum} : e^{-(\frac{\lambda-(\lambda_f+\Delta\lambda)}{\Delta_p})^2}; \text{filter} = e^{-(\frac{\lambda-\lambda_f}{\Delta_f})^2}, \tag{5.27}$$

where Δ_f is the spectral width of the filter, Δ_p is the spectral width of the pulse, λ_f is the central wavelength of the filter and $\Delta\lambda$ is the difference between it and the central wavelength of the pulse. After passing through the filter, the wavelength of the pulse gets closer to the center of the filter:

$$\begin{gathered} e^{-(\frac{\lambda-(\lambda_f+\Delta\lambda)}{\Delta_p})^2} \times e^{-(\frac{\lambda-\lambda_f}{\Delta_f})^2} \propto e^{-(\frac{\lambda-(\lambda_f+\Delta\lambda')}{\Delta_{p'}})^2}; \\ \Delta\lambda' = \frac{{\Delta_f}^2}{{\Delta_p}^2+{\Delta_f}^2}\Delta\lambda. \end{gathered} \tag{5.28}$$

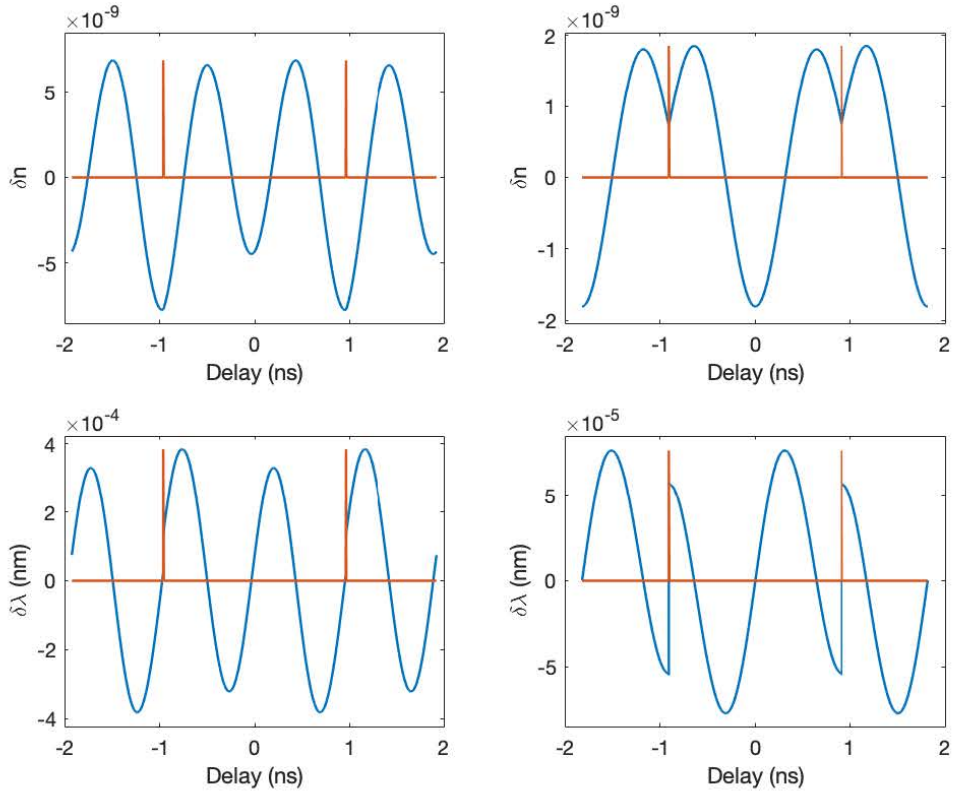

Figure 5.7: The refractive index modulation and wavelength shift for a regular pulse train at 520 MHz frequency (left) and a pulse train at 550 MHz (right). The orange spikes represent the optical ultrashort pulses and the blue curves represents the refractive index modulation or wavelength shift. The pulses are modeled as Dirac deltas, which causes a discontinuity in the derivative of δn and a jump discontinuity in $\delta\lambda$.

Writing $\delta\lambda$ as a function of the roundtrip, indexed by n, and the pulse position, τ_i, and adding the acoustically induced wavelength shift, $\delta\lambda(\tau_i)$,

$$\begin{aligned}\Delta\lambda(n,\tau_i) =& \frac{{\Delta_f}^2}{{\Delta_p}^2+{\Delta_f}^2}\Delta\lambda(n-1,\tau_i)+\delta\lambda(\tau)\\ \Longrightarrow& \Delta\lambda(\infty,\tau_i)=\frac{{\Delta_f}^2+{\Delta_p}^2}{{\Delta_p}^2}\delta\lambda(\tau_i),\end{aligned} \tag{5.29}$$

where $\Delta\lambda(\infty,\tau_i)$ is the accumulated wavelength shift at the position of the i^{th} pulse, τ_i. As discussed in section 2, we recognize that $\Delta\lambda(l,\tau_i)$ approaches $\Delta\lambda(\infty,\tau_i)$ in a negligibly short time and use this ultimate value to approximate the evolution of the pulse pattern. Therefore we drop the dependence on the roundtrip.

In the soliton regime, the spectrum of the filter, which arises from the finite bandwidth of the gain, is much wider than the pulse spectrum. Taking the spectral width of the pulse to be one order of magnitude smaller than that of the filter, we find that the accumulated wavelength shift is on the order of $10^{-3}nm$. The combination of dispersion and accumulated wavelength shift implies the relative pulse speeds:

$$\begin{aligned}\dot{\tau_i} &= D_{net}\Delta\lambda(\tau_i);\\ D_{net} &= \frac{D_{fiber}L_{fiber}}{T_R},\end{aligned} \tag{5.30}$$

where D_{net} is the total dispersion in the cavity in $\frac{ns}{nm.sec}$ and D_{fiber} is the dispersion property of the fiber in $\frac{ps}{nm.km}$. The second equation holds only in the absence of dispersive elements in the cavity other than the fiber. A typical all-fiber soliton laser at a central wavelength of 1.55 μm has a D_{net} of $\sim 0.4\times 10^4\frac{ns}{nm.sec}$. With $\delta\lambda$ on the order of $10^{-3}nm$, this implies that the relative pulse speeds are on the order of 10 ns/sec, which agrees with experiments [5].

In lasers with dispersion compensation, D_{net} is decreased. Also, a lower D_{net} is correlated with a wider pulse spectrum, Δ_p, which decreases the accumulated wavelength shift, $\Delta\lambda$. Therefore, one may conclude that dispersion-compensation decreases the relative pulse speeds. This has been observed experimentally in [69] and in [45], where it reportedly took on the order of minutes for the pulse organization to stabilize.

We would like to ascertain that harmonic mode-locking is a stable fixed point under the acoustically mediated interactions. Adding the contribution to the pulse speeds from both the refractive index modulation and its derivative:

$$\dot{\tau_i} = \frac{{\gamma_e}^2}{4cn^2\rho_0} \sum_{m=1}^{\infty} \int_{-\infty}^{+\infty} \frac{S_m^2 K_m^2 (\alpha + iw\beta)\widetilde{P}(w)}{v^2 K_m^2 - w^2 + 2iAwK_m^2} e^{iwt} dw, \tag{5.31}$$

where we have expressed the derivative in frequency domain and used α and β for the contribution of the index modulation and its derivative, respectively. The optical power can be modeled by taking the pulses as Dirac delta functions:

$$P(t) \propto \sum_{j=1}^{N} \delta(\tau - \tau_j). \tag{5.32}$$

Then, our dynamical system becomes:

$$\begin{aligned} \dot{\tau_i} &\propto \sum_{h=-\infty}^{+\infty} T_f(w_h)(\alpha + iw_h\beta) \sum_{j=1}^{N} e^{iw_h(\tau_i - \tau_j)}; \\ T_f(w) &= \sum_{m=1}^{\infty} \int_{-\infty}^{+\infty} \frac{S_m^2 K_m^2}{v^2 K_m^2 - w^2 + 2iAwK_m^2};\ w_h = \frac{2\pi h}{T_R}, \end{aligned} \tag{5.33}$$

where w_h denotes the frequencies that are permitted by the periodicity of the cavity. The derivatives of $\dot{\tau_i}$ are:

$$\begin{aligned} \frac{\partial \dot{\tau_i}}{\tau_i} &\propto \sum_{h=-\infty}^{+\infty} T_f(w_h)(\alpha + iw_h\beta)(iw_h) \sum_{j \neq i} e^{iw_h(\tau_i - \tau_j)}, \\ \frac{\partial \dot{\tau_i}}{\tau_j} &\propto \sum_{h=-\infty}^{+\infty} T_f(w_h)(\alpha + iw_h\beta)(-iw_h) e^{iw_h(\tau_i - \tau_j)};\ i \neq j. \end{aligned} \tag{5.34}$$

Then, the eigenvalues (equation 5.4) are found as:

$$\gamma_k \propto \sum_{h=-\infty}^{+\infty} T_f(w_h)(\alpha + iw_h\beta)(-iw_h) \sum_{j=2}^{N} e^{iw_h(\tau_1 - \tau_j) + i\frac{2\pi}{N}(j-1)k} - e^{iw_h(\tau_1 - \tau_j)}. \tag{5.35}$$

Noting the definition of w_h and the fact that $\tau_i = \frac{T_R}{N} i$ at harmonic mode-locking, and using the identity:

$$\begin{aligned} \sum_{j=0}^{N-1} e^{i\frac{2\pi}{N}j} &= N; j = lN, \\ \sum_{j=0}^{N-1} e^{i\frac{2\pi}{N}j} &= 0; j \neq lN, \end{aligned} \tag{5.36}$$

where l is any integer, then, equation 5.35 can be simplified:

$$\begin{aligned}\gamma_k &\propto \sum_{h=-\infty}^{+\infty} T_f(w_h)(\alpha + iw_h\beta)(-iw_h) \sum_{j=0}^{N-1} e^{i\frac{2\pi}{N}j(k-h)} \\ &= N \sum_{l=-\infty}^{+\infty} T_f(w_{l,k})(\alpha + iw_{l,k}\beta)(-iw_{l,k});\ w_{l,k} = \frac{2\pi}{T_R}(lN+k).\end{aligned} \tag{5.37}$$

Using the definition of T_f, the real parts of the eigenvalues are found as:

$$Re(\gamma_k) \propto \sum_{l=-\infty}^{+\infty} \sum_{m=1}^{\infty} \frac{S_m^2 K_m^2}{(v^2K_m^2 - w_{l,k}^2)^2 + (2Aw_{l,k}K_m^2)^2}[(v^2K_m^2 - w_{l,k}^2)w_{l,k}^2\beta - 2Aw_{l,k}^2K_m^2\alpha]. \tag{5.38}$$

From equation 5.38, it can be seen that the terms multiplying α are all negative. Similarly, the terms multiplying β sum up to negative values for each of the γ_ks as long as l reaches a sufficiently large number, i. e. as long as the pulse duration is sufficiently small. As α is always positive regardless of the mode-lock regime, lasers with positive β permit harmonic mode-locking as an attractor. This is the case for soliton (negative dispersion) lasers. Similarly, lasers with near-zero β also permit harmonic mode-locking as the α term dominates. This is the case for lasers with near-zero dispersion or narrow spectral filtering [46, 45, 43]. This result is consistent with the general tendency to realize harmonic mode-locking in soliton lasers but not in positive dispersion lasers.

This is, to our knowledge, the first analytical expression for the eigenvalues at harmonic mode-locking. In [66], the authors seem to have analyzed the stability of harmonic mode-locking semi-analytically and found mode-locking to be stable for only some harmonics of a given cavity length, which contradicts our experimental results, as well as others in the literature [41]. The reason behind this discrepancy is unclear because the authors in [66] did not present their analysis in sufficient detail.

In this analysis, we have implicitly assumed that the acoustic waves are always at their steady-state mandated by the pulse positions, even during the evolution of the pulse pattern. In other words, we have assumed that the acoustic oscillations are slaved to the pulse pattern. This is justified by its slow evolution.

In [5], the exact opposite assumption was implicitly made, where a fixed index modulation was used to write a modified master equation with acoustically induced phase modulation. This predicts harmonic mode-locking only around the acoustic eigenfrequencies, which contradicts the experimental results.

5.5 Our acoustically mediated emergent interactions

From the preceding discussion, we conclude that the wavelength shift cannot accumulate significantly in our Mamayshev oscillator because of the narrow filters. However, the observed pulse speeds are an order of magnitude higher than the speeds predicted from the direct effect of the index modulation alone (the α term). Moreover, the empirical fact that adjusting the filter positions changes the pulse organization suggests a connection between the β parameter and the filter positions in our oscillator.

The effect of the wavelength shift is similar to changing the pulse energy in that both processes change the filtered pulse energy by moving the outermost spectral lobe with respect to the filter. If we take the spectral broadening to be linear with the pulse energy, the wavelength shift is roughly equivalent to the following energy perturbation:

$$\frac{\delta E}{E_0} \approx \frac{+2\ \delta\lambda}{S_p}, \tag{5.39}$$

where S_p is the spectral width of the pulse and E_0 is the pulse energy without the perturbation. The positive sign assumes that the subsequent filter is red-shifted, which is true for the Kerr arm in our experiments; we neglect the acoustic oscillation and the associated wavelength shift in the similariton arm because of the large core diameter of its fiber, which weakens the acoustic oscillations in it (see figure 5.6).

Adding this energy perturbation to the energy map (see chapter 4), we see

that the energy perturbation accumulates:

$$\begin{aligned} E_0 + \Delta E(n, \tau_i) &= f(E_0 + \Delta E(n-1, \tau_i)) + \delta E(\tau_i) \\ &\approx f(E_0) + \left.\frac{df}{dE}\right|_{E_0} \Delta E(n-1, \tau_i) + \delta E(\tau_i) \\ \Longrightarrow \Delta E(\infty, \tau_i) &= \frac{\delta E(\tau_i)}{1 - \left.\frac{df}{dE}\right|_{E_0}}, \end{aligned} \tag{5.40}$$

where, as with the accumulated wavelength shift, we use $\Delta E(\infty, \tau_i)$ to calculate the pulse speeds and drop the dependence on the roundtrip. The magnitude of the accumulated energy perturbation can be adjusted by adjusting the filter positions relative to the spectra, with the highest accumulation of energy perturbation occurring when the filters are positioned such that $\frac{df}{dE}$ approaches 1. This is in line with the experimental behavior we reported in figure 5.4.

Since δE is negligible in the similariton arm, we use equation 5.40 to describe the accumulated pulse energy perturbation at the output of the Kerr arm only. Therefore, we name the accumulated perturbation ΔE_k. As discussed in chapter 4, the energy perturbation in the similariton arm, ΔE_s, is related to ΔE_k according to:

$$\begin{aligned} E_s = f_{s,k}(E_k) \Longrightarrow \Delta E_s &= \frac{df_{s,k}}{dE_k} \Delta E_k; \\ f(E) = f_{k,s}(f_{s,k}(E)) \Longrightarrow \frac{df}{dE} &= \frac{df_{k,s}}{dE_s} \frac{df_{s,k}}{dE_k}, \end{aligned} \tag{5.41}$$

where the function $f_{s,k}$ ($f_{k,s}$) maps the energy at the output of the Kerr arm (similariton arm) to the energy at the output of the similariton arm (Kerr arm). These two functions can be controlled separately, by adjusting the filter positions relative to the lobes in their respective spectra as long as the derivative of the energy map, $\frac{df}{dE}$, is kept below 1 so as to avoid pulse death (see chapter 4).

But how does the energy perturbation affect the speeds of the pulses? The answer lies in the combination of chirp and offset spectral filtering: because of the chirp, the different spectral components of the pulse are distributed over different temporal positions along the pulse. Consequently, the offset filter picks a part of the pulse that is offset in time compared to the original. This is illustrated in figure 5.8.

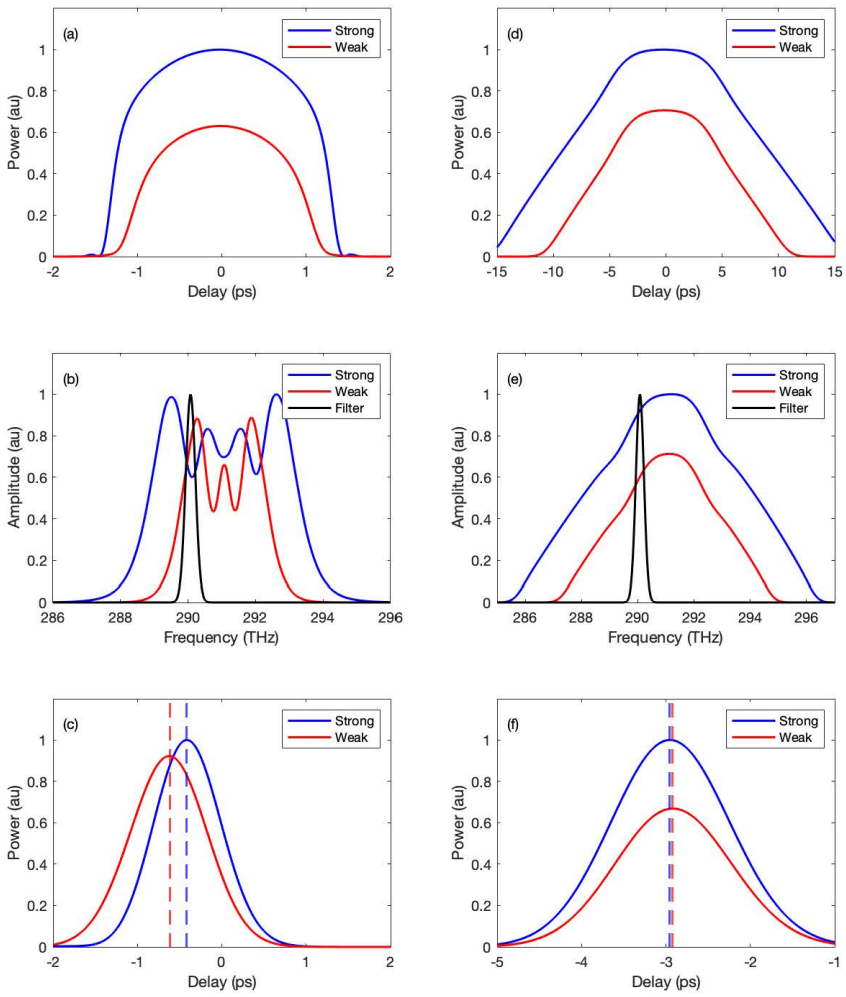

Figure 5.8: Simulation of the temporal shift due to offset filtering. The red curve refers to a low-energy pulse, and the blue curve refers to a high-energy pulse. The left-hand side (a, b, c) shows the result of simulating our Kerr arm, whereas the right-hand side (d, e, f) shows the result of the same simulation but with the passive fiber after amplification ten times as long. (a, b) the temporal and spectral shapes just before the filter in the Kerr arm; (c) the filtered pulse after the Kerr arm. The temporal shift decreases with higher energy; (d, e) the temporal and spectral shapes after propagating through a much longer arm; (f) the filtered pulse after the longer arm. The temporal shift increases slightly with higher energy. Increasing the pulse energy increases the temporal shift when dispersion is strong and decreases it when it's weak.

Assuming the spectrum is distributed linearly along the temporal shape of the pulse, the temporal shift due to offset filtering is:

$$\tau_o = -O\frac{T_p}{S_p}, \tag{5.42}$$

where τ_o is the temporal shift due to offset filtering, O is the filter offset in nanometers, positive for a red-shifted filter and negative for a blue-shifted filter, and T_p and S_p are the temporal and spectral widths of the pulse, respectively. The negative sign assumes the chirp is positive, which is the case in our laser.

This shift changes with ΔE according to:

$$\begin{aligned} \Delta\tau_o &= \frac{d\tau_o}{dE}\Delta E \\ &= O(\frac{T_p}{S_p^2}\frac{dS_p}{dE} - \frac{1}{S_p}\frac{dT_p}{dE})\Delta E \end{aligned} \tag{5.43}$$

The first derivative term corresponds to the effect of Kerr nonlinearity alone. Assuming the pulse propagation is dominated by Kerr nonlinearity, this derivative can be approximated as $\frac{S_p}{E_0}$. The second derivative corresponds to the effect of dispersion after the generation of the spectral components through nonlinearity: increasing the pulse energy strengthens Kerr nonlinearity such that the spectrum broadens earlier in its propagation through the fiber and, consequently, the pulse experiences dispersion for a longer distance. Whether one effect dominates over the other is determined by whether the temporal duration or spectral duration increases more with the pulse energy. In figure 5.8, two cases are shown, one in our Kerr arm, where the effect of Kerr nonlinearity is dominant, and one in a similar amplification arm but with a much longer passive fiber after amplification. In the Kerr-dominant case, the spectral duration broadens significantly more than the temporal duration and, so, increasing the pulse energy pulls the filtered pulse closer to the center of the original one. In the case of the long arm, on the other hand, dispersion is much more pronounced, and the temporal duration broadens slightly more than the spectral duration, which slightly pushes the filtered pulse away from the center of the original pulse upon increasing the pulse energy. This behavior can be achieved by approaching the active similariton attractor, where the spectral and temporal widths are both linear in the initial pulse energy [27]. This is achieved without the tens of meters of passive fiber needed to produce

the result of figure 5.8f. In Figure 5.9, we show the results of a simulation where we change the pulse energies in each of the two arms of our Mamyshev oscillator separately by adjusting the linear losses between the arms and the gain saturation energies. Increasing the pulse energy in either arm increases the delay of the pulse despite the opposite filter offset they have. This means that the spectral width broadens more than the temporal width in the Kerr arm and less than the temporal width in the similariton arm. The latter may be attributed in part to the similariton attractor.

Denoting the shift due to offset filtering after the Kerr arm as $\tau_{o,k}$ and the shift due to offset filtering after the similariton arm as $\tau_{o,s}$, the delays at both filters combined result in the following pulse speed:

$$\begin{aligned} \dot{\tau_i} &\approx \frac{1}{T_R}\left(\frac{d\tau_{o,k}}{dE_k} + \frac{d\tau_{o,s}}{dE_s}\frac{df_{s,k}}{dE_k}\right)\frac{2\ E_0}{S_p(1-\frac{df}{dE}\big|_{E_0})}\delta\lambda(\tau_i) \\ &= \frac{1}{T_R}\left(\frac{d\tau_{o,k}}{dE_k} + \frac{d\tau_{o,s}}{dE_s}\frac{df_{s,k}}{dE_k}\right)\frac{2\ E_0}{S_p(1-\frac{df}{dE}\big|_{E_0})}\frac{cL_{\delta n}}{\lambda}\frac{d(\delta n)}{dt}\ \big|_{\tau_i}. \end{aligned} \tag{5.44}$$

We now calculate the order of magnitude of the pulse speeds. Taking $\delta\lambda$ on the order of 10^{-4} nm, S_p and O on the order of a few nanometers, T_p on the order of few picoseconds, T_R on the order of 10^{-7} seconds and $\frac{1}{1-\frac{df}{dE}}$ on the order of 10 and taking only the shift due to the nonlinearity in one arm, the resulting $\dot{\tau_i}$ is on the order of 10 ns/sec, which agrees with our experimental observation.

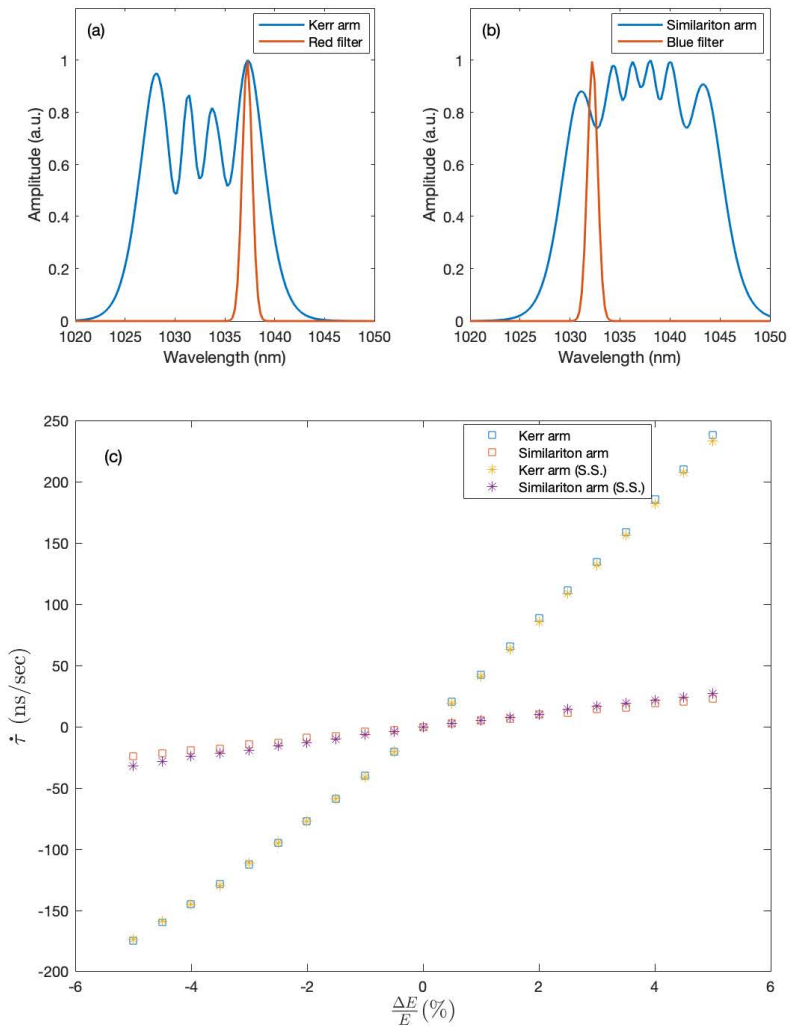

Figure 5.9: Simulation results for the delay experienced by a pulse in our Mamyshev oscillator upon changing the pulse energy in the Kerr arm and the similariton arm, separately. (a, b) the optical spectra and corresponding filters; (c) the delay versus the change in the pulse energy in each arm separately while fixing the pulse energy in the other arm. The stars represent simulations with self-steepening. The delay increases with pulse energy in both arms. Given the order of the filters, this means that the spectrum broadens more than the temporal duration in the Kerr arm but not in the similariton arm. This may be attributed to the similariton attractor.

For harmonic mode-locking to be stable, the coefficient of $\frac{d(\delta n)}{dt}$ in equation 5.44 (the β parameter in equation 5.38) has to be positive, which is the case as long as the net delay in the two arms increases with the pulse energy. However, our analysis here neglects multiple smaller effects. For example, we have neglected the small change in the filtered wavelength due to the motion of the spectral lobes with respect to the filters, which can be caused by the direct wavelength shift or the accumulated change in the pulse energy. We believe that this effect significantly decreased the delay caused by increasing the energy in the Kerr arm in figure 5.9 by red-shifting the pulse transmitted to the similariton arm with higher energies. We have also neglected the most obvious contribution to the pulse speeds, self-steepening, which is the dependence of the group velocity on the optical power. However, figure 5.9 shows that it is truly negligible.

From this analysis, we see that the pulse interactions in our laser emerge from its pulse shaping dynamics and not from the acoustic oscillations alone. This is why adjusting the filter positions, which does not affect the acoustic waves, affects the pulse interactions and the pulse pattern. The role of the acoustic waves is merely to facilitate the communication between the pulses. If another "messenger" mechanism is found, our analysis above can be used to *engineer* the pulse interactions.

5.6 Manipulation via a secondary loop

Here we present a novel technique to manipulate the pulse interactions using an orthogonally polarized secondary loop. A detailed schematic representation of the secondary loop was presented in chapter 3. We present a simplified schematic here in figure 5.10. It should be emphasized that the pulses sent by the secondary loop are orthogonally polarized. This means that they do not survive the polarizer after the Kerr arm. Each pulse sent by the secondary loop passes through the Kerr arm only once then directly gets extinguished at this polarizer. To distinguish these pulses, we refer to them as "secondary loop pulses" and refer to the pulses that circulate in the cavity as "cavity pulses."

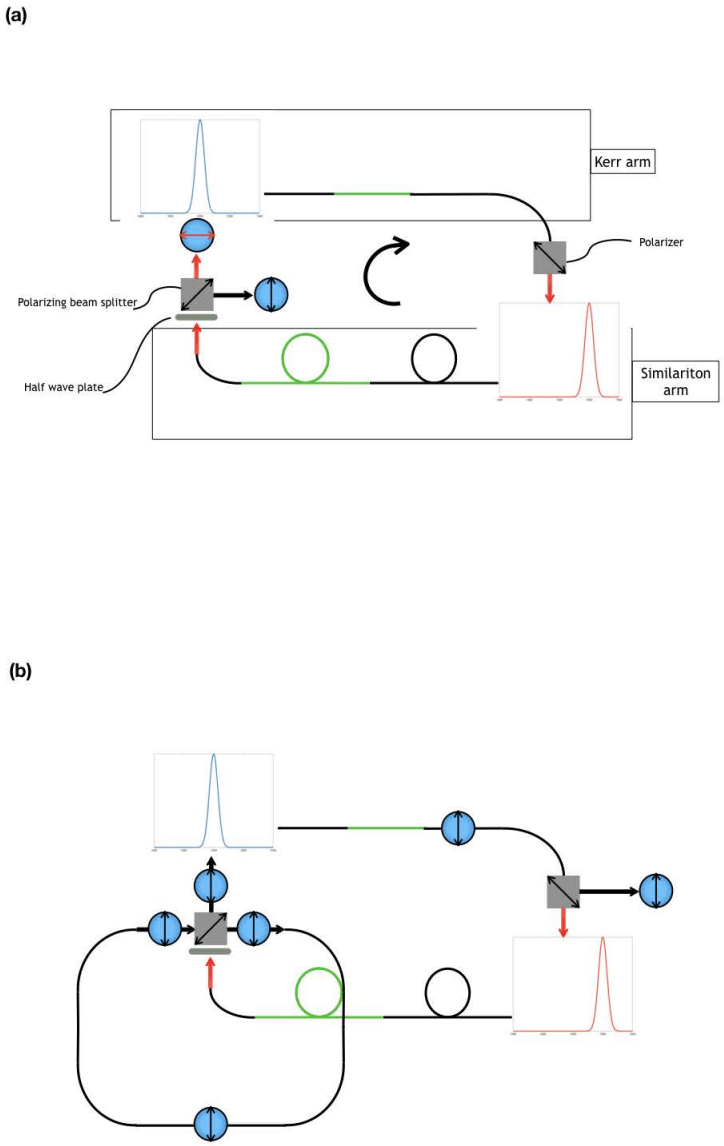

Figure 5.10: Schematic illustration of the orthogonally polarized secondary loop: (a) a simplified representation of our oscillator without the secondary loop. The combination of a half-wave plate and a polarization beam splitter splits the beam into two orthogonal polarization, one polarization continues to circulate in the cavity, and the other polarization leaves the cavity, (b) a simplified representation of the secondary loop and the travel of its pulses. The secondary loop takes the beam with the polarization that leaves the cavity and re-injects it into the cavity with a delay. This re-injected beam travels through the Kerr arm then gets extinguished by the polarizer after it due to its orthogonal polarization; it does not reach the similariton arm

The fact that the secondary loop pulses do not circulate in the cavity highlights the nature of the pulse interactions: each pulse influences the pulses following it by perturbing the fiber itself. In sections 3-5 we have argued that this perturbation is acoustic.

The difference introduced by the secondary loop pulses is that they drive the acoustic oscillations along with the cavity pulses but they are not affected by the acoustic oscillations; their temporal positions are fixed by the delay of the secondary loop. Mathematically, the secondary loop changes the driving force of the acoustic oscillations to:

$$\begin{aligned} P(\tau) &\propto \sum_{j=1}^{N} \delta(\tau - \tau_j) + \delta(\tau - (\tau_j + d)) \\ \implies \dot{\tau_i} &\propto \sum_{h=-\infty}^{+\infty} T_f(w_h)(\alpha + i w_h \beta) \sum_{j=1}^{N} e^{i w_h (\tau_i - \tau_j)}, + e^{i w_h (\tau_i - (\tau_j + d))} \end{aligned} \tag{5.45}$$

where d is the secondary loop delay and the second Dirac delta term represents the secondary loop pulse. Its position is written in terms of its parent cavity pulse to highlight that it does not add a new degree of freedom.

We now demonstrate the behavior of this new dynamical system experimentally.

If we start the state with two cavity pulses at a delay smaller than 3.5 ns, their delay increases up to $\sim$ 3.5 ns and stabilizes there. If we block the secondary loop, the delay starts to increase. If we unblock the secondary loop after a second or so, the delay stabilizes at ~ 8 ns, which is the secondary loop delay. If we block the secondary loop again for about a second, the delay moves and stabilizes at ~ 12 ns, and so on... This way, we have documented 13 different stable fixed points in addition to harmonic mode-locking, each of which can be reached from a smaller delay simply by blocking and unblocking the secondary loop by hand. These fixed points are plotted in figure 5.11.

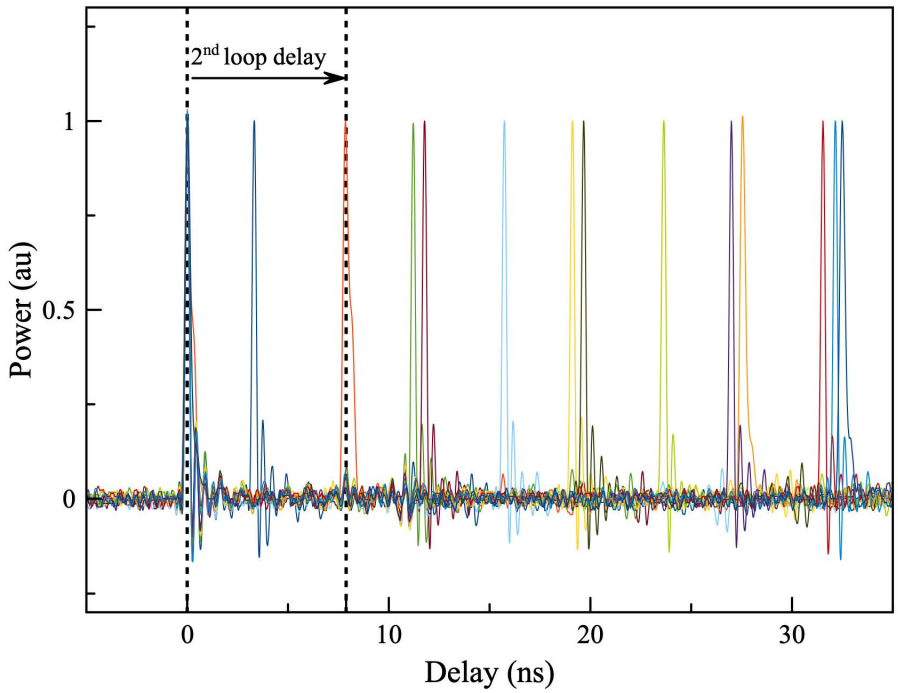

Figure 5.11: fixed delays between the cavity pulse under the effect of the secondary loop. Each of the 13 different colors represents a pair of pulses at a different stable delay. Transitions from smaller to larger delays are done by temporarily blocking the secondary loop.

These stable delays are yet another example of multistability. Choice of the attractor is determined by the initial state when the secondary loop is unblocked; blocking then unblocking the secondary loop changes the delay by delivering the pulse pair to the basin of attraction of the new stable delay.

This system also features bifurcation. This is to be expected from our discussion on the acoustic interactions and the adjustment of the β parameter with the filter positions. Figure 5.12 demonstrates a bifurcation where the delay between the pulses is moved back and forth between a pair of delays by moving the filter offset. Staring from, say, fixed point 1 and changing the filter offset beyond a critical point, the delay always moves to fixed point 2. This indicates that the fixed point is not turned unstable but is actually destroyed.

It's easy to explain this bifurcation in terms of our pulse interaction theory: At fixed point 1, the filters are positioned at steep slopes in their respective spectra (figure 5.12a and 5.12b). This implies that the derivative of the energy map is large, and the pulse energy perturbation is allowed to accumulate. Following the discussion in the previous section, this implies that the β parameter is large. Therefore, fixed point 1 is a fixed point of the system of equation 5.45 when the β term is dominant. When the filter offset is moved to that of figures 5.12c and 5.12d, the filters approach the peaks in their respective spectra, which means that the derivative of the energy map is approximately zero, and the energy perturbation cannot accumulate. This lowers the β parameter to approximately zero and allows the α term in equation 5.33 to dominate, under which, fixed point 1 is no longer a fixed point.

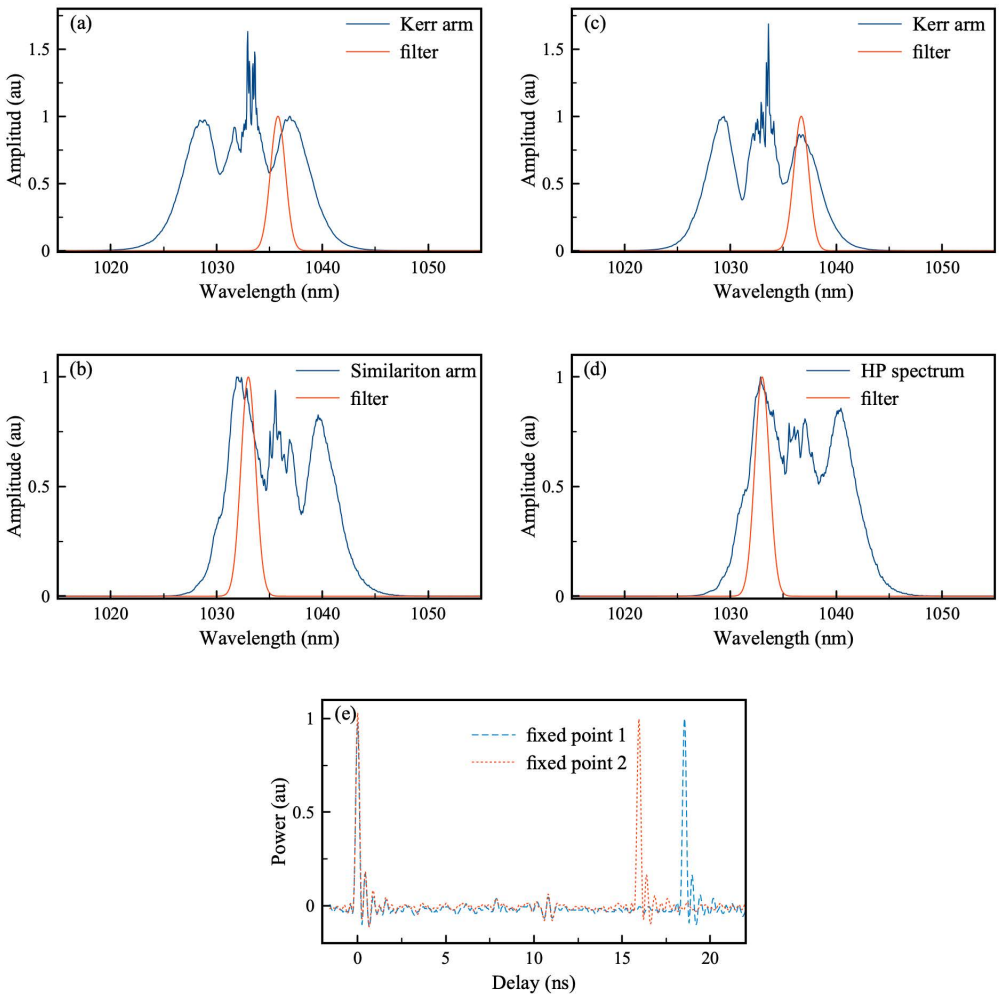

Figure 5.12: Bifurcation by changing filter offset: (a, b) the spectra and filter positions corresponding to fixed point 1, (c, d) the spectra and filter positions corresponding to fixed point 2, (e) oscilloscope traces for the two fixed points. Moving the filter positions from the steep slopes (a, b) to the peaks (c, d) destroys fixed point 1 and moves the delay to fixed point 2. Moving the filter offset back moves the delay back to fixed point 1

Our experimental account only scratches the surface of the possibilities with this technique. For example, we expect the positions of the fixed points to vary with the delay of the secondary loop, likely spanning all delays from $\sim$1 ns to half the cavity the period. Moreover, this technique can be applied with any number of cavity pulses, allowing many attractors with complicated pulse patterns. The choice of the attractor may be made by well-timed seeding of isolated pulses, as opposed to the stream of seed pulses we used. It may be possible to develop a precise numerical model for the acoustic response of the fiber semi-empirically by fitting its parameters to accurately predict all the fixed points. Much more research is needed to cover the full potential of this technique.

More directly, this technique may be exploited to synchronize oscillators by injecting part of the output of one into another. This may turn out to be very useful for optical parametric amplifiers and oscillators, where synchronous pumping is required.

Chapter 6

Conclusion

In this thesis, we have experimented with and theoretically analyzed complex multi-pulsing behavior with two goals in mind:

1. To demonstrate and solidify concepts in complex nonlinear dynamics that can be applied even outside the field of lasers
2. To gain robust control on this complex behavior so it can be used in technological applications

In chapter 4, we presented a procedure to control the number of pulses at tunable pulse energies using a synthetic quantization mechanism. This synthetic mechanism can also be exploited to produce period-doubled pulses and coexisting non-identical pulses as well.

In chapter 5, we presented a procedure to organize the pulses in harmonic mode-locking. As a result, we combined ultrashort pulse durations with high repetition rates and strong supermode suppression. The rare combination of these characteristics is very attractive for ablation-cooled material removal and frequency metrology, both of which require high repetition rates of short pulses. Our repetition rate and pulse duration were limited by the pump power. Therefore, we expect even higher repetition rates of even shorter pulses if we increase

the pump powers.

In addition, we have demonstrated a radical method of manipulating the pulse interactions using an orthogonally polarized secondary loop. We used this technique to control the delay between two pulses with a simple control procedure. More complex patterns with multiple pulses are likely controllable with complex control procedures that employ well-timed seeding of isolated pulses. Full exploitation of this technique may enable new technologies via new pulse patterns. Moreover, this method may enable different oscillators to interact and synchronize, which may be very useful for optical parametric processes.

The experimental behavior we have reported highlights phenomena of nonlinear dynamics such as stable fixed points, multistability, bifurcations, kinetic stability, and noise-induced transitions. The control procedures we have developed are merely management and exploitations of these dynamical phenomena. Therefore, our system can serve as an instructive example to develop control procedures for other complex systems.

Most notably, our analysis has repeatedly relied on the concept of slaving. The evolution of the slaved (fast) variables is simplified by taking the order parameters (slow) as constant parameters like we took the gain to be constant while the pulse energy evolves to a stable fixed point. The evolution of the order parameters, such as the gain, was simplified by taking the slaved variables, such as the pulse energies, at their stable fixed point. The simplification provided by slaving is what allowed us to analyze the dynamics with simple and standard techniques like plotting the trajectories and performing linear stability analysis. It is notable that slaving takes place at multiple levels in our system; the pulse shapes and speeds are slaved to the pulse energies, which are slaved to the gain and the acoustic waves, which are slaved to the pulse positions. This is why we describe the dynamics of our system as hierarchically slaved.

We are aiming to synthesize pulse interactions that strongly couple the evolution of the energies and positions of the pulses. We have conceived of a mechanism where we extract a "messenger" from each pulse and send it to interact with its

neighbor via the Raman process. Once implemented, we expect this technique to produce dense bursts of ultrashort pulses directly from the oscillator, which is very valuable for ablation-cooled material removal, also known as burst-mode ablation. This will be the focus of our efforts in the near future.

Bibliography

[1] L. E. Hargrove, R. L. Fork, and M. A. Pollack, "Locking of he–ne laser modes induced by synchronous intracavity modulation," *Appl. Phys. Lett.*, vol. 5, no. 1, pp. 4–5, 1964.

[2] H. Haus, "Theory of mode locking with a slow saturable absorber," *IEEE J. Quantum Electron.*, vol. 11, no. 9, pp. 736–746, 1975.

[3] H. A. Haus, "Theory of mode locking with a fast saturable absorber," *Journal of Applied Physics*, vol. 46, no. 7, pp. 3049–3058, 1975.

[4] A. B. Grudinin, D. J. Richardson, and D. N. Payne, "Energy quantisation in figure eight fibre laser," *Electronics Letters*, vol. 28, no. 1, pp. 67–68, 1992.

[5] A. B. Grudinin and S. Gray, "Passive harmonic mode locking in soliton fiber lasers," *J. Opt. Soc. Am. B*, vol. 14, pp. 144–154, Jan 1997.

[6] M. J. Lederer, B. Luther-Davies, H. H. Tan, C. Jagadish, N. N. Akhmediev, and J. M. Soto-Crespo, "Multipulse operation of a ti:sapphire laser mode locked by an ion-implanted semiconductor saturable-absorber mirror," *J. Opt. Soc. Am. B*, vol. 16, pp. 895–904, 1999.

[7] G. P. Agrawal, "Chapter 5 - optical solitons," in *Nonlinear Fiber Optics (Fourth Edition)* (G. P. Agrawal, ed.), Optics and Photonics, pp. 120 – 176, San Diego: Academic Press, fourth edition ed., 2006.

[8] B. N. Chichkov, C. Momma, S. Nolte, *et al.*, "Femtosecond, picosecond and nanosecond laser ablation of solids," *Appl. Phys. A*, vol. 63, p. 109–115, 1996.

[9] W. L. Peticolas, "Multiphoton spectroscopy," *Annu. Rev. Phys. Chem.*, vol. 18, no. 1, pp. 233–260, 1967.

[10] K. Tamura, E. P. Ippen, H. A. Haus, and L. E. Nelson, "77-fs pulse generation from a stretched-pulse mode-locked all-fiber ring laser," *Opt. Lett.*, vol. 18, pp. 1080–1082, Jul 1993.

[11] F. O. Ilday, J. R. Buckley, W. G. Clark, and F. W. Wise, "Self-similar evolution of parabolic pulses in a laser," *Phys. Rev. Lett.*, vol. 92, p. 213902, May 2004.

[12] A. Chong, J. Buckley, W. Renninger, and F. Wise, "All-normal-dispersion femtosecond fiber laser," *Opt. Express*, vol. 14, pp. 10095–10100, Oct 2006.

[13] B. Oktem, C. Ülgüdür, and F. Ilday, "Soliton–similariton fibre laser," *Nat. Photonics*, vol. 4, p. 307–311, 2010.

[14] W. H. Renninger, A. Chong, and F. W. Wise, "Self-similar pulse evolution in an all-normal-dispersion laser," *Phys. Rev. A*, vol. 82, p. 021805, Aug 2010.

[15] S. Pitois, C. Finot, L. Provost, and D. J. Richardson, "Generation of localized pulses from incoherent wave in optical fiber lines made of concatenated mamyshev regenerators," *J. Opt. Soc. Am. B*, vol. 25, pp. 1537–1547, Sep 2008.

[16] M. Rochette, L. R. Chen, K. Sun, and J. Hernandez-Cordero, "Multiwavelength and tunable self-pulsating fiber cavity based on regenerative spm spectral broadening and filtering," *IEEE Photonics Technol. Lett.*, vol. 20, no. 17, pp. 1497–1499, 2008.

[17] P. Sidorenko, W. Fu, L. G. Wright, M. Olivier, and F. W. Wise, "Self-seeded, multi-megawatt, mamyshev oscillator," *Opt. Lett.*, vol. 43, pp. 2672–2675, Jun 2018.

[18] K. Regelskis, J. Želudevičius, K. Viskontas, and G. Račiukaitis, "Ytterbium-doped fiber ultrashort pulse generator based on self-phase modulation and alternating spectral filtering," *Opt. Lett.*, vol. 40, pp. 5255–5258, Nov 2015.

[19] S.-S. Xu, M. Liu, Z.-W. Wei, A.-P. Luo, W.-C. Xu, and Z.-C. Luo, "Multi-pulse dynamics in a mamyshev oscillator," *Opt. Lett.*, vol. 45, pp. 2620–2623, May 2020.

[20] S. Strogatz, *Nonlinear Dynamics and Chaos: With Applications to Physics, Biology, Chemistry, and Engineering*. Studies in Nonlinearity, Avalon Publishing, 2014.

[21] J. B. MARION, "Chapter 9 - hamilton's principle—lagrangian and hamiltonian dynamics," in *Classical Dynamics of Particles and Systems* (J. B. MARION, ed.), pp. 214–266, Academic Press, 1965.

[22] H. Haken, *Synergetics: An Introduction : Nonequilibrium Phase Transitions and Self-organization in Physics, Chemistry, and Biology*. No. v. 3 in Recent Results in Cancer Research, Springer, 1983.

[23] W. Horsthemke and R. Lefever, *Noise-induced transitions*, vol. 15 of *Springer Series in Synergetics*. Springer, 1 ed., 1984.

[24] G. P. Agrawal, "Chapter 3 - group-velocity dispersion," in *Nonlinear Fiber Optics (Fourth Edition)* (G. P. Agrawal, ed.), Optics and Photonics, pp. 120 – 176, San Diego: Academic Press, fourth edition ed., 2006.

[25] G. P. Agrawal, "Chapter 4 - self-phase modulation," in *Nonlinear Fiber Optics (Fourth Edition)* (G. P. Agrawal, ed.), Optics and Photonics, pp. 120 – 176, San Diego: Academic Press, fourth edition ed., 2006.

[26] D. Anderson, M. Desaix, M. Karlsson, M. Lisak, and M. L. Quiroga-Teixeiro, "Wave-breaking-free pulses in nonlinear-optical fibers," *J. Opt. Soc. Am. B*, vol. 10, pp. 1185–1190, Jul 1993.

[27] M. E. Fermann, V. I. Kruglov, B. C. Thomsen, J. M. Dudley, and J. D. Harvey, "Self-similar propagation and amplification of parabolic pulses in optical fibers," *Phys. Rev. Lett.*, vol. 84, pp. 6010–6013, Jun 2000.

[28] M. Hofer, M. E. Fermann, F. Haberl, M. H. Ober, and A. J. Schmidt, "Mode locking with cross-phase and self-phase modulation," *Opt. Lett.*, vol. 16, pp. 502–504, Apr 1991.

[29] N. J. Doran and D. Wood, "Nonlinear-optical loop mirror," *Opt. Lett.*, vol. 13, pp. 56–58, Jan 1988.

[30] W. H. Renninger, A. Chong, and F. W. Wise, "Area theorem and energy quantization for dissipative optical solitons," *J. Opt. Soc. Am. B*, vol. 27, pp. 1978–1982, Oct 2010.

[31] L. M. Zhao, D. Y. Tang, and A. Q. Liu, "Chaotic dynamics of a passively mode-locked soliton fiber ring laser," *Chaos*, vol. 16, no. 1, p. 013128, 2006.

[32] L. Hua, S. Wang, X. Yang, X. Yao, L. Li, A. Komarov, M. Klimczak, D. Shen, D. Tang, L. Su, and L. Zhao, "Period doubling of multiple dissipative-soliton-resonance pulses in a fibre laser," *OSA Contin.*, vol. 3, pp. 911–920, Apr 2020.

[33] P. V. Mamyshev, "All-optical data regeneration based on self-phase modulation effect," in *24th European Conference on Optical Communication. ECOC '98 (IEEE Cat. No.98TH8398)*, vol. 1, pp. 475–476 vol.1, 1998.

[34] A. Gordon and B. Fischer, "Phase transition theory of many-mode ordering and pulse formation in lasers," *Phys. Rev. Lett.*, vol. 89, p. 103901, Aug 2002.

[35] A. Komarov, H. Leblond, and F. m. c. Sanchez, "Multistability and hysteresis phenomena in passively mode-locked fiber lasers," *Phys. Rev. A*, vol. 71, p. 053809, May 2005.

[36] E. Poeydebat, F. Scol, O. Vanvincq, G. Bouwmans, and E. Hugonnot, "All-fiber mamyshev oscillator with high average power and harmonic mode-locking," *Opt. Lett.*, vol. 45, pp. 1395–1398, Mar 2020.

[37] N. Tarasov, A. M. Perego, D. V. Churkin, K. Staliunas, and S. K. Turitsyn, "Mode-locking via dissipative faraday instability," *Nat. Commun.*, vol. 7, Aug 2016.

[38] I. Samartsev, A. Bordenyuk, and V. Gapontsev, "Environmentally stable seed source for high power ultrafast laser," in *Components and Packaging*

for Laser Systems III (A. L. Glebov and P. O. Leisher, eds.), vol. 10085, pp. 201 – 209, International Society for Optics and Photonics, SPIE, 2017.

[39] Z. Liu, Z. M. Ziegler, L. G. Wright, and F. W. Wise, "Megawatt peak power from a mamyshev oscillator," *Optica*, vol. 4, pp. 649–654, Jun 2017.

[40] Y.-H. Chen, P. Sidorenko, R. Thorne, and F. Wise, "Starting dynamics of a linear mamyshev oscillator," in *Conference on Lasers and Electro-Optics*, p. SF2H.4, Optical Society of America, 2020.

[41] S. Zhou, D. G. Ouzounov, and F. W. Wise, "Passive harmonic mode-locking of a soliton yb fiber laser at repetition rates to 1.5 ghz," *Opt. Lett.*, vol. 31, pp. 1041–1043, Apr 2006.

[42] Y. Wang, J. Li, K. Mo, Y. Wang, F. Liu, and Y. Liu, "14.5 ghz passive harmonic mode-locking in a dispersion compensated tm-doped fiber laser," *Sci. Rep.*, vol. 7, no. 1, 2017.

[43] B. Ortaç, A. Hideur, G. Martel, and M. Brunel, "2-ghz passive harmonically mode-locked yb-doped double-clad fiber laser," *Appl. Phys. B*, vol. 81, no. 4, p. 507–509, 2005.

[44] P. Grelu, F. Belhache, F. Gutty, and J.-M. Soto-Crespo, "Phase-locked soliton pairs in a stretched-pulse fiber laser," *Opt. Lett.*, vol. 27, pp. 966–968, Jun 2002.

[45] B. Ortaç, A. Hideur, and M. Brunel, "Passive harmonic mode locking with a high-power ytterbium-doped double-clad fiber laser," *Opt. Lett.*, vol. 29, pp. 1995–1997, Sep 2004.

[46] J. Wang, X. Bu, R. Wang, L. Zhang, J. Zhu, H. Teng, H. Han, and Z. Wei, "All-normal-dispersion passive harmonic mode-locking 220 fs ytterbium fiber laser," *Appl. Opt.*, vol. 53, pp. 5088–5091, Aug 2014.

[47] L.-J. Kong, X.-S. Xiao, and C.-X. Yang, "Passive harmonic mode locked all-normal-dispersion yb-doped fibre lasers," *Chin. Phys. B*, vol. 20, p. 024207, feb 2011.

[48] S. S. Huang, Y. G. Wang, P. G. Yan, G. L. Zhang, J. Q. Zhao, H. Q. Li, and R. Y. Lin, "High order harmonic mode-locking in an all-normal-dispersion yb-doped fiber laser with a graphene oxide saturable absorber," *Laser Phys.*, vol. 24, p. 015001, dec 2013.

[49] J. Koo, J. Park, J. Lee, Y. M. Jhon, and J. H. Lee, "Femtosecond harmonic mode-locking of a fiber laser at 3.27 ghz using a bulk-like, mose2-based saturable absorber," *Opt. Express*, vol. 24, pp. 10575–10589, May 2016.

[50] M. Baumgartl, C. Lecaplain, A. Hideur, J. Limpert, and A. Tünnermann, "66 w average power from a microjoule-class sub-100 fs fiber oscillator," *Opt. Lett.*, vol. 37, pp. 1640–1642, May 2012.

[51] I. M. Bomze, "Lotka-volterra equation and replicator dynamics: A two-dimensional classification," *Biol. Cybern.*, vol. 48, no. 3, p. 201–211, 1983.

[52] T. V. D. Burg and A. Prinz, "Progressive taxation as a means for improving competitive balance," *Scott. J. Political Econ.*, vol. 52, no. 1, p. 65–74, 2005.

[53] J. Zhou, W. Pan, and Y. Feng, "Period multiplication in mode-locked figure-of-9 fiber lasers," *Opt. Express*, vol. 28, pp. 17424–17433, Jun 2020.

[54] S. Namiki, E. P. Ippen, H. A. Haus, and C. X. Yu, "Energy rate equations for mode-locked lasers," *J. Opt. Soc. Am. B*, vol. 14, pp. 2099–2111, Aug 1997.

[55] H. Wei, B. Li, W. Shi, X. Zhu, R. A. Norwood, N. Peyghambarian, and S. Jian, "General description and understanding of the nonlinear dynamics of mode-locked fiber lasers," *Sci. Rep.*, vol. 7, no. 1, 2017.

[56] F. O. Ilday, *THEORY AND PRACTICE OF HIGH-ENERGY FEMTOSECOND FIBER LASERS*. PhD thesis, Cornell University, 2004.

[57] D. Kondepudi, F. Moss, and P. McClintock, "Branch selection in the presence of coloured noise," *Phys. Lett. A*, vol. 114, no. 2, pp. 68–74, 1986.

[58] F. O. Ilday, "Mode-locking dissected," *Nat. Phys.*, vol. 16, p. 504–505, 2020.

[59] N. N. Akhmediev, A. Ankiewicz, and J. M. Soto-Crespo, "Stable soliton pairs in optical transmission lines and fiber lasers," *J. Opt. Soc. Am. B*, vol. 15, pp. 515–523, Feb 1998.

[60] J. M. Soto-Crespo, N. Akhmediev, P. Grelu, and F. Belhache, "Quantized separations of phase-locked soliton pairs in fiber lasers," *Opt. Lett.*, vol. 28, pp. 1757–1759, Oct 2003.

[61] R. Weill, A. Bekker, V. Smulakovsky, B. Fischer, and O. Gat, "Noise-mediated casimir-like pulse interaction mechanism in lasers," *Optica*, vol. 3, pp. 189–192, Feb 2016.

[62] J. Kutz, B. Collings, K. Bergman, and W. Knox, "Stabilized pulse spacing in soliton lasers due to gain depletion and recovery," *IEEE J. Quantum Electron.*, vol. 34, no. 9, pp. 1749–1757, 1998.

[63] M. S. Kuznetsov, O. L. Antipov, A. A. Fotiadi, and P. Mégret, "Electronic and thermal refractive index changes in ytterbium-doped fiber amplifiers," *Opt. Express*, vol. 21, pp. 22374–22388, Sep 2013.

[64] K. Smith and L. F. Mollenauer, "Experimental observation of soliton interaction over long fiber paths: discovery of a long-range interaction," *Opt. Lett.*, vol. 14, pp. 1284–1286, Nov 1989.

[65] E. M. Dianov, A. V. Luchnikov, A. N. Pilipetskii, and A. N. Starodumov, "Electrostriction mechanism of soliton interaction in optical fibers," *Opt. Lett.*, vol. 15, pp. 314–316, Mar 1990.

[66] A. N. Pilipetskii, E. A. Golovchenko, and C. R. Menyuk, "Acoustic effect in passively mode-locked fiber ring lasers," *Opt. Lett.*, vol. 20, pp. 907–909, Apr 1995.

[67] M. S. Kang, A. Nazarkin, A. Brenn, and P. S. J. Russell, "Tightly trapped acoustic phonons in photonic crystal fibres as highly nonlinear artificial raman oscillators," *Nat. Phys.*, vol. 5, no. 4, p. 276–280, 2009.

[68] M. Pang, X. Jiang, W. He, G. K. L. Wong, G. Onishchukov, N. Y. Joly, G. Ahmed, C. R. Menyuk, and P. S. Russell, "Stable subpicosecond soliton

fiber laser passively mode-locked by gigahertz acoustic resonance in photonic crystal fiber core," *Optica*, vol. 2, pp. 339–342, Apr 2015.

[69] K. S. Lee, C. K. Ha, K. J. Moon, D. S. Han, and M. S. Kang, "Tailoring of multi-pulse dynamics in mode-locked laser via optoacoustic manipulation of quasi-continuous-wave background," *Commun. Phys.*, vol. 2, Nov 2019.

[70] R. W. Boyd, "Chapter 9 - stimulated brillouin and stimulated rayleigh scattering," in *Nonlinear Optics (Third Edition)* (R. W. Boyd, ed.), pp. 429–471, Burlington: Academic Press, third edition ed., 2008.

[71] C. Krischer, "Optical measurements of ultrasonic attenuation and reflection losses in fused silica," *J. Acoust. Soc. Am.*, vol. 48, no. 5B, pp. 1086–1092, 1970.

[72] D. B. Fraser, J. T. Krause, and A. H. Meitzler, "Physical limitations on the performance of vitreous silica in high-frequency ultrasonic and acousto-optical devices," *Appl. Phys. Lett.*, vol. 11, no. 10, pp. 308–310, 1967.

[73] J. Hult, "A fourth-order runge–kutta in the interaction picture method for simulating supercontinuum generation in optical fibers," *J. Light. Technol.*, vol. 25, no. 12, pp. 3770–3775, 2007.

Appendix A

Pulse Propagation Simulations

A.1 The Model in the Simulations

Figures 2.2-2.7, 3.1, 5.6, and 5.7 relied on numerical simulations of ultrashort pulse propagation. Here, we present the basic principle governing these simulations and the routines used in common for multiple figures. In Appendix B, we present the simulation settings and the main code for each of these simulation figures.

The simulation defines an initial pulse numerically on a finite time delay points. The pulse is determined by an input pulse shape (Gaussian or $sech^2$), the spectral width (full width at half maximum), the central wavelength, a linear chirp (measured as the ratio between the actual pulse duration and the transform-limited one, with a sign that determines the sign of the chirp), and the pulse energy.

The simulation propagates the pulse through a passive fiber by solving the following partial differential equation:

$$\frac{\partial A}{\partial z} = -i\frac{\beta_2}{2}\frac{\partial^2 A}{\partial \tau^2} + \frac{\beta_3}{6}\frac{\partial^3 A}{\partial \tau^3} + i\gamma\left|A\right|^2 A, \tag{A.1}$$

where β_2 refers to group velocity dispersion (GVD), β_3 refers to third order dispersion (TOD) , and γ is the Kerr nonlinearity coefficient. If self-steepening is

taken into account, the term

$$-\frac{\gamma}{w_0}\frac{\partial}{\partial\tau}\left|A\right|^2 A \tag{A.2}$$

is added to the right-hand side, where w_0 is the central frequency.

The propagation distance, z is divided to multiple small steps, within each, the propagation is carried out numerically using the "Runge-Kutta for interaction picture" method [73], which groups the linear, frequency dependent terms and solves them in the frequency domain in small sub-steps and solves the nonlinear term(s) in the time domain in small sub-steps and combines them in a manner similar to the Runge-Kutta methods for ordinary differential equations.

For propagation through a gain fiber, the following gain term is added to the linear, frequency-domain part:

$$\begin{gathered}\frac{\partial\tilde{A}}{\partial z} = \frac{g(w)}{2}\tilde{A}(w); \\ g(w) = \frac{G(w)}{1+\frac{E}{E_{sat}}};\ G(w) = \frac{G_{ss}}{1+(\frac{w-w_c}{\Delta w})^2},\end{gathered} \tag{A.3}$$

where G_{ss} is the small signal gain, Δw is the gain bandwidth (full width at half maximum), w_c is the central frequency of the gain spectrum, E is the total pulse energy, and E_{sat} is the saturation energy of the gain.

Linear losses are modeled as a nonlinear polarization evolution-based saturable absorber (NPE) with zero modulation depth. Effectively, this multiplies the complex pulse envelope, A by the square root of the transmission of the lossy element. Similarly, a spectral filter multiplies the pulse by the square root of the filter shape in the frequency domain.

A.2 The Main Simulation Codes

The simulations are done in Matlab. For each simulation there's a .txt file that contains the settings of the simulation, the name of the settings file is fed to the

function CommandLine(). The settings file is read through the function loadData(), which extracts segment settings and global settings. The later includes the width of the time window, the resolution in the time delay variable, the initial pulse parameters, the number of passes through the segments (roundtrips, used for oscillator simulations), and the saving frequency. A script named Assign_CommandLine is ran within CommandLine() to initialize the pulse and the time delay and frequency variables. Then, the code enters a loop over roundtrips, within which it enters a loop over segments. Within this inner loop it extracts all the settings about the segment and feeds them to a function named Propagation(). Propagation detects which type of segment it is and sends the pulse to a function that corresponds to the segment type. These include Passive(), Active(), NPE(), and Filter(). Our simulations involved only these segment types. In addition to the electric field envelope, the function Propagation returns multiple snapshots of the electric field taken at equidistant points along the propagation. These snapshots are, then, saved within the loop over roundtrips.

In all of the simulations except the one used for figure 5.7, the simulations are done using the CommandLine function, then the saved snapshots are recalled using the functions LoadPage and LoadE. Then, the recalled electric field data is used for plotting. Below, are the common routines and sub-routines used in multiple simulations in the thesis:

CommandLine():

```
function []=CommandLine(settings_file)
%% loading settings and segment data


[seg_data, global_data,segment_header,global_header] = loadData(settings_file,0);
% Assign variables from global/settings data and process the pulse with
% initial pulse shape
run Assign_CommandLine.m
%% main loop
while (lap<roundtrips)
    lap = lap + 1;
    if(mod(lap,saveevery)==0)
        snapstosave = [];
    end
    for i = 1:nOfSegments
% fprintf('Roundtrip: %d, Segment: %d\n',lap,i);
        % Propagate according to the segment info
        [E,Esnaps] = Propagation(E,Esnaps,t,w,wave,omegas,freq,edge_filter,frep,lambda_c,hr,tres,seg_data(i,:),snapshots(i),
              segment_header,0);
        if((mod(lap,saveevery)==0)||(saveevery==0))
           for k = 1:snapshots(i)
```

```
            snapstosave = [snapstosave Esnaps(k,:)];
        end
    end
    if Conv_typ==1 % convergence check based on pulse energy
        if i==Conv_seg
            Conv_mem=[Conv_mem(2:end) tres*(E*E')];
        end
    elseif Conv_typ==2 % convergence check based on peak power
        if i==Conv_seg
            Conv_mem=[Conv_mem(2:end) max(abs(E).^2)];
        end
    end
% fprintf('Energy = % f nJ \n',tres*(E*E')); % Print the pulse energy
end
if(mod(lap,saveevery)==0)
    SaveE(snapstosave(:),['Data' num2str(lap+(shape==3)*str2double(file_no)) '.bin'] ); % Save the for every N roundtrips to .
        bin file
    fprintf('lap=%d energy=%.10e nJ \n',lap+(shape==3)*str2double(file_no),tres*(E*E')); % Print the pulse energy
    % fprintf('Energy = % f nJ \n',tres*(E*E')); % Print the pulse energy
    % fprintf('saving \n');
end
Conv_MAX=max(Conv_mem); Conv_MIN=min(Conv_mem);
if (Conv_MAX-Conv_MIN)/Conv_MIN < Conv_th
    saveevery=lap+1;
    if converged==1
        break
    end
    converged=1;
end
end
%%
% soundsc([cos(1:.5:400), cos(1:.8:400), cos(1:.9:400)]); % Warning after simulation stops
fprintf('Done \n');
```

loadData():

```
function [segment_data,global_data,header_segment,header_global]=loadData(settings_file,segment)
% This file can extract segment data, global data and their headers
% It is both used in GUI Version and CommandLine version to extract segment data
% if segment = 0, it extracts all of the segments' data
% if segment = n, it extracts nth segment's data

%% Load Settings
fileName = settings_file;
fid = fopen(fileName,'r');
flag = 0;
str1 = [''];
while flag ~= 1
    text = fgetl(fid);
    array = strsplit(text,'\t');
    array = array(~cellfun('isempty',array));
    if sum(contains(array,"0") | contains(array,"1")) > 0 % Find the location of parameter inputs
        flag = 1;
    end
    if sum(contains(array,"Dw")) > 0 % Find and store header
        header_global = array;
    end
    if flag ~= 1 % Do not write parameter inputs now
        str1 = [str1 text '\r\n'];
    end
end % Stop the loop if the parameter inputs are found
flag = 0;
% Assign corresponding values of parameters from str, where we extracted
% information into
global_data = array; % Load parameter inputs
```

```
%% Load Segment
fileName = settings_file;
fid = fopen(fileName);
str = ["temp"];
while ~contains(str,'NaN')
    str = strsplit(fgetl(fid),'\t');
    str = str(~cellfun('isempty',str));
    if strcmp(str(1,1),'Seg_ID')
        header_segment = str; % Load Segment Header
    end
end
while ~feof(fid)
    get = strsplit(fgetl(fid),'\t');
    get = get(~cellfun('isempty',get));
    str = [str; get];
end
segment_data = str;
fclose(fid);
if segment ~= 0
    segment_data = segment_data(segment,:);
end
end
```

Assign_CommandLine:

```
% This script implements the initialization of the simulation on
% CommandLine code
% It assigns global values from what is written in .txt file
% Implemets the initial propagation of the pulse based on its shape
% Initializes variables
% It is included in CommandLine.m function


nOfSegments = length(seg_data(:,1));

file_no = global_data(contains(global_header,'File_No'));
page_no = global_data(contains(global_header,'Page_No'));
file_path = global_data(contains(global_header,'FilePath'));
if strcmp('null',file_path)
    file_path = '';
end

% Assign values of settings extracted above
roundtrips = str2double(global_data(contains(global_header,'Passes'))); % # of roundtrips
shape = str2double(global_data(contains(global_header,'Shape'))); % initial temporal shape (1 for sech^2, 2 for Gaussian, 3 for
      multiple Gaussian, 4 for noise)
lambda_c = str2double(global_data(contains(global_header,'CentW'))); % Central wavelength (nm)
Dw = str2double(global_data(contains(global_header,'Dw'))); % initial bandwidth (THz)
DT_T0 = str2double(global_data(contains(global_header,'DT'))); % chirp parameter (1 for transform limited)
frep = str2double(global_data(contains(global_header,'frep')))*1e-6; % laser rep rate (THz) (written as MHz*1e-6)
edge_filter = str2double(global_data(contains(global_header,'EdgeF'))); % Edge Filter
energy = str2double(global_data(contains(global_header,'Energy'))); % initial energy (nJ)
timewidth = str2double(global_data(contains(global_header,'TWidth'))); % Width of the time window in [ps]
tres1 = str2double(global_data(contains(global_header,'TRes')))*1e-3; % Resolution of the time window [ps] (written as fs*1e-3)
saveevery = str2double(global_data(contains(global_header,'SaveN')));
plotevery = str2double(global_data(contains(global_header,'plotN')));
plot_seg = str2double(global_data(contains(global_header,'plot_seg'))); % segment number where the state will be plotted; -1 for
      NPE rejection port
store_seg = str2double(global_data(contains(global_header,'store_seg'))); % segment number where the state will be stored; -1 for
      NPE rejection port
c = 299792.458; % [nm/ps]
timesteps=2^(ceil(log2(timewidth/tres1))); tres=timewidth/timesteps;
t = -timewidth*0.5+tres:tres:timewidth*0.5; % Time in [ps]
timesteps=length(t);
fs=1/timewidth; % Sampling rate in [THz]
freq=c/lambda_c+fs*linspace(-timesteps/2,timesteps/2-1,timesteps);
```

```
freq=fftshift(freq); % Frequency in [THz]
wave=c./freq; shiftedWave=fftshift(wave); % Wavelength in [nm]
w=2*pi*c/lambda_c; % Central angular frequency in [THz]
omegas = 2*pi*freq; % Angular frequency in [THz]

%% Calculation of Raman spectrum

% Calculation of Raman Spectrum
% REF: 1. Hollenbeck, D. & Cantrell, C. D. Multiple-vibrational-mode model
% for fiber-optic Raman gain spectrum and response function. J. Opt.
% Soc. Am. B 19, 2886?2892 (2002).
comp_pos=[56.25,100.00,231.25,362.50,463.00,497.00,611.50,691.67,793.67,835.50,930.00,1080.00,1215.00].*1e-7; %1/nm
peak_int=[1.00,11.40,36.67,67.67,74.00,4.50,6.80,4.60,4.20,4.50,2.70,3.10,3.00]; %Unitless
gau_FWHM=[52.10,110.42,175.00,162.50,135.33,24.50,41.50,155.00,59.50,64.30,150.00,91.00,160.00].*1e-7; %1/nm
lor_FWHM=[17.37,38.81,58.33,54.17,45.11,8.17,13.83,51.67,19.83,21.43,50.00,30.33,53.33].*1e-7; %1/nm
hr=zeros(1,timesteps);
for a=ceil(timesteps/2):timesteps
    for b=1:13
        hr(a)=hr(a)+peak_int(b)*exp(-pi*c*t(a)*lor_FWHM(b))*exp(-((pi*c*gau_FWHM(b))^2)*(t(a)^2)/4)*sin(2*pi*c*comp_pos(b)*t(a));
    end
end
hr_integral=trapz(t,hr);
hr=hr./hr_integral;
hr=fft(fftshift(hr));

%% initializing the state

if shape==1 %sech^2
    duration = 0.315/Dw*1.29414; %Pulse duration in [ps]
    spacing = str2double(global_data(contains(global_header,'spacing')));
    pulseno = str2double(global_data(contains(global_header,'pulse_no'))); % number of pulses in the initial time window
    jitter = 0.0; % jitter in the distance between pulses
    E = 0; % electrical field [kW^0.5]
    for pulseCount = 1:pulseno
        E = E + sqrt(energy/duration)*0.9417*sech((t+(pulseCount-pulseno/2-1/2+randn*jitter)*spacing)*2*sech(0.5)/duration);
    end
    if DT_T0^2 < 1; DT_T0=1; end
    B=B_calc(duration^2/(4*log(2))*sqrt(DT_T0^2-1)*sign(DT_T0),omegas,w);E=ifft(exp(B).*fft(E));
elseif shape==2 % Gaussian
    duration = 0.441/Dw; %Pulse duration in [ps]
    spacing = str2double(global_data(contains(global_header,'spacing')));
    pulseno = str2double(global_data(contains(global_header,'pulse_no'))); % number of pulses in the initial time window
    jitter = 0.0; % jitter in the distance between pulses
    E = 0; % electrical field [kW^0.5]
    for pulseCount = 1:pulseno
        E = E + sqrt(energy/duration)*0.969215*exp(-0.5*((t+(pulseCount-pulseno/2-1/2+randn*jitter)*spacing)/duration).^2*4*log(2)
              );
    end
    if DT_T0^2 < 1; DT_T0=1; end
    B=B_calc(duration^2/(4*log(2))*sqrt(DT_T0^2-1)*sign(DT_T0),omegas,w);E=ifft(exp(B).*fft(E));

elseif shape==3 %From Data File
    fileno = char(file_no);
    snapshotno = str2double(page_no);
    E = LoadPage(LoadE(['Data' fileno '.bin']),snapshotno,timesteps);

elseif shape==4 %Noise
    E=sqrt(energy/timewidth)*(rand(1,length(t))-0.5); % electrical field [kW^0.5]
    %[E,~] = Passive( E,t,w,0,B_calc(duration^2/(4*log(2))*sqrt(DT_T0^2-1)*sign(DT_T0),omegas,w),0,hr,1,1,1,tres,0, edge_filter );

elseif shape==5 %Custom %------------------modify here-------------------
% E = exp(t-d);
end

%% extracting snapshots vector
Esnaps = [];
snapshots = str2double(seg_data(:,contains(segment_header,'Snap')));
```

```
%% initializing settings for convergence check
Conv_typ = str2double(global_data(:,contains(global_header,'Conv_typ')));
Conv_th = str2double(global_data(:,contains(global_header,'Conv_th')))/100;
Conv_spn = str2double(global_data(:,contains(global_header,'Conv_spn')));
Conv_mem = [ones(1,Conv_spn-1) 1000];
Conv_seg = str2double(global_data(:,contains(global_header,'Conv_seg')));
converged=0;
%%
lap = 0; energies= [];
```

Propagation():

```
function [E,Esnaps,E_r,coords, pulsewidth, spectwidthf] = Propagation(E,Esnaps,t,w,wave,omegas,freq,edge_filter,frep,lambda_c,hr,
      tres,data,snapshots,segment_header,calcevo)
% PROPAGATION
% This function takes electric field, settings parameters and segment
% parameters and propagates.

if snapshots==0
    snapshots=1;
end
E_r=[];

type = data(contains(segment_header,'AcType'));
nsteps = str2double(data(contains(segment_header,'Steps'))); % Number of steps
nsteps=ceil(nsteps/snapshots)*snapshots;
if contains(type,'Passive')

    fiberlength = str2double(data(strcmp(segment_header,'L')))*1e7; % segment length in [nm]
    betas(1) = str2double(data(contains(segment_header,'GVD')))*1e-12; % GVD of the segment [ps^2/nm]
    betas(2) = str2double(data(contains(segment_header,'TOD')))*1e-15; % TOD of the segment [ps^3/nm]
    gamma = str2double(data(contains(segment_header,'Gamma')))*1e-9; % nonlinearity constant in [1/(KW.nm)]

    self_steep=str2double(data(contains(segment_header,'steep'))); % whether to include self-steepening (1) or not (0)
    fr = str2double(data(contains(segment_header,'f_R'))); % fraction of Raman scattering of the segment
    B = B_calc(betas,omegas,w); % dispersion coefficient of the fiber
    if calcevo == 1
        [Esnaps,coords, pulsewidth, spectwidthf] = Passive( E,t,w,gamma,self_steep,B,fr,hr,fiberlength,nsteps,snapshots,tres,
            calcevo,edge_filter); % propagation through the segment
    else
        [Esnaps,~,~,~] = Passive( E,t,w,gamma,self_steep,B,fr,hr,fiberlength,nsteps,snapshots,tres,calcevo,edge_filter); %
            propagation through the segment
    end
    E = Esnaps(snapshots,:); % because Esnaps is cumulative, the last raw is taken as result

elseif contains(type,'Eff_Gain')

    fiberlength = str2double(data(strcmp(segment_header,'L')))*1e7; % segment length in [nm]
    betas(1) = str2double(data(contains(segment_header,'GVD')))*1e-12; % GVD of the segment [ps^2/nm]
    betas(2) = str2double(data(contains(segment_header,'TOD')))*1e-15; % TOD of the segment [ps^3/nm]
    B = B_calc(betas,omegas,w); % dispersion coefficient of the fiber
    gamma = str2double(data(contains(segment_header,'Gamma')))*1e-9; % nonlinearity constant in [1/(KW.nm)]
    self_steep=str2double(data(contains(segment_header,'steep')));% whether to include self-steepening (1) or not (0)
    fr = str2double(data(contains(segment_header,'f_R'))); % fraction of Raman scattering of the segment

    gain_noise = str2double(data(contains(segment_header,'Noise'))); % Extract noise data [in percent]
    gss = 10^(str2double(data(contains(segment_header,'Unsat')))/10); % small signal gain (unsaturation gain)(linear scale,
        unitless)
    lambda_g = str2double(data(contains(segment_header,'Cent_WL'))); % gain central wavelength [nm]
    dl_g = str2double(data(contains(segment_header,'Gain_BW'))); % gain bandwidth [nm]
    Psat = str2double(data(contains(segment_header,'SatPow'))); % gain saturation power in [W]
    Esat = Psat/frep*1e-3; % saturation energy in [nJ]

    Ene_before = tres*(E*E');
    % addition of gain noise
    timesteps = length(t); % Time steps
```

```
    c = 299792.458; % Speed of light in [nm/ps]
    f0 = c/lambda_g; % Central frequency in [THz]
    df = c*dl_g/lambda_g^2; % Gain bandwidth in [THz]
    G = (log(gss)/fiberlength)*df^2./(4*(freq-f0).^2+df^2); % Gain coefficient
    nG=G/(log(gss)/fiberlength)/timesteps*tres; % normalized gain spectrum
    noise_strength = 10^(gain_noise/10)*nG/(1+Ene_before/Esat);
    noise = ifft(noise_strength.*(randn(1,length(E))+1i*randn(1,length(E))));%
    E = E + noise;
    % end adding noise

    if calcevo == 1
        [Esnaps, coords, pulsewidth, spectwidthf]=Active( E,t,w,freq,gamma,self_steep,B,fr,hr,fiberlength,nsteps,snapshots,tres,
            lambda_g,dl_g,Esat,gss,calcevo,edge_filter); % propagation through the segment
    else
        [Esnaps,~, ~, ~]=Active( E,t,w,freq,gamma,self_steep,B,fr,hr,fiberlength,nsteps,snapshots,tres,lambda_g,dl_g,Esat,gss,0,
            edge_filter); % propagation through the segment
    end
    E = Esnaps(snapshots,:); % because Esnaps is cumulative, the last raw is taken as result

elseif contains(type,'Dop_Gain_Yb') % Yb

    fiberlength = str2double(data(strcmp(segment_header,'L')))*1e7; % segment length in [nm]
    betas(1) = str2double(data(contains(segment_header,'GVD')))*1e-12; % GVD of the segment [ps^2/nm]
    betas(2) = str2double(data(contains(segment_header,'TOD')))*1e-15; % TOD of the segment [ps^3/nm]
    B = B_calc(betas,omegas,w); % dispersion coefficient of the fiber
    gamma = str2double(data(contains(segment_header,'Gamma')))*1e-9; % nonlinearity constant in [1/(KW.nm)]
    self_steep=str2double(data(contains(segment_header,'steep')));% whether to include self-steepening (1) or not (0)
    fr = str2double(data(contains(segment_header,'f_R'))); % fraction of Raman scattering of the segment

    gain_noise = str2double(data(contains(segment_header,'Noise'))); % Extract noise data [in percent]
    doping = str2double(data(contains(segment_header,'DopConc'))); % Doping Concentration
    Pp = str2double(data(contains(segment_header,'PumpPow')))*1e-3; % Pump Power in [W]
    lambda_p = str2double(data(contains(segment_header,'Pump_WL'))); % Pump Wavelength in [nm]
    dl_p = str2double(data(contains(segment_header,'PmpFWHM'))); % Pump FWHM in [nm]

    Ene_before = tres*(E*E');
    % addition of gain noise
    noise_strength = gain_noise/100;
    fprintf('Noise:␣%d␣\n',noise_strength);
    noise_percent = noise_strength/Ene_before; % originally noise_strength*E;
    noise = noise_percent.*randn(1,length(E));
    E = E + noise;
    % end adding noise

    if calcevo == 1
        [Esnaps, coords, pulsewidth, spectwidthf]=SMYbFiber2(E,t,w,freq,gamma,self_steep,B,fr,hr,fiberlength,nsteps,snapshots,tres
            ,Pp,lambda_p,dl_p,frep,doping,calcevo); % propagation through the segment
    else
        [Esnaps,~,~,~]=SMYbFiber2(E,t,w,freq,gamma,self_steep,B,fr,hr,fiberlength,nsteps,snapshots,tres,Pp,lambda_p,dl_p,frep,
            doping,calcevo); % propagation through the segment
    end
    E = Esnaps(snapshots,:); % because Esnaps is cumulative, the last raw is taken as result

elseif contains(type,'Dop_Gain_Er') % Er

    fiberlength = str2double(data(strcmp(segment_header,'L')))*1e7; % segment length in [nm]
    betas(1) = str2double(data(contains(segment_header,'GVD')))*1e-12; % GVD of the segment [ps^2/nm]
    betas(2) = str2double(data(contains(segment_header,'TOD')))*1e-15; % TOD of the segment [ps^3/nm]
    B = B_calc(betas,omegas,w); % dispersion coefficient of the fiber
    gamma = str2double(data(contains(segment_header,'Gamma')))*1e-9; % nonlinearity constant in [1/(KW.nm)]
    self_steep=str2double(data(contains(segment_header,'steep')));% whether to include self-steepening (1) or not (0)
    fr = str2double(data(contains(segment_header,'f_R'))); % fraction of Raman scattering of the segment

    gain_noise = str2double(data(contains(segment_header,'Noise'))); % Extract noise data [in percent]
    doping = str2double(data(contains(segment_header,'DopConc'))); % Doping Concentration
    Pp = str2double(data(contains(segment_header,'PumpPow')))*1e-3; % Pump Power in [W]
    lambda_p = str2double(data(contains(segment_header,'Pump_WL'))); % Pump Wavelength in [nm]
    dl_p = str2double(data(contains(segment_header,'PmpFWHM'))); % Pump FWHM in [nm]
```

```
    Ene_before = tres*(E*E');
    % addition of gain noise
    noise_strength = gain_noise/100;
    fprintf('Noise:␣%d␣\n',noise_strength);
    noise_percent = noise_strength/Ene_before; % originally noise_strength*E;
    noise = noise_percent.*randn(1,length(E));
    E = E + noise;
    % end adding noise

    if calcevo == 1
        [Esnaps, coords, pulsewidth, spectwidthf]=SMErFiber2(E,t,w,freq,gamma,self_steep,B,fr,hr,fiberlength,nsteps,snapshots,tres
            ,Pp,lambda_p,dl_p,frep,doping,calcevo); % propagation through the segment
    else
        [Esnaps,~,~,~]=SMErFiber2(E,t,w,freq,gamma,self_steep,B,fr,hr,fiberlength,nsteps,snapshots,tres,Pp,lambda_p,dl_p,frep,
            doping,calcevo); % propagation through the segment
    end
    E = Esnaps(snapshots,:); % because Esnaps is cumulative, the last raw is taken as result

elseif contains(type,'Dop_Gain_Tm') % Tm

    fiberlength = str2double(data(strcmp(segment_header,'L')))*1e7; % segment length in [nm]
    betas(1) = str2double(data(contains(segment_header,'GVD')))*1e-12; % GVD of the segment [ps^2/nm]
    betas(2) = str2double(data(contains(segment_header,'TOD')))*1e-15; % TOD of the segment [ps^3/nm]
    B = B_calc(betas,omegas,w); % dispersion coefficient of the fiber
    gamma = str2double(data(contains(segment_header,'Gamma')))*1e-9; % nonlinearity constant in [1/(KW.nm)]
    self_steep=str2double(data(contains(segment_header,'steep')));% whether to include self-steepening (1) or not (0)
    fr = str2double(data(contains(segment_header,'f_R'))); % fraction of Raman scattering of the segment

    gain_noise = str2double(data(contains(segment_header,'Noise'))); % Extract noise data [in percent]
    doping = str2double(data(contains(segment_header,'DopConc'))); % Doping Concentration
    Pp = str2double(data(contains(segment_header,'PumpPow')))*1e-3; % Pump Power in [W]
    lambda_p = str2double(data(contains(segment_header,'Pump_WL'))); % Pump Wavelength in [nm]
    dl_p = str2double(data(contains(segment_header,'PmpFWHM'))); % Pump FWHM in [nm]

    Ene_before = tres*(E*E');
    % addition of gain noise
    noise_strength = gain_noise/100;
    fprintf('Noise:␣%d␣\n',noise_strength);
    noise_percent = noise_strength/Ene_before; % originally noise_strength*E;
    noise = noise_percent.*randn(1,length(E));
    E = E + noise;
    % end adding noise

    if calcevo == 1
        [Esnaps, coords, pulsewidth, spectwidthf]=SMTmFiber2(E,t,w,freq,gamma,self_steep,B,fr,hr,fiberlength,nsteps,snapshots,tres
            ,Pp,lambda_p,dl_p,frep,doping,calcevo); % propagation through the segment
    else
        [Esnaps,~,~,~]=SMTmFiber2(E,t,w,freq,gamma,self_steep,B,fr,hr,fiberlength,nsteps,snapshots,tres,Pp,lambda_p,dl_p,frep,
            doping,calcevo); % propagation through the segment
    end
    E = Esnaps(snapshots,:); % because Esnaps is cumulative, the last raw is taken as result

elseif contains(type,'B_W_gain') % effective gain with backwards pumping and spectrum-weighted energy calculation.
    fiberlength = str2double(data(strcmp(segment_header,'L')))*1e7; % segment length in [nm]
    betas(1) = str2double(data(contains(segment_header,'GVD')))*1e-12; % GVD of the segment [ps^2/nm]
    betas(2) = str2double(data(contains(segment_header,'TOD')))*1e-15; % TOD of the segment [ps^3/nm]
    B = B_calc(betas,omegas,w); % dispersion coefficient of the fiber
    gamma = str2double(data(contains(segment_header,'Gamma')))*1e-9; % nonlinearity constant in [1/(KW.nm)]
    self_steep=str2double(data(contains(segment_header,'steep')));% whether to include self-steepening (1) or not (0)
    fr = str2double(data(contains(segment_header,'f_R'))); % fraction of Raman scattering of the segment

    gain_noise = str2double(data(contains(segment_header,'Noise'))); % Extract noise data [in percent]
    gss = 10^(str2double(data(contains(segment_header,'Unsat')))/10); % small signal gain (unsaturation gain)(linear scale,
        unitless)
    lambda_g = str2double(data(contains(segment_header,'Cent_WL'))); % gain central wavelength [nm]
    dl_g = str2double(data(contains(segment_header,'Gain_BW'))); % gain bandwidth [nm]
    Psat = str2double(data(contains(segment_header,'SatPow'))); % gain saturation power in [W]
```

```
    Esat0 = Psat/frep*1e-3; % saturation energy in [nJ]
    alpha= str2double(data(contains(segment_header,'alpha'))); % linear pump absorption constant in [dB/m]

    Ene_before = tres*(E*E');
    % addition of gain noise
    noise_strength = gain_noise/100;
    noise_percent = noise_strength/Ene_before; % originally noise_strength*E;
    noise = noise_percent.*randn(1,length(E));
    E = E + noise;
    % end adding noise

    if calcevo == 1
        [Esnaps, coords, pulsewidth, spectwidthf]=Active_B_W( E,t,w,freq,gamma,self_steep,B,fr,hr,fiberlength,nsteps,snapshots,
              tres,lambda_g,dl_g,Esat0,alpha,gss,1,edge_filter); % propagation through the segment
    else
        [Esnaps,~, ~, ~]=Active_B_W( E,t,w,freq,gamma,self_steep,B,fr,hr,fiberlength,nsteps,snapshots,tres,lambda_g,dl_g,Esat0,
              alpha,gss,0,edge_filter); % propagation through the segment
    end
    E = Esnaps(snapshots,:); % because Esnaps is cumulative, the last raw is taken as result

elseif contains(type,'NPE')

    snapshots = 1;
    q_0 = str2double(data(contains(segment_header,'q_0'))); % linear loss of NPE in [unitless]
    q_1 = str2double(data(contains(segment_header,'q_1'))); % modulation depth of NPE in [unitless]
    I_sat = str2double(data(contains(segment_header,'I_sat'))); % saturation power of NPE or SESAM in [W]
    f_0 = str2double(data(contains(segment_header,'Phi')))*pi/180; % phase shift of NPE tranmission in [rad]

    % fprintf('Peak Power (kW):%f\n',max(abs(E).^2));
    [E,E_r]=NPE(E,q_0,q_1,I_sat,f_0,t,edge_filter); % propagation through the segment
    Esnaps(1,:) = E;
    if calcevo == 1
        [coordsx,coordsy, pulsewidth, spectwidthf] = PhaseSpacePoint(E,t,4);
        coords = [coordsx' coordsy'];
    end
elseif contains(type,'SESAM')

    snapshots = 1;
    q_0 = str2double(data(contains(segment_header,'q_0'))); % linear loss of NPE in [unitless]
    q_1 = str2double(data(contains(segment_header,'q_1'))); % modulation depth of NPE in [unitless]
    I_sat = str2double(data(contains(segment_header,'I_sat'))); % saturation power of NPE or SESAM in [W]
    EsatSesam = I_sat/frep*1e-3;
    tau = str2double(data(contains(segment_header,'Tau'))); % Recovery time in [ps]

    E=SESAM(E,t,q_0,q_1,tau,EsatSesam,edge_filter); % propagation through the segment
    Esnaps(1,:) = E;
    if calcevo == 1
        [coordsx,coordsy, pulsewidth, spectwidthf] = PhaseSpacePoint(E,t,4);
        coords = [coordsx' coordsy'];
    end
elseif contains(type,'Filter')

    snapshots = 1;
    shape_filter = str2double(data(contains(segment_header,'Shape'))); % Shape of Filter
    fcent_w = str2double(data(contains(segment_header,'FCent_W'))); % Central Wavelength of Filter
    f_bw = str2double(data(contains(segment_header,'F_BW'))); % Bandwidth of Filter
    E = Filter(E,wave,shape_filter,fcent_w,f_bw);
    Esnaps(1,:) = E;
    if calcevo == 1
        [coordsx,coordsy, pulsewidth, spectwidthf] = PhaseSpacePoint(E,t,4);
        coords = [coordsx' coordsy'];
    end
elseif contains(type,'2filter') % a two-Gaussians filter with a time delay between them
    lambdas = [str2double(data(contains(segment_header,'blue_w'))) str2double(data(contains(segment_header,'red_w')))]; % Central
          Wavelengths array
    BWs = [str2double(data(contains(segment_header,'blue_BW'))) str2double(data(contains(segment_header,'red_BW')))]; %
          Bandwidths array
    delay= str2double(data(contains(segment_header,'delay')));
```

```
    E=DoubleFilter( E,wave,omegas,delay,lambdas,BWs);
    Esnaps(1,:) = E;
    if calcevo == 1
        [coordsx,coordsy, pulsewidth, spectwidthf] = PhaseSpacePoint(E,t,4);
        coords = [coordsx' coordsy'];
    end
end
end
```

Passive():

```
function [Esnaps,coords, p_widths, s_widths] = Passive( E,t,w,gamma,self_steep,B,fr,hr,fiberlength,nsteps,pages,tres,calcevo,
      edge_filter )
%This function simulates propagation in a passive fiber using RK4IP method.
%Time unit: ps
%Length unit: nm
%Energy unit: nJ


timesteps = length(E);
dz = fiberlength/nsteps;
eB=exp(B*dz/2);

coords = zeros(pages,2);
Esnaps = zeros(pages,length(E));
p_widths = zeros(1,pages);
s_widths = zeros(1,pages);
for i=1:nsteps
    E = Prop(E,w,gamma,eB,self_steep,fr,hr,dz,tres,timesteps); % Propagation through the segment
    if edge_filter == 1 % edgefiltering
        E = recenter(E,t); % recenter
        E = EdgeFilter(E,t);
    end
    if(mod(i,nsteps/pages)==0)
        if (calcevo==1)
            [a,b, p_width, s_width] = PhaseSpacePoint(E,t,4);
            coords(i/(nsteps/pages),1) = a;
            coords(i/(nsteps/pages),2) = b;
            p_widths(i/(nsteps/pages)) = p_width;
            s_widths(i/(nsteps/pages)) = s_width;
        end
        Esnaps(i/(nsteps/pages),:) = E;
    end
end


end
function [Eout] = Prop(Ein,w,gamma,eB,self_steep,fr,hr,dz,tres,timesteps)
% This function propagates the pulse through the segment using improved
% split-step Fourier transform method with 4th order Runge-Kutta method.
% REF: Agrawal, Nonlinear fiber optics, 5th ed., Ch. 2, Page 43

Ai=DSProp(Ein,eB,dz/2);
k05=NLProp(Ein,w,gamma,self_steep,fr,hr,dz,tres,timesteps);
k1=DSProp(k05,eB,dz/2);
k2=NLProp(Ai+k1/2,w,gamma,self_steep,fr,hr,dz,tres,timesteps);
k3=NLProp(Ai+k2/2,w,gamma,self_steep,fr,hr,dz,tres,timesteps);
k35=DSProp(Ai+k3,eB,dz/2);
k4=NLProp(k35,w,gamma,self_steep,fr,hr,dz,tres,timesteps);
k5=DSProp(Ai+k1/6+k2/3+k3/3,eB,dz/2);
Eout=k5+k4/6;
end

function [Eout] = NLProp(Ein,w,gamma,self_steep,fr,hr,dz,tres,timesteps)
%% Nonlinear operator
power=abs(Ein).^2;
```

```
if fr==0
    I=Ein.*power;
else
    I=(ifft(hr.*fft(power))).*Ein*tres*fr+(1-fr).*Ein.*power;
end
if self_steep==0
    Eout=-dz*gamma*(I*1i); % No self-steepening
else
    Eout=-dz*gamma*(I*1i+1/w*dif(I,tres,timesteps)); % self-steepening
end

end

function [Eout] = DSProp(Ein,eB,dz)
%% Dispersion operator
Ef=(fft(Ein));
Eout=ifft((Ef.*eB));
end


function [out] = dif(in,tres,len)
% Differentiation calculation using five-point stencil method
out=zeros(1,len);
out(1)=(in(4)-9*in(3)+45*in(2)-45*in(len)+9*in(len-1)-in(len-2))/(60*tres);
out(2)=(in(5)-9*in(4)+45*in(3)-45*in(1)+9*in(len)-in(len-1))/(60*tres);
out(3)=(in(6)-9*in(5)+45*in(4)-45*in(2)+9*in(1)-in(len))/(60*tres);
out(4:len-3)=(in(7:len)-9*in(6:len-1)+45*in(5:len-2)-45*in(3:len-4)+9*in(2:len-5)-in(1:len-6))/(60*tres);
out(len-2)=(in(1)-9*in(len)+45*in(len-1)-45*in(len-3)+9*in(len-4)-in(len-5))/(60*tres);
out(len-1)=(in(2)-9*in(1)+45*in(len)-45*in(len-2)+9*in(len-3)-in(len-4))/(60*tres);
out(len)=(in(3)-9*in(2)+45*in(1)-45*in(len-1)+9*in(len-2)-in(len-3))/(60*tres);
end
% Last modified: 15 January 2021
```

B_calc():

```
function [ B ] = B_calc( betas,omegas,w )
% Calculates the dispersion coefficient of the fiber

B=0;
for i = 1:length(betas) % Taylor expansion of betas
    B = B - 1i*betas(i)/factorial(i+1).*(omegas-w).^(i+1);
end

end

% Last modified: 22 September 2014
```

Active():

```
function [ Esnaps,coords, p_widths, s_widths] = Active( E,t,w,freq,gamma,self_steep,B,fr,hr,fiberlength,nsteps,pages,tres,
      lambda_g,dl_g,Esat,gss,calcevo,edge_filter)
%This function simulates propagation in a single-mode active fiber using RK4IP method.
%Time unit: ps
%Length unit: nm
%Energy unit: nJ


c = 299792.458; % Speed of light in [nm/ps]
dz = fiberlength/nsteps; % Step size
timesteps = length(t); % Time steps
eB=exp(B*dz/2);

f0 = c/lambda_g; % Central frequency of pump in [THz]
df = c*dl_g/lambda_g^2; % Gain bandwidth of pump in [THz]
```

```
G = (log(gss)/fiberlength)*df^2./(4*(freq-f0).^2+df^2); % Gain coefficient

coords = zeros(pages,2);
Esnaps = zeros(pages,length(E));
p_widths = zeros(1,pages);
s_widths = zeros(1,pages);

for i=1:nsteps
    E=Prop(E,w,gamma,self_steep,fr,hr,dz,tres,timesteps,eB,t,G,Esat);
    if edge_filter == 1 % edgefiltering
        E = recenter(E,t); % recenter
        E = EdgeFilter(E,t);
    end
    if(mod(i,nsteps/pages)==0)
        if (calcevo==1)
            [a,b, p_width, s_width] = PhaseSpacePoint(E,t,4);
            coords(i/(nsteps/pages),1) = a;
            coords(i/(nsteps/pages),2) = b;
            p_widths(i/(nsteps/pages)) = p_width;
            s_widths(i/(nsteps/pages)) = s_width;
        end
        Esnaps(i/(nsteps/pages),:) = E;
    end
end

end

function [Eout] = Prop(Ein,w,gamma,self_steep,fr,hr,dz,tres,timesteps,eB,t,G,Esat)
% This function propagates the pulse through the segment using improved
% split-step Fourier transform method with 4th order Runge-Kutta method.
% REF: Agrawal, Nonlinear fiber optics, 5th ed., Ch. 2, Page 43

[Ai]=DSProp(Ein,eB,t,tres,G,Esat,dz/2);
k1=DSProp(NLProp(Ein,w,gamma,self_steep,fr,hr,dz,tres,timesteps),eB,t,tres,G,Esat,dz/2);
k2=NLProp(Ai+k1/2,w,gamma,self_steep,fr,hr,dz,tres,timesteps);
k3=NLProp(Ai+k2/2,w,gamma,self_steep,fr,hr,dz,tres,timesteps);
k4=NLProp(DSProp(Ai+k3,eB,t,tres,G,Esat,dz/2),w,gamma,self_steep,fr,hr,dz,tres,timesteps);
Eout=DSProp(Ai+k1./6+k2./3+k3./3,eB,t,tres,G,Esat,dz/2);
Eout=Eout+k4./6;
end

function [Eout] = DSProp(Ein,eB,t,tres,G,Esat,dz)
%% Dispersion operator
Energy = tres*(Ein*Ein');
if Energy==0
    Eout = Ein;
else
    Ef=(fft(Ein));
    Ef = Ef.*exp( 0.5*G./(1+Energy/Esat).*dz);
    Eout=ifft((Ef.*eB));
end

end

function [Eout] = NLProp(Ein,w,gamma,self_steep,fr,hr,dz,tres,timesteps)
%% Nonlinear operator
power=abs(Ein).^2;
if fr==0
    I=Ein.*power;
else
    I=(ifft(hr.*fft(power))).*Ein*tres*fr+(1-fr).*Ein.*power;
end
if self_steep==0
    Eout=-dz*gamma*(I*1i); % No self-steepening
else
    Eout=-dz*gamma*(I*1i+1/w*dif(I,tres,timesteps)); % self-steepening
end
end
```

```
function [out] = dif(in,tres,len)
% Differentiation calculation using five-point stencil method
out=zeros(1,len);
out(1)=(in(4)-9*in(3)+45*in(2)-45*in(len)+9*in(len-1)-in(len-2))/(60*tres);
out(2)=(in(5)-9*in(4)+45*in(3)-45*in(1)+9*in(len)-in(len-1))/(60*tres);
out(3)=(in(6)-9*in(5)+45*in(4)-45*in(2)+9*in(1)-in(len))/(60*tres);
out(4:len-3)=(in(7:len)-9*in(6:len-1)+45*in(5:len-2)-45*in(3:len-4)+9*in(2:len-5)-in(1:len-6))/(60*tres);
out(len-2)=(in(1)-9*in(len)+45*in(len-1)-45*in(len-3)+9*in(len-4)-in(len-5))/(60*tres);
out(len-1)=(in(2)-9*in(1)+45*in(len)-45*in(len-2)+9*in(len-3)-in(len-4))/(60*tres);
out(len)=(in(3)-9*in(2)+45*in(1)-45*in(len-1)+9*in(len-2)-in(len-3))/(60*tres);
end
```

NPE():

```
function [ E_out, E_r] = NPE( E,q_0,q_1,I_sat,f_0,t,edge_filter )
%This function simulates a saturable absorber with a similar transmission
%function to NPE

% T(I)=q_0+q_1*sin^2(I/I_sat+f_0)
% q_0: Minimum transmission [unitless]
% q_1: Modulation depth [unitless]
% I_sat: Saturation power in [kW]
% f_0: Phase shift for the transmission curve in [rad]

if edge_filter == 1 % edgefiltering
    E = recenter(E,t); % recenter
    E = EdgeFilter(E,t);
end

power=abs(E).^2;

E_out = E.*sqrt(q_0+q_1*(sin(pi*0.5*power/I_sat+f_0)).^2);
E_r = E.*sqrt(1-(q_0+q_1*(sin(pi*0.5*power/I_sat+f_0)).^2));

end

% Last modified: 15 January 2021
```

SaveE():

```
function [ ] = SaveE(E,filename)

fid = fopen(filename,'W');

for i=1:length(E)
    fwrite(fid,real(E(i)),'double');
    fwrite(fid,imag(E(i)),'double');
end

fclose(fid);

end
```

LoadPage():

```
function [ Etemp ] = LoadPage( E,page,timesteps )

Etemp = E(((page-1)*timesteps+1):timesteps*page);

end
```

A.3 Figure 2.2 (dispersion)

The code (code4ThesisDispersion.m):

```
% code4ThesisDispersion
clear
settings_file="settings4ThesisDispersion.txt";

[seg_data, global_data,segment_header,global_header] = loadData(settings_file,0);
lambda_c = str2double(global_data(contains(global_header,'CentW'))); % Central wavelength (nm)

timewidth = str2double(global_data(contains(global_header,'TWidth'))); % Width of the time window in [ps]
tres1 = str2double(global_data(contains(global_header,'TRes')))*1e-3; % Resolution of the time window [ps] (written as fs*1e-3)

c = 299792.458; % [nm/ps]
timesteps=2^(ceil(log2(timewidth/tres1))); tres=timewidth/(timesteps);
t = -timewidth*0.5+tres:tres:timewidth*0.5; % Time in [ps]
timesteps=length(t);
fs=1/timewidth; % Sampling rate in [THz]
freq=c/lambda_c+fs*linspace(-timesteps/2-1,timesteps/2,timesteps);
freq=fftshift(freq); % Frequency in [THz]
wave=c./freq; shiftedWave=fftshift(wave); % Wavelength in [nm]
w=2*pi*c/lambda_c; % Central angular frequency in [THz]
omegas = 2*pi*freq; % Angular frequency in [THz]

% lambda_c = str2double(global_data(contains(global_header,'CentW'))); % Central wavelength (nm)
%
% timewidth = str2double(global_data(contains(global_header,'TWidth'))); % Width of the time window in [ps]
% tres1 = str2double(global_data(contains(global_header,'TRes')))*1e-3; % Resolution of the time window [ps] (written as fs*1e-3)
%
% timesteps=2^(ceil(log2(timewidth/tres1))); tres=timewidth/(timesteps-1);
% t = -timewidth*0.5:tres:timewidth*0.5; % Time in [ps]
% timesteps=length(t);
% fs=1/timewidth; % Sampling rate in [THz]
% freq=c/lambda_c+fs*linspace(-(timesteps-1)/2,(timesteps-1)/2,timesteps);
% freq=fftshift(freq); % Frequency in [THz]
% wave=c./freq; shiftedWave=fftshift(wave); % Wavelength in [nm]
% w=2*pi*c/lambda_c; % Central angular frequency in [THz]
% omegas = 2*pi*freq; % Angular frequency in [THz]

CommandLine(settings_file);

% Before dispersion
BeforeDispersion=LoadPage(LoadE(['Data' num2str(1) '.bin']),1,timesteps);
powerBeforeDispersion=abs(BeforeDispersion).^2;powerMax=max(powerBeforeDispersion);

phase=unwrap(angle(BeforeDispersion));
chirpBeforeDispersion=(phase(2:end)-phase(1:end-1))./(t(2:end)-t(1:end-1));
t_chirp=(t(1:end-1)+t(2:end))/2;

spectrumBeforeDispersion=fftshift(abs(fft(BeforeDispersion)).^2);spectrumMax=max(spectrumBeforeDispersion);

% After dispersion
AfterDispersion=LoadPage(LoadE(['Data' num2str(1) '.bin']),2,timesteps);
powerAfterDispersion=abs(AfterDispersion).^2;

phase=unwrap(angle(AfterDispersion));
chirpAfterDispersion=(phase(2:end)-phase(1:end-1))./(t(2:end)-t(1:end-1));

spectrumAfterDispersion=fftshift(abs(fft(AfterDispersion)).^2);

f=figure('position',[800 800 500 800]);f.Color='w';

subplot(3,1,1)
```

```
plot(t,powerBeforeDispersion/powerMax,'.',"LineWidth",1.6);xlabel('Time␣(ps)');ylabel('Power␣(a.u.)');xlim([-1 +1]);ylim([0 1.1])
      ;
hold on; plot(t,powerAfterDispersion/powerMax,"LineWidth",1.1); hold off; legend("Before dispersion", "After dispersion");
text(0.03,0.92,'(a)','Units','normalized','fontsize',11)

subplot(3,1,2)
plot(shiftedWave,spectrumBeforeDispersion/spectrumMax,'.',"LineWidth",1.6);xlabel('Wavelength␣(nm)');ylabel('Amplitude␣(a.u.)');
      xlim([1020 +1040]);ylim([-0 1.1]);
hold on; plot(shiftedWave,spectrumAfterDispersion/spectrumMax,"LineWidth",1.1); hold off; legend("Before dispersion", "After
      dispersion");
text(0.03,0.92,'(b)','Units','normalized','fontsize',11)


subplot(3,1,3)
plot(t_chirp,chirpBeforeDispersion,'.',"LineWidth",1.6);xlabel('Time␣(ps)');ylabel('Chirp␣(THz)');xlim([-1 +1]);ylim([-10 10]);
hold on; plot(t_chirp,chirpAfterDispersion,"LineWidth",1.1); hold off; legend("Before dispersion", "After dispersion");
text(0.03,0.92,'(c)','Units','normalized','fontsize',11)
```

The settings file (settings4ThesisDispersion.txt):

```
-----------------------------------------------------------------------------------------------------------------------------------------------
TWidth TRes frep CentW pulse_no spacing Shape Dw DT Energy File_No Page_No SaveN plotN plot_seg store_seg Passes Conv_typ
      Conv_spn Conv_seg Conv_th EdgeF
ps fs MHz nm integer ps index THz ratio nJ integer page RundTrp RundTrp integer integer RundTrp index RundTrp integer percent
      logical
-----------------------------------------------------------------------------------------------------------------------------------------------
30 10 1000 1030 1 19.999 2 1 1 2e-2 1410 20 1 1 2 -1 1 1 10 4 0.000002 0
-----------------------------------------------------------------------------------------------------------------------------------------------
  - - - - - - - - - - - - - - - - - - - - - S - - - - - - - - - -
  - - - - - - - - - - - - - - - - - - - - - A P - - - - - - - - -
  - - - - - - - - - - - - - - - - - - - - - T H - - - - - - - - -
  - - - - - - - - - - - - - - - - - - - - - U A - - - - - - - - -
  - - - - - - - - - - - - - - - - - - - - - R S - - - - - - - - -
  - - - - - - - - - - - - - - - - - - - - - A E - - - - - - - - -
  - - - - - - - - - - - - - - - - - - - - - T - - - - - - - - - -
  - - - - G - - R - - - - - - - - - - - - - I S - - F - - - - - -
  - - - - R - - A - - - - - - - - - - - - - O H - - I - - - - - -
  - - - - O - N M - - - - - - - - - - - - - N I - - L - - - - - -
  - - - - U T O A - - - - - - - - - - - - - F - - T - - B - - -
  - - - - P H N N - - - - - - - - - - - - - P T - - E - - L R B -
  - - - - - I L - - - - - - - - - - - - - - O - - - R - - U E L R
  - N - - V R I S - - - - - - - - - - - - - W o - - - - D E D U E
  - U - - E D N C - - - C - - - - - - - P - - E F - - C - O - - E D
  - M - - L - E A - - - E - - - D - - U - - R - - - E - U F F - -
  - B - - O O A T - - U N - S - O - - M - M - N - - N F B I I F F
  - E N L C R R T S - N T - A P P - P P - O O P - - T I L L L I I
  - R U E I D I E E - S R G T U I - U - - D F E - - R L E T T L L
  - - M N T E T R L - A A A U M N - M S - U - - R - A T - E E T T
  - O B G Y R Y I F - T L I R P G - P P - L N T E F L E F R R E E
  M F E T - - - N _ - U - N A - - - - E L A P R C I - R I - - R R
  E - R H D D C G S G R W - T A C P W C I T E A O L W - L W W - -
  D S - - I I O - T A A A B I B O U A T N I - N V T A B T A A B B
  I N O O S S F F E I T V A O S N M V R E O O S E E V A E V V A A
  U A F F P P F R E N E E N N O C P E A A N R M R R E N R E E N N
  M P - - E E I A P - D L D - R E - L L R - - I Y - L D - L L D D
  - S S F R R C C E N - E W P P N P E - - D S S - S E W D E E W W
  T H T I S S I T N O G N I O T T O N F L E E S T H N I E N N I I
  Y O E B I I E I I I A G D W I I W G W O P S I I A G D L G G D D
  P T P E O O N O N S I T T E O O E T H S T A O M P T T A T T T T
  E S S R N N T N G E N H H R N N R H M S H M N E E H H Y H H H H
-----------------------------------------------------------------------------------------------------------------------------------------------
Seg_ID AcType  Snap Steps L GVD TOD Gamma f_R steep Noise Unsat Cent_WL Gain_BW SatPow alpha DopConc PumpPow Pump_WL PmpFWHM q_0
      q_1 I_sat Phi Tau Shape FCent_W F_BW delay blue_w red_w blue_BW red_BW
ID Name Snap Step cm fs2/mm fs3/mm 1/kW/m fraction logical dB dB nm nm W dB/m nm-3 W nm nm None None kW deg ps Index nm nm ps nm
      nm nm nm
-----------------------------------------------------------------------------------------------------------------------------------------------
```

```
seg_1 Passive 1 1 1 1 0 0 0 0 NaN NaN NaN NaN NaN NaN NaN NaN NaN NaN NaN NaN NaN NaN NaN NaN NaN NaN NaN NaN NaN NaN NaN NaN
seg_2 Passive 1 1 400 22 0 0 0 0 NaN NaN NaN NaN NaN NaN NaN NaN NaN NaN NaN NaN NaN NaN NaN NaN NaN NaN NaN NaN NaN NaN NaN NaN
```

A.4 Figure 2.3 (Kerr nonlinearity)

The code (code4ThessisNonlinearity.m):

```
% code4ThesisDispersion
clear
settings_file="settings4ThesisNonlinearity.txt";

[seg_data, global_data,segment_header,global_header] = loadData(settings_file,0);
lambda_c = str2double(global_data(contains(global_header,'CentW'))); % Central wavelength (nm)

timewidth = str2double(global_data(contains(global_header,'TWidth'))); % Width of the time window in [ps]
tres1 = str2double(global_data(contains(global_header,'TRes')))*1e-3; % Resolution of the time window [ps] (written as fs*1e-3)

c = 299792.458; % [nm/ps]
timesteps=2^(ceil(log2(timewidth/tres1))); tres=timewidth/(timesteps);
t = -timewidth*0.5+tres:tres:timewidth*0.5; % Time in [ps]
timesteps=length(t);
fs=1/timewidth; % Sampling rate in [THz]
freq=c/lambda_c+fs*linspace(-timesteps/2-1,timesteps/2,timesteps);
freq=fftshift(freq); % Frequency in [THz]
wave=c./freq; shiftedWave=fftshift(wave); % Wavelength in [nm]
w=2*pi*c/lambda_c; % Central angular frequency in [THz]
omegas = 2*pi*freq; % Angular frequency in [THz]


CommandLine(settings_file);

% Before dispersion
BeforeNonlinearity=LoadPage(LoadE(['Data' num2str(1) '.bin']),1,timesteps);
powerBeforeNonlinearity=abs(BeforeNonlinearity).^2;powerMax=max(powerBeforeNonlinearity);

phase=unwrap(angle(BeforeNonlinearity));
chirpBeforeNonlinearity=(phase(2:end)-phase(1:end-1))./(t(2:end)-t(1:end-1));
t_chirp=(t(1:end-1)+t(2:end))/2;

spectrumBeforeNonlinearity=fftshift(abs(fft(BeforeNonlinearity)).^2);spectrumMaxBefore=max(spectrumBeforeNonlinearity);

% After dispersion
AfterNonlinearity=LoadPage(LoadE(['Data' num2str(1) '.bin']),2,timesteps);
powerAfterNonlinearity=abs(AfterNonlinearity).^2;

phase=unwrap(angle(AfterNonlinearity));
chirpAfterNonlinearity=(phase(2:end)-phase(1:end-1))./(t(2:end)-t(1:end-1));

spectrumAfterNonlinearity=fftshift(abs(fft(AfterNonlinearity)).^2);spectrumMaxAfter=max(spectrumAfterNonlinearity);

f=figure('position',[800 800 500 800]);f.Color='w';

subplot(3,1,1)
plot(t,powerBeforeNonlinearity/powerMax,'.',"LineWidth",1.6);xlabel('Time␣(ps)');ylabel('Power␣(a.u.)');xlim([-1 +1]);ylim([0
      1.1]);
hold on; plot(t,powerAfterNonlinearity/powerMax,"LineWidth",1.1); hold off;legend("Before nonlinearity", "After nonlinearity");
text(0.03,0.92,'(a)','Units','normalized','fontsize',11)

subplot(3,1,2)
```

```
plot(shiftedWave,spectrumBeforeNonlinearity/spectrumMaxBefore,'.',"LineWidth",1.6);xlabel('Wavelength␣(nm)');ylabel('Amplitude␣(a
      .u.)');xlim([1000 +1060]);ylim([-0 1.2]);
hold on; plot(shiftedWave,spectrumAfterNonlinearity/spectrumMaxAfter,"LineWidth",1.1); hold off; legend("Before nonlinearity", "
      After nonlinearity");
text(0.03,0.92,'(b)','Units','normalized','fontsize',11)


subplot(3,1,3)
plot(t_chirp,chirpBeforeNonlinearity,'.',"LineWidth",1.6);xlabel('Time␣(ps)');ylabel('Chirp␣(THz)');xlim([-1 +1]);ylim([-30 30]);
hold on; plot(t_chirp,chirpAfterNonlinearity,"LineWidth",1.1); hold off; legend("Before nonlinearity", "After nonlinearity");
text(0.03,0.92,'(c)','Units','normalized','fontsize',11)
```

The settings file (settings4ThesisNonlinearity.txt):

```
-------------------------------------------------------------------------------------------------------------------------------
TWidth TRes frep CentW pulse_no spacing Shape Dw DT Energy File_No Page_No SaveN plotN plot_seg store_seg Passes Conv_typ
      Conv_spn Conv_seg Conv_th EdgeF
ps fs MHz nm integer ps index THz ratio nJ integer page RundTrp RundTrp integer integer RundTrp index RundTrp integer percent
      logical
-------------------------------------------------------------------------------------------------------------------------------
30 10 1000 1030 1 19.999 2 1 1 1 1410 20 1 1 2 -1 1 1 10 4 0.000002 0
-------------------------------------------------------------------------------------------------------------------------------
  - - - - - - - - - - - - - - - - - - - - - - S - - - - - - - - - - -
  - - - - - - - - - - - - - - - - - - - - - - A P - - - - - - - - - -
  - - - - - - - - - - - - - - - - - - - - - - T H - - - - - - - - - -
  - - - - - - - - - - - - - - - - - - - - - - U A - - - - - - - - - -
  - - - - - - - - - - - - - - - - - - - - - - R S - - - - - - - - - -
  - - - - - - - - - - - - - - - - - - - - - - A E - - - - - - - - - -
  - - - - - - - - - - - - - - - - - - - - - - T - - - - - - - - - - -
  - - - - G - - R - - - - - - - - - - - - - - I S - - F - - - - - - -
  - - - - R - - A - - - - - - - - - - - - - - O H - - I - - - - - - -
  - - - - O - N M - - - - - - - - - - - - - - N I - - L - - - - - - -
  - - - - U T O A - - - - - - - - - - - - - - - F - - T - - B - - - -
  - - - - P H N N - - - - - - - - - - - - - - P T - - E - - L R B -
  - - - - - I L - - - - - - - - - - - - - - - O - - - R - - U E L R
  - N - - V R I S - - - - - - - - - - - - - - W o - - - - D E D U E
  - U - - E D N C - - - C - - - - - - - P - - E F - - C - O - - E D
  - M - - L - E A - - - E - - - D - - U - - R - - - E - U F F - -
  - B - - O O A T - - U N - S - O - - M - M - N - - N F B I I F F
  - E N L C R R T S - N T - A P P - P P - O O P - - T I L L L I I
  - R U E I D I E E - S R G T U I - U - - D F E - - R L E T T L L
  - - M N T E T R L - A A A U M N - M S - U - - R - A T - E E T T
  - O B G Y R Y I F - T L I R P G - P P - L N T E F L E F R R E E
  M F E T - - - N _ - U - N A - - - - E L A P R C I - R I - - R R
  E - R H D D C G S G R W - T A C P W C I T E A O L W - L W W - -
  D S - - I I O - T A A A B I B O U A T N I - N V T A B T A A B B
  I N O O S S F F E I T V A O S N M V R E O O S E E V A E V V A A
  U A F F P P F R E N E E N N O C P E A A N R M R R E N R E E N N
  M P - - E E I A P - D L D - R E - L L R - - I Y - L D - L L D D
  - S S F R R C C E N - E W P P N P E - - D S S - S E W D E E W W
  T H T I S S I T N O G N I O T T O N F L E E S T H N I E N N I I
  Y O E B I I E I I I A G D W I I W G W O P S I I A G D L G G D D
  P T P E O O N O N S I T T E O O E T H S T A O M P T T A T T T T
  E S S R N N T N G E N H H R N N R H M S H M N E E H H Y H H H H
-------------------------------------------------------------------------------------------------------------------------------
Seg_ID AcType  Snap Steps L GVD TOD Gamma f_R steep Noise Unsat Cent_WL Gain_BW SatPow alpha DopConc PumpPow Pump_WL PmpFWHM q_0
      q_1 I_sat Phi Tau Shape FCent_W F_BW delay blue_w red_w blue_BW red_BW
ID Name Snap Step cm fs2/mm fs3/mm 1/kW/m fraction logical dB dB nm nm W dB/m nm-3 W nm nm None None kW deg ps Index nm nm ps nm
      nm nm nm
-------------------------------------------------------------------------------------------------------------------------------
seg_1 Passive 1 1 1 1 0 0 0 0 NaN NaN NaN NaN NaN NaN NaN NaN NaN NaN NaN NaN NaN NaN NaN NaN NaN NaN NaN NaN NaN NaN NaN NaN
seg_2 Passive 1 100 80 0 0 4.5 0 0 NaN NaN NaN NaN NaN NaN NaN NaN NaN NaN NaN NaN NaN NaN NaN NaN NaN NaN NaN NaN NaN NaN NaN
```

A.5 Figure 2.4 (soliton)

The code (code4ThesisSoliton.m):

```
% code4ThesisSoliton
clear
settings_file1="settings4ThesisSoliton1.txt";
settings_file2="settings4ThesisSoliton2.txt";

[seg_data, global_data,segment_header,global_header] = loadData(settings_file1,0);
lambda_c = str2double(global_data(contains(global_header,'CentW'))); % Central wavelength (nm)

timewidth = str2double(global_data(contains(global_header,'TWidth'))); % Width of the time window in [ps]
tres1 = str2double(global_data(contains(global_header,'TRes')))*1e-3; % Resolution of the time window [ps] (written as fs*1e-3)

c = 299792.458; % [nm/ps]
timesteps=2^(ceil(log2(timewidth/tres1))); tres=timewidth/(timesteps);
t = -timewidth*0.5+tres:tres:timewidth*0.5; % Time in [ps]
timesteps=length(t);
fs=1/timewidth; % Sampling rate in [THz]
freq=c/lambda_c+fs*linspace(-timesteps/2-1,timesteps/2,timesteps);
freq=fftshift(freq); % Frequency in [THz]
wave=c./freq; shiftedWave=fftshift(wave); % Wavelength in [nm]
w=2*pi*c/lambda_c; % Central angular frequency in [THz]
omegas = 2*pi*freq; % Angular frequency in [THz]


CommandLine(settings_file1);

% Soliton Before
SolitonBefore=LoadPage(LoadE(['Data' num2str(1) '.bin']),1,timesteps);
powerSolitonBefore=abs(SolitonBefore).^2;powerSolitonMax=max(powerSolitonBefore);

phase=unwrap(angle(SolitonBefore));
chirpSolitonBefore=(phase(2:end)-phase(1:end-1))./(t(2:end)-t(1:end-1));
t_chirp=(t(1:end-1)+t(2:end))/2;

spectrumSolitonBefore=fftshift(abs(fft(SolitonBefore)).^2);spectrumSolitonMaxBefore=max(spectrumSolitonBefore);

% Soliton After
SolitonAfter=LoadPage(LoadE(['Data' num2str(1) '.bin']),2,timesteps);
powerSolitonAfter=abs(SolitonAfter).^2;powerSolitonMax=max(powerSolitonMax,max(powerSolitonAfter));

phase=unwrap(angle(SolitonAfter));
chirpSolitonAfter=(phase(2:end)-phase(1:end-1))./(t(2:end)-t(1:end-1));

spectrumSolitonAfter=fftshift(abs(fft(SolitonAfter)).^2);spectrumMaxSolitonAfter=max(spectrumSolitonAfter);

f=figure('position',[800 800 700 800]);f.Color='w';

subplot(3,2,1)
semilogy(t,powerSolitonBefore/powerSolitonMax,'.',"LineWidth",1.7);xlabel('Time␣(ps)');ylabel('Power␣(a.u.)');xlim([-2 +2]);ylim
      ([1e-6 10]);
hold on; semilogy(t,powerSolitonAfter/powerSolitonMax,"LineWidth",1.1); hold off;legend("Before", "After");
text(0.03,0.92,'(a)','Units','normalized','fontsize',11)

subplot(3,2,3)
plot(shiftedWave,spectrumSolitonBefore/spectrumSolitonMaxBefore,'.',"LineWidth",1.7);xlabel('Wavelength␣(nm)');ylabel('Amplitude␣
      (a.u.)');xlim([1020 +1040]);ylim([-0 1.2]);
hold on; plot(shiftedWave,spectrumSolitonAfter/spectrumMaxSolitonAfter,"LineWidth",1.1); hold off; legend("Before", "After");
text(0.03,0.92,'(b)','Units','normalized','fontsize',11)

subplot(3,2,5)
plot(t_chirp,chirpSolitonBefore,'.',"LineWidth",1.7);xlabel('Time␣(ps)');ylabel('Chirp␣(THz)');xlim([-2 +2]);ylim([-30 30]);
hold on; plot(t_chirp,chirpSolitonAfter,"LineWidth",1.1); hold off; legend("Before", "After");
```

```
text(0.03,0.92,'(c)','Units','normalized','fontsize',11)

CommandLine(settings_file2);

% Gaussian Before
GaussianBefore=LoadPage(LoadE(['Data' num2str(1) '.bin']),1,timesteps);
powerGaussianBefore=abs(GaussianBefore).^2;powerGaussianMax=max(powerGaussianBefore);

phase=unwrap(angle(GaussianBefore));
chirpGaussianBefore=(phase(2:end)-phase(1:end-1))./(t(2:end)-t(1:end-1));
t_chirp=(t(1:end-1)+t(2:end))/2;

spectrumGaussianBefore=fftshift(abs(fft(GaussianBefore)).^2);spectrumGaussianMaxBefore=max(spectrumGaussianBefore);

% Gaussian After
GaussianAfter=LoadPage(LoadE(['Data' num2str(1) '.bin']),2,timesteps);
powerGaussianAfter=abs(GaussianAfter).^2;powerGaussianMax=max(powerGaussianMax,max(powerGaussianAfter));

phase=unwrap(angle(GaussianAfter));
chirpGaussianAfter=(phase(2:end)-phase(1:end-1))./(t(2:end)-t(1:end-1));

spectrumGaussianAfter=fftshift(abs(fft(GaussianAfter)).^2);spectrumMaxGaussianAfter=max(spectrumGaussianAfter);

subplot(3,2,2)
semilogy(t,powerGaussianBefore/powerGaussianMax,'.',"LineWidth",1.7);xlabel('Time␣(ps)');ylabel('Power␣(a.u.)');xlim([-2 +2]);
      ylim([1e-6 10]);
hold on; semilogy(t,powerGaussianAfter/powerGaussianMax,"LineWidth",1.1); hold off;legend("Before", "After");
text(0.03,0.92,'(d)','Units','normalized','fontsize',11)

subplot(3,2,4)
plot(shiftedWave,spectrumGaussianBefore/spectrumGaussianMaxBefore,'.',"LineWidth",1.7);xlabel('Wavelength␣(nm)');ylabel('
      Amplitude␣(a.u.)');xlim([1020 +1040]);ylim([-0 1.2]);
hold on; plot(shiftedWave,spectrumGaussianAfter/spectrumMaxGaussianAfter,"LineWidth",1.1); hold off; legend("Before", "After");
text(0.03,0.92,'(e)','Units','normalized','fontsize',11)

subplot(3,2,6)
plot(t_chirp,chirpGaussianBefore,'.',"LineWidth",1.7);xlabel('Time␣(ps)');ylabel('Chirp␣(THz)');xlim([-2 +2]);ylim([-30 30]);
hold on; plot(t_chirp,chirpGaussianAfter,"LineWidth",1.1); hold off; legend("Before", "After");
text(0.03,0.92,'(f)','Units','normalized','fontsize',11)
```

The settings files:

1. settings4ThesisSoliton1.txt:

```
-------------------------------------------------------------------------------------------------------------------------------

TWidth TRes frep CentW pulse_no spacing Shape Dw DT Energy File_No Page_No SaveN plotN plot_seg store_seg Passes
      Conv_typ Conv_spn Conv_seg Conv_th EdgeF
ps fs MHz nm integer ps index THz ratio nJ integer page RundTrp RundTrp integer integer RundTrp index RundTrp integer
      percent logical
-------------------------------------------------------------------------------------------------------------------------------

30 30 1000 1030 1 19.999 1 1 1 0.0427 1410 20 1 1 2 -1 1 1 10 4 0.000002 0
-------------------------------------------------------------------------------------------------------------------------------

  - - - - - - - - - - - - - - - - - - - - - - S - - - - - - - - - - -
  - - - - - - - - - - - - - - - - - - - - - - A P - - - - - - - - - -
  - - - - - - - - - - - - - - - - - - - - - - T H - - - - - - - - - -
  - - - - - - - - - - - - - - - - - - - - - - U A - - - - - - - - - -
  - - - - - - - - - - - - - - - - - - - - - - R S - - - - - - - - - -
  - - - - - - - - - - - - - - - - - - - - - - A E - - - - - - - - - -
  - - - - - - - - - - - - - - - - - - - - - - T - - - - - - - - - - -
  - - - - G - - R - - - - - - - - - - - - - - I S - - F - - - - - - -
```

```
 - - - - R - - A - - - - - - - - - - - - - - O H - - I - - - - - -
 - - - - O - N M - - - - - - - - - - - - - - N I - - L - - - - - -
 - - - - U T O A - - - - - - - - - - - - - - - F - - T - - B - - -
 - - - - P H N N - - - - - - - - - - - - - - P T - - E - - L R B -
 - - - - - I L - - - - - - - - - - - - - - - O - - - R - - U E L R
 - N - - V R I S - - - - - - - - - - - - - - W o - - - - - D E D U E
 - U - - E D N C - - - C - - - - - - - P - - E F - - C - O - - E D
 - M - - L - E A - - - E - - - D - - U - - R - - - E - U F F - -
 - B - - O O A T - - U N - S - O - - M - M - N - - N F B I I F F
 - E N L C R R T S - N T - A P P - P P - O O P - - T I L L L I I
 - R U E I D I E E - S R G T U I - U - - D F E - - R L E T T L L
 - - M N T E T R L - A A A U M N - M S - U - - R - A T - E E T T
 - O B G Y R Y I F - T L I R P G - P P - L N T E F L E F R R E E
 M F E T - - - N _ - U - N A - - - - E L A P R C I - R I - - R R
 E - R H D D C G S G R W - T A C P W C I T E A O L W - L W W - -
 D S - - I I O - T A A A B I B O U A T N I - N V T A B T A A B B
 I N O O S S F F E I T V A O S N M V R E O O S E E V A E V V A A
 U A F F P P F R E N E E N N O C P E A A N R M R R E N R E E N N
 M P - - E E I A P - D L D - R E - L L R - - I Y - L D - L L D D
 - S S F R R C C E N - E W P P N P E - - D S S - S E W D E E W W
 T H T I S S I T N O G N I O T T O N F L E E S T H N I E N N I I
 Y O E B I I E I I I A G D W I I W G W O P S I I A G D L G G D D
 P T P E O O N O N S I T T E O O E T H S T A O M P T T A T T T T
 E S S R N N T N G E N H H R N N R H M S H M N E E H H Y H H H H
```

```
Seg_ID AcType  Snap Steps L GVD TOD Gamma f_R steep Noise Unsat Cent_WL Gain_BW SatPow alpha DopConc PumpPow Pump_WL
      PmpFWHM q_0 q_1 I_sat Phi Tau Shape FCent_W F_BW delay blue_w red_w blue_BW red_BW
ID Name Snap Step cm fs2/mm fs3/mm 1/kW/m fraction logical dB dB nm nm W dB/m nm-3 W nm nm None None kW deg ps Index nm
      nm ps nm nm nm nm
```

```
seg_1 Passive 1 1 1 1 0 0 0 0 NaN NaN NaN NaN NaN NaN NaN NaN NaN NaN NaN NaN NaN NaN NaN NaN NaN NaN NaN NaN NaN NaN NaN
      NaN
seg_2 Passive 1 1000 1000 -22 0 4.5 0 0 NaN NaN NaN NaN NaN NaN NaN NaN NaN NaN NaN NaN NaN NaN NaN NaN NaN NaN NaN NaN
      NaN NaN NaN
```

2. settings4ThesisSoliton2.txt:

```
TWidth TRes frep CentW pulse_no spacing Shape Dw DT Energy File_No Page_No SaveN plotN plot_seg store_seg Passes
      Conv_typ Conv_spn Conv_seg Conv_th EdgeF
ps fs MHz nm integer ps index THz ratio nJ integer page RundTrp RundTrp integer integer RundTrp index RundTrp integer
      percent logical
```

```
30 30 1000 1030 1 19.999 2 1 1 0.0427 1410 20 1 1 2 -1 1 1 10 4 0.000002 0
```

```
 - - - - - - - - - - - - - - - - - - - - - - S - - - - - - - - - -
 - - - - - - - - - - - - - - - - - - - - - - A P - - - - - - - - -
 - - - - - - - - - - - - - - - - - - - - - - T H - - - - - - - - -
 - - - - - - - - - - - - - - - - - - - - - - U A - - - - - - - - -
 - - - - - - - - - - - - - - - - - - - - - - R S - - - - - - - - -
 - - - - - - - - - - - - - - - - - - - - - - A E - - - - - - - - -
 - - - - - - - - - - - - - - - - - - - - - - T - - - - - - - - - -
 - - - - G - - R - - - - - - - - - - - - - - I S - - F - - - - - -
 - - - - R - - A - - - - - - - - - - - - - - O H - - I - - - - - -
 - - - - O - N M - - - - - - - - - - - - - - N I - - L - - - - - -
 - - - - U T O A - - - - - - - - - - - - - - - F - - T - - B - - -
 - - - - P H N N - - - - - - - - - - - - - - P T - - E - - L R B -
 - - - - - I L - - - - - - - - - - - - - - - O - - - R - - U E L R
 - N - - V R I S - - - - - - - - - - - - - - W o - - - - - D E D U E
 - U - - E D N C - - - C - - - - - - - P - - E F - - C - O - - E D
 - M - - L - E A - - - E - - - D - - U - - R - - - E - U F F - -
```

```
 - B - - 0 0 A T - - U N - S - 0 - - M - M - N - - N F B I I F F
 - E N L C R R T S - N T - A P P - P P - 0 0 P - - T I L L L I I
 - R U E I D I E E - S R G T U I - U - - D F E - - R L E T T L L
 - - M N T E T R L - A A A U M N - M S - U - - R - A T - E E T T
 - 0 B G Y R Y I F - T L I R P G - P P - L N T E F L E F R R E E
 M F E T - - - N _ - U - N A - - - - E L A P R C I - R I - - R R
 E - R H D D C G S G R W - T A C P W C I T E A O L W - L W W - -
 D S - - I I O - T A A A B I B O U A T N I - N V T A B T A A B B
 I N O O S S F F E I T V A O S N M V R E O O S E E V A E V V A A
 U A F F P P F R E N E E N N O C P E A A N R M R R E N R E E N N
 M P - - E E I A P - D L D - R E - L L R - - I Y - L D - L L D D
 - S S F R R C C E N - E W P P N P E - - D S S - S E W D E E W W
 T H T I S S I T N O G N I O T T O N F L E E S T H N I E N N I I
 Y O E B I I E I I I A G D W I I W G W O P S I I A G D L G G D D
 P T P E O O N O N S I T T E O O E T H S T A O M P T T A T T T T
 E S S R N N T N G E N H H R N N R H M S H M N E E H H Y H H H H
```

```
Seg_ID AcType  Snap Steps L GVD TOD Gamma f_R steep Noise Unsat Cent_WL Gain_BW SatPow alpha DopConc PumpPow Pump_WL
      PmpFWHM q_0 q_1 I_sat Phi Tau Shape FCent_W F_BW delay blue_w red_w blue_BW red_BW
ID Name Snap Step cm fs2/mm fs3/mm 1/kW/m fraction logical dB dB nm nm W dB/m nm-3 W nm nm None None kW deg ps Index nm
      nm ps nm nm nm nm
```

```
seg_1 Passive 1 1 1 1 0 0 0 0 NaN NaN NaN NaN NaN NaN NaN NaN NaN NaN NaN NaN NaN NaN NaN NaN NaN NaN NaN NaN NaN NaN
      NaN
seg_2 Passive 1 1000 1000 -22 0 4.5 0 0 NaN NaN NaN NaN NaN NaN NaN NaN NaN NaN NaN NaN NaN NaN NaN NaN NaN NaN NaN
      NaN NaN NaN
```

A.6 Figure 2.5 (passive similariton)

The code (code4ThesisPassiveSimilariton.m):

```
% code4ThesisPassiveSimilariton
clear
settings_file1="settings4ThesisPassiveSimilariton1.txt";
settings_file2="settings4ThesisPassiveSimilariton2.txt";

[seg_data, global_data,segment_header,global_header] = loadData(settings_file1,0);
lambda_c = str2double(global_data(contains(global_header,'CentW'))); % Central wavelength (nm)

timewidth = str2double(global_data(contains(global_header,'TWidth'))); % Width of the time window in [ps]
tres1 = str2double(global_data(contains(global_header,'TRes')))*1e-3; % Resolution of the time window [ps] (written as fs*1e-3)

c = 299792.458; % [nm/ps]
timesteps=2^(ceil(log2(timewidth/tres1))); tres=timewidth/(timesteps);
t = -timewidth*0.5+tres:tres:timewidth*0.5; % Time in [ps]
timesteps=length(t);
fs=1/timewidth; % Sampling rate in [THz]
freq=c/lambda_c+fs*linspace(-timesteps/2-1,timesteps/2,timesteps);
freq=fftshift(freq); % Frequency in [THz]
wave=c./freq; shiftedWave=fftshift(wave); % Wavelength in [nm]
w=2*pi*c/lambda_c; % Central angular frequency in [THz]
omegas = 2*pi*freq; % Angular frequency in [THz]

% Tight Soliton
CommandLine(settings_file1);

% Soliton Before
SolitonBefore=LoadPage(LoadE(['Data' num2str(1) '.bin']),1,timesteps);
```

```
powerSolitonBefore=abs(SolitonBefore).^2;powerMaxBefore=max(powerSolitonBefore);

phase=unwrap(angle(SolitonBefore));
chirpSolitonBefore=(phase(2:end)-phase(1:end-1))./(t(2:end)-t(1:end-1));
t_chirp=(t(1:end-1)+t(2:end))/2;

spectrumSolitonBefore=fftshift(abs(fft(SolitonBefore)).^2);spectrumSolitonMaxBefore=max(spectrumSolitonBefore);

% Soliton After
SolitonAfter=LoadPage(LoadE(['Data' num2str(1) '.bin']),2,timesteps);
powerSolitonAfter=abs(SolitonAfter).^2;powerMaxAfter=max(powerSolitonAfter);

phase=unwrap(angle(SolitonAfter));
chirpSolitonAfter=(phase(2:end)-phase(1:end-1))./(t(2:end)-t(1:end-1));

spectrumSolitonAfter=fftshift(abs(fft(SolitonAfter)).^2);spectrumSolitonMaxAfter=max(spectrumSolitonAfter);


% Broad Gaussian
CommandLine(settings_file2);

% Gaussian Before
GaussianBefore=LoadPage(LoadE(['Data' num2str(1) '.bin']),1,timesteps);
powerGaussianBefore=abs(GaussianBefore).^2;powerMaxBefore=max(max(powerGaussianBefore),powerMaxBefore);

phase=unwrap(angle(GaussianBefore));
chirpGaussianBefore=(phase(2:end)-phase(1:end-1))./(t(2:end)-t(1:end-1));
t_chirp=(t(1:end-1)+t(2:end))/2;

spectrumGaussianBefore=fftshift(abs(fft(GaussianBefore)).^2);spectrumGaussianMaxBefore=max(spectrumGaussianBefore);

% Gaussian After
GaussianAfter=LoadPage(LoadE(['Data' num2str(1) '.bin']),2,timesteps);
powerGaussianAfter=abs(GaussianAfter).^2;powerMaxAfter=max(max(powerGaussianAfter),powerMaxAfter);

phase=unwrap(angle(GaussianAfter));
chirpGaussianAfter=(phase(2:end)-phase(1:end-1))./(t(2:end)-t(1:end-1));

spectrumGaussianAfter=fftshift(abs(fft(GaussianAfter)).^2);spectrumGaussianMaxAfter=max(spectrumGaussianAfter);


f=figure('position',[800 800 700 800]);f.Color='w';

subplot(3,2,1)
plot(t,powerSolitonBefore/powerMaxBefore,"LineWidth",1.4);xlabel('Time␣(ps)');ylabel('Power␣(a.u.)');xlim([-1 +1]);ylim([0 1.1]);
hold on;plot(t,powerGaussianBefore/powerMaxBefore,"LineWidth",1.4);hold off;
text(0.03,0.92,'(a)','Units','normalized','fontsize',11)

subplot(3,2,2)
plot(t,powerSolitonAfter/powerMaxAfter,"LineWidth",1.4);xlabel('Time␣(ps)');ylabel('Power␣(a.u.)');xlim([-10 +10]);ylim([0 1.1]);
hold on; plot(t,powerGaussianAfter/powerMaxAfter,"LineWidth",1.4); hold off;
text(0.03,0.92,'(d)','Units','normalized','fontsize',11)

subplot(3,2,3)
plot(shiftedWave,spectrumSolitonBefore/spectrumSolitonMaxBefore,"LineWidth",1.4);xlabel('Wavelength␣(nm)');ylabel('Amplitude␣(a.u
      .)');xlim([1000 +1060]);ylim([-0 1.1]);
hold on;plot(shiftedWave,spectrumGaussianBefore/spectrumGaussianMaxBefore,"LineWidth",1.4);hold off;
text(0.03,0.92,'(b)','Units','normalized','fontsize',11)

subplot(3,2,4)
plot(shiftedWave,spectrumSolitonAfter/spectrumSolitonMaxAfter,"LineWidth",1.4);xlabel('Wavelength␣(nm)');ylabel('Amplitude␣(a.u.)
      ');xlim([1000 +1060]);ylim([-0 1.1]);
hold on; plot(shiftedWave,spectrumGaussianAfter/spectrumGaussianMaxAfter,"LineWidth",1.4); hold off;
text(0.03,0.92,'(e)','Units','normalized','fontsize',11)

subplot(3,2,5)
plot(t_chirp,chirpSolitonBefore,"LineWidth",1.4);xlabel('Time␣(ps)');ylabel('Chirp␣(THz)');xlim([-1 +1]);ylim([-60 60]);
hold on;plot(t_chirp,chirpGaussianBefore,"LineWidth",1.4);hold off;
```

```
text(0.03,0.92,'(c)','Units','normalized','fontsize',11)

subplot(3,2,6)
plot(t_chirp,chirpSolitonAfter,"LineWidth",1.4);xlabel('Time␣(ps)');ylabel('Chirp␣(THz)');xlim([-10 +10]);ylim([-60 60]);
hold on; plot(t_chirp,chirpGaussianAfter,"LineWidth",1.4); hold off;
text(0.03,0.92,'(f)','Units','normalized','fontsize',11)
```

The settings files:

1. settings4ThesisPassiveSimilariton1.txt:

```
      ------------------------------------------------------------------------------------------------------------------------------------------------------

TWidth TRes frep CentW pulse_no spacing Shape Dw DT Energy File_No Page_No SaveN plotN plot_seg store_seg Passes
      Conv_typ Conv_spn Conv_seg Conv_th EdgeF
ps fs MHz nm integer ps index THz ratio nJ integer page RundTrp RundTrp integer integer RundTrp index RundTrp integer
      percent logical
------------------------------------------------------------------------------------------------------------------------------------------------------

90 30 1000 1030 1 19.999 1 3 1 0.3 1410 20 1 1 2 -1 1 1 10 4 0.000002 0
------------------------------------------------------------------------------------------------------------------------------------------------------

  - - - - - - - - - - - - - - - - - - - - - - S - - - - - - - - - -
  - - - - - - - - - - - - - - - - - - - - - - A P - - - - - - - - -
  - - - - - - - - - - - - - - - - - - - - - - T H - - - - - - - - -
  - - - - - - - - - - - - - - - - - - - - - - U A - - - - - - - - -
  - - - - - - - - - - - - - - - - - - - - - - R S - - - - - - - - -
  - - - - - - - - - - - - - - - - - - - - - - A E - - - - - - - - -
  - - - - - - - - - - - - - - - - - - - - - - T - - - - - - - - - -
  - - - - G - - R - - - - - - - - - - - - - I S - - F - - - - - - -
  - - - - R - - A - - - - - - - - - - - - - O H - - I - - - - - - -
  - - - - O - N M - - - - - - - - - - - - - N I - - L - - - - - - -
  - - - - U T O A - - - - - - - - - - - - - - F - - T - - B - - - -
  - - - - P H N N - - - - - - - - - - - - - P T - - E - - L R B -
  - - - - - I L - - - - - - - - - - - - - - O - - - R - - U E L R
  - N - - V R I S - - - - - - - - - - - - - W o - - - - D E D U E
  - U - - E D N C - - - C - - - - - - - P - - E F - - C - O - - E D
  - M - - L - E A - - - E - - - D - - U - - R - - - E - U F F - -
  - B - - O O A T - - U N - S - O - - M - M - N - - N F B I I F F
  - E N L C R R T S - N T - A P P - P P - O O P - - T I L L L I I
  - R U E I D I E E - S R G T U I - U - - D F E - - R L E T T L L
  - - M N T E T R L - A A A U M N - M S - U - - R - A T - E E T T
  - O B G Y R Y I F - T L I R P G - P P - L N T E F L E F R R E E
  M F E T - - - N _ - U - N A - - - - E L A P R C I - R I - - R R
  E - R H D D C G S G R W - T A C P W C I T E A O L W - L W W - -
  D S - - I I O - T A A A B I B O U A T N I - N V T A B T A A B B
  I N O O S S F F E I T V A O S N M V R E O O S E E V A E V V A A
  U A F F P P F R E N E E N N O C P E A A N R M R R E N R E E N N
  M P - - E E I A P - D L D - R E - L L R - - I Y - L D - L L D D
  - S S F R R C C E N - E W P P N P E - - D S S - S E W D E E W W
  T H T I S S I T N O G N I O T T O N F L E E S T H N I E N N I I
  Y O E B I I E I I I A G D W I I W G W O P S I I A G D L G G D D
  P T P E O O N O N S I T T E O O E T H S T A O M P T T A T T T T
  E S S R N N T N G E N H H R N N R H M S H M N E E H H Y H H H H
------------------------------------------------------------------------------------------------------------------------------------------------------

Seg_ID AcType  Snap Steps L GVD TOD Gamma f_R steep Noise Unsat Cent_WL Gain_BW SatPow alpha DopConc PumpPow Pump_WL
      PmpFWHM q_0 q_1 I_sat Phi Tau Shape FCent_W F_BW delay blue_w red_w blue_BW red_BW
ID Name Snap Step cm fs2/mm fs3/mm 1/kW/m fraction logical dB dB nm nm W dB/m nm-3 W nm nm None None kW deg ps Index nm
      nm ps nm nm nm nm
------------------------------------------------------------------------------------------------------------------------------------------------------
```

```
seg_1 Passive 1 1 1 1 0 0 0 0 NaN NaN NaN NaN NaN NaN NaN NaN NaN NaN NaN NaN NaN NaN NaN NaN NaN NaN NaN NaN NaN NaN NaN NaN
      NaN
seg_2 Passive 1 10000 600 23 0 4.5 0 0 NaN NaN NaN NaN NaN NaN NaN NaN NaN NaN NaN NaN NaN NaN NaN NaN NaN NaN NaN NaN NaN
      NaN NaN NaN
```

2. settings4ThesisPassiveSimilariton2.txt:

```
      ------------------------------------------------------------------------------------------------------------------------------------------------

TWidth TRes frep CentW pulse_no spacing Shape Dw DT Energy File_No Page_No SaveN plotN plot_seg store_seg Passes
      Conv_typ Conv_spn Conv_seg Conv_th EdgeF
ps fs MHz nm integer ps index THz ratio nJ integer page RundTrp RundTrp integer integer RundTrp index RundTrp integer
      percent logical
------------------------------------------------------------------------------------------------------------------------------------------------

90 30 1000 1030 1 19.999 2 3 1 0.3 1410 20 1 1 2 -1 1 1 10 4 0.000002 0
------------------------------------------------------------------------------------------------------------------------------------------------

  - - - - - - - - - - - - - - - - - - - - - - S - - - - - - - - - -
  - - - - - - - - - - - - - - - - - - - - - - A P - - - - - - - - -
  - - - - - - - - - - - - - - - - - - - - - - T H - - - - - - - - -
  - - - - - - - - - - - - - - - - - - - - - - U A - - - - - - - - -
  - - - - - - - - - - - - - - - - - - - - - - R S - - - - - - - - -
  - - - - - - - - - - - - - - - - - - - - - - A E - - - - - - - - -
  - - - - - - - - - - - - - - - - - - - - - - T - - - - - - - - - -
  - - - - G - - R - - - - - - - - - - - - - I S - - F - - - - - - -
  - - - - R - - A - - - - - - - - - - - - - O H - - I - - - - - - -
  - - - - O - N M - - - - - - - - - - - - - N I - - L - - - - - - -
  - - - - U T O A - - - - - - - - - - - - - - F - - T - - B - - - -
  - - - - P H N N - - - - - - - - - - - - - P T - - E - - L R B -
  - - - - - I L - - - - - - - - - - - - - - O - - - R - - U E L R
  - N - - V R I S - - - - - - - - - - - - - W o - - - - D E D U E
  - U - - E D N C - - - C - - - - - - - P - - E F - - C - O - - E D
  - M - - L - E A - - - E - - - D - - U - - R - - - E - U F F - -
  - B - - O O A T - - U N - S - O - - M - M - N - - N F B I I F F
  - E N L C R R T S - N T - A P P - P P - O O P - - T I L L L I I
  - R U E I D I E E - S R G T U I - U - - D F E - - R L E T T L L
  - - M N T E T R L - A A A U M N - M S - U - - R - A T - E E T T
  - O B G Y R Y I F - T L I R P G - P P - L N T E F L E F R R E E
  M F E T - - - N _ - U - N A - - - - E L A P R C I - R I - - R R
  E - R H D D C G S G R W - T A C P W C I T E A O L W - L W W - -
  D S - - I I O - T A A A B I B O U A T N I - N V T A B T A A B B
  I N O O S S F F E I T V A O S N M V R E O O S E E V A E V V A A
  U A F F P P F R E N E E N N O C P E A A N R M R R E N R E E N N
  M P - - E E I A P - D L D - R E - L L R - - I Y - L D - L L D D
  - S S F R R C C E N - E W P P N P E - - D S S - S E W D E E W W
  T H T I S S I T N O G N I O T T O N F L E E S T H N I E N N I I
  Y O E B I I E I I I A G D W I I W G W O P S I I A G D L G G D D
  P T P E O O N O N S I T T E O O E T H S T A O M P T T A T T T T
  E S S R N N T N G E N H H R N N R H M S H M N E E H H Y H H H H
------------------------------------------------------------------------------------------------------------------------------------------------

Seg_ID AcType  Snap Steps L GVD TOD Gamma f_R steep Noise Unsat Cent_WL Gain_BW SatPow alpha DopConc PumpPow Pump_WL
      PmpFWHM q_0 q_1 I_sat Phi Tau Shape FCent_W F_BW delay blue_w red_w blue_BW red_BW
ID Name Snap Step cm fs2/mm fs3/mm 1/kW/m fraction logical dB dB nm nm W dB/m nm-3 W nm nm None None kW deg ps Index nm
      nm ps nm nm nm nm
------------------------------------------------------------------------------------------------------------------------------------------------

seg_1 Passive 1 1 50 23 0 0 0 0 NaN NaN NaN NaN NaN NaN NaN NaN NaN NaN NaN NaN NaN NaN NaN NaN NaN NaN NaN NaN NaN NaN NaN
      NaN
seg_2 Passive 1 10000 600 23 0 4.5 0 0 NaN NaN NaN NaN NaN NaN NaN NaN NaN NaN NaN NaN NaN NaN NaN NaN NaN NaN NaN NaN NaN
      NaN NaN NaN
```

A.7 Figure 2.6 (active similariton)

The code (code4ThesisActiveSimilariton.m):

```
% code4ThesisActiveSimilariton
clear
settings_file1="settings4ThesisActiveSimilariton1.txt";
settings_file2="settings4ThesisActiveSimilariton2.txt";

[seg_data, global_data,segment_header,global_header] = loadData(settings_file1,0);
lambda_c = str2double(global_data(contains(global_header,'CentW'))); % Central wavelength (nm)

timewidth = str2double(global_data(contains(global_header,'TWidth'))); % Width of the time window in [ps]
tres1 = str2double(global_data(contains(global_header,'TRes')))*1e-3; % Resolution of the time window [ps] (written as fs*1e-3)

c = 299792.458; % [nm/ps]
timesteps=2^(ceil(log2(timewidth/tres1))); tres=timewidth/(timesteps);
t = -timewidth*0.5+tres:tres:timewidth*0.5; % Time in [ps]
timesteps=length(t);
fs=1/timewidth; % Sampling rate in [THz]
freq=c/lambda_c+fs*linspace(-timesteps/2-1,timesteps/2,timesteps);
freq=fftshift(freq); % Frequency in [THz]
wave=c./freq; shiftedWave=fftshift(wave); % Wavelength in [nm]
w=2*pi*c/lambda_c; % Central angular frequency in [THz]
omegas = 2*pi*freq; % Angular frequency in [THz]

% Tight Soliton
CommandLine(settings_file1);

% Soliton Before
SolitonBefore=LoadPage(LoadE(['Data' num2str(1) '.bin']),1,timesteps);
powerSolitonBefore=abs(SolitonBefore).^2;powerMaxBefore=max(powerSolitonBefore);

phase=unwrap(angle(SolitonBefore));
chirpSolitonBefore=(phase(2:end)-phase(1:end-1))./(t(2:end)-t(1:end-1));
t_chirp=(t(1:end-1)+t(2:end))/2;

spectrumSolitonBefore=fftshift(abs(fft(SolitonBefore)).^2);spectrumSolitonMaxBefore=max(spectrumSolitonBefore);

% Soliton After
SolitonAfter=LoadPage(LoadE(['Data' num2str(1) '.bin']),2,timesteps);
powerSolitonAfter=abs(SolitonAfter).^2;powerMaxAfter=max(powerSolitonAfter);

phase=unwrap(angle(SolitonAfter));
chirpSolitonAfter=(phase(2:end)-phase(1:end-1))./(t(2:end)-t(1:end-1));

spectrumSolitonAfter=fftshift(abs(fft(SolitonAfter)).^2);spectrumSolitonMaxAfter=max(spectrumSolitonAfter);


% Broad Gaussian
CommandLine(settings_file2);

% Gaussian Before
GaussianBefore=LoadPage(LoadE(['Data' num2str(1) '.bin']),1,timesteps);
powerGaussianBefore=abs(GaussianBefore).^2;powerMaxBefore=max(max(powerGaussianBefore),powerMaxBefore);

phase=unwrap(angle(GaussianBefore));
chirpGaussianBefore=(phase(2:end)-phase(1:end-1))./(t(2:end)-t(1:end-1));
t_chirp=(t(1:end-1)+t(2:end))/2;

spectrumGaussianBefore=fftshift(abs(fft(GaussianBefore)).^2);spectrumGaussianMaxBefore=max(spectrumGaussianBefore);

% Gaussian After
GaussianAfter=LoadPage(LoadE(['Data' num2str(1) '.bin']),2,timesteps);
powerGaussianAfter=abs(GaussianAfter).^2;powerMaxAfter=max(max(powerGaussianAfter),powerMaxAfter);
```

```
phase=unwrap(angle(GaussianAfter));
chirpGaussianAfter=(phase(2:end)-phase(1:end-1))./(t(2:end)-t(1:end-1));

spectrumGaussianAfter=fftshift(abs(fft(GaussianAfter)).^2);spectrumGaussianMaxAfter=max(spectrumGaussianAfter);


f=figure('position',[800 800 700 800]);f.Color='w';

subplot(3,2,1)
plot(t,powerSolitonBefore/powerMaxBefore,"LineWidth",1.4);xlabel('Time␣(ps)');ylabel('Power␣(a.u.)');xlim([-1 +1]);ylim([0 1.1]);
hold on;plot(t,powerGaussianBefore/powerMaxBefore,"LineWidth",1.4);hold off;
text(0.03,0.92,'(a)','Units','normalized','fontsize',11)

subplot(3,2,2)
plot(t,powerSolitonAfter/powerMaxAfter,"LineWidth",1.4);xlabel('Time␣(ps)');ylabel('Power␣(a.u.)');xlim([-10 +10]);ylim([0 1.1]);
hold on; plot(t,powerGaussianAfter/powerMaxAfter,"LineWidth",1.4); hold off;
text(0.03,0.92,'(d)','Units','normalized','fontsize',11)

subplot(3,2,3)
plot(shiftedWave,spectrumSolitonBefore/spectrumSolitonMaxBefore,"LineWidth",1.4);xlabel('Wavelength␣(nm)');ylabel('Amplitude␣(a.u
      .)');xlim([1000 +1080]);ylim([-0 1.1]);
hold on;plot(shiftedWave,spectrumGaussianBefore/spectrumGaussianMaxBefore,"LineWidth",1.4);hold off;
text(0.03,0.92,'(b)','Units','normalized','fontsize',11)

subplot(3,2,4)
plot(shiftedWave,spectrumSolitonAfter/spectrumSolitonMaxAfter,"LineWidth",1.4);xlabel('Wavelength␣(nm)');ylabel('Amplitude␣(a.u.)
      ');xlim([1000 +1080]);ylim([-0 1.1]);
hold on; plot(shiftedWave,spectrumGaussianAfter/spectrumGaussianMaxAfter,"LineWidth",1.4); hold off;
text(0.03,0.92,'(e)','Units','normalized','fontsize',11)

subplot(3,2,5)
plot(t_chirp,chirpSolitonBefore,"LineWidth",1.4);xlabel('Time␣(ps)');ylabel('Chirp␣(THz)');xlim([-1 +1]);ylim([-80 80]);
hold on;plot(t_chirp,chirpGaussianBefore,"LineWidth",1.4);hold off;
text(0.03,0.92,'(c)','Units','normalized','fontsize',11)

subplot(3,2,6)
plot(t_chirp,chirpSolitonAfter,"LineWidth",1.4);xlabel('Time␣(ps)');ylabel('Chirp␣(THz)');xlim([-10 +10]);ylim([-80 80]);
hold on; plot(t_chirp,chirpGaussianAfter,"LineWidth",1.4); hold off;
text(0.03,0.92,'(f)','Units','normalized','fontsize',11)
```

The settings files:

1. settings4ThesisActiveSimilariton1.txt:

```
-------------------------------------------------------------------------------------------------------------------------------
TWidth TRes frep CentW pulse_no spacing Shape Dw DT Energy File_No Page_No SaveN plotN plot_seg store_seg Passes
      Conv_typ Conv_spn Conv_seg Conv_th EdgeF
ps fs MHz nm integer ps index THz ratio nJ integer page RundTrp RundTrp integer integer RundTrp index RundTrp integer
      percent logical
-------------------------------------------------------------------------------------------------------------------------------

90 25 1000 1040 1 19.999 1 3 1 0.3 1410 20 1 1 2 -1 1 1 10 4 0.000002 0
-------------------------------------------------------------------------------------------------------------------------------

  - - - - - - - - - - - - - - - - - - - - - - S - - - - - - - - - - -
  - - - - - - - - - - - - - - - - - - - - - - A P - - - - - - - - - -
  - - - - - - - - - - - - - - - - - - - - - - T H - - - - - - - - - -
  - - - - - - - - - - - - - - - - - - - - - - U A - - - - - - - - - -
  - - - - - - - - - - - - - - - - - - - - - - R S - - - - - - - - - -
  - - - - - - - - - - - - - - - - - - - - - - A E - - - - - - - - - -
  - - - - - - - - - - - - - - - - - - - - - - T - - - - - - - - - - -
  - - - - G - - R - - - - - - - - - - - - - - I S - - F - - - - - - -
  - - - - R - - A - - - - - - - - - - - - - - O H - - I - - - - - - -
```

```
 - - - - O - N M - - - - - - - - - - - - - N I - - L - - - - - -
 - - - - U T O A - - - - - - - - - - - - - - F - - T - - B - - -
 - - - - P H N N - - - - - - - - - - - - - P T - - E - - L R B -
 - - - - - I L - - - - - - - - - - - - - - O - - - R - - U E L R
 - N - - V R I S - - - - - - - - - - - - - W o - - - - D E D U E
 - U - - E D N C - - - C - - - - - - - P - - E F - - C - O - - E D
 - M - - L - E A - - - E - - - D - - U - - R - - - E - U F F - -
 - B - - O O A T - - U N - S - O - - M - M - N - - N F B I I F F
 - E N L C R R T S - N T - A P P - P P - O O P - - T I L L L I I
 - R U E I D I E E - S R G T U I - U - - D F E - - R L E T T L L
 - - M N T E T R L - A A A U M N - M S - U - - R - A T - E E T T
 - O B G Y R Y I F - T L I R P G - P P - L N T E F L E F R R E E
 M F E T - - - N _ - U - N A - - - - E L A P R C I - R I - - R R
 E - R H D D C G S G R W - T A C P W C I T E A O L W - L W W - -
 D S - - I I O - T A A A B I B O U A T N I - N V T A B T A A B B
 I N O O S S F F E I T V A O S N M V R E O O S E E V A E V V A A
 U A F F P P F R E N E E N N O C P E A A N R M R R E N R E E N N
 M P - - E E I A P - D L D - R E - L L R - - I Y - L D - L L D D
 - S S F R R C C E N - E W P P N P E - - D S S - S E W D E E W W
 T H T I S S I T N O G N I O T T O N F L E E S T H N I E N N I I
 Y O E B I I E I I I A G D W I I W G W O P S I I A G D L G G D D
 P T P E O O N O N S I T T E O O E T H S T A O M P T T A T T T T
 E S S R N N T N G E N H H R N N R H M S H M N E E H H Y H H H H
```

```
Seg_ID AcType  Snap Steps L GVD TOD Gamma f_R steep Noise Unsat Cent_WL Gain_BW SatPow alpha DopConc PumpPow Pump_WL
      PmpFWHM q_0 q_1 I_sat Phi Tau Shape FCent_W F_BW delay blue_w red_w blue_BW red_BW
ID Name Snap Step cm fs2/mm fs3/mm 1/kW/m fraction logical dB dB nm nm W dB/m nm-3 W nm nm None None kW deg ps Index nm
      nm ps nm nm nm nm
```

```
seg_1 Passive 1 1 1 1 0 0 0 0 NaN NaN NaN NaN NaN NaN NaN NaN NaN NaN NaN NaN NaN NaN NaN NaN NaN NaN NaN NaN NaN NaN
      NaN
seg_2 Eff_Gain 1 6000 600 23 0 4.5 0 0 -200 25 1040 100 200 NaN NaN NaN NaN NaN NaN  NaN  NaN  NaN NaN  NaN  NaN
      NaN NaN NaN NaN NaN
```

2. settings4ThesisActiveSimilariton2.txt:

```
TWidth TRes frep CentW pulse_no spacing Shape Dw DT Energy File_No Page_No SaveN plotN plot_seg store_seg Passes
      Conv_typ Conv_spn Conv_seg Conv_th EdgeF
ps fs MHz nm integer ps index THz ratio nJ integer page RundTrp RundTrp integer integer RundTrp index RundTrp integer
      percent logical
```

```
90 25 1000 1040 1 19.999 2 1.5 1 0.3 1410 20 1 1 2 -1 1 1 10 4 0.000002 0
```

```
 - - - - - - - - - - - - - - - - - - - - - S - - - - - - - - - -
 - - - - - - - - - - - - - - - - - - - - - A P - - - - - - - - -
 - - - - - - - - - - - - - - - - - - - - - T H - - - - - - - - -
 - - - - - - - - - - - - - - - - - - - - - U A - - - - - - - - -
 - - - - - - - - - - - - - - - - - - - - - R S - - - - - - - - -
 - - - - - - - - - - - - - - - - - - - - - A E - - - - - - - - -
 - - - - - - - - - - - - - - - - - - - - - T - - - - - - - - - -
 - - - - G - - R - - - - - - - - - - - - - I S - - F - - - - - -
 - - - - R - - A - - - - - - - - - - - - - O H - - I - - - - - -
 - - - - O - N M - - - - - - - - - - - - - N I - - L - - - - - -
 - - - - U T O A - - - - - - - - - - - - - - F - - T - - B - - -
 - - - - P H N N - - - - - - - - - - - - - P T - - E - - L R B -
 - - - - - I L - - - - - - - - - - - - - - O - - - R - - U E L R
 - N - - V R I S - - - - - - - - - - - - - W o - - - - D E D U E
 - U - - E D N C - - - C - - - - - - - P - - E F - - C - O - - E D
 - M - - L - E A - - - E - - - D - - U - - R - - - E - U F F - -
 - B - - O O A T - - U N - S - O - - M - M - N - - - N F B I I F F
```

```
 - E N L C R R T S - N T - A P P - P P - O O P - - T I L L L I I
 - R U E I D I E E - S R G T U I - U - - D F E - - R L E T T L L
 - - M N T E T R L - A A A U M N - M S - U - - R - A T - E E T T
 - O B G Y R Y I F - T L I R P G - P P - L N T E F L E F R R E E
 M F E T - - - N _ - U - N A - - - - E L A P R C I - R I - - R R
 E - R H D D C G S G R W - T A C P W C I T E A O L W - L W W - -
 D S - - I I O - T A A A B I B O U A T N I - N V T A B T A A B B
 I N O O S S F F E I T V A O S N M V R E O O S E E V A E V V A A
 U A F F P P F R E N E E N N O C P E A A N R M R R E N R E E N N
 M P - - E E I A P - D L D - R E - L L R - - I Y - L D - L L D D
 - S S F R R C C E N - E W P P N P E - - D S S - S E W D E E W W
 T H T I S S I T N O G N I O T T O N F L E E S T H N I E N N I I
 Y O E B I I E I I I A G D W I I W G W O P S I I A G D L G G D D
 P T P E O O N O N S I T T E O O E T H S T A O M P T T A T T T T
 E S S R N N T N G E N H H R N N R H M S H M N E E H H Y H H H H
```

```
Seg_ID AcType  Snap Steps L GVD TOD Gamma f_R steep Noise Unsat Cent_WL Gain_BW SatPow alpha DopConc PumpPow Pump_WL
      PmpFWHM q_0 q_1 I_sat Phi Tau Shape FCent_W F_BW delay blue_w red_w blue_BW red_BW
ID Name Snap Step cm fs2/mm fs3/mm 1/kW/m fraction logical dB dB nm nm W dB/m nm-3 W nm nm None None kW deg ps Index nm
      nm ps nm nm nm nm
```

```
seg_1 Passive 1 1 170 23 0 0 0 0 NaN NaN NaN NaN NaN NaN NaN NaN NaN NaN NaN NaN NaN NaN NaN NaN NaN NaN NaN NaN NaN NaN
       NaN
seg_2 Eff_Gain 1 6000 600 23 0 4.5 0 0 -200 25 1040 100 200 NaN NaN NaN NaN NaN NaN  NaN  NaN  NaN  NaN NaN  NaN  NaN
      NaN NaN NaN NaN NaN
```

A.8 Figure 2.7 (Narrow filtering)

The code (code4ThesisNarrowFiltering.m):

```
settings_file1="settings4ThesisNarrowFiltering1.txt";
settings_file2="settings4ThesisNarrowFiltering2.txt";

[seg_data, global_data,segment_header,global_header] = loadData(settings_file1,0);

lambda_c = str2double(global_data(contains(global_header,'CentW'))); % Central wavelength (nm)

timewidth = str2double(global_data(contains(global_header,'TWidth'))); % Width of the time window in [ps]
tres1 = str2double(global_data(contains(global_header,'TRes')))*1e-3; % Resolution of the time window [ps] (written as fs*1e-3)

c = 299792.458; % [nm/ps]
timesteps=2^(ceil(log2(timewidth/tres1))); tres=timewidth/(timesteps-1);
t = -timewidth*0.5:tres:timewidth*0.5; % Time in [ps]
timesteps=length(t);
fs=1/timewidth; % Sampling rate in [THz]
freq=c/lambda_c+fs*linspace(-(timesteps-1)/2,(timesteps-1)/2,timesteps); freq=fftshift(freq); % Frequency in [THz]
wave=c./freq; shiftedWave=fftshift(wave); % Wavelength in [nm]
w=2*pi*c/lambda_c; % Central angular frequency in [THz]
omegas = 2*pi*freq; % Angular frequency in [THz]


CommandLine(settings_file1);
MyPulseBeforeFiltering=LoadPage(LoadE(['Data' num2str(1) '.bin']),4,timesteps);

MyPulseBeforeFiltering_power=abs(MyPulseBeforeFiltering).^2;

% my pulse before the filter
phase=unwrap(angle(MyPulseBeforeFiltering));
```

```
MyPulseBeforeFiltering_chirp=(phase(2:end)-phase(1:end-1))./(t(2:end)-t(1:end-1));
t_chirp=(t(1:end-1)+t(2:end))/2;
upperChirpLimit=1.1*max(MyPulseBeforeFiltering_chirp(find((t_chirp>-2).* (t_chirp<2)) ));
lowerChirpLimit=1.1*min(MyPulseBeforeFiltering_chirp(find((t_chirp>-2).* (t_chirp<2)) ));

MyPulseBeforeFiltering_spectrum=fftshift(abs(fft(MyPulseBeforeFiltering)).^2);


% my pulse after the filter
MyPulseAfterFiltering=LoadPage(LoadE(['Data' num2str(1) '.bin']),5,timesteps);

MyPulseAfterFiltering_power=abs(MyPulseAfterFiltering).^2;

phase=unwrap(angle(MyPulseAfterFiltering));
MyPulseAfterFiltering_chirp=(phase(2:end)-phase(1:end-1))./(t(2:end)-t(1:end-1));

MyPulseAfterFiltering_spectrum=fftshift(abs(fft(MyPulseAfterFiltering)).^2);


% Soliton Pulse after the filter
CommandLine(settings_file2);

SolitonPulseBeforeFiltering=LoadPage(LoadE(['Data' num2str(1) '.bin']),1,timesteps);

SolitonPulseBeforeFiltering_power=abs(SolitonPulseBeforeFiltering).^2;

phase=unwrap(angle(SolitonPulseBeforeFiltering));
SolitonPulseBeforeFiltering_chirp=(phase(2:end)-phase(1:end-1))./(t(2:end)-t(1:end-1));

SolitonPulseBeforeFiltering_spectrum=fftshift(abs(fft(SolitonPulseBeforeFiltering)).^2);

% Soliton pulse after the filter
SolitonPulseAfterFiltering_spectrum=fftshift(abs(fft(SolitonPulseBeforeFiltering)).^2);

SolitonPulseAfterFiltering=LoadPage(LoadE(['Data' num2str(1) '.bin']),2,timesteps);

SolitonPulseAfterFiltering_power=abs(SolitonPulseAfterFiltering).^2;

phase=unwrap(angle(SolitonPulseAfterFiltering));
SolitonPulseAfterFiltering_chirp=(phase(2:end)-phase(1:end-1))./(t(2:end)-t(1:end-1));

SolitonPulseAfterFiltering_spectrum=fftshift(abs(fft(SolitonPulseAfterFiltering)).^2);



% plotting
f=figure('position',[800 800 700 800]);f.Color='w';

plot1Max=max([MyPulseBeforeFiltering_power SolitonPulseBeforeFiltering_power]);
subplot(3,2,1)
plot(t,MyPulseBeforeFiltering_power/plot1Max,'LineWidth',1.4); xlim([-2 +2]); ylim([0 1.1]);hold on
plot(t,SolitonPulseBeforeFiltering_power/plot1Max,'LineWidth',1.4);xlabel('Delay␣(ps)');ylabel('Power␣(au)');
legend('pulse␣1','pulse␣2');text(0.03,0.9,'(a)','Units','normalized')


subplot(3,2,5)
plot(t_chirp,MyPulseBeforeFiltering_chirp,'LineWidth',1.4);xlim([-2 +2]);ylim([-15 +15]);hold on
plot(t_chirp,SolitonPulseBeforeFiltering_chirp,'LineWidth',1.4);xlabel('Delay␣(ps)');ylabel('Chirp␣(THz)');
legend('pulse␣1','pulse␣2');text(0.03,0.9,'(b)','Units','normalized')
legend('Location','southeast');

plot5Max=[max(MyPulseBeforeFiltering_spectrum) max(SolitonPulseBeforeFiltering_spectrum)];
subplot(3,2,3)
plot(shiftedWave,MyPulseBeforeFiltering_spectrum/plot5Max(1),'LineWidth',1.4); xlim([1010 1050]);hold on
plot(shiftedWave,SolitonPulseBeforeFiltering_spectrum/plot5Max(2),'LineWidth',1.4); ylim([-0 1.1]);
xlabel('Wavelength␣(nm)'); ylabel('Amplitude␣(au)');
legend('pulse␣1','pulse␣2');text(0.03,0.9,'(e)','Units','normalized')
```

```
plot2Max=max([MyPulseAfterFiltering_power SolitonPulseAfterFiltering_power]);
subplot(3,2,2)
plot(t,MyPulseAfterFiltering_power/plot2Max,'LineWidth',1.4); xlim([-2 +2]);hold on; ylim([0 1.1]);
plot(t,SolitonPulseAfterFiltering_power/plot2Max,'LineWidth',1.4);xlabel('Delay␣(ps)');ylabel('Power␣(au)');
legend('pulse␣1','pulse␣2');text(0.03,0.9,'(d)','Units','normalized')


subplot(3,2,6)
plot(t_chirp,MyPulseAfterFiltering_chirp,'LineWidth',1.4); xlim([-2 +2]);ylim([-15 +15]);hold on
plot(t_chirp,SolitonPulseAfterFiltering_chirp,'LineWidth',1.4);xlabel('Delay␣(ps)');ylabel('Chirp␣(THz)');
legend('pulse␣1','pulse␣2');text(0.03,0.9,'(d)','Units','normalized')


plot6Max=[max(MyPulseAfterFiltering_spectrum) max(SolitonPulseAfterFiltering_spectrum)];
subplot(3,2,4)
plot(shiftedWave, MyPulseAfterFiltering_spectrum/plot6Max(1),'LineWidth',1.4);xlim([1010 1050]); hold on;
plot(shiftedWave, SolitonPulseAfterFiltering_spectrum/plot6Max(2),'LineWidth',1.4); ylim([0 1.1]);
xlabel('Wavelength␣(nm)'); ylabel('Amplitude␣(au)');
legend('pulse␣1','pulse␣2');text(0.03,0.9,'(f)','Units','normalized')

% plot the filter
sigma=(1.2/2.355)^2;
subplot(3,2,3)
plot(shiftedWave,exp(-(shiftedWave-1033.5).^2/sigma),'-k','LineWidth',1.4);
legend('pulse␣1','pulse␣2','filter');text(0.03,0.9,'(c)','Units','normalized')
```

The settings files:

1. settings4ThesisNarrowFiltering1.txt:

```
-------------------------------------------------------------------------------------------------------------------------------------------

TWidth TRes frep CentW pulse_no spacing Shape Dw DT Energy File_No Page_No SaveN plotN plot_seg store_seg Passes
      Conv_typ Conv_spn Conv_seg Conv_th EdgeF
ps fs MHz nm integer ps index THz ratio nJ integer page RundTrp RundTrp integer integer RundTrp index RundTrp integer
      percent logical
-------------------------------------------------------------------------------------------------------------------------------------------

20 20 1000 1030 1 19.999 2 0.47 1 2e-2 1410 20 1 1 2 -1 1 1 10 4 0.000002 0
-------------------------------------------------------------------------------------------------------------------------------------------

  - - - - - - - - - - - - - - - - - - - - - - S - - - - - - - - - -
  - - - - - - - - - - - - - - - - - - - - - - A P - - - - - - - - -
  - - - - - - - - - - - - - - - - - - - - - - T H - - - - - - - - -
  - - - - - - - - - - - - - - - - - - - - - - U A - - - - - - - - -
  - - - - - - - - - - - - - - - - - - - - - - R S - - - - - - - - -
  - - - - - - - - - - - - - - - - - - - - - - A E - - - - - - - - -
  - - - - - - - - - - - - - - - - - - - - - - T - - - - - - - - - -
  - - - - G - - R - - - - - - - - - - - - - I S - - F - - - - - - -
  - - - - R - - A - - - - - - - - - - - - - O H - - I - - - - - - -
  - - - - O - N M - - - - - - - - - - - - - N I - - L - - - - - - -
  - - - - U T O A - - - - - - - - - - - - - - F - - T - - B - - - -
  - - - - P H N N - - - - - - - - - - - - - P T - - E - - L R B -
  - - - - - I L - - - - - - - - - - - - - - O - - - R - - U E L R
  - N - - V R I S - - - - - - - - - - - - - W o - - - - D E D U E
  - U - - E D N C - - - C - - - - - - - P - - E F - - C - O - - E D
  - M - - L - E A - - - E - - - D - - U - - R - - - E - U F F - -
  - B - - O O A T - - U N - S - O - - M - M - N - - N F B I I F F
  - E N L C R R T S - N T - A P P - P P - O O P - - T I L L L I I
  - R U E I D I E E - S R G T U I - U - - D F E - - R L E T T L L
```

```
 - - M N T E T R L - A A A U M N - M S - U - - R - A T - E E T T
 - O B G Y R Y I F - T L I R P G - P P - L N T E F L E F R R E E
 M F E T - - - N _ - U - N A - - - - E L A P R C I - R I - - R R
 E - R H D D C G S G R W - T A C P W C I T E A O L W - L W W - -
 D S - - I I O - T A A A B I B O U A T N I - N V T A B T A A B B
 I N O O S S F F E I T V A O S N M V R E O O S E E V A E V V A A
 U A F F P P F R E N E E N N O C P E A A N R M R R E N R E E N N
 M P - - E E I A P - D L D - R E - L L R - - I Y - L D - L L D D
 - S S F R R C C E N - E W P P N P E - - D S S - S E W D E E W W
 T H T I S S I T N O G N I O T T O N F L E E S T H N I E N N I I
 Y O E B I I E I I I A G D W I I W G W O P S I I A G D L G G D D
 P T P E O O N O N S I T T E O O E T H S T A O M P T T A T T T T
 E S S R N N T N G E N H H R N N R H M S H M N E E H H Y H H H H
```

```
Seg_ID AcType  Snap Steps L GVD TOD Gamma f_R steep Noise Unsat Cent_WL Gain_BW SatPow alpha DopConc PumpPow Pump_WL
      PmpFWHM q_0 q_1 I_sat Phi Tau Shape FCent_W F_BW delay blue_w red_w blue_BW red_BW
ID Name Snap Step cm fs2/mm fs3/mm 1/kW/m fraction logical dB dB nm nm W dB/m nm-3 W nm nm None None kW deg ps Index nm
      nm ps nm nm nm nm
```

```
seg_1 Passive 1 10 200 22 40 4.5 0 0 NaN NaN NaN NaN NaN NaN NaN NaN NaN NaN NaN NaN NaN NaN NaN NaN NaN NaN NaN NaN
       NaN NaN
seg_2 Eff_Gain 1 100 80 21 40 1.5 0 0 -200 20 1030 80 100 NaN NaN NaN NaN NaN NaN  NaN  NaN  NaN  NaN NaN  NaN  NaN NaN
      NaN NaN NaN NaN
seg_3 NPE 1 1 NaN NaN NaN NaN NaN NaN NaN NaN NaN NaN NaN NaN NaN NaN NaN NaN NaN NaN 0.85 0 1 0 NaN NaN NaN NaN NaN NaN NaN NaN
       NaN
seg_4 Passive 1 240 120 22 40 4.5 0 0 NaN NaN NaN NaN NaN NaN NaN NaN NaN NaN NaN NaN NaN NaN NaN NaN NaN NaN NaN NaN
      NaN NaN NaN
seg_5 Filter 1 1 NaN NaN NaN NaN NaN NaN NaN NaN NaN NaN NaN NaN NaN NaN NaN NaN NaN NaN NaN NaN NaN NaN NaN 1 1033.5 1.2 NaN
      NaN NaN NaN NaN
```

2. settings4ThesisNarrowFiltering2.txt:

```
TWidth TRes frep CentW pulse_no spacing Shape Dw DT Energy File_No Page_No SaveN plotN plot_seg store_seg Passes
      Conv_typ Conv_spn Conv_seg Conv_th EdgeF
ps fs MHz nm integer ps index THz ratio nJ integer page RundTrp RundTrp integer integer RundTrp index RundTrp integer
      percent logical
```

```
20 20 1000 1030 1 19.999 1 3 1 1 1410 20 1 1 2 -1 1 1 10 4 0.000002 0
```

```
 - - - - - - - - - - - - - - - - - - - - - - S - - - - - - - - - -
 - - - - - - - - - - - - - - - - - - - - - - A P - - - - - - - - -
 - - - - - - - - - - - - - - - - - - - - - - T H - - - - - - - - -
 - - - - - - - - - - - - - - - - - - - - - - U A - - - - - - - - -
 - - - - - - - - - - - - - - - - - - - - - - R S - - - - - - - - -
 - - - - - - - - - - - - - - - - - - - - - - A E - - - - - - - - -
 - - - - - - - - - - - - - - - - - - - - - - T - - - - - - - - - -
 - - - - G - - R - - - - - - - - - - - - - I S - - F - - - - - - -
 - - - - R - - A - - - - - - - - - - - - - O H - - I - - - - - - -
 - - - - O - N M - - - - - - - - - - - - - N I - - L - - - - - - -
 - - - - U T O A - - - - - - - - - - - - - - F - - T - - B - - - -
 - - - - P H N N - - - - - - - - - - - - - P T - - E - - L R B -
 - - - - - I L - - - - - - - - - - - - - - O - - - R - - U E L R
 - N - - V R I S - - - - - - - - - - - - - W o - - - - D E D U E
 - U - - E D N C - - - C - - - - - - - P - - E F - - C - O - - E D
 - M - - L - E A - - - E - - - D - - U - - R - - - E - U F F - -
 - B - - O O A T - - U N - S - O - - M - M - N - - N F B I I F F
 - E N L C R R T S - N T - A P P - P P - O O P - - T I L L L I I
 - R U E I D I E E - S R G T U I - U - - D F E - - R L E T T L L
 - - M N T E T R L - A A A U M N - M S - U - - R - A T - E E T T
 - O B G Y R Y I F - T L I R P G - P P - L N T E F L E F R R E E
```

```
  M F E T - - - N _ - U - N A - - - - E L A P R C I - R I - - R R
  E - R H D D C G S G R W - T A C P W C I T E A O L W - L W W - -
  D S - - I I O - T A A A B I B O U A T N I - N V T A B T A A B B
  I N O O S S F F E I T V A O S N M V R E O O S E E V A E V V A A
  U A F F P P F R E N E E N N O C P E A A N R M R R E N R E E N N
  M P - - E E I A P - D L D - R E - L L R - - I Y - L D - L L D D
  - S S F R R C C E N - E W P P N P E - - D S S - S E W D E E W W
  T H T I S S I T N O G N I O T T O N F L E E S T H N I E N N I I
  Y O E B I I E I I I A G D W I I W G W O P S I I A G D L G G D D
  P T P E O O N O N S I T T E O O E T H S T A O M P T T A T T T T
  E S S R N N T N G E N H H R N N R H M S H M N E E H H Y H H H H
```

```
Seg_ID AcType  Snap Steps L GVD TOD Gamma f_R steep Noise Unsat Cent_WL Gain_BW SatPow alpha DopConc PumpPow Pump_WL
      PmpFWHM q_0 q_1 I_sat Phi Tau Shape FCent_W F_BW delay blue_w red_w blue_BW red_BW
ID Name Snap Step cm fs2/mm fs3/mm 1/kW/m fraction logical dB dB nm nm W dB/m nm-3 W nm nm None None kW deg ps Index nm
      nm ps nm nm nm nm
```

```
seg_1 Passive 1 1 0.1 -0.1 0 1.5 0 0 NaN NaN NaN NaN NaN NaN NaN NaN NaN NaN NaN NaN NaN NaN NaN NaN NaN NaN NaN NaN NaN
       NaN NaN
seg_2 Filter 1 1 NaN NaN NaN NaN NaN NaN NaN NaN NaN NaN NaN NaN NaN NaN NaN NaN NaN NaN NaN NaN NaN NaN NaN 1 1033.5 1.2 NaN
      NaN NaN NaN NaN
```

A.9 Figure 3.1 (Mamyshev)

The code (code4ThesisTypicalMamyshev.m):

```
% code4ThesisTypicalMamyshev
settings_file="settings4ThesisTypicalMamyshev.txt";

[seg_data, global_data,segment_header,global_header] = loadData(settings_file,0);

c = 299792.458; % [nm/ps]

lambda_c = str2double(global_data(contains(global_header,'CentW'))); % Central wavelength (nm)

timewidth = str2double(global_data(contains(global_header,'TWidth'))); % Width of the time window in [ps]
tres1 = str2double(global_data(contains(global_header,'TRes')))*1e-3; % Resolution of the time window [ps] (written as fs*1e-3)

timesteps=2^(ceil(log2(timewidth/tres1))); tres=timewidth/timesteps;
t = -timewidth*0.5+tres:tres:timewidth*0.5; % Time in [ps]
timesteps=length(t);
fs=1/timewidth; % Sampling rate in [THz]
freq=c/lambda_c+fs*linspace(-timesteps/2,timesteps/2-1,timesteps);
freq=fftshift(freq); % Frequency in [THz]
wave=c./freq; shiftedWave=fftshift(wave); % Wavelength in [nm]
w=2*pi*c/lambda_c; % Central angular frequency in [THz]
omegas = 2*pi*freq; % Angular frequency in [THz]

% Simulate the cavity
CommandLine(settings_file);

n=15; in_snap=2;xmin=1005;xmax=1065;linewidth=2;
% retrieve the spectra
filteredBlue=LoadPage(LoadE(['Data' num2str(n) '.bin']),18,timesteps);
filteredBlueSpectrum=fftshift(abs(fft(filteredBlue)).^2);
figure;plot(shiftedWave,filteredBlueSpectrum/max(filteredBlueSpectrum),"LineWidth",linewidth,'Color',[1 0 1]);ylim([0 1.1]);xlim
      ([xmin xmax]);xticks([]);yticks([])
saveas(gcf,'ThesisMamyshevBlue_filtered.fig');saveas(gcf,'ThesisMamyshevBlue_filtered.png');
```

```
amplifiedBlue=LoadPage(LoadE(['Data' num2str(n) '.bin']),in_snap,timesteps);
amplifiedBlueSpectrum=fftshift(abs(fft(amplifiedBlue)).^2);
figure;plot(shiftedWave,amplifiedBlueSpectrum/max(amplifiedBlueSpectrum),"LineWidth",linewidth,'Color',[1 0 1]);ylim([0 1.1]);
      xlim([xmin xmax]);xticks([]);yticks([])
saveas(gcf,'ThesisMamyshevEvolvingBlue.fig');saveas(gcf,'ThesisMamyshevEvolvingBlue.png');

BeforeRedFilter=LoadPage(LoadE(['Data' num2str(n) '.bin']),7,timesteps);
BeforeRedFilterSpectrum=fftshift(abs(fft(BeforeRedFilter)).^2);
figure;plot(shiftedWave,BeforeRedFilterSpectrum/max(BeforeRedFilterSpectrum),"LineWidth",linewidth,'Color',[1 0 1]);ylim([0 1.1])
      ;xlim([xmin xmax]);xticks([]);yticks([])
hold on; sigma=(3/2.355)^2; plot(shiftedWave,exp(-(shiftedWave-1040).^2/sigma),'-r','LineWidth',linewidth);hold off;
saveas(gcf,'ThesisMamyshevAtRed.fig');saveas(gcf,'ThesisMamyshevAtRed.png');

filteredRed=LoadPage(LoadE(['Data' num2str(n) '.bin']),9,timesteps);
filteredRedSpectrum=fftshift(abs(fft(filteredRed)).^2);
figure;plot(shiftedWave,filteredRedSpectrum/max(filteredRedSpectrum),"LineWidth",linewidth,'Color',[1 0 1]);ylim([0 1.1]);xlim([
      xmin xmax]);xticks([]);yticks([])
saveas(gcf,'ThesisMamyshevRed_filtered.fig');saveas(gcf,'ThesisMamyshevRed_filtered.png');

amplifiedRed=LoadPage(LoadE(['Data' num2str(n) '.bin']),in_snap+9,timesteps);
amplifiedRedSpectrum=fftshift(abs(fft(amplifiedRed)).^2);
figure;plot(shiftedWave,amplifiedRedSpectrum/max(amplifiedRedSpectrum),"LineWidth",linewidth,'Color',[1 0 1]);ylim([0 1.1]);xlim
      ([xmin xmax]);xticks([]);yticks([])
saveas(gcf,'ThesisMamyshevEvolvingRed.fig');saveas(gcf,'ThesisMamyshevEvolvingRed.png');

BeforeBlueFilter=LoadPage(LoadE(['Data' num2str(n) '.bin']),7+9,timesteps);
BeforeBlueFilterSpectrum=fftshift(abs(fft(BeforeBlueFilter)).^2);
figure;plot(shiftedWave,BeforeBlueFilterSpectrum/max(BeforeBlueFilterSpectrum),"LineWidth",linewidth,'Color',[1 0 1]);ylim([0
      1.1]);xlim([xmin xmax]);xticks([]);yticks([])
hold on; sigma=(3/2.355)^2; plot(shiftedWave,exp(-(shiftedWave-1030).^2/sigma),'LineWidth',linewidth,'Color','b');hold off;
saveas(gcf,'ThesisMamyshevAtBlue.fig');saveas(gcf,'ThesisMamyshevAtBlue.png');
```

The settings file (settings4ThesisTypicalMamyshev.txt):

```
-------------------------------------------------------------------------------------------------------------------------------
TWidth TRes frep CentW pulse_no spacing Shape Dw DT Energy File_No Page_No SaveN plotN plot_seg store_seg Passes Conv_typ
      Conv_spn Conv_seg Conv_th EdgeF
ps fs MHz nm integer ps index THz ratio nJ integer page RundTrp RundTrp integer integer RundTrp index RundTrp integer percent
      logical
-------------------------------------------------------------------------------------------------------------------------------
40 20 1000 1035 1 19.999 2 0.9 1 1e-1 1410 20 15 1 2 -1 15 1 10 4 0.000002 0
-------------------------------------------------------------------------------------------------------------------------------
  - - - - - - - - - - - - - - - - - - - - S - - - - - - - - - -
  - - - - - - - - - - - - - - - - - - - - A P - - - - - - - - -
  - - - - - - - - - - - - - - - - - - - - T H - - - - - - - - -
  - - - - - - - - - - - - - - - - - - - - U A - - - - - - - - -
  - - - - - - - - - - - - - - - - - - - - R S - - - - - - - - -
  - - - - - - - - - - - - - - - - - - - - A E - - - - - - - - -
  - - - - - - - - - - - - - - - - - - - - T - - - - - - - - - -
  - - - - G - - R - - - - - - - - - - - - I S - - F - - - - - -
  - - - - R - - A - - - - - - - - - - - - O H - - I - - - - - -
  - - - - O - N M - - - - - - - - - - - - N I - - L - - - - - -
  - - - - U T O A - - - - - - - - - - - - F - - T - - B - - -
  - - - - P H N N - - - - - - - - - - - - P T - - E - - L R B -
  - - - - - I L - - - - - - - - - - - - - O - - - R - - U E L R
  - N - - V R I S - - - - - - - - - - - - W o - - - - D E D U E
  - U - - E D N C - - - C - - - - - - P - - E F - - C - O - - E D
  - M - - L - E A - - - E - - - D - - U - - R - - - E - U F F - -
  - B - - O O A T - - U N - S - O - - M - M - N - - N F B I I F F
  - E N L C R R T S - N T - A P P - P P - O O P - - T I L L L I I
  - R U E I D I E E - S R G T U I - U - - D F E - - R L E T T L L
  - - M N T E T R L - A A A U M N - M S - U - - R - A T - E E T T
  - O B G Y R Y I F - T L I R P G - P P - L N T E F L E F R R E E
  M F E T - - - N _ - U - N A - - - - E L A P R C I - R I - - R R
  E - R H D D C G S G R W - T A C P W C I T E A O L W - L W W - -
```

```
  D S - - I I O - T A A A B I B O U A T N I - N V T A B T A A B B
  I N O O S S F F E I T V A O S N M V R E O O S E E V A E V V A A
  U A F F P P F R E N E E N N O C P E A A N R M R R E N R E E N N
  M P - - E E I A P - D L D - R E - L L R - - I Y - L D - L L D D
  - S S F R R C C E N - E W P P N P E - - D S S - S E W D E E W W
  T H T I S S I T N O G N I O T T O N F L E E S T H N I E N N I I
  Y O E B I I E I I I A G D W I I W G W O P S I I A G D L G G D D
  P T P E O O N O N S I T T E O O E T H S T A O M P T T A T T T T
  E S S R N N T N G E N H H R N N R H M S H M N E E H H Y H H H H
```

```
Seg_ID AcType  Snap Steps L GVD TOD Gamma f_R steep Noise Unsat Cent_WL Gain_BW SatPow alpha DopConc PumpPow Pump_WL PmpFWHM q_0
      q_1 I_sat Phi Tau Shape FCent_W F_BW delay blue_w red_w blue_BW red_BW
ID Name Snap Step cm fs2/mm fs3/mm 1/kW/m fraction logical dB dB nm nm W dB/m nm-3 W nm nm None None kW deg ps Index nm nm ps nm
      nm nm nm
seg_1 Passive 1 10 200 22 30 4.5 0 0 NaN NaN NaN NaN NaN NaN NaN NaN NaN NaN NaN NaN NaN NaN NaN NaN NaN NaN NaN NaN NaN
seg_2 Eff_Gain 1 300 250 22 30 4.5 0 0 -200 20 1035 80 15 NaN NaN NaN NaN NaN NaN  NaN  NaN  NaN  NaN NaN  NaN  NaN NaN NaN NaN
      NaN NaN
seg_3 Passive 5 200 200 22 30 4.5 0 0 NaN NaN NaN NaN NaN NaN NaN NaN NaN NaN NaN NaN NaN NaN NaN NaN NaN NaN NaN NaN NaN NaN
seg_4 Filter 1 1 NaN NaN NaN NaN NaN NaN NaN NaN NaN NaN NaN NaN NaN NaN NaN NaN NaN NaN NaN NaN NaN NaN 1 1040 3 NaN NaN NaN NaN NaN
seg_5 NPE 1 1 NaN NaN NaN NaN NaN NaN NaN NaN NaN NaN NaN NaN NaN NaN NaN NaN 0.2 0 1 0 NaN NaN NaN NaN NaN NaN NaN NaN NaN
seg_6 Passive 1 10 200 22 30 4.5 0 0 NaN NaN NaN NaN NaN NaN NaN NaN NaN NaN NaN NaN NaN NaN NaN NaN NaN NaN NaN NaN NaN NaN
seg_7 Eff_Gain 1 300 250 22 30 4.5 0 0 -200 20 1035 80 15 NaN NaN NaN NaN NaN NaN  NaN  NaN  NaN  NaN NaN  NaN  NaN NaN NaN NaN
      NaN NaN
seg_8 Passive 5 200 200 22 30 4.5 0 0 NaN NaN NaN NaN NaN NaN NaN NaN NaN NaN NaN NaN NaN NaN NaN NaN NaN NaN NaN NaN NaN NaN
seg_9 Filter 1 1 NaN NaN NaN NaN NaN NaN NaN NaN NaN NaN NaN NaN NaN NaN NaN NaN NaN NaN NaN NaN NaN NaN 1 1030 3 NaN NaN NaN NaN NaN
seg_10 NPE 1 1 NaN NaN NaN NaN NaN NaN NaN NaN NaN NaN NaN NaN NaN NaN NaN NaN 0.2 0 1 0 NaN NaN NaN NaN NaN NaN NaN NaN NaN
```

A.10 Figure 5.6 (Temporal Shift Due to Offset filtering)

The code (code4Energy_filteredPosition.m):

```
settings_file1="settings4Energy_filteredPosition1.txt";
settings_file2="settings4Energy_filteredPosition2.txt";
settings_file3="settings4Energy_filteredPosition3.txt";
settings_file4="settings4Energy_filteredPosition4.txt";

[seg_data, global_data,segment_header,global_header] = loadData(settings_file1,0);

lambda_c = str2double(global_data(contains(global_header,'CentW'))); % Central wavelength (nm)

timewidth = str2double(global_data(contains(global_header,'TWidth'))); % Width of the time window in [ps]
tres1 = str2double(global_data(contains(global_header,'TRes')))*1e-3; % Resolution of the time window [ps] (written as fs*1e-3)

c = 299792.458; % [nm/ps]
timesteps=2^(ceil(log2(timewidth/tres1))); tres=timewidth/(timesteps-1);
t = -timewidth*0.5:tres:timewidth*0.5; % Time in [ps]
timesteps=length(t);
fs=1/timewidth; % Sampling rate in [THz]
freq=c/lambda_c+fs*linspace(-(timesteps-1)/2,(timesteps-1)/2,timesteps); freq=fftshift(freq); % Frequency in [THz]
wave=c./freq; shiftedWave=fftshift(wave); % Wavelength in [nm]
w=2*pi*c/lambda_c; % Central angular frequency in [THz]
omegas = 2*pi*freq; % Angular frequency in [THz]

% Strong pulse simulation
CommandLine(settings_file1);
```

```
% before filtering
strongPulseBeforeFiltering=LoadPage(LoadE(['Data' num2str(1) '.bin']),4,timesteps);

strongPulseBeforeFiltering_power=abs(strongPulseBeforeFiltering).^2;

strongPulseBeforeFiltering_spectrum=fftshift(abs(fft(strongPulseBeforeFiltering)).^2);

% after filtering
strongPulseAfterFiltering=LoadPage(LoadE(['Data' num2str(1) '.bin']),5,timesteps);

strongPulseAfterFiltering_power=abs(strongPulseAfterFiltering).^2;

strongPulseAfterFiltering_spectrum=fftshift(abs(fft(strongPulseAfterFiltering)).^2);


% Weak pulse simulation
CommandLine(settings_file2);

% before filtering
weakPulseBeforeFiltering=LoadPage(LoadE(['Data' num2str(1) '.bin']),4,timesteps);

weakPulseBeforeFiltering_power=abs(weakPulseBeforeFiltering).^2;

weakPulseBeforeFiltering_spectrum=fftshift(abs(fft(weakPulseBeforeFiltering)).^2);

% after filtering
weakPulseAfterFiltering=LoadPage(LoadE(['Data' num2str(1) '.bin']),5,timesteps);

weakPulseAfterFiltering_power=abs(weakPulseAfterFiltering).^2;

weakPulseAfterFiltering_spectrum=fftshift(abs(fft(weakPulseAfterFiltering)).^2);


% plotting
f=figure('position',[800 800 700 800]);f.Color='w';

plot1max=max(strongPulseBeforeFiltering_power);
subplot(3,2,1)
plot(t,strongPulseBeforeFiltering_power/plot1max,'-b','LineWidth',1.5);
xlim([-2 2]);ylim([0 1.199]);xlabel('Delay␣(ps)');ylabel('Power␣(au)');
hold on;plot(t,weakPulseBeforeFiltering_power/plot1max,'-r','LineWidth',1.5);
legend('Strong','Weak');text(0.03,0.9,'(a)','Units','normalized')

plot2max=max([strongPulseBeforeFiltering_spectrum weakPulseBeforeFiltering_spectrum]);
subplot(3,2,3)
plot(ifftshift(freq),strongPulseBeforeFiltering_spectrum/plot2max,'-b','LineWidth',1.5);
xlim([286 296]);ylim([0 1.199]);xlabel('Frequency␣(THz)');ylabel('Amplitude␣(au)');
hold on; plot(ifftshift(freq),weakPulseBeforeFiltering_spectrum/plot2max,'-r','LineWidth',1.5);
sigma=(1.7/2.355)^2; plot(ifftshift(freq),exp(-(shiftedWave-1033.5).^2/sigma),'-k','LineWidth',1.5);
legend('Strong','Weak','Filter');text(0.03,0.9,'(b)','Units','normalized')

plot3max=max([weakPulseAfterFiltering_power strongPulseAfterFiltering_power]);
strongPulseDelay=t(find(strongPulseAfterFiltering_power==max(strongPulseAfterFiltering_power)));
weakPulseDelay=t(find(weakPulseAfterFiltering_power==max(weakPulseAfterFiltering_power)));
subplot(3,2,5)
plot(t,strongPulseAfterFiltering_power/plot3max,'-b','LineWidth',1.5);
xlim([-2 2]);ylim([0 1.199]);xlabel('Delay␣(ps)');ylabel('Power␣(au)');
hold on;plot(t,weakPulseAfterFiltering_power/plot3max,'-r','LineWidth',1.5);
xline(strongPulseDelay,'--b','LineWidth',1.5);xline(weakPulseDelay,'--r','LineWidth',1.5);
% quiver(weakPulseDelay,0.25,0.3,0,0,"- k","LineWidth",1.4,"MaxHeadSize",1.6)
legend('Strong','Weak');text(0.03,0.9,'(c)','Units','normalized')


% Strong pulse simulation (dispersion)
CommandLine(settings_file3);

% before filtering
strongPulseBeforeFiltering=LoadPage(LoadE(['Data' num2str(1) '.bin']),4,timesteps);
```

```
strongPulseBeforeFiltering_power=abs(strongPulseBeforeFiltering).^2;

strongPulseBeforeFiltering_spectrum=fftshift(abs(fft(strongPulseBeforeFiltering)).^2);

% after filtering
strongPulseAfterFiltering=LoadPage(LoadE(['Data' num2str(1) '.bin']),5,timesteps);

strongPulseAfterFiltering_power=abs(strongPulseAfterFiltering).^2;

strongPulseAfterFiltering_spectrum=fftshift(abs(fft(strongPulseAfterFiltering)).^2);


% Weak pulse simulation (dispersion
CommandLine(settings_file4);

% before filtering
weakPulseBeforeFiltering=LoadPage(LoadE(['Data' num2str(1) '.bin']),4,timesteps);

weakPulseBeforeFiltering_power=abs(weakPulseBeforeFiltering).^2;

weakPulseBeforeFiltering_spectrum=fftshift(abs(fft(weakPulseBeforeFiltering)).^2);

% after filtering
weakPulseAfterFiltering=LoadPage(LoadE(['Data' num2str(1) '.bin']),5,timesteps);

weakPulseAfterFiltering_power=abs(weakPulseAfterFiltering).^2;

weakPulseAfterFiltering_spectrum=fftshift(abs(fft(weakPulseAfterFiltering)).^2);

% plotting

plot1max=max(strongPulseBeforeFiltering_power);
subplot(3,2,2)
plot(t,strongPulseBeforeFiltering_power/plot1max,'-b','LineWidth',1.5);
xlim([-15 15]);ylim([0 1.199]);xlabel('Delay␣(ps)');ylabel('Power␣(au)');
hold on;plot(t,weakPulseBeforeFiltering_power/plot1max,'-r','LineWidth',1.5);
legend('Strong','Weak');text(0.03,0.9,'(d)','Units','normalized')

plot2max=max([strongPulseBeforeFiltering_spectrum weakPulseBeforeFiltering_spectrum]);
subplot(3,2,4)
plot(ifftshift(freq),strongPulseBeforeFiltering_spectrum/plot2max,'-b','LineWidth',1.5);
xlim([285 297]);ylim([0 1.199]);xlabel('Frequency␣(THz)');ylabel('Amplitude␣(au)');
hold on; plot(ifftshift(freq),weakPulseBeforeFiltering_spectrum/plot2max,'-r','LineWidth',1.5);
sigma=(1.7/2.355)^2; plot(ifftshift(freq),exp(-(shiftedWave-1033.5).^2/sigma),'-k','LineWidth',1.5);
legend('Strong','Weak','Filter');text(0.03,0.9,'(e)','Units','normalized')

plot3max=max([weakPulseAfterFiltering_power strongPulseAfterFiltering_power]);
strongPulseDelay=t(find(strongPulseAfterFiltering_power==max(strongPulseAfterFiltering_power)));
weakPulseDelay=t(find(weakPulseAfterFiltering_power==max(weakPulseAfterFiltering_power)));
subplot(3,2,6)
plot(t,strongPulseAfterFiltering_power/plot3max,'-b','LineWidth',1.5);
xlim([-5 -1]);ylim([0 1.199]);xlabel('Delay␣(ps)');ylabel('Power␣(au)');
hold on;plot(t,weakPulseAfterFiltering_power/plot3max,'-r','LineWidth',1.5);
xline(strongPulseDelay,'--b','LineWidth',1.5);xline(weakPulseDelay,'--r','LineWidth',1.5);
% quiver(weakPulseDelay,0.25,-0.3,0,0,"- k","LineWidth",1.4,"MaxHeadSize",1.6)
legend('Strong','Weak');text(0.03,0.9,'(f)','Units','normalized')
```

The settings files:

1. settings4Energy_filteredPosition1.txt:

```
-------------------------------------------------------------------------------------------------------------------------------------------------------

TWidth TRes frep CentW pulse_no spacing Shape Dw DT Energy File_No Page_No SaveN plotN plot_seg store_seg Passes
      Conv_typ Conv_spn Conv_seg Conv_th EdgeF
ps fs MHz nm integer ps index THz ratio nJ integer page RundTrp RundTrp integer integer RundTrp index RundTrp integer
      percent logical
-------------------------------------------------------------------------------------------------------------------------------------------------------

-40 20 1000 1030 1 19.999 2 0.46 1 1.8e-2 1410 20 1 1 2 -1 1 1 10 4 0.000002 0
-------------------------------------------------------------------------------------------------------------------------------------------------------

- - - - - - - - - - - - - - - - - - - - - - S - - - - - - - - - -
  - - - - - - - - - - - - - - - - - - - - - - A P - - - - - - - - -
  - - - - - - - - - - - - - - - - - - - - - - T H - - - - - - - - -
  - - - - - - - - - - - - - - - - - - - - - - U A - - - - - - - - -
  - - - - - - - - - - - - - - - - - - - - - - R S - - - - - - - - -
  - - - - - - - - - - - - - - - - - - - - - - A E - - - - - - - - -
  - - - - - - - - - - - - - - - - - - - - - - T - - - - - - - - - -
  - - - - G - - R - - - - - - - - - - - - - I S - - F - - - - - - -
  - - - - R - - A - - - - - - - - - - - - - O H - - I - - - - - - -
  - - - - O - N M - - - - - - - - - - - - - N I - - L - - - - - - -
  - - - - U T O A - - - - - - - - - - - - - - F - - T - - B - - - -
  - - - - P H N N - - - - - - - - - - - - - P T - - E - - L R B -
  - - - - - I L - - - - - - - - - - - - - - O - - - R - - U E L R
  - N - - V R I S - - - - - - - - - - - - - W o - - - - D E D U E
  - U - - E D N C - - - C - - - - - - - P - - E F - - C - O - - E D
  - M - - L - E A - - - E - - - D - - U - - R - - - E - U F F - -
  - B - - O O A T - - U N - S - O - - M - M - N - - N F B I I F F
  - E N L C R R T S - N T - A P P - P P - O O P - - T I L L L I I
  - R U E I D I E E - S R G T U I - U - - D F E - - R L E T T L L
  - - M N T E T R L - A A A U M N - M S - U - - R - A T - E E T T
  - O B G Y R Y I F - T L I R P G - P P - L N T E F L E F R R E E
  M F E T - - - N _ - U - N A - - - - E L A P R C I - R I - - R R
  E - R H D D C G S G R W - T A C P W C I T E A O L W - L W W - -
  D S - - - I I O - T A A A B I B O U A T N I - N V T A B T A A B B
  I N O O S S F F E I T V A O S N M V R E O O S E E V A E V V A A
  U A F F P P F R E N E E N N O C P E A A N R M R R E N R E E N N
  M P - - E E I A P - D L D - R E - L L R - - I Y - L D - L L D D
  - S S F R R C C E N - E W P P N P E - - D S S - S E W D E E W W
  T H T I S S I T N O G N I O T T O N F L E E S T H N I E N N I I
  Y O E B I I E I I I A G D W I I W G W O P S I I A G D L G G D D
  P T P E O O N O N S I T T E O O E T H S T A O M P T T A T T T T
  E S S R N N T N G E N H H R N N R H M S H M N E E H H Y H H H H
-------------------------------------------------------------------------------------------------------------------------------------------------------

-Seg_ID AcType  Snap Steps L GVD TOD Gamma f_R steep Noise Unsat Cent_WL Gain_BW SatPow alpha DopConc PumpPow Pump_WL
      PmpFWHM q_0 q_1 I_sat Phi Tau Shape FCent_W F_BW delay blue_w red_w blue_BW red_BW
ID Name Snap Step cm fs2/mm fs3/mm 1/kW/m fraction logical dB dB nm nm W dB/m nm-3 W nm nm None None kW deg ps Index nm
      nm ps nm nm nm nm
-------------------------------------------------------------------------------------------------------------------------------------------------------

-seg_1 Passive 1 10 200 22 40 4.5 0 0 NaN NaN NaN NaN NaN NaN NaN NaN NaN NaN NaN NaN NaN NaN NaN NaN NaN NaN NaN
      NaN NaN NaN
seg_2 Eff_Gain 1 400 65 22 40 1.5 0 0 -200 20 1030 80 100 NaN NaN NaN NaN NaN NaN  NaN  NaN  NaN  NaN NaN  NaN  NaN NaN
      NaN NaN NaN NaN
seg_3 NPE 1 1 NaN NaN NaN NaN NaN NaN NaN NaN NaN NaN NaN NaN NaN NaN NaN NaN NaN 0.9 0 1 0 NaN NaN NaN NaN NaN NaN NaN NaN
      NaN
seg_4 Passive 1 240 220 22 40 4.5 0 0 NaN NaN NaN NaN NaN NaN NaN NaN NaN NaN NaN NaN NaN NaN NaN NaN NaN NaN NaN
      NaN NaN NaN
seg_5 Filter 1 1 NaN NaN NaN NaN NaN NaN NaN NaN NaN NaN NaN NaN NaN NaN NaN NaN NaN NaN NaN NaN NaN NaN NaN 1 1033.5 1.67 NaN
      NaN NaN NaN NaN
```

2. settings4Energy_filteredPosition2.txt:

```
-------------------------------------------------------------------------------------------------------------------------------------------------------

TWidth TRes frep CentW pulse_no spacing Shape Dw DT Energy File_No Page_No SaveN plotN plot_seg store_seg Passes
      Conv_typ Conv_spn Conv_seg Conv_th EdgeF
ps fs MHz nm integer ps index THz ratio nJ integer page RundTrp RundTrp integer integer RundTrp index RundTrp integer
      percent logical
-------------------------------------------------------------------------------------------------------------------------------------------------------

40 20 1000 1030 1 19.999 2 0.46 1 0.9e-2 1410 20 1 1 2 -1 1 1 10 4 0.000002 0
-------------------------------------------------------------------------------------------------------------------------------------------------------

  - - - - - - - - - - - - - - - - - - - - - - S - - - - - - - - - -
  - - - - - - - - - - - - - - - - - - - - - - A P - - - - - - - - - -
  - - - - - - - - - - - - - - - - - - - - - - T H - - - - - - - - - -
  - - - - - - - - - - - - - - - - - - - - - - U A - - - - - - - - - -
  - - - - - - - - - - - - - - - - - - - - - - R S - - - - - - - - - -
  - - - - - - - - - - - - - - - - - - - - - - A E - - - - - - - - - -
  - - - - - - - - - - - - - - - - - - - - - - T - - - - - - - - - - -
  - - - - G - - R - - - - - - - - - - - - - - I S - - F - - - - - - -
  - - - - R - - A - - - - - - - - - - - - - - O H - - I - - - - - - -
  - - - - O - N M - - - - - - - - - - - - - - N I - - L - - - - - - -
  - - - - U T O A - - - - - - - - - - - - - - F - - T - - B - - - -
  - - - - P H N N - - - - - - - - - - - - - - P T - - E - - L R B -
  - - - - - I L - - - - - - - - - - - - - - - O - - - R - - U E L R
  - N - - V R I S - - - - - - - - - - - - - - W o - - - - D E D U E
  - U - - E D N C - - - C - - - - - - - P - - E F - - C - O - - E D
  - M - - L - E A - - - E - - - D - - U - - R - - - E - U F F - -
  - B - - O O A T - - U N - S - O - - M - M - N - - N F B I I F F
  - E N L C R R T S - N T - A P P - P P - O O P - - T I L L L I I
  - R U E I D I E E - S R G T U I - U - - D F E - - R L E T T L L
  - - M N T E T R L - A A A U M N - M S - U - - R - A T - E E T T
  - O B G Y R Y I F - T L I R P G - P P - L N T E F L E F R R E E
  M F E T - - - N _ - U - N A - - - - E L A P R C I - R I - - R R
  E - R H D D C G S G R W - T A C P W C I T E A O L W - L W W - -
  D S - - - I I O - T A A A B I B O U A T N I - N V T A B T A A B B
  I N O O S S F F E I T V A O S N M V R E O O S E E V A E V V A A
  U A F F P P F R E N E E N N O C P E A A N R M R R E N R E E N N
  M P - - E E I A P - D L D - R E - L L R - - I Y - L D - L L D D
  - S S F R R C C E N - E W P P N P E - - D S S - S E W D E E W W
  T H T I S S I T N O G N I O T T O N F L E E S T H N I E N N I I
  Y O E B I I E I I I A G D W I I W G W O P S I I A G D L G G D D
  P T P E O O N O N S I T T E O O E T H S T A O M P T T A T T T T
  E S S R N N T N G E N H H R N N R H M S H M N E E H H Y H H H H
-------------------------------------------------------------------------------------------------------------------------------------------------------

Seg_ID AcType  Snap Steps L GVD TOD Gamma f_R steep Noise Unsat Cent_WL Gain_BW SatPow alpha DopConc PumpPow Pump_WL
      PmpFWHM q_0 q_1 I_sat Phi Tau Shape FCent_W F_BW delay blue_w red_w blue_BW red_BW
ID Name Snap Step cm fs2/mm fs3/mm 1/kW/m fraction logical dB dB nm nm W dB/m nm-3 W nm nm None None kW deg ps Index nm
      nm ps nm nm nm nm
-------------------------------------------------------------------------------------------------------------------------------------------------------

seg_1 Passive 1 10 200 22 40 4.5 0 0 NaN NaN NaN NaN NaN NaN NaN NaN NaN NaN NaN NaN NaN NaN NaN NaN NaN NaN NaN NaN
       NaN NaN
seg_2 Eff_Gain 1 400 65 22 40 1.5 0 0 -200 20 1030 80 100 NaN NaN NaN NaN NaN NaN  NaN  NaN  NaN  NaN NaN  NaN  NaN NaN
      NaN NaN NaN NaN
seg_3 NPE 1 1 NaN NaN NaN NaN NaN NaN NaN NaN NaN NaN NaN NaN NaN NaN NaN NaN NaN 0.9 0 1 0 NaN NaN NaN NaN NaN NaN NaN NaN
      NaN
seg_4 Passive 1 240 220 22 40 4.5 0 0 NaN NaN NaN NaN NaN NaN NaN NaN NaN NaN NaN NaN NaN NaN NaN NaN NaN NaN NaN NaN
      NaN NaN NaN
seg_5 Filter 1 1 NaN NaN NaN NaN NaN NaN NaN NaN NaN NaN NaN NaN NaN NaN NaN NaN NaN NaN NaN NaN NaN NaN NaN 1 1033.5 1.67 NaN
      NaN NaN NaN NaN
```

3. settings4Energy_filteredPosition3.txt:

```
-------------------------------------------------------------------------------------------------------------------------------------------------------

TWidth TRes frep CentW pulse_no spacing Shape Dw DT Energy File_No Page_No SaveN plotN plot_seg store_seg Passes
      Conv_typ Conv_spn Conv_seg Conv_th EdgeF
ps fs MHz nm integer ps index THz ratio nJ integer page RundTrp RundTrp integer integer RundTrp index RundTrp integer
      percent logical
-------------------------------------------------------------------------------------------------------------------------------------------------------

40 20 1000 1030 1 19.999 2 0.46 1 1.8e-2 1410 20 1 1 2 -1 1 1 10 4 0.000002 0
-------------------------------------------------------------------------------------------------------------------------------------------------------

  - - - - - - - - - - - - - - - - - - - - - - S - - - - - - - - - -
  - - - - - - - - - - - - - - - - - - - - - - A P - - - - - - - - - -
  - - - - - - - - - - - - - - - - - - - - - - T H - - - - - - - - - -
  - - - - - - - - - - - - - - - - - - - - - - U A - - - - - - - - - -
  - - - - - - - - - - - - - - - - - - - - - - R S - - - - - - - - - -
  - - - - - - - - - - - - - - - - - - - - - - A E - - - - - - - - - -
  - - - - - - - - - - - - - - - - - - - - - - T - - - - - - - - - - -
  - - - - G - - R - - - - - - - - - - - - - - I S - - F - - - - - - -
  - - - - R - - A - - - - - - - - - - - - - - O H - - I - - - - - - -
  - - - - O - N M - - - - - - - - - - - - - - N I - - L - - - - - - -
  - - - - U T O A - - - - - - - - - - - - - - F - - T - - B - - - -
  - - - - P H N N - - - - - - - - - - - - - - P T - - E - - L R B -
  - - - - - I L - - - - - - - - - - - - - - - O - - - R - - U E L R
  - N - - V R I S - - - - - - - - - - - - - - W o - - - - D E D U E
  - U - - E D N C - - - C - - - - - - - P - - E F - - C - O - - E D
  - M - - L - E A - - - E - - - D - - U - - R - - - E - U F F - -
  - B - - O O A T - - U N - S - O - - M - M - N - - N F B I I F F
  - E N L C R R T S - N T - A P P - P P - O O P - - T I L L L I I
  - R U E I D I E E - S R G T U I - U - - D F E - - R L E T T L L
  - - M N T E T R L - A A A U M N - M S - U - - R - A T - E E T T
  - O B G Y R Y I F - T L I R P G - P P - L N T E F L E F R R E E
  M F E T - - - N _ - U - N A - - - - E L A P R C I - R I - - R R
  E - R H D D C G S G R W - T A C P W C I T E A O L W - L W W - -
  D S - - - I I O - T A A A B I B O U A T N I - N V T A B T A A B B
  I N O O S S F F E I T V A O S N M V R E O O S E E V A E V V A A
  U A F F P P F R E N E E N N O C P E A A N R M R R E N R E E N N
  M P - - E E I A P - D L D - R E - L L R - - I Y - L D - L L D D
  - S S F R R C C E N - E W P P N P E - - D S S - S E W D E E W W
  T H T I S S I T N O G N I O T T O N F L E E S T H N I E N N I I
  Y O E B I I E I I I A G D W I I W G W O P S I I A G D L G G D D
  P T P E O O N O N S I T T E O O E T H S T A O M P T T A T T T T
  E S S R N N T N G E N H H R N N R H M S H M N E E H H Y H H H H
-------------------------------------------------------------------------------------------------------------------------------------------------------

Seg_ID AcType  Snap Steps L GVD TOD Gamma f_R steep Noise Unsat Cent_WL Gain_BW SatPow alpha DopConc PumpPow Pump_WL
      PmpFWHM q_0 q_1 I_sat Phi Tau Shape FCent_W F_BW delay blue_w red_w blue_BW red_BW
ID Name Snap Step cm fs2/mm fs3/mm 1/kW/m fraction logical dB dB nm nm W dB/m nm-3 W nm nm None None kW deg ps Index nm
      nm ps nm nm nm nm
-------------------------------------------------------------------------------------------------------------------------------------------------------

seg_1 Passive 1 10 200 22 40 4.5 0 0 NaN NaN NaN NaN NaN NaN NaN NaN NaN NaN NaN NaN NaN NaN NaN NaN NaN NaN NaN NaN
       NaN NaN
seg_2 Eff_Gain 1 400 65 22 40 1.5 0 0 -200 20 1030 80 100 NaN NaN NaN NaN NaN NaN  NaN  NaN  NaN  NaN NaN  NaN  NaN NaN
      NaN NaN NaN NaN
seg_3 NPE 1 1 NaN NaN NaN NaN NaN NaN NaN NaN NaN NaN NaN NaN NaN NaN NaN NaN NaN 0.9 0 1 0 NaN NaN NaN NaN NaN NaN NaN NaN
      NaN
seg_4 Passive 1 2000 2200 22 40 4.5 0 0 NaN NaN NaN NaN NaN NaN NaN NaN NaN NaN NaN NaN NaN NaN NaN NaN NaN NaN NaN NaN
      NaN NaN NaN
seg_5 Filter 1 1 NaN NaN NaN NaN NaN NaN NaN NaN NaN NaN NaN NaN NaN NaN NaN NaN NaN NaN NaN NaN NaN NaN NaN 1 1033.5 1.67 NaN
      NaN NaN NaN NaN
```

4. settings4Energy_filteredPosition4.txt:

```
------------------------------------------------------------------------------------------------------------------------------------------

TWidth TRes frep CentW pulse_no spacing Shape Dw DT Energy File_No Page_No SaveN plotN plot_seg store_seg Passes
      Conv_typ Conv_spn Conv_seg Conv_th EdgeF
ps fs MHz nm integer ps index THz ratio nJ integer page RundTrp RundTrp integer integer RundTrp index RundTrp integer
      percent logical
------------------------------------------------------------------------------------------------------------------------------------------

40 20 1000 1030 1 19.999 2 0.46 1 0.9e-2 1410 20 1 1 2 -1 1 1 10 4 0.000002 0
------------------------------------------------------------------------------------------------------------------------------------------

  - - - - - - - - - - - - - - - - - - - - - - S - - - - - - - - - -
  - - - - - - - - - - - - - - - - - - - - - - A P - - - - - - - - -
  - - - - - - - - - - - - - - - - - - - - - - T H - - - - - - - - -
  - - - - - - - - - - - - - - - - - - - - - - U A - - - - - - - - -
  - - - - - - - - - - - - - - - - - - - - - - R S - - - - - - - - -
  - - - - - - - - - - - - - - - - - - - - - - A E - - - - - - - - -
  - - - - - - - - - - - - - - - - - - - - - - T - - - - - - - - - -
  - - - - G - - R - - - - - - - - - - - - - I S - - F - - - - - - -
  - - - - R - - A - - - - - - - - - - - - - O H - - I - - - - - - -
  - - - - O - N M - - - - - - - - - - - - - N I - - L - - - - - - -
  - - - - U T O A - - - - - - - - - - - - - - F - - T - - B - - - -
  - - - - P H N N - - - - - - - - - - - - - P T - - E - - L R B -
  - - - - - I L - - - - - - - - - - - - - - O - - - R - - U E L R
  - N - - V R I S - - - - - - - - - - - - - W o - - - - D E D U E
  - U - - E D N C - - - C - - - - - - - P - - E F - - C - O - - E D
  - M - - L - E A - - - E - - - D - - U - - R - - - E - U F F - -
  - B - - O O A T - - U N - S - O - - M - M - N - - N F B I I F F
  - E N L C R R T S - N T - A P P - P P - O O P - - T I L L L I I
  - R U E I D I E E - S R G T U I - U - - D F E - - R L E T T L L
  - - M N T E T R L - A A A U M N - M S - U - - R - A T - E E T T
  - O B G Y R Y I F - T L I R P G - P P - L N T E F L E F R R E E
  M F E T - - - N _ - U - N A - - - - E L A P R C I - R I - - R R
  E - R H D D C G S G R W - T A C P W C I T E A O L W - L W W - -
  D S - - I I O - T A A A B I B O U A T N I - N V T A B T A A B B
  I N O O S S F F E I T V A O S N M V R E O O S E E V A E V V A A
  U A F F P P F R E N E E N N O C P E A A N R M R R E N R E E N N
  M P - - E E I A P - D L D - R E - L L R - - I Y - L D - L L D D
  - S S F R R C C E N - E W P P N P E - - D S S - S E W D E E W W
  T H T I S S I T N O G N I O T T O N F L E E S T H N I E N N I I
  Y O E B I I E I I I A G D W I I W G W O P S I I A G D L G G D D
  P T P E O O N O N S I T T E O O E T H S T A O M P T T A T T T T
  E S S R N N T N G E N H H R N N R H M S H M N E E H H Y H H H H
------------------------------------------------------------------------------------------------------------------------------------------

Seg_ID AcType  Snap Steps L GVD TOD Gamma f_R steep Noise Unsat Cent_WL Gain_BW SatPow alpha DopConc PumpPow Pump_WL
      PmpFWHM q_0 q_1 I_sat Phi Tau Shape FCent_W F_BW delay blue_w red_w blue_BW red_BW
ID Name Snap Step cm fs2/mm fs3/mm 1/kW/m fraction logical dB dB nm nm W dB/m nm-3 W nm nm None None kW deg ps Index nm
      nm ps nm nm nm nm
------------------------------------------------------------------------------------------------------------------------------------------

seg_1 Passive 1 10 200 22 40 4.5 0 0 NaN NaN NaN NaN NaN NaN NaN NaN NaN NaN NaN NaN NaN NaN NaN NaN NaN NaN NaN NaN
       NaN NaN
seg_2 Eff_Gain 1 400 65 22 40 1.5 0 0 -200 20 1030 80 100 NaN NaN NaN NaN NaN NaN  NaN  NaN  NaN  NaN NaN  NaN  NaN NaN
      NaN NaN NaN NaN
seg_3 NPE 1 1 NaN NaN NaN NaN NaN NaN NaN NaN NaN NaN NaN NaN NaN NaN NaN NaN NaN 0.9 0 1 0 NaN NaN NaN NaN NaN NaN NaN NaN
      NaN
seg_4 Passive 1 2000 2200 22 40 4.5 0 0 NaN NaN NaN NaN NaN NaN NaN NaN NaN NaN NaN NaN NaN NaN NaN NaN NaN NaN NaN NaN
      NaN NaN NaN
seg_5 Filter 1 1 NaN NaN NaN NaN NaN NaN NaN NaN NaN NaN NaN NaN NaN NaN NaN NaN NaN NaN NaN NaN NaN NaN NaN 1 1033.5 1.67 NaN
      NaN NaN NaN NaN
```

A.11 Figure 5.7 (Speed versus pulse energy in our Mamyshev oscillator)

The code (code4ThesisEnergy_speed.m):

```
Efactors=1+[-0.05:0.005:0.05];
Kerr_tau_dot=zeros(1,length(Efactors));
Similariton_tau_dot=zeros(1,length(Efactors));
Kerr_tau_dot_s=zeros(1,length(Efactors));
Similariton_tau_dot_s=zeros(1,length(Efactors));
settingsFile1="settings4ThesisEnergy_speed1.txt";
settingsFile2="settings4ThesisEnergy_speed2.txt";

[seg_data, global_data,segment_header,global_header] = loadData(settingsFile1,0);

timewidth = str2double(global_data(contains(global_header,'TWidth'))); % Width of the time window in [ps]
tres1 = str2double(global_data(contains(global_header,'TRes')))*1e-3; % Resolution of the time window [ps] (written as fs*1e-3)
c = 299792.458; % [nm/ps]
timesteps=2^(ceil(log2(timewidth/tres1))); tres=timewidth/timesteps;
t = -timewidth*0.5+tres:tres:timewidth*0.5; % Time in [ps]
timesteps=length(t);
fs=1/timewidth; % Sampling rate in [THz]
freq=c/lambda_c+fs*linspace(-timesteps/2,timesteps/2-1,timesteps);
freq=fftshift(freq); % Frequency in [THz]
wave=c./freq; shiftedWave=fftshift(wave); % Wavelength in [nm]
w=2*pi*c/lambda_c; % Central angular frequency in [THz]
omegas = 2*pi*freq; % Angular frequency in [THz]

CommandLine(settingsFile1);

KerrIn=LoadPage(LoadE(['Data' num2str(50) '.bin']),10,timesteps);KerrInE=tres*(KerrIn*KerrIn');
SimilaritonIn=LoadPage(LoadE(['Data' num2str(50) '.bin']),10,timesteps);SimilaritonInE=tres*(SimilaritonIn*SimilaritonIn');
q_0toKerrOriginal=str2double(seg_data(11,contains(segment_header,'q_0'))) ;
q_0toSimilaritonOriginal= str2double(seg_data(6,contains(segment_header,'q_0'))) ;

f=figure('position',[800 800 600 260]);f.Color='w';
subplot(1,2,1)
KerrOutput=LoadPage(LoadE(['Data' num2str(50) '.bin']),4,timesteps);
KerrOutputSpectrum=fftshift(abs(fft(KerrOutput)).^2);
plot(shiftedWave,KerrOutputSpectrum/max(KerrOutputSpectrum),'LineWidth',1.4);xlim([1020 1050]);ylim([0 1.199]);xlabel("Wavelength
       (nm)");ylabel("Amplitude (a.u.)")
sigma1=(1.65/2.355)^2;hold on;plot(shiftedWave,exp(-(shiftedWave-1037.25).^2/sigma1),'LineWidth',1.4);hold off;text(0.04,0.93,'(a
      )','Units','normalized','fontsize',11)
legend("Kerr arm", "Red filter")

subplot(1,2,2)
SimilaritonOutput=LoadPage(LoadE(['Data' num2str(50) '.bin']),9,timesteps);
SimilaritonOutputSpectrum=fftshift(abs(fft(SimilaritonOutput)).^2);
plot(shiftedWave,SimilaritonOutputSpectrum/max(SimilaritonOutputSpectrum),'LineWidth',1.4);xlim([1020 1050]);ylim([0 1.199]);
      xlabel("Wavelength (nm)");ylabel("Amplitude (a.u.)")
sigma2=(1.69/2.355)^2;hold on;plot(shiftedWave,exp(-(shiftedWave-1032.25).^2/sigma2),'LineWidth',1.4);hold off;text(0.04,0.93,'(b
      )','Units','normalized','fontsize',11);
legend("Similariton arm", "Blue filter")

f=figure('position',[800 800 600 600]);f.Color='w';
% without self-steepening
for trial=1:length(Efactors)
   [seg_data, global_data,segment_header,global_header] = loadData(settingsFile1,0);
   seg_data(2,contains(segment_header,'SatPow'))={num2str(str2double(seg_data(2,contains(segment_header,'SatPow')))*Efactors(
         trial))};
   % initial pulse shape
   run Assign_CommandLine.m
   %% main loop
```

```
    while (lap<roundtrips)
        lap = lap + 1;
        if(mod(lap,saveevery)==0)
            snapstosave = [];
        end
        for i = 1:nOfSegments
            % fprintf('Roundtrip: %d, Segment: %d\n',lap,i);
            % Propagate according to the segment info
            [E,Esnaps] = Propagation(E,Esnaps,t,w,wave,omegas,freq,edge_filter,frep,lambda_c,hr,tres,seg_data(i,:),snapshots(i),
                  segment_header,0);
            if((mod(lap,saveevery)==0)||(saveevery==0))
                for k = 1:snapshots(i)
                    snapstosave = [snapstosave Esnaps(k,:)];
                end
            end
            if Conv_typ==1 % convergence check based on pulse energy
                if i==Conv_seg
                    Conv_mem=[Conv_mem(2:end) tres*(E*E')];
                end
            elseif Conv_typ==2 % convergence check based on peak power
                if i==Conv_seg
                    Conv_mem=[Conv_mem(2:end) max(abs(E).^2)];
                end
            end
            % fprintf('Energy = % f nJ \n',tres*(E*E')); % Print the pulse energy
            if i==5
                currentE=tres*(E*E');
                seg_data(6,contains(segment_header,'q_0'))={num2str(q_0toSimilaritonOriginal*SimilaritonInE/currentE)};
            elseif i==10
                currentE=tres*(E*E');
                seg_data(11,contains(segment_header,'q_0'))={num2str(q_0toKerrOriginal*KerrInE*Efactors(trial)/currentE)};
            end
        end
        if(mod(lap,saveevery)==0)
            SaveE(snapstosave(:),['Data' num2str(lap+(shape==3)*str2double(file_no)) '.bin'] ); % Save the for every N roundtrips
                  to .bin file
            fprintf('lap=%d␣energy=%.10e␣nJ␣\n',lap+(shape==3)*str2double(file_no),tres*(E*E')); % Print the pulse energy
            % fprintf('Energy = % f nJ \n',tres*(E*E')); % Print the pulse energy
            % fprintf('saving \n');
        end
        Conv_MAX=max(Conv_mem); Conv_MIN=min(Conv_mem);
        if (Conv_MAX-Conv_MIN)/Conv_MIN < Conv_th
            saveevery=lap+1;
            if converged==1
                break
            end
            converged=1;
        end
    end
    E10=LoadPage(LoadE(['Data' num2str(10) '.bin']),11,timesteps);
    E20=LoadPage(LoadE(['Data' num2str(50) '.bin']),11,timesteps);
    power10=abs(E10).^2;power20=abs(E20).^2;
    max10=max(power10);max20=max(power20);
    tau10=t(power10==max10);tau50=t(power20==max20);
    Delta_tau=tau50-tau10;
    tau_dot=Delta_tau*15/4*10^2;
    Kerr_tau_dot(trial)=tau_dot;
end

Kerr_tau_dot=Kerr_tau_dot-Kerr_tau_dot((length(Efactors)-1)/2+1);
plot((Efactors-1)*100,Kerr_tau_dot,"s");
xlabel("${\frac{\Delta E}{E} (\%)}$",'interpreter','latex','FontSize',15,'FontWeight','bold')
ylabel("$\mathbf{\dot{\tau}}$ (ns/sec)",'interpreter','latex','FontSize',15,'FontWeight','bold')


for trial=1:length(Efactors)
    [seg_data, global_data,segment_header,global_header] = loadData(settingsFile1,0);
```

```
    seg_data(8,contains(segment_header,'SatPow'))={num2str(str2double(seg_data(8,contains(segment_header,'SatPow')))*Efactors(
        trial))};
    % initial pulse shape
    run Assign_CommandLine.m
    %% main loop
    while (lap<roundtrips)
        lap = lap + 1;
        if(mod(lap,saveevery)==0)
            snapstosave = [];
        end
        for i = 1:nOfSegments
            % fprintf('Roundtrip: %d, Segment: %d\n',lap,i);
            % Propagate according to the segment info
            [E,Esnaps] = Propagation(E,Esnaps,t,w,wave,omegas,freq,edge_filter,frep,lambda_c,hr,tres,seg_data(i,:),snapshots(i),
                segment_header,0);
            if((mod(lap,saveevery)==0)||(saveevery==0))
                for k = 1:snapshots(i)
                    snapstosave = [snapstosave Esnaps(k,:)];
                end
            end
            if Conv_typ==1 % convergence check based on pulse energy
                if i==Conv_seg
                    Conv_mem=[Conv_mem(2:end) tres*(E*E')];
                end
            elseif Conv_typ==2 % convergence check based on peak power
                if i==Conv_seg
                    Conv_mem=[Conv_mem(2:end) max(abs(E).^2)];
                end
            end
            % fprintf('Energy = % f nJ \n',tres*(E*E')); % Print the pulse energy
            if i==5
                currentE=tres*(E*E');
                seg_data(6,contains(segment_header,'q_0'))={num2str(q_0toSimilaritonOriginal*SimilaritonInE*Efactors(trial)/
                    currentE)};
            elseif i==10
                currentE=tres*(E*E');
                seg_data(11,contains(segment_header,'q_0'))={num2str(q_0toKerrOriginal*KerrInE/currentE)};
            end
        end
        if(mod(lap,saveevery)==0)
            SaveE(snapstosave(:),['Data' num2str(lap+(shape==3)*str2double(file_no)) '.bin'] ); % Save the for every N roundtrips
                to .bin file
            fprintf('lap=%d␣energy=%.10e␣nJ␣\n',lap+(shape==3)*str2double(file_no),tres*(E*E')); % Print the pulse energy
            % fprintf('Energy = % f nJ \n',tres*(E*E')); % Print the pulse energy
            % fprintf('saving \n');
        end
        Conv_MAX=max(Conv_mem); Conv_MIN=min(Conv_mem);
        if (Conv_MAX-Conv_MIN)/Conv_MIN < Conv_th
            saveevery=lap+1;
            if converged==1
                break
            end
            converged=1;
        end
    end
    E10=LoadPage(LoadE(['Data' num2str(10) '.bin']),11,timesteps);
    E20=LoadPage(LoadE(['Data' num2str(50) '.bin']),11,timesteps);
    power10=abs(E10).^2;power20=abs(E20).^2;
    max10=max(power10);max20=max(power20);
    tau10=t(power10==max10);tau50=t(power20==max20);
    Delta_tau=tau50-tau10;
    tau_dot=Delta_tau*15/4*10^2;
    Similariton_tau_dot(trial)=tau_dot;
end

Similariton_tau_dot=Similariton_tau_dot-Similariton_tau_dot((length(Efactors)-1)/2+1);
hold on;plot((Efactors-1)*100,Similariton_tau_dot,"s");
xlabel("${\frac{\Delta E}{E} (\%)}$",'interpreter','latex','FontSize',15,'FontWeight','bold')
```

```
ylabel("$\mathbf{\dot{\tau}}$ (ns/sec)",'interpreter','latex','FontSize',15,'FontWeight','bold')
% legend('Kerr arm','Similariton arm')

% with self-steepening
for trial=1:length(Efactors)
    [seg_data, global_data,segment_header,global_header] = loadData(settingsFile2,0);
    seg_data(2,contains(segment_header,'SatPow'))={num2str(str2double(seg_data(2,contains(segment_header,'SatPow')))*Efactors(
          trial))};
    % initial pulse shape
    run Assign_CommandLine.m
    %% main loop
    while (lap<roundtrips)
        lap = lap + 1;
        if(mod(lap,saveevery)==0)
            snapstosave = [];
        end
        for i = 1:nOfSegments
            % fprintf('Roundtrip: %d, Segment: %d\n',lap,i);
            % Propagate according to the segment info
            [E,Esnaps] = Propagation(E,Esnaps,t,w,wave,omegas,freq,edge_filter,frep,lambda_c,hr,tres,seg_data(i,:),snapshots(i),
                segment_header,0);
            if((mod(lap,saveevery)==0)||(saveevery==0))
                for k = 1:snapshots(i)
                    snapstosave = [snapstosave Esnaps(k,:)];
                end
            end
            if Conv_typ==1 % convergence check based on pulse energy
                if i==Conv_seg
                    Conv_mem=[Conv_mem(2:end) tres*(E*E')];
                end
            elseif Conv_typ==2 % convergence check based on peak power
                if i==Conv_seg
                    Conv_mem=[Conv_mem(2:end) max(abs(E).^2)];
                end
            end
            % fprintf('Energy = % f nJ \n',tres*(E*E')); % Print the pulse energy
            if i==5
                currentE=tres*(E*E');
                seg_data(6,contains(segment_header,'q_0'))={num2str(q_0toSimilaritonOriginal*SimilaritonInE/currentE)};
            elseif i==10
                currentE=tres*(E*E');
                seg_data(11,contains(segment_header,'q_0'))={num2str(q_0toKerrOriginal*KerrInE*Efactors(trial)/currentE)};
            end
        end
        if(mod(lap,saveevery)==0)
            SaveE(snapstosave(:),['Data' num2str(lap+(shape==3)*str2double(file_no)) '.bin'] ); % Save the for every N roundtrips
                to .bin file
            fprintf('lap=%d␣energy=%.10e␣nJ␣\n',lap+(shape==3)*str2double(file_no),tres*(E*E')); % Print the pulse energy
            % fprintf('Energy = % f nJ \n',tres*(E*E')); % Print the pulse energy
            % fprintf('saving \n');
        end
        Conv_MAX=max(Conv_mem); Conv_MIN=min(Conv_mem);
        if (Conv_MAX-Conv_MIN)/Conv_MIN < Conv_th
            saveevery=lap+1;
            if converged==1
                break
            end
            converged=1;
        end
    end
    E10=LoadPage(LoadE(['Data' num2str(10) '.bin']),11,timesteps);
    E20=LoadPage(LoadE(['Data' num2str(50) '.bin']),11,timesteps);
    power10=abs(E10).^2;power20=abs(E20).^2;
    max10=max(power10);max20=max(power20);
    tau10=t(power10==max10);tau50=t(power20==max20);
    Delta_tau=tau50-tau10;
    tau_dot=Delta_tau*15/4*10^2;
    Kerr_tau_dot_s(trial)=tau_dot;
```

```
end

Kerr_tau_dot_s=Kerr_tau_dot_s-Kerr_tau_dot_s((length(Efactors)-1)/2+1);
hold on;plot((Efactors-1)*100,Kerr_tau_dot_s,"*");
xlabel("${\frac{\Delta E}{E} (\%)}$",'interpreter','latex','FontSize',15,'FontWeight','bold')
ylabel("$\mathbf{\dot{\tau}}$ (ns/sec)",'interpreter','latex','FontSize',15,'FontWeight','bold')


for trial=1:length(Efactors)
    [seg_data, global_data,segment_header,global_header] = loadData(settingsFile2,0);
    seg_data(8,contains(segment_header,'SatPow'))={num2str(str2double(seg_data(8,contains(segment_header,'SatPow')))*Efactors(
          trial))};
    % initial pulse shape
    run Assign_CommandLine.m
    %% main loop
    while (lap<roundtrips)
        lap = lap + 1;
        if(mod(lap,saveevery)==0)
            snapstosave = [];
        end
        for i = 1:nOfSegments
            % fprintf('Roundtrip: %d, Segment: %d\n',lap,i);
            % Propagate according to the segment info
            [E,Esnaps] = Propagation(E,Esnaps,t,w,wave,omegas,freq,edge_filter,frep,lambda_c,hr,tres,seg_data(i,:),snapshots(i),
                  segment_header,0);
            if((mod(lap,saveevery)==0)||(saveevery==0))
                for k = 1:snapshots(i)
                    snapstosave = [snapstosave Esnaps(k,:)];
                end
            end
            if Conv_typ==1 % convergence check based on pulse energy
                if i==Conv_seg
                    Conv_mem=[Conv_mem(2:end) tres*(E*E')];
                end
            elseif Conv_typ==2 % convergence check based on peak power
                if i==Conv_seg
                    Conv_mem=[Conv_mem(2:end) max(abs(E).^2)];
                end
            end
            % fprintf('Energy = % f nJ \n',tres*(E*E')); % Print the pulse energy
            if i==5
                currentE=tres*(E*E');
                seg_data(6,contains(segment_header,'q_0'))={num2str(q_0toSimilaritonOriginal*SimilaritonInE*Efactors(trial)/
                      currentE)};
            elseif i==10
                currentE=tres*(E*E');
                seg_data(11,contains(segment_header,'q_0'))={num2str(q_0toKerrOriginal*KerrInE/currentE)};
            end
        end
        if(mod(lap,saveevery)==0)
            SaveE(snapstosave(:),['Data' num2str(lap+(shape==3)*str2double(file_no)) '.bin'] ); % Save the for every N roundtrips
                  to .bin file
            fprintf('lap=%d␣energy=%.10e␣nJ␣\n',lap+(shape==3)*str2double(file_no),tres*(E*E')); % Print the pulse energy
            % fprintf('Energy = % f nJ \n',tres*(E*E')); % Print the pulse energy
            % fprintf('saving \n');
        end
        Conv_MAX=max(Conv_mem); Conv_MIN=min(Conv_mem);
        if (Conv_MAX-Conv_MIN)/Conv_MIN < Conv_th
            saveevery=lap+1;
            if converged==1
                break
            end
            converged=1;
        end
    end
    E10=LoadPage(LoadE(['Data' num2str(10) '.bin']),11,timesteps);
    E20=LoadPage(LoadE(['Data' num2str(50) '.bin']),11,timesteps);
    power10=abs(E10).^2;power20=abs(E20).^2;
```

```
    max10=max(power10);max20=max(power20);
    tau10=t(power10==max10);tau50=t(power20==max20);
    Delta_tau=tau50-tau10;
    tau_dot=Delta_tau*15/4*10^2;
    Similariton_tau_dot_s(trial)=tau_dot;
end

Similariton_tau_dot_s=Similariton_tau_dot_s-Similariton_tau_dot_s((length(Efactors)-1)/2+1);
hold on;plot((Efactors-1)*100,Similariton_tau_dot_s,"*");
xlabel("${\frac{\Delta E}{E} (\%)}$",'interpreter','latex','FontSize',15,'FontWeight','bold')
ylabel("$\mathbf{\dot{\tau}}$ (ns/sec)",'interpreter','latex','FontSize',15,'FontWeight','bold')
legend('Kerr␣arm','Similariton␣arm','Kerr␣arm␣(S.S.)','Similariton␣arm␣(S.S.)')
```

The settings files:

1. settings4ThesisEnergy_speed1.txt:

```
-------------------------------------------------------------------------------------------------------------------------------------------

TWidth TRes frep CentW pulse_no spacing Shape Dw DT Energy File_No Page_No SaveN plotN plot_seg store_seg Passes
      Conv_typ Conv_spn Conv_seg Conv_th EdgeF
ps fs MHz nm integer ps index THz ratio nJ integer page RundTrp RundTrp integer integer RundTrp index RundTrp integer
      percent logical
-------------------------------------------------------------------------------------------------------------------------------------------

14 5 1000 1035 1 19.999 2 0.48 1 1e-1 1410 20 10 1 2 -1 50 0 10 4 0.000002 0
-------------------------------------------------------------------------------------------------------------------------------------------

  - - - - - - - - - - - - - - - - - - - - - - S - - - - - - - - - -
  - - - - - - - - - - - - - - - - - - - - - - A P - - - - - - - - -
  - - - - - - - - - - - - - - - - - - - - - - T H - - - - - - - - -
  - - - - - - - - - - - - - - - - - - - - - - U A - - - - - - - - -
  - - - - - - - - - - - - - - - - - - - - - - R S - - - - - - - - -
  - - - - - - - - - - - - - - - - - - - - - - A E - - - - - - - - -
  - - - - - - - - - - - - - - - - - - - - - - T - - - - - - - - - -
  - - - - G - - R - - - - - - - - - - - - - I S - - F - - - - - - -
  - - - - R - - A - - - - - - - - - - - - - O H - - I - - - - - - -
  - - - - O - N M - - - - - - - - - - - - - N I - - L - - - - - - -
  - - - - U T O A - - - - - - - - - - - - - - F - - T - - B - - - -
  - - - - P H N N - - - - - - - - - - - - - P T - - E - - L R B -
  - - - - - I L - - - - - - - - - - - - - - O - - - R - - U E L R
  - N - - - V R I S - - - - - - - - - - - - - W o - - - - D E D U E
  - U - - E D N C - - - C - - - - - - - P - - E F - - C - O - - E D
  - M - - L - E A - - - E - - - D - - U - - R - - - E - U F F - -
  - B - - O O A T - - U N - S - O - - M - M - N - - N F B I I F F
  - E N L C R R T S - N T - A P P - P P - O O P - - T I L L L I I
  - R U E I D I E E - S R G T U I - U - - D F E - - R L E T T L L
  - - M N T E T R L - A A A U M N - M S - U - - R - A T - E E T T
  - O B G Y R Y I F - T L I R P G - P P - L N T E F L E F R R E E
  M F E T - - - N _ - U - N A - - - - E L A P R C I - R I - - R R
  E - R H D D C G S G R W - T A C P W C I T E A O L W - L W W - -
  D S - - I I O - T A A A B I B O U A T N I - N V T A B T A A B B
  I N O O S S F F E I T V A O S N M V R E O O S E E V A E V V A A
  U A F F P P F R E N E E N N O C P E A A N R M R R E N R E E N N
  M P - - E E I A P - D L D - R E - L L R - - I Y - L D - L L D D
  - S S F R R C C E N - E W P P N P E - - D S S - S E W D E E W W
  T H T I S S I T N O G N I O T T O N F L E E S T H N I E N N I I
  Y O E B I I E I I I A G D W I I W G W O P S I I A G D L G G D D
  P T P E O O N O N S I T T E O O E T H S T A O M P T T A T T T T
  E S S R N N T N G E N H H R N N R H M S H M N E E H H Y H H H H
-------------------------------------------------------------------------------------------------------------------------------------------
```

```
Seg_ID AcType  Snap Steps L GVD TOD Gamma f_R steep Noise Unsat Cent_WL Gain_BW SatPow alpha DopConc PumpPow Pump_WL
      PmpFWHM q_0 q_1 I_sat Phi Tau Shape FCent_W F_BW delay blue_w red_w blue_BW red_BW
ID Name Snap Step cm fs2/mm fs3/mm 1/kW/m fraction logical dB dB nm nm W dB/m nm-3 W nm nm None None kW deg ps Index nm
      nm ps nm nm nm nm
-------------------------------------------------------------------------------------------------------------------------------------

seg_1 Passive 1 40 200 22 40 1.6 0 0 NaN NaN NaN NaN NaN NaN NaN NaN NaN NaN NaN NaN NaN NaN NaN NaN NaN NaN NaN NaN
       NaN NaN
seg_2 Eff_Gain 1 250 80 22 40 1.6 0 0 -200 21 1035 80 0.7 NaN NaN NaN NaN NaN NaN  NaN  NaN  NaN  NaN NaN  NaN  NaN NaN
      NaN NaN NaN NaN
seg_3 NPE 1 1 NaN NaN NaN NaN NaN NaN NaN NaN NaN NaN NaN NaN NaN NaN NaN NaN NaN NaN 0.9 0 1 0 NaN NaN NaN NaN NaN NaN NaN NaN
      NaN
seg_4 Passive 1 300 220 22 40 4.5 0 0 NaN NaN NaN NaN NaN NaN NaN NaN NaN NaN NaN NaN NaN NaN NaN NaN NaN NaN NaN NaN
      NaN NaN NaN
seg_5 Filter 1 1 NaN NaN NaN NaN NaN NaN NaN NaN NaN NaN NaN NaN NaN NaN NaN NaN NaN NaN NaN NaN NaN NaN NaN NaN 1 1037.25 1.65 NaN
      NaN NaN NaN NaN
seg_6 NPE 1 1 NaN NaN NaN NaN NaN NaN NaN NaN NaN NaN NaN NaN NaN NaN NaN NaN NaN NaN 0.55 0 1 0 NaN NaN NaN NaN NaN NaN NaN NaN
       NaN
seg_7 Passive 1 100 400 22 40 4.5 0 0 NaN NaN NaN NaN NaN NaN NaN NaN NaN NaN NaN NaN NaN NaN NaN NaN NaN NaN NaN NaN
      NaN NaN NaN
seg_8 Eff_Gain 1 300 275 22 40 1.6 0 0 -200 43 1035 80 1.6 NaN NaN NaN NaN NaN  NaN  NaN  NaN  NaN NaN  NaN  NaN NaN
       NaN NaN NaN NaN
seg_9 Passive 1 150 90 22 40 1.6 0 0 NaN NaN NaN NaN NaN NaN NaN NaN NaN NaN NaN NaN NaN NaN NaN NaN NaN NaN NaN NaN
       NaN NaN
seg_10 Filter 1 1 NaN NaN NaN NaN NaN NaN NaN NaN NaN NaN NaN NaN NaN NaN NaN NaN NaN NaN NaN NaN NaN NaN NaN NaN 1 1032.75 1.69 NaN
       NaN NaN NaN NaN
seg_11 NPE 1 1 NaN NaN NaN NaN NaN NaN NaN NaN NaN NaN NaN NaN NaN NaN NaN NaN NaN NaN 0.09 0 1 0 NaN NaN NaN NaN NaN NaN NaN
      NaN NaN
```

2. settings4ThesisEnergy_speed2.txt:

```
      ---------------------------------------------------------------------------------------------------------------------------------------

TWidth TRes frep CentW pulse_no spacing Shape Dw DT Energy File_No Page_No SaveN plotN plot_seg store_seg Passes
      Conv_typ Conv_spn Conv_seg Conv_th EdgeF
ps fs MHz nm integer ps index THz ratio nJ integer page RundTrp RundTrp integer integer RundTrp index RundTrp integer
      percent logical
-------------------------------------------------------------------------------------------------------------------------------------

14 5 1000 1035 1 19.999 2 0.48 1 1e-1 1410 20 10 1 2 -1 50 0 10 4 0.000002 0
-------------------------------------------------------------------------------------------------------------------------------------

  - - - - - - - - - - - - - - - - - - - - - - S - - - - - - - - - -
  - - - - - - - - - - - - - - - - - - - - - - A P - - - - - - - - - -
  - - - - - - - - - - - - - - - - - - - - - - T H - - - - - - - - - -
  - - - - - - - - - - - - - - - - - - - - - - U A - - - - - - - - - -
  - - - - - - - - - - - - - - - - - - - - - - R S - - - - - - - - - -
  - - - - - - - - - - - - - - - - - - - - - - A E - - - - - - - - - -
  - - - - - - - - - - - - - - - - - - - - - - T - - - - - - - - - - -
  - - - - G - - R - - - - - - - - - - - - - I S - - F - - - - - - -
  - - - - R - - A - - - - - - - - - - - - - O H - - I - - - - - - -
  - - - - O - N M - - - - - - - - - - - - - N I - - L - - - - - - -
  - - - - U T O A - - - - - - - - - - - - - - F - - T - - B - - - -
  - - - - P H N N - - - - - - - - - - - - - P T - - E - - L R B -
  - - - - - I L - - - - - - - - - - - - - - O - - - R - - U E L R
  - N - - V R I S - - - - - - - - - - - - - W o - - - - D E D U E
  - U - - E D N C - - - C - - - - - - P - - E F - - C - O - - E D
  - M - - L - E A - - - E - - - D - - U - - R - - - E - U F F - -
  - B - - O O A T - - U N - S - O - - M - M - N - - N F B I I F F
  - E N L C R R T S - N T - A P P - P P - O O P - - T I L L L I I
  - R U E I D I E E - S R G T U I - U - - D F E - - R L E T T L L
  - - M N T E T R L - A A A U M N - M S - U - - R - A T - E E T T
  - O B G Y R Y I F - T L I R P G - P P - L N T E F L E F R R E E
  M F E T - - - N _ - U - N A - - - - E L A P R C I - R I - - R R
  E - R H D D C G S G R W - T A C P W C I T E A O L W - L W W - -
  D S - - I I O - T A A A B I B O U A T N I - N V T A B T A A B B
```

```
  I N O O S S F F E I T V A O S N M V R E O O S E E V A E V V A A
  U A F F P P F R E N E E N N O C P E A A N R M R R E N R E E N N
  M P - - E E I A P - D L D - R E - L L R - - I Y - L D - L L D D
  - S S F R R C C E N - E W P P N P E - - D S S - S E W D E E W W
  T H T I S S I T N O G N I O T T O N F L E E S T H N I E N N I I
  Y O E B I I E I I I A G D W I I W G W O P S I I A G D L G G D D
  P T P E O O N O N S I T T E O O E T H S T A O M P T T A T T T T
  E S S R N N T N G E N H H R N N R H M S H M N E E H H Y H H H H
```

```
Seg_ID AcType  Snap Steps L GVD TOD Gamma f_R steep Noise Unsat Cent_WL Gain_BW SatPow alpha DopConc PumpPow Pump_WL
      PmpFWHM q_0 q_1 I_sat Phi Tau Shape FCent_W F_BW delay blue_w red_w blue_BW red_BW
ID Name Snap Step cm fs2/mm fs3/mm 1/kW/m fraction logical dB dB nm nm W dB/m nm-3 W nm nm None None kW deg ps Index nm
      nm ps nm nm nm nm
```

```
seg_1 Passive 1 40 200 22 40 1.6 0 1 NaN NaN NaN NaN NaN NaN NaN NaN NaN NaN NaN NaN NaN NaN NaN NaN NaN NaN NaN NaN
       NaN NaN
seg_2 Eff_Gain 1 250 80 22 40 1.6 0 1 -200 21 1035 80 0.7 NaN NaN NaN NaN NaN NaN  NaN  NaN  NaN  NaN NaN  NaN  NaN NaN
      NaN NaN NaN NaN
seg_3 NPE 1 1 NaN NaN NaN NaN NaN NaN NaN NaN NaN NaN NaN NaN NaN NaN NaN NaN NaN 0.9 0 1 0 NaN NaN NaN NaN NaN NaN NaN NaN
      NaN
seg_4 Passive 1 300 220 22 40 4.5 0 1 NaN NaN NaN NaN NaN NaN NaN NaN NaN NaN NaN NaN NaN NaN NaN NaN NaN NaN NaN NaN
      NaN NaN NaN
seg_5 Filter 1 1 NaN NaN NaN NaN NaN NaN NaN NaN NaN NaN NaN NaN NaN NaN NaN NaN NaN NaN NaN NaN NaN NaN NaN 1 1037.25 1.65 NaN
      NaN NaN NaN NaN
seg_6 NPE 1 1 NaN NaN NaN NaN NaN NaN NaN NaN NaN NaN NaN NaN NaN NaN NaN NaN NaN 0.55 0 1 0 NaN NaN NaN NaN NaN NaN NaN NaN
       NaN
seg_7 Passive 1 100 400 22 40 4.5 0 1 NaN NaN NaN NaN NaN NaN NaN NaN NaN NaN NaN NaN NaN NaN NaN NaN NaN NaN NaN NaN
      NaN NaN NaN
seg_8 Eff_Gain 1 300 275 22 40 1.6 0 1 -200 43 1035 80 1.6 NaN NaN NaN NaN NaN NaN  NaN  NaN  NaN  NaN NaN  NaN  NaN NaN
       NaN NaN NaN NaN
seg_9 Passive 1 150 90 22 40 1.6 0 1 NaN NaN NaN NaN NaN NaN NaN NaN NaN NaN NaN NaN NaN NaN NaN NaN NaN NaN NaN NaN
       NaN NaN
seg_10 Filter 1 1 NaN NaN NaN NaN NaN NaN NaN NaN NaN NaN NaN NaN NaN NaN NaN NaN NaN NaN NaN NaN NaN NaN NaN 1 1032.75 1.69 NaN
       NaN NaN NaN NaN
seg_11 NPE 1 1 NaN NaN NaN NaN NaN NaN NaN NaN NaN NaN NaN NaN NaN NaN NaN NaN NaN 0.09 0 1 0 NaN NaN NaN NaN NaN NaN NaN
      NaN NaN
```